ISSN 0021-9673

VOL. 498 , NO. 1 JANUARY 5, 1990

NAL OF HROMATOGRAPHY

INTERNATIONAL JOURNAL ON CHROMATOGRAPHY, ELECTROPHORESIS AND RELATED METHODS

ELSEVIER

JOURNAL OF CHROMATOGRAPHY

Scope. The *Journal of Chromatography* publishes papers on all aspects of chromatography, electrophoresis and related methods. Contributions consist mainly of research papers dealing with chromatographic theory, instrumental development and their applications. The section *Biomedical Applications*, which is under separate editorship, deals with the following aspects: developments in and applications of chromatographic and electrophoretic techniques related to clinical diagnosis or alterations during medical treatment; screening and profiling of body fluids or tissues with special reference to metabolic disorders; results from basic medical research with direct consequences in clinical practice; drug level monitoring and pharmacokinetic studies; clinical toxicology; analytical studies in occupational medicine.

Submission of Papers. Papers in English, French and German may be submitted, in three copies. Manuscripts should be submitted to: The Editor of *Journal of Chromatography*, P.O. Box 681, 1000 AR Amsterdam, The Netherlands, or to: The Editor of *Journal of Chromatography, Biomedical Applications*, P.O. Box 681, 1000 AR Amsterdam, The Netherlands. Review articles are invited or proposed by letter to the Editors. An outline of the proposed review should first be forwarded to the Editors for preliminary discussion prior to preparation. Submission of an article is understood to imply that the article is original and unpublished and is not being considered for publication elsewhere. For copyright regulations, see below.

Subscription Orders. Subscription orders should be sent to: Elsevier Science Publishers B.V., P.O. Box 211, 1000 AE Amsterdam, The Netherlands, Tel. 5803 911, Telex 18582 ESPA NL. The *Journal of Chromatography* and the *Biomedical Applications* section can be subscribed to separately.

Publication. The *Journal of Chromatography* (incl. *Biomedical Applications*) has 37 volumes in 1990. The subscription prices for 1990 are:

J. Chromatogr. (incl. *Cum. Indexes, Vols. 451–500)* + *Biomed. Appl.* (Vols. 498–534):
Dfl. 6734.00 plus Dfl. 1036.00 (p.p.h.) (total *ca.* US$ 3564.25)

J. Chromatogr. (incl. *Cum. Indexes, Vols. 451–500*) only (Vols. 498–524):
Dfl. 5616.00 plus Dfl. 756.00 (p.p.h.) (total *ca.* US$ 2923.00)

Biomed. Appl. only (Vols. 525–534):
Dfl. 2080.00 plus Dfl. 280.00 (p.p.h.) (total *ca.* US$ 1082.50).

Our p.p.h. (postage, package and handling) charge includes surface delivery of all issues, except to subscribers in Argentina, Australia, Brasil, Canada, China, Hong Kong, India, Israel, Malaysia, Mexico, New Zealand, Pakistan, Singapore, South Africa, South Korea, Taiwan, Thailand and the U.S.A. who receive all issues by air delivery (S.A.L. — Surface Air Lifted) at no extra cost. For Japan, air delivery requires 50% additional charge; for all other countries airmail and S.A.L. charges are available upon request. Back volumes of the *Journal of Chromatography* (Vols. 1–497) are available at Dfl. 195.00 (plus postage). Claims for missing issues will be honoured, free of charge, within three months after publication of the issue. Customers in the U.S.A. and Canada wishing information on this and other Elsevier journals, please contact Journal Information Center, Elsevier Science Publishing Co. Inc., 655 Avenue of the Americas, New York, NY 10010. Tel. (212) 633-3750.

Abstracts/Contents Lists published in Analytical Abstracts, ASCA, Biochemical Abstracts, Biological Abstracts, Chemical Abstracts, Chemical Titles, Chromatography Abstracts, Clinical Chemistry Lookout, Current Contents/Physical, Chemical & Earth Sciences, Current Contents/Life Sciences, Deep-Sea Research/Part B: Oceanographic Literature Review, Excerpta Medica, Index Medicus, Mass Spectrometry Bulletin, PASCAL-CNRS, Pharmaceutical Abstracts, Referativnyi Zhurnal, Science Citation Index and Trends in Biotechnology.

See inside back cover for Publication Schedule, Information for Authors and information on Advertisements.

0021-9673/90/$03.50

Printed in The Netherlands

CONTENTS

(Abstracts/Contents Lists published in Analytical Abstracts, ASCA, Biochemical Abstracts, Biological Abstracts, Chemical Abstracts, Chemical Titles, Chromatography Abstracts, Current Contents/Physical, Chemical & Earth Sciences, Current Contents/Life Sciences, Deep-Sea Research/Part B: Oceanographic Literature Review, Excerpta Medica, Index Medicus, Mass Spectrometry Bulletin, PASCAL-CNRS, Referativnyi Zhurnal and Science Citation Index)

(Continued overleaf)

JOURNAL OF CHROMATOGRAPHY

VOL. 498 (1990)

JOURNAL
of
CHROMATOGRAPHY

INTERNATIONAL JOURNAL ON CHROMATOGRAPHY,
ELECTROPHORESIS AND RELATED METHODS

ELSEVIER
AMSTERDAM — OXFORD — NEW YORK — TOKYO

0021-9673/90/$03.50

Printed in The Netherlands

Journal of Chromatography, 498 (1990) 1–9
Elsevier Science Publishers B.V., Amsterdam — Printed in The Netherlands

CHROM. 21 981

PROGRAMMED-TEMPERATURE RETENTION INDICES

A SURVEY OF CALCULATION METHODS

E. FERNÁNDEZ-SÁNCHEZ, J. A. GARCÍA-DOMÍNGUEZ*, V. MENÉNDEZ and J. M. SANTIUSTE

Instituto de Química Física "Rocasolano", CSIC, Serrano 119, 28006 Madrid (Spain)

(First received April 28th, 1989; revised manuscript received September 8th, 1989)

SUMMARY

Retention temperatures of various solutes were measured on an OV-105 column under different heating rates. The experimental results agree with those evaluated by means of the equation of Curvers *et al.* Several methods of assigning programmed-temperature retention indices to each solute were tested. Comparison of the results does not allow a clear choice of any of the methods, although a procedure based on an interpolation through the use of cubic splines polynomials is preferred. The sensitivity of the various procedures towards small changes in the input data is reported.

INTRODUCTION

A number of workers have attempted to report retention data in a systematic way in order to identify compounds and characterize stationary phases. In 1958 Kováts[1] formulated his well known isothermal retention index. A generalization of the Kováts definition to the field of programmed-temperature chromatography was made by van den Doole and Kratz[2] by the use of the retention temperature (T_R) as the parameter that characterizes each solute, and with the assumption that the retention temperatures of the *n*-alkanes are linearly dependent on their retention index as defined by Kováts.

Van den Doole and Kratz's equation is written as

$$PTRI = 100Z + 100 \cdot \frac{T_{RX} - T_{RZ}}{T_{RZ+1} - T_{RZ}} \quad (1)$$

where *PTRI* represents the programmed-temperature retention index, and $T_{RZ} < T_{RX} < T_{RZ+1}$ are the retention temperatures of the *n*-alkane with Z carbon atoms, the solute and the *n*-alkane with $Z+1$ carbon atoms, respectively.

The use of programmed-temperature gas chromatography has increased enormously as it is a valuable tool in many fields, such as pharmaceutical drugs, petroleum, foods, spirits, flavours and cosmetics, where complex mixtures occur.

0021-9673/90/$03.50

TABLE I

EXPERIMENTAL RETENTION TEMPERATURES (°C) AND VALUES OBTAINED ACCORDING TO EQN. 2

r (°C/min) is the heating rate T_0 = 80°C.

Solute	*r = 1*		*r = 2*		*r = 3*		*r = 5*		*r = 6*		*r = 8*	
	Exp.	*Calc.*	*Exp.*	*Calc.*	*Exp.*	*Calc.*	*Exp.*	*Calc.*	*Exp.*	*Calc.*	*Exp.*	*Calc.*
n-Hexane	83.4	83.7	86.7	87.1	89.9	90.4	95.3	96.3	98.6	99.2	104.5	104.6
n-Heptane	85.8	85.9	91.2	91.2	96.0	96.0	104.1	104.3	108.8	108.2	116.6	115.2
n-Octane	90.3	90.4	98.6	98.6	105.7	105.5	116.7	116.8	122.5	121.5	132.2	130.0
n-Nonane	97.6	97.7	109.2	109.3	118.4	118.1	132.1	131.6	138.7	137.1	150.0	146.5
n-Decane	107.1	107.7	121.3	122.3	132.6	132.6	148.8	147.6	155.6	153.5	168.3	163.3
n-Undecane	119.3	120.3	135.8	136.8	148.3	148.0	165.5	163.5	172.7	169.6		
n-Dodecane	132.3	133.6	150.7	151.2	163.4	162.6						
Benzene	85.1	85.3	89.2	90.2	94.1	94.6			106.4	106.3		
1-Butanol	85.8	85.8	90.4	90.0	95.4	95.6			108.1	107.6		
2-Pentanone	86.0	86.5	91.5	92.2	96.9	97.3			110.4	110.2		
1-Nitropropane	88.8	89.4	96.3	97.0	103.2	103.5			119.8	119.1		
Pyridine	89.1	89.2	95.7	96.8	102.6	103.3			119.5	119.1		
2-Methyl-2-pentanol	88.3	88.3	95.3	95.2	101.5	101.2			117.2	115.7		
1-Iodobutane	92.4	92.5	102.1	102.0	110.1	109.8			129.4	127.7		
2-Octyne	95.2	95.6	105.1	106.4	114.5	114.8			134.5	133.1		
1,4-Dioxane	86.6	86.8	91.8	92.8	97.6	98.1			111.9	111.5		
cis-Hydrindane	107.2	107.6	122.5	122.8	133.8	133.7			158.5	155.9		

Therefore, the definition of a retention index similar to that of Kováts is required. Several equations have been reported[3–13]; however, none of them has gained universal recognition as in isothermal gas chromatography. This paper shows again the ability of the equation of Curvers *et al.*[14], based on the work of Grant and Hollis[3], to evaluate the retention temperature of a solute. The calculation of a *PTRI* according to the definition of van den Doole and Kratz is considered to be impractical in some instances, and retention indices calculated according to different procedures are reported here in an attempt to establish a method of choice.

EXPERIMENTAL

C_6–C_{12} *n*-alkanes and the ten McReynolds' probes[15] were used as solutes. Chromatograms were obtained on a Perkin-Elmer Sigma 2 gas chromatograph with a 2 m × 1/8 in. O.D. stainless-steel column packed with OV-105 on Chromosorb W and a flame ionization detector was used. The oven temperature was monitored to within ±0.2°C with the aid of a thermocouple. Nitrogen was used as the carrier gas, regulated at 10 ml/min with a mass flow regulator. Calculations were carried out in a CYBER 855 computer. IMSL routines were used when required.

RESULTS AND DISCUSSION

Retention temperatures in programmed-temperature gas chromatography

An interesting problem that has attracted the attention of many workers is to find of a method for evaluating programmed-temperature parameters from readily available isothermal data. Habgood and Harris[16] found the retention temperature by means of the dependence between isothermal and temperature-programmed retention volumes. A modified equation was offered by Grant and Hollis[3]. According to Curvers *et al.*[14], the equation may be written as

$$\int_{T_0}^{T_R} \frac{dT}{t_m(T)\left[1 + \frac{a}{\beta}\exp(\Delta H/RT)\right]} = r \qquad (2)$$

where the T_R of a solute is evaluated as the higher limit of the definite integral; $a = \exp(\Delta S/R)$, a/β and $\Delta H/R$ are entropic and enthalpic parameters, r is the heating rate of the oven and $t_m(T)$ is the time function, usually taken as linear. Other symbols have their usual meanings.

Table I shows the retention temperatures found experimentally and those calculated by eqn. 2 for several heating rates. The reported values are the averages of at least three independent runs. The agreement observed gives support to the use of eqn. 2 for the calculation of retention temperatures in programmed-temperature gas chromatography. At the higher heating rates there is a discrepancy between the experimental and calculated values of T_R probably because the temperatures reported are oven temperatures and the column is colder. Most experiments considered in this paper correspond to an initial column temperature of 80°C. We have carried out experiments at $T_0 = 50$°C and also at higher flow-rates using hydrogen as the carrier gas. The results were similar to those reported.

Retention indices in programmed-temperature gas chromatography

The *PTRI* of a solute is closely related to its retention temperature under given experimental conditions. The first step in establishing a retention index is therefore to determine the retention temperature. The different procedures discussed here used to calculate *PTRI* values follow two different approaches: in the first, the procedures are really methods of calculation of the retention temperatures of the different solutes of the mixture from isothermal data, leaving the determination of the *PTRI* to the application of an equation such as that of van den Doole and Kratz. Sometimes the methods find "equivalent temperatures", which are then used in the *PTRI* calculation. In the second group of procedures, the methods use values of T_R calculated or measured experimentally and apply equations that are different from the linear interpolation mentioned.

Giddings[4] defined an equivalent retention temperature as 0.92 times the experimental T_R. Guiochon[5] proposed for the same purpose subtracting 20°C from the experimental value of T_R. These empirical approaches have been shown to be acceptable. They are not considered in this discussion, however.

Lee and Taylor[6] used as an equivalent temperature (T_{eq}) the harmonic mean of the experimental T_R and the starting temperature of the heating programme T_0. That is,

$$T_{eq} = 2\ T_0 T_R/(T_0 + T_R) \tag{3}$$

Krupčík *et al.*[7] avoided the numerical evaluation of an integral. Their equation thus appears to be more suited to manual calculations:

$$T_{RX} = \frac{[I(T_1) - 100\,Z - T_1(\mathrm{d}I/\mathrm{d}T)](T_{RZ+1} - T_{RZ}) + 100\,T_{RZ}}{100 - (\mathrm{d}I/\mathrm{d}T)(T_{RZ+1} - T_{RZ})} \tag{4}$$

where T_{RX} is the retention temperature of compound X, $I(T_1)$ is the isothermal retention index at temperature T_1, not necessarily the initial temperature, $\mathrm{d}I/\mathrm{d}T$ is the rate of change of the isothermal retention index of the compound *versus* temperature and the other symbols have their usual meanings.

The indices of the ten McReynolds' standards found by the linear interpolation procedure (eqn. 1), using both experimental and calculated retention temperatures, are given in Table II. Values of *PTRI* found with equivalent temperatures obtained by eqn. 3 do not differ from those obtained by the direct use of the experimental T_R, or that calculated with eqn. 2. Values of *PTRI* evaluated using the retention temperatures deduced with the help of eqn. 4 tend to be higher.

As mentioned earlier, other methods do not calculate values of T_R. They are procedures of finding the *PTRI* of a solute under temperature-programmed conditions. Golovnya and Uraletz[8] propose a simple equation:

$$PTRI = I(T_0) + 0.5\,rt_R(\mathrm{d}I/\mathrm{d}T) \tag{5}$$

where $I(T_0)$ is the Kováts' retention index of the solute at the programme starting temperature (T_0) and r is the constant heating rate.

The approach of Erdey *et al.*[9] avoids data related to the *n*-alkanes, as does eqn. 5,

TABLE II

PTRI OF VARIOUS SUBSTANCES OBTAINED BY EQN. 1 USING EXPERIMENTAL AND CALCULATED VALUES OF T_R

Heating rate 3°C/min. T_0 = 80°C.

Solute	*Exp.*	*Calc.*[a]	*Eqn. 3*		*Eqn. 4*	
			Exp.[b]	*Calc.*[c]	*Exp.*[b]	*Calc.*[c]
Benzene	672	673	669	674	682	685
1-Butanol	689	693	690	693	693	695
2-Pentanone	708	714	709	714	714	717
1-Nitropropane	775	779	776	780	784	785
Pyridine	768	777	767	777	785	785
2-Methyl-2-pentanol	756	755	758	755	760	760
1-Iodobutane	835	834	836	835	843	844
2-Octyne	869	874	870	874	875	875
1,4-Dioxane	717	722	718	723	728	728
cis-Hydrindane	1008	1007	1009	1008	1018	1018

[a] T_R values found by eqn. 2.
[b] T_{eq} or T_{RX} calculated with experimental values of T_R.
[c] T_{eq} or T_{RX} calculated with values of T_R obtained by eqn. 2.

and assumes that the temperature dependence of the isothermal retention index is given by an expression such as

$$I(T) = A + \frac{B}{T + C} \tag{6}$$

The coefficients A, B and C are evaluated by obtaining isothermal experimental data at three temperatures (100, 120 and 140°C in our case), and the use of the following expressions:

$$C = \frac{(T_2 - T_1)(I_3T_3 - I_1T_1) + (T_3 - T_1)(I_1T_1 - I_2T_2)}{(T_3 - T_1)(I_2 - I_1) - (T_2 - T_1)(I_3 - I_1)} \tag{7}$$

$$A = \frac{I_3T_3 - I_1T_1 + C(I_3 - I_1)}{(T_3 - T_1)} \tag{8}$$

$$B = I_3T_3 + I_3C - A(T_3 + C) \tag{9}$$

where I_i is the isothermal retention index at the temperature T_i.

The *PTRI* of a solute eluting with a retention temperature T_R in a programme starting at T_0 is calculated as

$$PTRI = A + \frac{B \ln\left(\frac{T_R + C}{T_0 + C}\right)}{T_R - T_0} \tag{10}$$

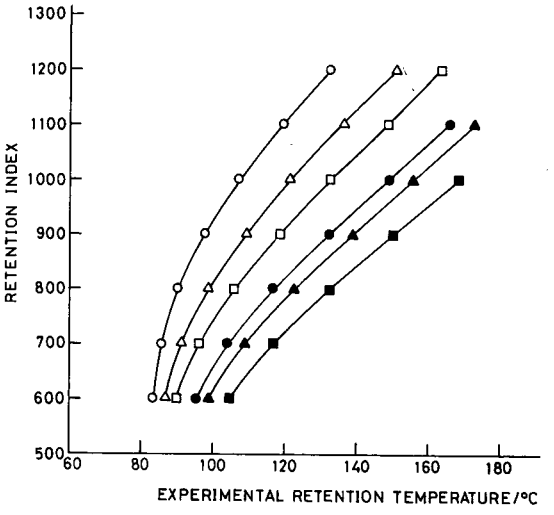

Fig. 1. Plot of retention indices *versus* retention temperatures for various *n*-alkanes at different heating rates (○, 1.0; △, 2.0; □, 3.0; ●, 5.0; ▲, 6.0; ■, 8.0°C/min. Column, OV-105 on Chromosorb W (2 m × $\frac{1}{8}$ in. O.D.). Carrier gas, nitrogen at 10 ml/min. T_0 = 80°C.

Fig. 1 shows a plot of the Kováts retention indices of various *n*-alkanes *versus* the experimental value of T_R obtained at six different heating rates. A clear curvature may be observed at the low values of T_R. As mentioned earlier, the same shapes have been found for plots drawn using values obtained at lower initial column temperatures and also at higher flow-rates, for this and other columns. We used a mass flow regulator for the carrier gas in our experiments. The use of a pressure regulator (capillary gas chromatography) would result in a more pronounced curvature. Other workers[7,8,13,17–20] have reported the same type of curvatures under different chromatographic conditions, or the curves may be deduced from their results. The question now being posed is how the curve joining the points must be drawn. The mathematical answer is that an interpolation procedure should be used. Following these lines, various equations have been proposed.

Zenkevich and Ioffe[10,11] performed a linear logarithmic interpolation between *n*-alkanes of Z and $Z + K$ carbon atoms. The "generalized retention index" (GI_X) of a solute X with a retention time of t'_{RX} is given by

$$GI_X = 100Z + 100K\frac{(t'_{RX} + q\log t'_{RX}) - (t'_{RZ} + q\log t'_{RZ})}{(t'_{RZ+K} + q\log t'_{RZ+K}) - (t'_{RZ} + q\log t'_{RZ})} \tag{11}$$

with

$$q = \frac{(n_2 - n_1)t'_{R1} + (n_3 - n_2)t'_{R3} - (n_3 - n_1)t'_{R2}}{\log(t'^2_{R2}/t'_{R1}t'_{R3})} \tag{12}$$

Where n_1, n_2 and n_3 are the number of carbon atoms of *n*-alkanes 1, 2 and 3 eluting under the same experimental conditions.

TABLE III

RETENTION INDICES OBTAINED BY EQNS. 5[8], 10[9], 11[11] AND 13[12] AND BY THE CUBIC SPLINES METHOD[13]

Temperature programmed from 80 to 180°C at 3°C/min. Retention temperature used were calculated by eqn. 2.

Solute	*Eqn. 5*	*Eqn. 10*	*Eqn. 11*	*Eqn. 13*	*Cubic splines*
Benzene	681	682	680	680	678
1-Butanol	696	701	694	694	694
2-Pentanone	715	715	717	715	719
1-Nitropropane	783	783	783	780	783
Pyridine	781	783	780	778	782
2-Methyl-2-pentanol	760	759	759	761	763
1-Iodobutane	839	837	837	841	835
2-Octyne	877	877	876	874	875
1,4-Dioxane	726	726	727	727	729
cis-Hidrindane	1003	1004	1007	1000	1007

Wang and Sun[12] modified the expression for GI_x:

$$GI_X = 100N + 100 \cdot \frac{(q \ln Y_X + Y_X^B) - (q \ln Y_Z + Y_Z^B}{(q \ln Y_{Z+1} + Y_{Z+1}^B) - (q \ln Y_Z + Y_Z^B)} \qquad (13)$$

with $B > 1$; q is calculated according to eqn. 12. Y_i represents a retention parameter which may be volume or time.

The procedure of Halang *et al.*[13] for assigning the *PTRI* of a solute is based on a direct interpolation through the T_R values of the *n*-alkanes. The interpolation polynomials chosen are cubic splines. A short description of the numerical properties of this kind of polynomial and a computer program were given by Press *et al.*[21], and a broader mathematical treatment of the subject was given by de Boor[22].

Results obtained with eqns. 5, 10, 11 and 13 and the cubic splines method, using the values of T_R deduced with the help of eqn. 2 applied to our experimental isothermal data, are presented in Table III. The differences observed among the various values of the *PTRI* of a substance are now smaller than those which can be deduced from Table II.

Fig. 1 shows that the plots of the retention indices of *n*-alkanes *versus* their T_R are curves for low values of the difference $T_R - T_0$. It seems clear that any deduction of the *PTRI* of a substance eluting between two *n*-alkanes in this region must be carried out bearing in mind the existence of this curvature, and not using the linear interpolation method proposed by van den Doole and Kratz. It is therefore reasonable to consider that the value obtained using the cubic splines procedure is closer to the real *PTRI* of the compound. Unfortunately, unlike the situation with T_R, where calculated values can be compared with experimental results, the *PTRI* of a substance cannot be compared with any standard value. Therefore, direct comparison of the different methods of deducing a *PTRI* is not possible. However, if we accept that the method of Halang *et al.*[13] is a good choice for calculating a *PTRI*, a comparison of the various

TABLE IV

SENSITIVITY TEST: CHANGE IN RETENTION INDEX UNITS PER MINUTE CHANGE IN RETENTION TIME

Temperature programmed from 50 to 180°C at 2°C/min.

Eqn.	*Low-temperature value*	*High-temperature value*
1	20	12
10	0.06	0.1
11	42	5.6
13	55	0.6
Cubic splines	28	13

columns in Table III indicates that the differences are sufficiently small to consider all five methods to be approximately correct. Experimental errors in the determination of Kováts retention indices are frequently as large as those found among the various values corresponding to the same substance in Table III.

From the experimental point of view, those methods which do not require the injection of the *n*-alkanes seem to offer certain advantages. Reality is different however. The methods of Golovnya and Uraletz[8] and Erdey *et al.*[9] do not require the injection of *n*-alkanes with the sample but they are not useful for finding the *PTRI* of an unknown peak in a chromatogram (isothermal retention indices of the substance are needed). The increasing availability of personal computers and microprocessor-controlled chromatographs makes the cubic splines interpolation a useful procedure, as it takes into account automatically the fact that the points defined by the retention indices of the *n*-alkanes do not lie on a straight line.

Sensitivity of the various methods

In order to compare further the different methods discussed, a sensitivity analysis was carried out so that the robustness of the procedures towards small changes in the retention input data could be established. Derivatives of the different equations were evaluated numerically for a temperature programme from 50 to 180°C at 2°C/min. With the equation of Erdey *et al.*[9], benzene was the solute used in the sensitivity test.

Table IV gives the results obtained, presented in the form of the change in retention index units per minute. The sensitivity of an equation based on a linear interpolation is, of course, the slope of the straight line obtained by a least-squares method. It is clear that in this instance the sensitivity remains constant. Fig. 1, however, shows that interpolation between two consecutive *n*-alkanes means that the straight line that should be used depends on the region where the value of T_R lies. The values in Table IV are the two extreme values corresponding to the low- and high-temperature ends of the plot. In all other instances the sensitivity changes more smoothly with retention time. The sensitivity of the cubic splines interpolation becomes close to that of the linear interpolation procedure when retention times increase, in agreement with the fact that the curvature decreases. Van den Doole and Kratz's equation becomes sound for solutes eluting with long retention times.

ACKNOWLEDGEMENTS

The computing facilities provided by the Centro de Cálculo of the Consejo Superior de Investigaciones Científicas are gratefully acknowledged. This work was carried out under Project number PB87-0393 of the Direccción General de Ciencia y Tecnologia (DGCYT).

REFERENCES

1 E. Kováts, *Helv. Chim. Acta*, 41 (1958) 1915.
2 H. van den Doole and P. D. Kratz, *J. Chromatogr.*, 11 (1963) 463.
3 D. W. Grant and M. G. Hollis, *J. Chromatogr.*, 158 (1978) 3.
4 J. C. Giddings, in N. Brenner, J. E. Callen and M. D. Weiss (Editors), *Gas Chromatography*, Academic Press, New York, 1962, p. 57.
5 G. Guiochon, *Anal. Chem.*, 36 (1964) 661.
6 J. Lee and D. R. Taylor, *Chromatographia*, 16 (1982) 286.
7 J. Krupčik, P. Cellar, D. Repka, J. Garaj and G. Guiochon, *J. Chromatogr.*, 351 (1986) 111.
8 R. V. Golovnya and V. P. Uraletz, *J. Chromatogr.*, 36 (1968) 276.
9 L. Erdey, J. Takács and E. Szalánczy, *J. Chromatogr.*, 46 (1970) 29.
10 I. G. Zenkevich, *Zh. Anal. Khim.*, 39 (1984) 1297.
11 I. G. Zenkevich and B. V. Ioffe, *J. Chromatogr.*, 439 (1988) 185.
12 T. Wang and Y. Sun, *J. Chromatogr.*, 390 (1987) 261.
13 W. A. Halang, R. Langlais and E. Kugler, *Anal. Chem.*, 50 (1978) 1829.
14 J. Curvers, J. Rijks, C. Cramers, K. Knaus and P. Larson, *J. High Resolut. Chromatogr. Chromatogr. Commun.*, 8 (1985) 607.
15 W. O. McReynolds, *J. Chromatogr. Sci.*, 8 (1970) 685.
16 H. W. Habgood and W. E. Harris, *Anal. Chem.*, 32 (1960) 450.
17 G. Janssens, *Anal. Chim. Acta*, 95 (1977) 153.
18 P. Kusz and W. Czelakowski, *Int. Lab.*, (1987) 92.
19 J. Krupčik, D. Repka, E. Benická, T. Hevesi, J. Nolte, B. Paschold and H. Mayer, *J. Chromatogr.*, 448 (1988) 203.
20 E. E. Akporhonor, S. Le Vent and D. R. Taylor, *J. Chromatogr.*, 463 (1989) 271.
21 W. H. Press, B. P. Flannery, S. A. Tenkolsky and W. T. Vetterling, *Numerical Recipes*, Cambridge University Press, Cambridge, 1986, p. 77.
22 C. de Boor, *A Practical Guide to Splines*, Springer, New York, Heidelberg, Berlin, 1978.

Journal of Chromatography, 498 (1990) 11–24
Elsevier Science Publishers B.V., Amsterdam — Printed in The Netherlands

CHROM. 22 017

INVESTIGATION INTO THE FACTORS AFFECTING PERFORMANCE IN THE DETERMINATION OF POLYCYCLIC AROMATIC HYDROCARBONS USING CAPILLARY GAS CHROMATOGRAPHY–MASS SPECTROMETRY WITH SPLITLESS INJECTION

IAN D. BRINDLE* and XING-FANG LI
Chemistry Department, Brock University, St. Catharines, Ontario L2S 3A1 (Canada)
(First received July 4th, 1989; revised manuscript received September 21st, 1989)

SUMMARY

The importance of solvent choice and temperature program for the separation and quantification of sixteen polycyclic aromatic hydrocarbons (PAHs), considered as priority pollutants, was investigated. For the eight late-eluting PAHs, higher boiling solvents, such as toluene and the xylenes, gave enhanced signals that were between 1 and 100 times greater than those from splitless injections in solvents such as dichloromethane, hexane, acetonitrile, benzene and isooctane. The results indicate that the greatest enhancement can be found by choosing a proper solvent for a specific range of PAHs coupled with an appropriate initial column temperature. Further studies of other parameters were accomplished with toluene as solvent. Simplex optimization of the injection temperature and the initial column temperature gave 260 and 120°C, respectively, as the optima. These optimum conditions also improved the peak shape and resolution. The dependence of the initial column temperature on solvent is discussed with respect of sensitivity and resolution. Detection limits (signal-to-noise ratio = 3) range from 2.4 pg for naphthalene to 86 pg for benzo-[*ghi*]perylene. Relative standard deviations of seven replicate determinations of a 3-ng injection ranged from 2.2 to 10.5% when measured by peak area and from 3.9 to 11.0% when measured by peak height. The studies further illustrate that the sensitivity of late-eluting PAHs can be further improved when xylenes are used as solvents.

INTRODUCTION

Polycyclic aromatic hydrocarbons (PAHs) have been shown to contain several potent carcinogens. One of them (benzo[*a*]pyrene) was identified as the causative agent of scrotal cancer among English chimney sweeps in the eighteenth century[1], the first reported case of occupational carcinogenesis. PAHs are emitted from a wide range of activities such as coal burning, coking operations, household fireplaces, automobiles and cigarette smoking[2]. These activities have resulted in the discovery of PAHs in natural waters, sediment, air and the fatty tissue of exposed animals. The occurrence and potential hazards of this class of compounds have stimulated developments in analytical methods for PAHs, their nitration products and their metabolites[3,4].

0021-9673/90/$03.50

High-performance liquid chromatography (HPLC) and gas chromatography (GC) have usually been considered as most sensitive techniques for the determination of PAHs. Reversed-phase HPLC on C_{18} columns with fluorescence detection has been developed over the last decade. This technique offers both low cost and high sensitivity, but usually requires the collection of fractions composed of isomers or small number of PAHs, before the PAHs can be separated[5–8]. Gas chromatography–mass spectrometry (GC–MS) has the advantage of providing comprehensive information that allows qualitative identification and quantification of the analyte of interest. It also separates a wide range of PAHs in a single run. However, it appears to give relatively poor signals for late-eluting PAH peaks[9].

One way to improve the sensitivity and separation of PAHs by GC is to search for the optimum conditions for the determination. One of the most important factors, the solvent effect, was described by Grob and Grob[10,11] when the analytes such as *n*-heptane, *n*-octane and *n*-nonane were introduced by splitless injection. Cold trapping was originally described as the mechanism operating in the splitless injection mode. Further work[11,12] led to a description of the solvent effect, which is now considered to be an important mechanism for both splitless injection and on-column injection. Grob and Grob's work[12] also suggested that the solvent effect was controlled by four independent factors: column temperature, volatility of the solvent, amount of solvent and injection time. Based on Grob and Grob's studies, Jennings *et al.*[13] described the theoretical basis of the solvent effect. Cold trapping and the solvent effect were described as the two functions that led to the reconcentration of eluates on the top of the column.

The effect of solvent on the response factors of PAHs was recently reported by Lee *et al.*[14]. Their work indicated that different solvents can change drastically the response of an analyte under the same GC conditions. Hence, they suggested that there should be consistency in the solvent used for standards and samples in capillary GC. They used the same conditions of analysis to show the effect so that the other factors, *e.g.*, the relationship between the boiling point of the solvent and the GC conditions, such as injector temperature and oven program, were not investigated.

To achieve the best separation and the highest sensitivity in the determination of PAHs, especially the late-eluting PAHs, by capillary GC, it was felt necessary to study the effect of solvent, the relationship between the boiling point of the solvent and the optimum initial temperature of the column and other factors that might affect the performance in the determination of PAHs by GC–MS.

EXPERIMENTAL

A Hewlett-Packard Model 5890 gas chromatograph equipped with a Model 5970 mass spectrometer, Model 7673A autosampler and Model 300 computer system was used for all determinations. A Hewlett-Packard Ultra 1 (25 m × 0.2 mm I.D., film thickness 0.33 μm) fused-silica capillary column coated with cross-linked methylsilicone gum as the stationary phase was used with splitless injection. Temperature program I in Table I was used to obtain the results in Table II and Fig. 1. With a number of optimization experiments temperature program II in Table I was used for the remainder of the experiments except that initial temperature was changed (see Results and Discussion). Helium (Linde "Zero gas") was used as the carrier gas at

TABLE I
TEMPERATURE PROGRAMS

Program No.[a]	*Level*	*Initial temperature (°C)*	*Initial time (min)*	*Rate (°C/min)*	*Final temperature (°C)*	*Final time (min)*
I	1	100	1	20.0	150	1.5
	2			30.0	200	4.0
	3			30.0	220	4.0
	4			30.0	250	0.2
	5			1.0	263	2.0
	6			50.0	270	0.0
	7			1.0	280	0.0
II	1	120	8	20.0	150	0.0
	2			5.0	187	0.0
	3			30.0	220	0.0
	4			20.0	260	25

[a] Injection port temperature, 250°C; transfer-line temperature, (I) 250°C; (II) 260°C.

a flow-rate of 0.8 ml min^{-1} at ambient temperature. Sample solution (3 μl) was injected onto the column by using the autosampler with a fast injection speed. Peak area and height were integrated by using the computer program.

A commercially available solution of a mixture of sixteen PAHs [2000 μg ml^{-1} of each PAH in dichloromethane–benzene (50:50)] was obtained from Supelco (Oakville, Canada). This standard was dissolved in benzene to give a stock solution containing 40 μg ml^{-1} of each PAH, and 2 μg ml^{-1} solutions of PAHs in different solvents were prepared by dilution of appropriate volumes of this stock solution. All the solvents were of HPLC grade.

RESULTS AND DISCUSSION

Effect of solvent

The sixteen PAHs available commercially represented a reasonably wide range of compounds from the list of priority pollutants. They are listed in Table II with their boiling points. The order of the list in Table II also corresponds to the order in which the PAHs are eluted from the capillary GC column.

Several solvents with different boiling points and different polarities were used to investigate the effect of solvent on the determination of PAHs by GC–MS. In an initial trial, the seven solvents with the lowest boiling points, listed in Table II, were chosen as solvents for the injection of the PAHs. Each of these solvents was used separately to prepare a standard solution containing 2 μg ml^{-1} of each of the sixteen PAHs. An aliquot of 3 μl of this solution was then introduced into the capillary GC column by splitless injection. Both the peak area and peak height of each PAH were determined from the total ion current (TIC) chromatogram with selected ion monitoring. For comparison, the peak areas and peak heights of all PAH peaks, with all seven solvents, were normalized, based on the results obtained with toluene as the solvent. The relative peak areas and peak heights are given in Table II. The peak areas generally increase with increasing boiling point of the solvent, except for the first five peaks in isooctane.

TABLE II

RELATIVE PEAK AREAS AND PEAK HEIGHTS (%) OF PAHs IN DIFFERENT SOLVENTS

Conditions: temperature program I (Table I) and injection volume 3 μl.

Component	*B.p. (°C)*	*Peak No.*	*Parameter*	*Solvent*[a]						
				Dichloromethane (9.080, 40°C)	*Hexane (1.890, 68°C)*	*Benzene (2.284, 80.1°C)*	*Cyclohexane (2.023, 80.7°C)*	*Acetonitrile (38.8, 81.6°C)*	*Isooctane (1.940, 99.2°C)*	*Toluene (2.379, 110.6°C)*
Naphthalene	218	1	Relative peak area	84	89	79	81	64	118	100
Acenaphthylene	270	2		77	84	75	78	63	118	100
Acenaphthene	274	3		77	83	75	76	63	115	100
Fluorene	294	4		69	77	71	72	61	111	100
Phenanthrene	338	5		55	67	62	63	53	112	100
Anthracene	340	6		61	78	73	72	61	99	100
Fluoranthene	383	7		44	63	59	63	54	97	100
Pyrene	393	8		42	61	57	60	53	94	100
Benzo[*a*]anthracene	431	9		15	30	33	35	33	60	100
Chrysene	414	10		24	65	50	52	49	69	100
Benzo[*b*]fluoranthene	481	11		6	17	20	21	25	37	100
Benzo[*k*]fluoranthene	481	12		11	26	31	32	36	47	100
Benzo[*a*]pyrene	496	13		5	17	21	21	27	35	100
Indeno[1,2,3-*cd*]pyrene	–	14		21	6	9	7	14	16	100

Dibenz[*a,h*]anthracene	–	15		0(nd)[a]	6	11	8	14	16	100
Benzo[*ghi*]perylene	–	16		1	8	12	9	17	17	100
Naphthalene	218	1	Relative peak height	18	23	37	35	19	103	100
Acenaphthylene	270	2		56	75	79	79	54	84	100
Acenaphthene	274	3		65	82	86	87	61	87	100
Fluorene	294	4		85	106	108	107	84	107	100
Phenanthrene	338	5		92	115	107	110	92	119	100
Anthracene	340	6		85	107	109	108	91	113	100
Fluoranthene	383	7		65	95	89	96	82	111	100
Pyrene	393	8		61	91	85	87	78	106	100
Benzo[*a*]anthracene	431	9		20	42	45	48	45	69	100
Chrysene	414	10		23	50	52	55	50	73	100
Benzo[*b*]fluoranthene	481	11		7	23	26	27	33	45	100
Benzo[*k*]fluoranthene	481	12		8	23	27	29	32	44	100
Benzo[*a*]pyrene	496	13		5	17	27	21	27	37	100
Indeno[1,2,3-*cd*]pyrene	–	14		1	5	9	6	14	16	100
Dibenz[*ah*]anthracene	–	15		0	4	8	6	11	13	100
Benzo[*ghi*]perylene	–	16		1	7	11	8	16	17	100

[a] With dielectric constants and boiling points in parentheses.
[b] Not detected.

TABLE III
RELATIVE PEAK HEIGHTS (%) ON TIC CHROMATOGRAMS OF PAHs
Conditions: temperature program II (Table I) and injection volume 3 μl.

Peak No.[a]	*Solvent*[b]			
	Benzene (2.284, 80.1°C)	*Toluene (2.379, 110.6°C)*	*p-Xylene (2.270, 138°C)*	*o-Xylene (2.568, 144°C)*
1	37	100	94	109
2	60	100	142	167
3	40	100	138	157
4	45	100	92	61
5	38	100	52	65
6	54	100	50	45
7	55	100	49	49
8	55	100	59	53
9	45	100	91	92
10	46	100	71	70
11	70	100	117	109
12	66	100	99	96
13	41	100	112	107
14	24	100	147	120
15	21	100	162	134
16	27	100	143	118

[a] As in Table II.
[b] With dielectic constants and boiling points in parentheses.

The late-eluting peaks from the toluene solution are much larger than those from all the other solvents, which suggests that toluene is much more efficient in transferring the higher molecular weight PAHs onto the column. The peaks from fluorene, phenanthrene, anthracene, fluoranthene and pyrene in low-boiling solvents are more comparable in height with similar peaks from the toluene solutions.

In order to confirm the importance of the boiling point of the solvent on the determination of PAHs by GC–MS, benzene, toluene, *o*-xylene and *p*-xylene, which have similar polarities, with dielectric constants of 2.284, 2.379, 2.568 and 2.270, respectively, but different boiling points, were used as solvents. The TIC chromatograms of PAHs in these four solvents were obtained, under similar conditions, as discussed above, except that the initial temperature was increased from 100 to 120°C. The peak height of each PAH, relative to that of the same PAH in toluene as 100%, are given in Table III. Despite their similar polarities, these solvents caused significant differences in the signals from the PAHs, probably owing to the difference in their volatilities. Again, the greater the difference in boiling point between these solvents, the greater is the difference in relative peak height. Similar observations were made by Lee *et al.*[14], solvents with similar polarity, such as acetonitrile and methanol, giving significantly different responses. This also suggests that this difference in behaviour might be due to the difference in the boiling points of these two solvents.

Determinations of the same amount of PAHs in benzene and toluene as solvents gave the chromatograms shown in Fig. 1 when the initial temperature was 100°C. Comparing Fig. 1a and b, the enhancement of the chromatographic signals when the

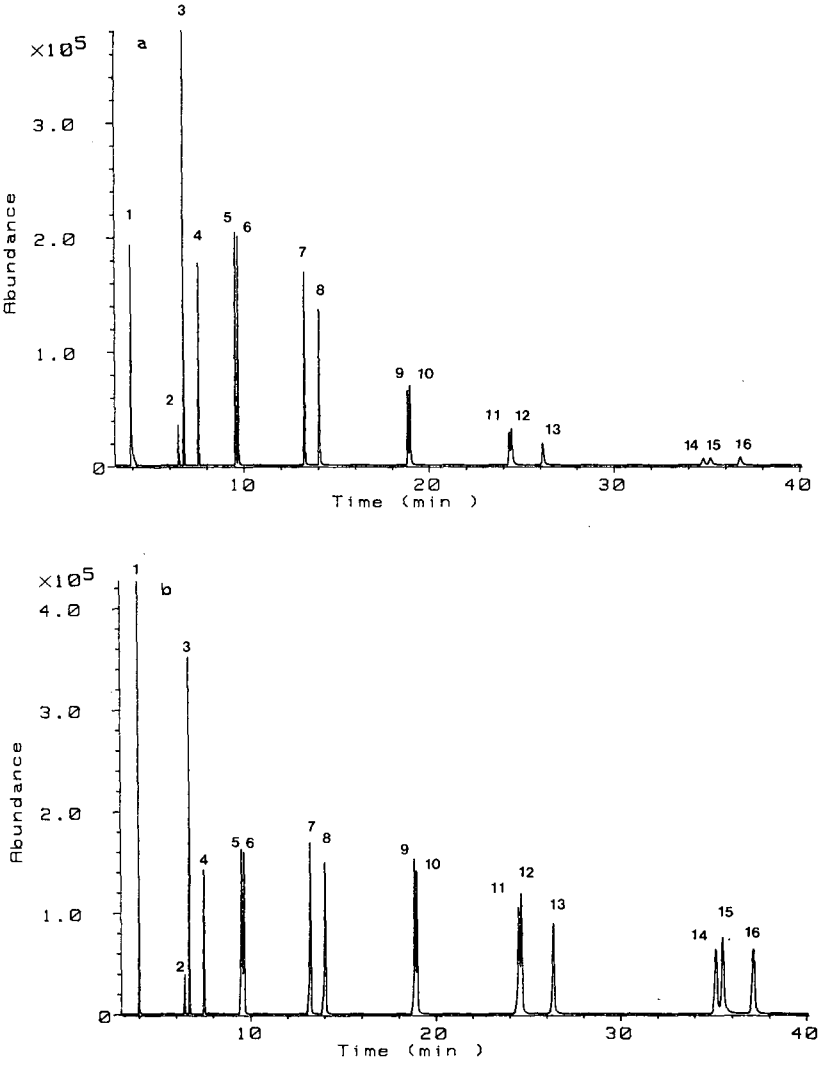

Fig. 1. Chromatograms of the sixteen PAHs: 3 μl of 2 μg ml^{-1} solutions in (a) benzene and (b) toluene. Peak numbering as in Table II.

solvent is toluene can be clearly seen, especially the dramatic enhancement of the late-eluting peaks. The enhancing effect of the higher boiling solvent on the TIC signal can be interpreted as reconcentration of PAHs by the solvent effect. In Grob and Grob's model of the solvent effect[12], the vaporized material is transferred onto the column essentially as a mixture. In the first stage of separation on the column, the solvent shifts away from the sample components and the relatively wider band of solvent blocks the expansion of the vapors of the solutes so that the solutes are reconcentrated in a narrow band. This effect appears to become more pronounced as

the boiling point of the solvent increases. Thus the responses of the solutes are greater from toluene than from benzene solutions.

The solvent itself would not be expected to change the ionization process in mass spectrometric detector as the solutes and solvent will be separated in time. This, was confirmed by the observations that the ratio $[M+1]^+/M^+$ for each PAH was independent of the solvent. If the solvent participated in the process of ionization of the PAH, the abundance of $[M+1]^+$ would be changed owing to chemical ionization in addition to electron-impact ionization.

Effect of initial temperature

Column temperature and temperature programming were found to affect the resolution and sensitivity of the mixture of PAHs. The temperature program mentioned under Experimental was found to be optimum for the determination of PAHs in toluene solution with regard to both resolution and sensitivity. This temperature program was also appropriate when PAHs were dissolved in other solvents, except that the initial temperature was changed. The effect of the initial temperature on the determination of PAHs was found to be more significant than the temperatures during the later stages. Therefore, studies on the effect of initial

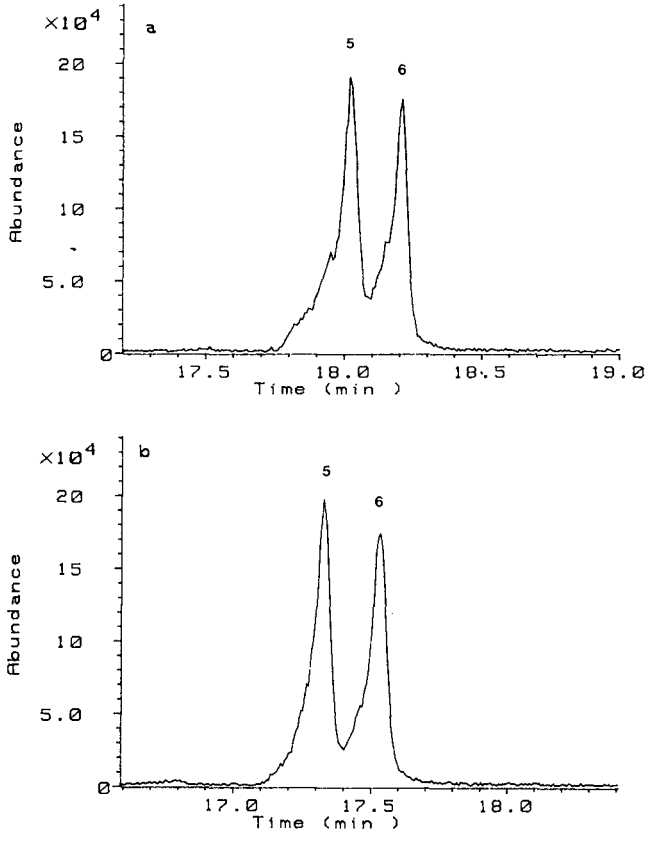

Fig. 2.

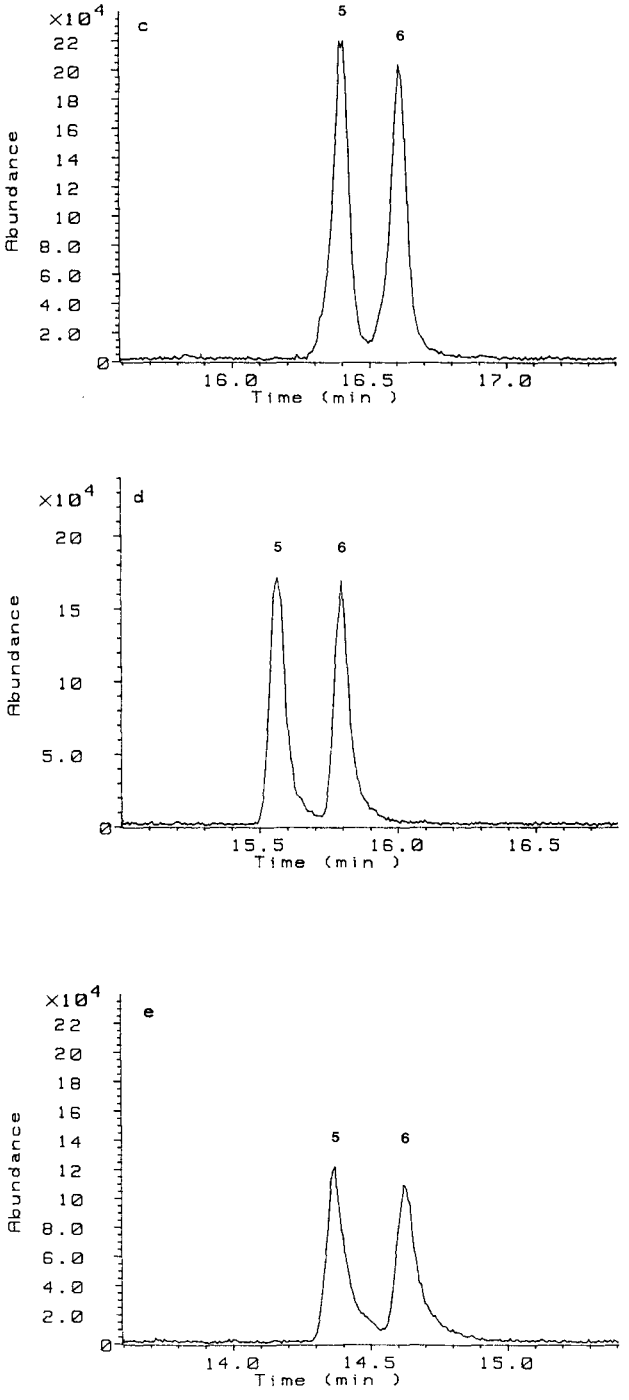

Fig. 2. Effect of initial temperature on peak shape of (5) phenanthrene and (6) anthracene: (a) 100; (b) 110; (c) 120; (d) 130; (e) 140°C.

temperature were carried out while the remainder of the temperature program was kept unchanged.

The effect of initial temperature on peak resolution and peak shape is clearly demonstrated in Fig. 2, which compares chromatograms of phenanthrene and anthracene in toluene at initial temperatures of (a) 100, (b) 110, (c) 120 (d) 130 and (e) 140°C. At the lowest initial temperature, fronting of the peak appeared (Fig. 2a). With increase in the initial temperature from 100 to 120°C, the fronting of the peaks gradually disappeared, and a symmetrical peak was obtained when the initial temperature was 120°C (Fig. 2c). With a further increase in initial temperature from 120 to 140°C, tailing of the peaks occurred, leaving asymmetric peaks (Fig. 2e). Similar results were obtained using other solvents. Fronting appeared at initial temperatures lower than the boiling point of the solvent; tailing appeared at initial temperatures higher than 20°C above the boiling point of the solvent. This effect is more significant for the eight early-eluting peaks than for the late-eluting peaks.

In order to determine the effect of initial temperature on peak height and area, aliquots of 3 μl of 2 μg ml^{-1} PAH solutions in benzene, toluene, *o*-xylene and *p*-xylene were injected sequentially. At different initial temperatures varying within 10–20°C above and below the boiling point of the solvent, TIC chromatograms of the sixteen PAHs were obtained. Peak heights and peak areas were determined, and the relative peak height and area of each PAH were then calculated and compared with those determined at 10°C above the boiling point of the solvent. The results are summarized in Table IV. The optimum initial temperature depends on the solvent used; at an initial temperature between the boiling point of the solvent and 10–20°C higher than the boiling point, the highest response, measured by peak area and peak height, was achieved. The results in Table IV indicate that the solvent with the lowest boiling point (*i.e.*, benzene, 80°C) showed the smallest range of optimum initial temperature. If a higher boiling (*e.g.*, xylene) was used, the changes in response of the PAHs were small within a relatively wider initial temperature range. Hence the most symmetrical peaks with the highest responses were achieved by using an initial temperature 10–20°C above the boiling point of the solvent used. The data in Table V are based on these conditions. Initial temperatures of 90 and 120°C are optimum for benzene and toluene as solvents, respectively. The peak area and peak height of the PAHs in Table V show that toluene gives a higher sensitivity than benzene.

While other parameters were kept constant and the initial time was varied from 2 to 10 min, a series of determinations of the PAHs in toluene and *p*-xylene were carried out. The effect of the length of time at the initial column temperature is not as significant as the initial temperature itself. Resolutions of peaks 5 and 6, 9 and 10, 11 and 12, and 14 and 15, at different initial times, were not obviously changed. The relatively better resolution between the closest pairs of peaks and sensitivity for the sixteen PAHs were achieved with an initial time of 8 min for toluene and 4 min for *p*-xylene. When a higher boiling solvent was used, a different initial temperature was necessary for optimum sensitivity and resolution. Thus, for *p*-xylene the initial temperature was 148°C and the initial time was kept at 4 min.

Other factors

The injection port temperature directly affects the efficiency of sample vaporization, and therefore also affects the sensitivity of determination. As the

TABLE IV

RELATIVE PEAK AREAS AND HEIGHTS (%) OF PAHs IN AROMATIC SOLVENTS AT DIFFERENT INITIAL COLUMN TEMPERATURES

Conditions: temperature program II (Table I) and injection volume 3 μl.

Peak No.[a]	*Parameter*	*Benzene (80°C)*[b]			*Toluene (110.6°C)*[b]					*p-Xylene (138°C)*[b]			*o-Xylene (144°C)*[b]			
		80°C	*90°C*	*100°C*	*100°C*	*110°C*	*120°C*	*130°C*	*140°C*	*128°C*	*138°C*	*148°C*	*158°C*	*144°C*	*154°C*	*164°C*
1	Relative	167	100	54	92	113	100	88	75	–	–	–	–	–	–	–
2	peak area	142	100	72	81	108	100	89	81	113	120	100	89	18	100	–
3		147	100	73	83	114	100	114	83	106	112	100	85	113	100	–
4		135	100	78	88	111	100	121	84	108	111	100	85	116	100	87
5		138	100	71	90	111	100	113	72	104	113	100	97	109	100	80
6		134	100	74	78	106	100	108	75	105	111	100	94	108	100	78
7		136	100	74	85	106	100	114	75	107	108	100	98	104	100	86
8		126	100	72	87	107	100	112	75	102	105	100	96	102	100	85
9		127	100	70	104	112	100	113	73	120	115	100	140	98	100	77
10		121	100	70	85	103	100	109	78	91	96	100	101	123	100	96
11		126	100	65	100	104	100	115	87	110	112	100	97	106	100	78
12		120	100	70	95	101	100	101	86	96	94	100	100	125	100	93
13		111	100	71	100	112	100	111	70	101	101	100	99	112	100	84
14		118	100	71	94	101	100	120	63	104	105	100	108	118	100	75
15		122	100	67	92	102	100	120	54	101	109	100	106	118	100	78
16		114	100	50	111	126	100	120	92	98	105	100	102	125	100	84
1	Relative	114	100	68	64	88	100	48	15	–	–	–	–	–	–	–
2	peak height	106	100	76	98	109	100	50	32	86	98	100	68	77	100	–
3		108	100	80	94	98	100	71	33	113	90	100	73	86	100	–
4		104	100	74	90	95	100	80	42	138	125	100	83	101	100	99
5		109	100	67	89	93	100	79	56	67	88	100	67	161	100	98
6		106	100	68	90	91	100	85	56	67	88	100	67	113	100	100
7		108	100	75	81	96	100	83	59	73	84	100	82	136	100	111
8		110	100	78	76	90	100	79	63	64	76	100	82	129	100	114
9		113	100	71	87	104	100	79	70	96	95	100	99	115	100	96
10		116	100	71	79	97	100	82	71	85	87	100	100	156	100	100
11		121	100	70	95	103	100	88	83	102	101	100	100	114	100	86
12		118	100	66	86	96	100	88	79	91	100	100	97	128	100	94
13		113	100	60	91	109	100	81	75	99	95	100	95	122	100	92
14		117	100	51	100	108	100	74	66	101	102	100	107	126	100	88
15		115	100	54	88	100	100	74	66	100	103	100	100	116	100	77
16		116	100	60	94	104	100	80	96	98	97	100	100	78	100	90

[a] As in Table II.

[b] Boiling point.

TABLE V
RELATIVE PEAK AREAS AND HEIGHTS (%)
Conditions: temperature program II (Table I) and injection volume 3 μl.

Peak No.[a]	*Relative peak area*		*Relative peak height*	
	Benzene (90°C)[b]	*Toluene (120°C)*[b]	*Benzene (90°C)*	*Toluene (120°C)*
1	76	100	59	100
2	66	100	107	100
3	67	100	120	100
4	65	100	125	100
5	67	100	111	100
6	63	100	99	100
7	61	100	71	100
8	60	100	73	100
9	45	100	48	100
10	49	100	51	100
11	37	100	39	100
12	37	100	37	100
13	33	100	34	100
14	24	100	25	100
15	22	100	22	100
16	24	100	24	100

[a] As in Table II.
[b] Initial column temperature.

injection port temperature was increased from 200 to 250°C, the peak areas of most of the sixteen PAHs gradually increased, reaching a maximum at 250°C and remaining similar between 250 and 260°C. When the injection port temperature was increased further to 270 and 280°C, a decrease in peak area was observed. A similar effect was also obtained for peak heights.

To obtain optimum conditions for both injection port temperature and initial temperature in the determination of PAHs, a simplex optimization method was applied to optimize these two factors. The mean value of the heights of all sixteen individual PAH peaks on the TIC chromatogram was used as the response as all the peaks changed in a similar fashion. Toluene was used to prepare standard solutions. Both factors were varied at the same time, regulated by the simplex optimization method. A full simplex optimization was accomplished with nine experimental units. The results indicate that the highest response for the sixteen PAHs was obtained under the optimum conditions of an injection port temperature of 260°C and an initial column temperature of 120°C.

The temperature of the interface (*i.e.*, transfer line) between the GC column and the mass spectrometer is also a factor that could influence sensitivity. It was found that a relatively high temperature of the interface is needed in order to achieve the highest sensitivity. An interface temperature of 260°C was chosen as it gave sufficient sensitivity and was the highest temperature in the temperature program and reasonably below the limiting temperature (300°C, suggested by the manufacturer). Although the sensitivity of PAHs depended on the interface temperature, the

TABLE VI
DETECTION LIMITS OF PAHs IN TOLUENE AND *p*-XYLENE
Conditions: temperature program II (Table I) and injection volume 3 μl.

Peak No.[a]	*Detection limit (3σ) (pg)*	
	Toluene (120°C)[b]	*p-Xylene (148°C)*[b]
1	2.4	4.4
2	10.5	7.5
3	8.7	8.0
4	24.6	8.8
5	27.0	3.0
6	49.2	3.0
7	16.8	2.7
8	13.5	2.8
9	34.5	4.4
10	17.4	4.1
11	33.3	11.7
12	28.2	10.7
13	94.7	17.1
14	69.0	43.6
15	85.8	43.6
16	62.1	30.8

[a] As in Table II.
[b] Initial column temperature.

resolution of peaks was not affected appreciably by this factor within the range of temperatures used. Also, the length of the interface (20 cm) is very short compared with the 25-m length of the capillary column, and would not be expected to have a significant effect on resolution.

Analytical figures

Calibrations for the sixteen PAHs in toluene were carried out under the optimum conditions, as discussed above, for PAH concentrations in the range 0.02–6 μg ml^{-1}. Both peak area and peak height were used as response. The correlation coefficients of the calibration graphs in the concentration range 0.20–6.0 μg ml^{-1} were better than 0.97 for all sixteen PAHs.

Seven replicate determinations of 3 ng (3 μl of 1 μg ml^{-1} solution) of each of the sixteen PAHs in toluene were carried out under the optimum conditions in order to determine the precision. Relative standard deviations (R.S.D.s) in the range 3.9–11.0% based on peak height, and 2.2–10.5% based on peak area were obtained for the sixteen PAHs. Nine replicate determinations of 3 ng of the sixteen PAHs gave R.S.D.s for the retention time of 0.45% for naphthalene and less than 0.1% for the other fifteen PAHs.

The detection limits (signal-to-noise ratio = 3) for the determination of the sixteen PAHs by GC–MS were at low picogram levels, as shown in Table VI, ranging from 2.4 pg for naphthalene to 94.7 pg for benzo[*a*]pyrene when determinations were made in toluene and from 4.4 pg for naphthalene to 30.8 pg for benzo[*a*]pyrene for determinations in *p*-xylene.

CONCLUSIONS

When toluene and xylenes are used as solvents to prepare solutions of PAHs for injection into the GC–MS column, enhancement of signals can be obtained. The optimum initial temperature is based on the boiling point of the solvent. The results could be applied to the determination of PAHs in environmental samples.

ACKNOWLEDGEMENT

The authors thank the Ontario Ministry of the Environment for funding this research (project 357G) and for funding the purchase of the Hewlett-Packard GC–MS system.

REFERENCES

1 P. Pott, 1775, quoted by A. Bjørseth and T. Ramdahl, in A. Bjørseth and T. Ramdahl (Editors), *Handbook of Polycyclic Aromatic Hydrocarbons, Vol. 2, Emission Sources and Recent Progress in Analytical Chemistry,* Marcel Dekker, New York, 1985, p. 1.
2 K. D. Bartle, M. L. Lee and S. A. Wise, *Chem. Soc. Rev.*, 10 (1981) 113.
3 M. L. Lee, M. V. Novotny and K. D. Bartle, *Analytical Chemistry of Polycyclic Aromatic Compounds,* Academic Press, New York, 1981, pp. 50–73.
4 K. D. Bartle, in A. Bjørseth and T. Ramdahl (Editors), *Handbook of Polycyclic Aromatic Hydrocarbons, Vol. 2, Emission Sources and Recent Progress in Analytical Chemistry,* Marcel Dekker, New York, 1985, p. 193.
5 M. V. Novotny, L. Lee and K. D. Bartle, *J. Chromatogr. Sci.*, 12 (1974) 606–607.
6 M. J. Dennis, R. C. Massey and D. J. McWeeny, *J. Chromatogr.*, 285 (1984) 127–133.
7 P. G. Sim, R. K. Boyd, R. M. Gershey, R. Guevremeont, W. D. Jamieson, M. A. Quilliam and R. J. Gergely, *Biomed. Environ. Mass Spectrom.*, 14 (1987) 357–381.
8 S. A. Wise, B. A. Benner, G. D. Byrd, S. N. Chesler, R. E. Rebbert and M. M. Schantz, *Anal. Chem.*, 60 (1988) 887–894.
9 H. G. Nowicki, C. A. Kieda and D. O. Bassett, in A. Bjørseth and A. J. Dennis (Editors), *Polynuclear Aromatic Hydrocarbons: Chemical and Biological Effects*, Battelle Press, Columbus, OH, 1980, pp. 75–87.
10 K. Grob and K. Grob, Jr., *J. Chromatogr. Sci.*, 7 (1969) 584–591.
11 K. Grob and K. Grob, Jr., *J. Chromatogr.*, 94 (1974) 53–64.
12 K. Grob and K. Grob, Jr., *J. High Resolut. Chromatogr. Chromatogr. Commun.*, 1 (1978) 57–64.
13 W. G. Jennings, R. R. Freemann and T. A. Rooney, *J. High Resolut. Chromatogr. Chromatogr. Commun.*, 1 (1978) 275–276.
14 H.-B. Lee, R. Szawiola and A. S. Y. Chau, *J. Assoc. Off. Anal. Chem.*, 70 (1987) 929–930.

Journal of Chromatography, 498 (1990) 25–33
Elsevier Science Publishers B.V., Amsterdam — Printed in The Netherlands

CHROM. 21 977

SEPARATION AND IDENTIFICATION OF MONOMETHYLATED POLYCYCLIC AROMATIC HYDROCARBONS IN HEAVY OIL

SADAO MATSUZAWA*
National Research Institute for Pollution and Resources, 16-3, Onogawa, Tsukuba, Ibaraki 305 (Japan)
PHILIPPE GARRIGUES
UA 348 CNRS Université de Bordeaux I, 33405 Talence Cedex (France)
and
OSAMU SETOKUCHI, MASARU SATO, TADATO YAMAMOTO, YUKIO SHIMIZU and MITSUHISA TAMURA
National Research Institute for Pollution and Resources, 16-3, Onogawa, Tsukuba, Ibaraki 305 (Japan)
(First received May 19th, 1989; revised manuscript received August 28th, 1989)

SUMMARY

The application of high-performance liquid chromatographic fractionation using a column-switching technique to the identification of monomethylated polycyclic aromatic hydrocarbons by capillary gas chromatography and high-resolution (Shpol'skii effect) fluorescence spectroscopy is described. The column-switching technique with silica and aminosilane columns permitted the rapid fractionation of both aromatics and each aromatic ring type in heavy oils. The existence of methylphenanthrenes, methylchrysenes and methylbenz[*a*]anthracenes in Kuwait 340–500°C distillate was confirmed by the two methods.

INTRODUCTION

The determination of polycyclic aromatic hydrocarbons (PAHs) in oils, sediments and particulate extracts has attracted considerable attention for many years, because these compounds show biological activity[1,2]. For example, monomethylated PAHs are of particular interest because of their potential carcinogenic and mutagenic activities[1,2]. Therefore, various methods for quantitative and qualitative analysis of samples for PAHs have been reported[3–13].

In the determination of PAHs in oil, the usual method includes the separation of aliphatics and polar compounds from aromatics by open-column chromatography to concentrate the PAHs[3–5], then the resulting aromatics are separated into individual PAHs by capillary gas chromatography or fractionated into each aromatic ring type by high-performance liquid chromatography (HPLC) for the subsequent instrumental analysis. The time required for these methods is generally long because of the use of open-column chromatography.

In this paper, we report the application of HPLC fractionation using a column-

0021-9673/90/$03.50

switching technique to the identification of monomethylated PAHs by capillary gas chromatography and high-resolution (Shpol'skii effect) fluorescence spectroscopy. The column-switching technique permits the rapid fractionation of both aromatics and each aromatic ring type in heavy oils.

EXPERIMENTAL

Apparatus

A Model Trirotar-III liquid chromatograph (JASCO) was used with a Model R-401 refractive index (RI) detector (Waters Assoc.) and a Shimazu SPD-1 UV–visible spectrophotometric detector. Sample solution (20 μl) was injected with a Model 7120 injector (Rheodyne). Column switching was performed with two high-pressure valves. Chromatograms with the RI and UV detectors were recorded on a Model VP-6621A recorder (Matsushita Electric). Nucleosil 50-5 (300 × 4 mm I.D.) and μBondapak-NH_2 (300 × 4 mm I.D.) separation columns were used. The configuration of the system and three flow modes for the column-switching technique are presented in Fig. 1. A sample is first separated into saturates (S) and aromatics (Total A) on the silica column in flow mode I, then aromatics are backflushed and further separated into monoaromatics (1A), diaromatics (2A) and polycyclic aromatic hydrocarbons (PAHs) on the aminosilane column in flow mode II. Flow mode III is used for the direct elution of aromatics.

A Model G3000 gas chromatograph (Hitachi), equipped with a flame ionization detector and a splitless injector, was used for separating aromatics obtained by HPLC (in flow mode III). Separation was performed with an SPD-5 fused-silica

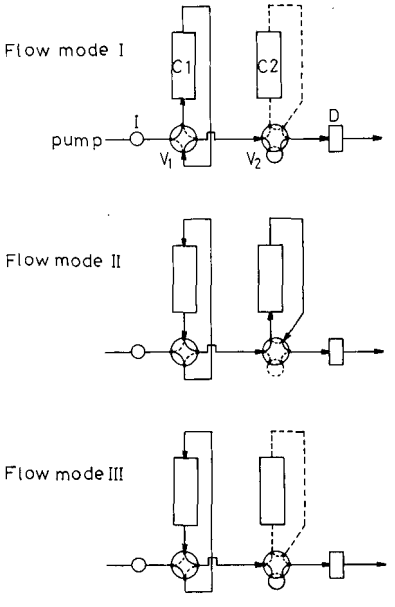

Fig. 1. Flow modes for the column-switching technique. I = Injector; V_1 and V_2 = high-pressure valves; C_1 = silica column; C_2 = aminosilane (NH_2-silica) column; D = detector.

capillary column (Supelco) (30 m × 0.25 mm I.D.); the stationary phase is slightly polar. Helium was used as the carrier gas at a flow-rate of 1.70 ml/min. Retention data were obtained with a Model D-2100 data processor (Hitachi).

High-resolution (Shpol'skii effect) fluorescence spectra of monomethylated PAHs were obtained with a laboratory-made apparatus. *n*-Alkane solutions of samples, contained in quartz tubes, were frozen by attachment to the cold head of a closed-cycle helium cryogenerator (Daikin Cryo Kelvin 202A 5L) operating at 15 K. The light from the excitation source (500-W xenon lamp; JASCO) was dispersed by a monochromator (JASCO CT-25C) and focused on the rigid solution of a sample (excitation band width 6 nm). Fluorescence was observed at 90° through a high-resolution monochromator (JASCO CT-50CS; focal distance 0.5 m, emission band width 0.08 nm) and detected with a photomultiplier (Hamamatsu R928). Aromatic compounds in HPLC fractions were identified by comparison of the high-resolution spectra of the fractions with those of reference standards recorded in this study or reported previously[2,8,10].

Samples

Taching 290–340°C and Kuwait 340–500°C distillates were used as sample.

Reagents

For the removal of polar compounds from oil, 30 g of Florisil (200–300 mesh) and 600 ml of methylene chloride–*n*-hexane (HPLC grade) (20:80) were used. Compounds insoluble in *n*-hexane in the fraction of non-polar compounds were filtered off using a polytetrafluoroethylene (PTFE) filter (Chromatodisc 25N; Kurabou) and the *n*-hexane fraction was collected. *n*-Hexane, used as a mobile phase in HPLC or as a solvent in high-resolution fluorescence spectroscopy, and *n*-octane, used in the latter, were of HPLC grade (Wako and Tokyo Kasei). PAHs of analytical-reagent grade (purity >97%) were supplied by Tokyo Kasei or Aldrich. A C_{18} cartridge (Sep-Pak C_{18}; Waters Assoc.) and methanol were used for separating high-molecular weight PAHs in HPLC fractions.

Procedure

Fig. 2 shows the flow scheme for the qualitative analysis of heavy oils. Prior to the HPLC separation, a sample (1 g) was treated with Florisil and a PTFE filter to remove polar compounds and *n*-hexane-insoluble compounds (high-molecular-weight *n*-alkanes). *n*-Hexane-soluble compounds were diluted to 25 ml and aliquots (20 μl of the solution) were further separated into each group type by HPLC with the column-switching technique. Identification of monomethylated PAHs by capillary gas chromatography and high-resolution fluorescence spectroscopy was carried out using fractions of aromatics (Total A), tricyclic aromatics (3A)-2 (mixture of anthracenes and phenanthrenes) and tetracyclicaromatics (4A)-2 (mixture of chrysenes and benz[*a*]anthracenes). The eluent (*n*-hexane) was removed from each fraction by using Model S-3 mini-evaporator (Tokyo Rikakikai).

For capillary gas chromatography, aromatics, from a double HPLC fractionation in flow mode III, were dissolved in a small amount of *n*-hexane and 2 μl of the solution were injected. The temperature of the column oven was programmed from 120 to 310°C at 3°C/min. Retention indices for each peak were calculated according to Lee *et al.*'s method[14].

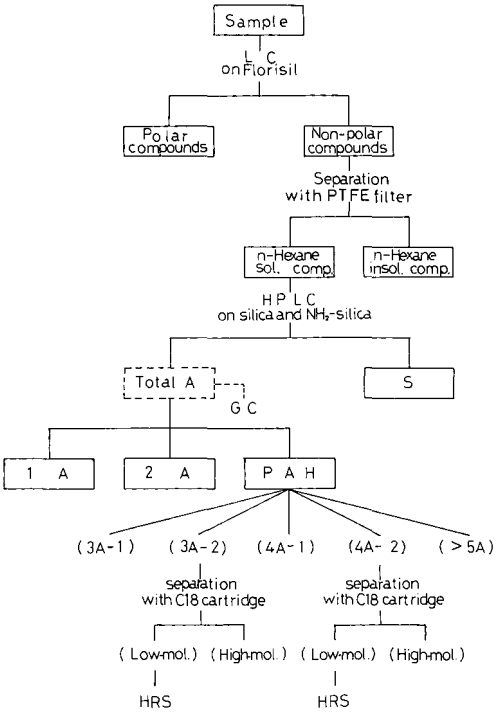

Fig. 2. Flow scheme for qualitative analysis of heavy oils. S, 1A, 2A, 3A, 4A, 5A and PAH indicate saturates, monocyclic aromatics, dicyclic aromatics, tricyclic aromatics, tetracyclic aromatics, pentacyclic aromatics and polycyclic aromatic hydrocarbons, respectively. 3A-1 and 3A-2 indicate the parent tricyclic aromatic compound and monomethylated tricyclic aromatics, respectively HRS = high-resolution fluorescence spectroscopy.

For high-resolution fluorescence spectroscopy, the 3A-2 and 4A-2 fractions were further percolated through C_{18} cartridges to remove high-molecular-weight PAHs with long alkyl chains [$>C_5$ for tricyclic aromatics and $>C_4$ for tetracyclic aromatics, judging from the percentage of retention for *n*-octylbenzene (64.5%) and *n*-butylbenzene (4.1%) and from the elution characteristics of alkylated aromatic hydrocarbons on C_{18} cartridges[15]]. Methanol (1 ml) was used as the eluent. The methanol was removed from the eluate under vacuum and monomethylated PAHs were dissolved in a suitable *n*-alkane[2,8,10] for high-resolution fluorescence spectroscopy. Tricyclic aromatics were dissolved in *n*-hexane and tetracyclic aromatics in *n*-octane.

RESULTS AND DISCUSSION

Separation by column-switching technique

Fig. 3 shows chromatograms of a high-boiling (Taching 290–340°C) petroleum distillate separated by HPLC using different columns and different techniques. The sample injected is a typical oil with a paraffinic base[16]. As Fig. 3a shows, the aminosi-

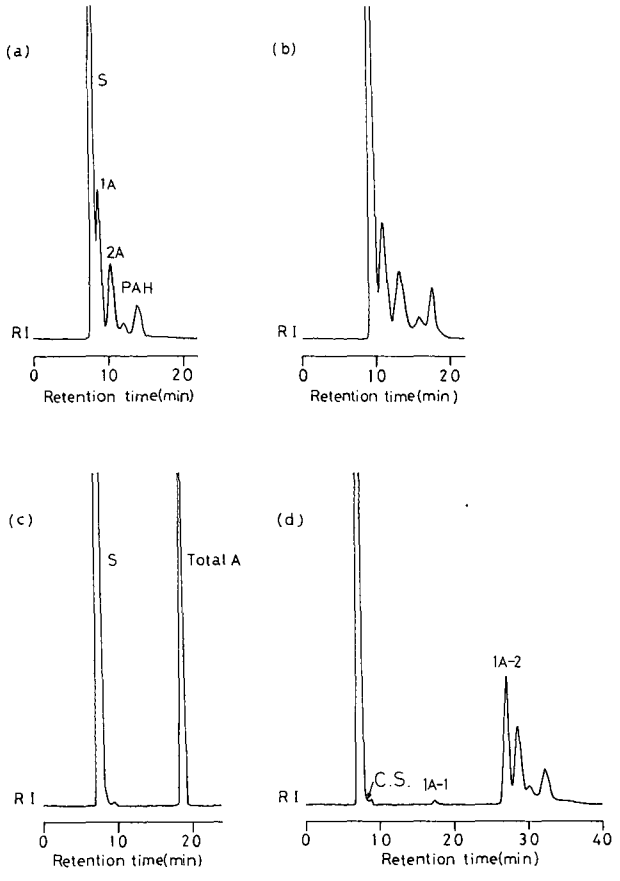

Fig. 3. HPLC traces for a Taching 290–340°C distillate. Columns or method of separation are as follows: (a) on μBondapak NH_2; (b) on μBondapak NH_2 connected with a silica column (LiChrosorb Si 100); (c) on Nucleosil 50-5, aromatics were back-flushed; (d) by the column-switching technique with Nucleosil 50-5 and μBondapak NH_2 columns. Eluent, *n*-hexane; flow-rate, 0.5 ml/min. CS = column-switching point; S = saturates; 1A = monocyclic aromatics; 2A = dicyclic aromatics; 1A-1 = monocyclic aromatics trapped between valves; 1A-2 = main band of monocyclic aromatics.

lane column does not satisfactorily separate saturates (S) from monoaromatics (1A). The use of two aminosilane columns for complete separation was reported by Grizzle and Sablotny[17]. However, this is not effective for the separation of the present kind of paraffinic oil. Fig. 3b shows that the addition of a short silica column (LiChrosorb Si 100) (50 × 4 mm I.D.) to the aminosilane column, in series, slightly increases the resolution between saturates and monoaromatics. However, the length of the silica column cannot be increased, as the resolution for ring class separation of aromatic hydrocarbons with an aminosilane column would be decreased. Better resolution between saturates and monoaromatics is obtained on the silica column, as can be seen in Fig. 3c. This advantage of the silica column and the ability of the aminosilane column to perform ring class separation was combined in the column-switching tech-

nique described here. As Fig. 3d shows, the column-switching technique permits both the separation of saturates–aromatics and separation according to ring class. Monoaromatics are separated as two peaks. The first peak (1A-1) contains early eluting monoaromatics trapped between high-pressure valves V_1 and V_2 during the elution of saturates in flow mode I. With the column-switching technique, direct elution of aromatics (Fig. 3c) is also possible in flow mode III. In spite of these improvements, monoaromatics having a large alkyl chain ($>C_{19}$) are still eluted with saturates.

Identification of monomethylated polycyclic aromatic hydrocarbons

The column-switching technique was applied to the identification of methylphenanthrene (MP), methylchrysene (MC) and methylbenz[*a*]anthracene (MBA) isomers in Kuwait 340–500°C distillate as a preparative method for capillary gas chromatography and high-resolution fluorescence spectroscopy. Fig. 4 shows a capillary gas chromatogram of aromatics (Total A in Fig. 2) obtained in flow mode III. For comparison, the chromatogram of triaromatics-2 obtained in flow mode II (fractionation was carried out five times) is also shown. The chromatogram of the aromatics shows that PAHs are clearly separated from saturated hydrocarbons.

Retention indices[14] were used for determination of MP and MC from a given chromatogram. MP and MC could be determined from the retention indices on Ultra 2 (Hewlett-Packard), reported by Radke *et al.*[18], since the characteristics of Ultra 2 are very similar (slightly polar) to those of SPD-5, as indicated in Table I. Peaks 1–4, in Fig. 4 correspond to MP. According to the retention indices, 3MP (peak 1), 2MP (peak 2), 4MP and 9MP (peak 3) and 1MP (peak 4) are determined. Distinction between 4MP and 9MP (peak 3) is impossible owing to overlapping. Similarly, 3MC (peak 8), 2MC (peak 9), 5MC (peak 10), 6MC and 4MC (peak 11) and 1MC (peak 12) are determined using retention indices. However, 2MC overlaps with 5MBA and 5MC with 4MBA, according to the retention indices on SE-52 reported by Lee *et al.*[14]

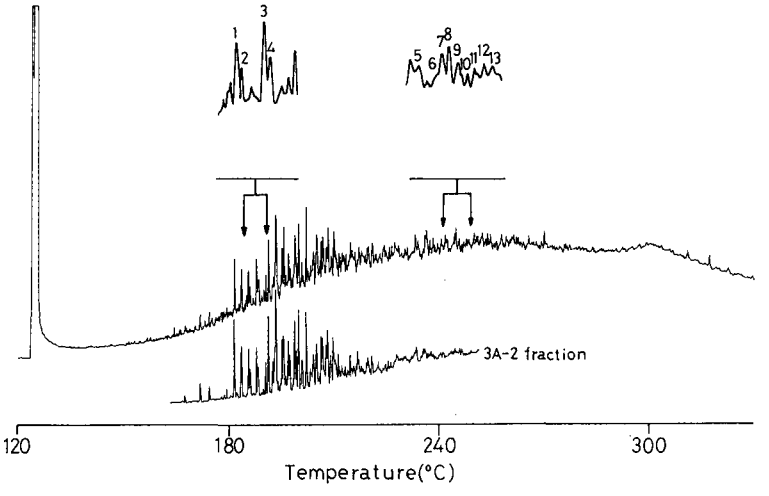

Fig. 4. Capillary gas chromatogram of aromatics from Kuwait 340–500°C distillate. Peaks 1–4 correspond to methylphenanthrene (MP) isomers and 5–13 to methylchrysene (MC) and methylbenz[*a*]anthracene (MBA) isomers.

TABLE I

RETENTION INDICES OF POLYCYCLIC AROMATIC HYDROCARBONS

Retention indices for Ultra 2 and SE-52 are taken from refs. 18 and 14, respectively.

Compound	*Retention index*		
	SPD-5	*Ultra 2*	*SE-52*
Phenanthrene	300	300	300
3-Methylphenanthrene		318.37	319.46
2-Methylphenanthrene	318.91	319.09	320.17
9-Methylphenanthrene		322.51	323.06
4-Methylphenanthrene		322.51	323.17
1-Methylphenanthrene	322.63	323.36	323.90
3,6-Dimethylphenanthrene	335.57	336.18	337.83
Fluranthene	343.18	343.52	344.01
Pyrene	350.87	350.20	351.22
Benz[*a*]anthracene	398.57		398.50
Chrysene	400	400	400
Triphenylene	400		400
11--Methylbenz[*a*]anthracene			412.72
2-Methylbenz[*a*]anthracene			413.78
1-Methylbenz[*a*]anthracene			414.37
9-Methylbenz[*a*]anthracene			416.50
3-Methylbenz[*a*]anthracene			416.63
8-Methylbenz[*a*]anthracene			417.56
6-Methylbenz[*a*]anthracene			417.57
3-Methylchrysene		416.98	418.10
5-Methylbenz[*a*]anthracene			418.72
2-Methylchrysene		418.28	418.80
12-Methylbenz[*a*]anthracene			419.39
4-Methylbenz[*a*]anthracene			419.67
5-Methylchrysene		419.56	419.68
6-Methylchrysene		420.31	420.61
4-Methylchrysene		420.31	420.87
1-Methylchrysene		422.38	422.87
7-Methylbenz[*a*]anthracene			423.14
Benzo[*e*]pyrene	452.41	453.18	450.18
Benzo[*a*]pyrene	454.11	454.83	453.44
Perylene	457.43	457.88	456.22

(Table I). Other monomethylated tetracyclic aromatic compounds (methylbenzo[*c*]phenanthrenes, -triphenylenes and -tetracenes) could also be present and eluted with MC and MBA, giving only a tentative identification of MC.

High-resolution fluorescence spectroscopy is a powerful tool for the identification of isomers of methylated PAHs[8,10]. The existence of several monomethylated PAH in sample were confirmed by this technique. The tricyclic aromatics-2 (3A-2) in Fig. 2 and tetracyclic aromatics-2 (4A-2) in Fig. 2 were obtained as illustrated in Fig. 5. Fig. 6 shows the spectrum of tricyclic aromatics-2 containing anthracenes and phenanthrenes. Owing to the selectivity of high-resolution fluorescence spectroscopy, only the last compound series is observed. In this spectrum, the existence of 9MP is shown by a strong peak. On the other hand, fluorescence from 4MP is weak. This

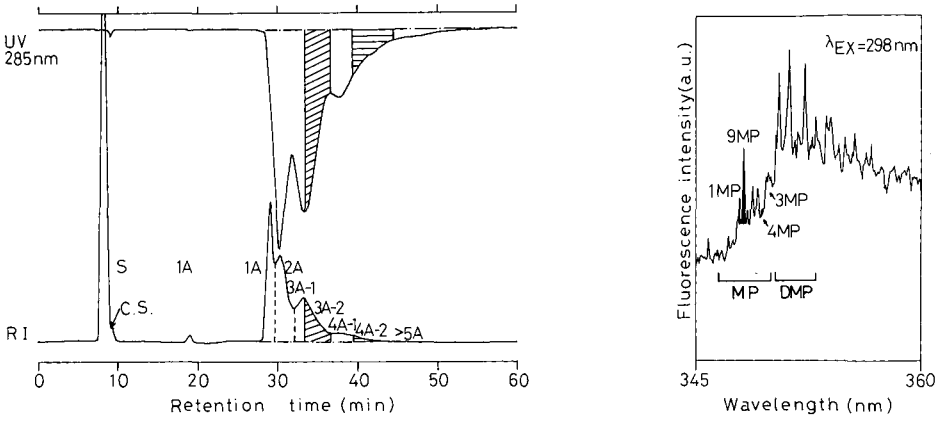

Fig. 5. Chromatograms of a Kuwait 340–500°C distillate obtained by the column-switching technique. Abbreviations as in Figs. 2 and 3. Flow-rate, 0.44 ml/min.

Fig. 6. High-resolution fluorescence spectrum of tricyclic aromatics-2 fraction. MP and DMP correspond to the methylphenanthrene and.dimethylphenanthrene isomers, respectively, as reported elsewhere[19].

trend coincides with that reported by Garrigues and Ewald[8]. Although fluorescence from 1MP is also detected, that from 3MP is not clear because of overlap with the fluorescence from some of the dimethylphenanthrenes[19]. This overlapping problem may be easily eliminated by fractionating methylphenanthrenes concentrated by HPLC using an ODS column[8].

Fig. 7 shows the spectra of tetracyclic aromatics-2, containing MC and MBA, obtained by excitation at 274 and 294 nm. The spectrum obtained by selective excitation at 274 nm indicates that 1-, 2-, 3-, 4- and 6MC are contained in the tetracyclic aromatics-2. The existence of 5MC is not clear in this spectrum. On the other hand, the spectrum obtained by selective excitation at 294 nm indicates that 5-, 6-, 7- and 11MBA are also contained in the tetracyclic aromatics-2.

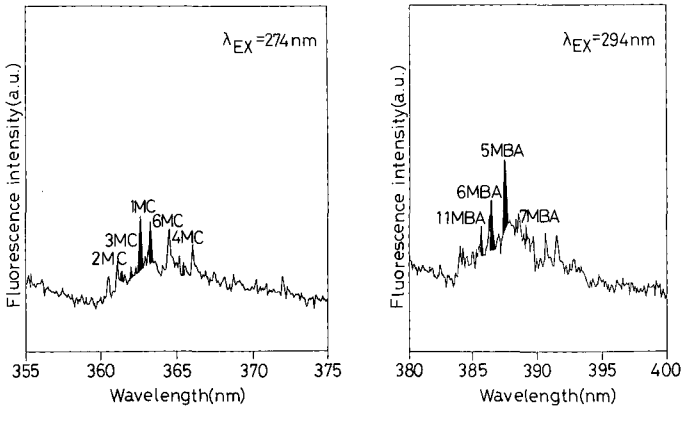

Fig. 7. High-resolution fluorescence spectrum of tetracyclic aromatics-2 fraction. MC and MBA represent methylchrysene and methylbenz[*a*]anthracene isomers, respectively.

CONCLUSION

A column-switching technique permitted the rapid fractionation of both aromatics and each aromatic ring type. It was applied as a preparative method to the identification of monomethylated PAHs by using gas chromatography and high-resolution (Shpol'skii) fluorescence spectroscopy. It was demonstrated that the separation by this technique is very reliable and is applicable to the analysis of heavy oils.

ACKNOWLEDGEMENT

Dr. P. Lightfoot is thanked for reviewing the manuscript.

REFERENCES

1 J. Jacob, W. Karcher and P. J. Wagstaffe, *Fresenius Z. Anal. Chem.*, 317 (1984) 101.
2 *Spectral Atlas of Polycyclic Aromatic Compounds*, Vol 1, edited by W. Karcher, R. J. Fordham, J. J. Dubois, P. G. J. M. Glaude and J. A. M. Ligthart, Reidel, Dordrecht, 1985 and Vol. 2, edited by W. Karcher, Kluwer, Amsterdam, 1988.
3 M. Popl, M. Stejskal and J. Mostecky, *Anal. Chem.*, 47 (1975) 1947.
4 D. L. Pullen and D. V. Scammells, *Fuel*, 67 (1988) 251.
5 Y. L. Tan, *Anal. Lett.*, 21 (1988) 553.
6 J. F. Mckay and D. R. Latham, *Anal. Chem.*, 44 (1972) 2132.
7 J. F. Mckay and D. R. Latham, *Anal. Chem.*, 45 (1973) 1050.
8 P. Garrigues and M. Ewald, *Anal. Chem.*, 55 (1983) 2155.
9 W. Giger and M. Blumer, *Anal. Chem.*, 46 (1974) 1663.
10 P. Garrigues, M.-P. Marniesse, S. A. Wise, J. Bellocq and M. Ewald, *Anal. Chem.*, 59 (1987) 1695.
11 T. Spitzer and W. Dannecker, *J. Chromatogr.*, 267 (1983) 167.
12 W. E. May and S. A. Wise, *Anal. Chem.*, 56 (1984) 225.
13 S. A. Wise, B. A. Benner, S. N. Chesler, L. R. Hilpert, C. R. Vogt and W. E. May, *Anal. Chem.*, 58 (1986) 3067.
14 M. L. Lee, D. L. Vassilaros, C. M. White and M. Novotny, *Anal. Chem.*, 51 (1979) 768.
15 N. Theobald, *Anal. Chim. Acta*, 204 (1988) 135.
16 W. L. Nelson, *Petroleum Refinery Engineering*, McGraw-Hill Kougakusha, Tokyo, 4th ed., 1958, p. 81.
17 P. L. Grizzle and D. M. Sablotny, *Anal. Chem.*, 58 (1986) 2389.
18 M. Radke, H. Willsch and D. H. Welte, *Anal. Chem.*, 56 (1984) 2538.
19 P. Garrigues and R. Lapouyade, in *Proceeding of the 11th International Symposium on Polycyclic Aromatic Hydrocarbons, Gaithersburg, MD, September 1987*, in press.

Journal of Chromatography, 498 (1990) 35–40
Elsevier Science Publishers B.V., Amsterdam — Printed in The Netherlands

CHROM. 22 011

GAS CHROMATOGRAPHIC–MASS SPECTROMETRIC INVESTIGATION OF DEXTROMORAMIDE (PALFIUM) METABOLISM IN THE HORSE

P. J. REILLY, C. J. SUANN and A. M. DUFFIELD*
Australian Jockey Club Laboratory, P.O. Box 3, Randwick, N.S.W. 2031 (Australia)
(First received July 24th, 1989; revised manuscript received September 13th, 1989)

SUMMARY

Dextromoramide (Palfium) was given by intravenous injection to a Thoroughbred horse at a dosage of 20 mg and urine was collected 2, 4, 6 and 8 h after drug administration. Enzymatic hydrolysis of the urine followed by solvent extraction gave a residue which was back-extracted into 0.1 *M* sulphuric acid. After basification to pH 9 and solvent extraction, the resulting residue was submitted to gas chromatographic–mass spectrometric analysis. Both electron-impact and ammonia chemical-ionization mass spectra were recorded and, based on the observed fragmentation patterns, the principal metabolites in horse urine were shown to be 2,2-diphenyl-3-methyl-4-morpholinobutyramide (compound **2**) and the product of hydroxylation of one phenyl ring in dextromoramide (compound **3**), respectively. The electron-impact mass spectra of compounds **2** and **3**, and of their derivatisation products from on-column methylation in the gas chromatograph, are reported.

INTRODUCTION

Dextromoramide (Palfium, compound **1**, see Fig. 1) is a potent analgesic, first described in 1956[1], which is commonly believed to enhance the racing performance of Thoroughbred and Standardbred horses. Methods used for the analysis of dextromoramide include paper and thin-layer chromatography[2–5] and ultraviolet spectrophotometry[6] but these methods lack the sensitivity and specificity required for this drug's detection in human or equine urine. Thermal degradation of dextromoramide was reported[7] to be a problem with a method based upon the gas chromatographic (GC) quantitation of **1**. Alternatively, dextromoramide was quantitated using a procedure incorporating its initial oxidation with permanganate to benzophenone which was then detected by GC or high-performance liquid chromatography[7].

Several pharmacokinetic parameters have been determined for dextromoramide in humans[7]. A report[7] has described the human metabolism of **1** as occurring by formation of the morpholine-N-oxide, *para*-hydroxylation of one of the phenyl rings and hydrolysis of the pyrrolidinylamide linkage in **1** to a substituted butyric acid. However, nothing has been published on the metabolic fate of dextromoramide in the horse.

0021-9673/90/$03.50

We were unable to detect dextromoramide in equine urine 2 h after an intravenous 20-mg dose. In the present study the urinary metabolites of dextromoramide have been identified as having structures **2** (2,2-diphenyl-3-methyl-4-morpholinobutyramide) and **3** (the product of hydroxylation of one phenyl ring in dextromoramide), respectively (see Fig. 1). These assignments were based upon their mass spectral fragmentation patterns and structure **2** was confirmed from direct comparison with a reference compound of known structure. It follows that the GC–mass spectrometric (MS) identification of **2** in an equine urine swab is direct evidence for the prior administration of dextromoramide. The method described can identify **2** in equine urine after a single intravenous dose of 20 mg of dextromoramide for at least 8 h after administration of this dose.

EXPERIMENTAL

Chemicals and solvents

All solvents were obtained from Mallinckrodt Australia (Clayton, Australia) and were of nanograde quality. MethElute was purchased from Pierce (Rockford, IL, U.S.A.).

Drug administration

Dextromoramide (Palfium) was a product of Janssen Pharmaceutica (Beerse, Belgium) and was purchased from F. H. Faulding (Thebarton, Australia). Four 5-mg tablets were crushed and extracted with dichloromethane to isolate dextromoramide which was suspended in water and administered intravenously to a healthy Thoroughbred horse. Under GC–MS conditions no indication was obtained for the presence of metabolites **2** and **3** in extracts of dextromoramide isolated from this procedure. Urine samples were collected 2, 4, 6 and 8 h after drug administration.

GC–MS instrumentation

The mass spectrometer used in this study was a Kratos MS-80RFAQ instrument interfaced to the same manufacturer's Model DS-90 data system. Electron-impact (EI) mass spectra were recorded at 70 eV with a trap current of 100 μA. Chemical-ionization (CI) mass spectra were obtained using alternating EI and CI scans and ammonia as the CI reagent gas. Scan speeds of 1 s decade^{-1} were used and the ion source temperature was maintained at 200°C. Typically the electron multiplier was operated at 4.5 kV.

GC separations were achieved using a Carlo Erba gas chromatograph operating under the following conditions. A cross-linked fused-silica 5% phenylmethylsilicone column (Hewlett-Packard, North Ryde, Australia) (20 m × 0.31 mm I.D.; 0.17 μm film thickness) was used in all the studies reported and it terminated in the MS ion source. Helium served as the GC carrier gas at a flow-rate of 1 ml min^{-1}. Urine extracts were injected at an initial oven temperature of 100°C which was programmed 2 min after sample injection at 20°C min^{-1} to 200°C, then at 30°C to a final temperature of 280°C. The GC injector was maintained at 250°C and the interface line between the GC and MS ion source at 250°C.

Urine extraction

Urine (9 ml), collected 2 h after dextromoramide administration, was hydrolysed at 37°C overnight by β-glucuronidase/arylsulphatase (Boehringer Mannheim, North Ryde, Australia). The hydrolysed solution was extracted with dichloromethane (1 × 10 ml) and the organic phase washed with 0.1 *M* sulphuric acid (1 × 1 ml). The aqueous phase was adjusted to pH 9 (sodium carbonate) and the organic bases were extracted into dichloromethane (2 × 10 ml). After drying over anhydrous sodium sulphate the residue was dissolved in ethyl acetate (20 μl) prior to GC–MS analysis.

Reference standard of structure **2**

Compound **2** was a gift from Janssen Research Foundation (Beerse, Belgium) and it had an identical GC retention time and EI and ammonia CI mass spectra with the metabolite of dextromoramide occurring in equine urine. Under CI conditions using a resolving power of 10 000 (10% valley) the $[MH]^+$ ion of **2** was measured to be 339.2059 (calculated for $C_{21}H_{27}N_2O_2$: 339.2066).

RESULTS AND DISCUSSION

The EI mass spectrum of **1** has been published[8]. The base peak of this spectrum occurs at *m/z* 100 with prominent ions at *m/z* 128 and 265 with a low-abundance (3%) molecular ion visible at *m/z* 392. This fragmentation can formally be accommodated by the bond fissions depicted in Fig. 1. Thus, metabolic transformations of dextromoramide should be readily identified by MS from displacement of the *m/z* values of these diagnostic ions.

In contrast to the EI mass spectrum[8] of **1** where high mass ions are of low abundance, the ammonia CI mass spectrum of this compound has the protonted molecular ion $[MH]^+$ at *m/z* 393 as the base peak.

Equine urine, collected 2 h after drug administration, was enzymatically hydrolysed (β-glucuronidase) and the products were analysed by GC–EI-MS. The total ion

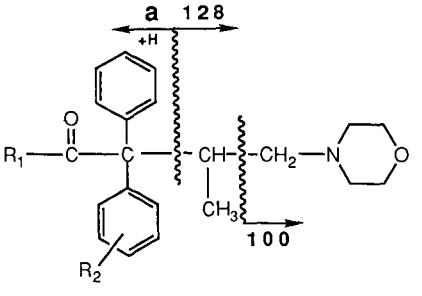

Fig. 1. Rationalisation of the principal bond fissions in the EI mass spectrum of dextromoramide (**1**), its urinary metabolites (**2** and **3**) and their products after derivatisation with MethElute. Structures **4** and **5** derived from metabolite **2** and structure **6** from metabolite **3**. **1**: R_1 = N-pyrrolidinyl; R_2 = H; a = *m/z* 265; **2**: R_1 = NH_2; R_2 = H; a = *m/z* 211; **3**: R_1 = N-pyrrolidinyl; R_2 = OH; a = *m/z* 281; **4**: R_1 = $NHCH_3$; R_2 = H; a = *m/z* 225; **5**: R_1 = $N(CH_3)_2$; R_2 = H; a = *m/z* 239; **6**: R_1 = N-pyrrolidinyl; R_2 = OCH_3; a = *m/z* 295.

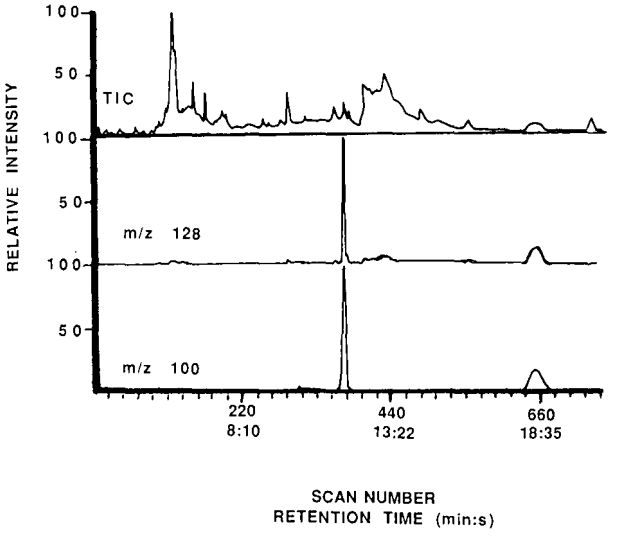

Fig. 2. Total ion chromatogram and mass chromatograms of *m/z* 100 and 128 of the basic fraction from horse urine collected 2 h after intravenous administration of dextromoramide (Palfium, 20 mg).

chromatogram (Fig. 2) was searched for the peak profiles of *m/z* 100 and 128, respectively. This identified two GC peaks with the first occurring at a retention time of 11 min 40 s. The EI mass spectrum of this component (Fig. 3) did not detect an obvious molecular ion and no ions were observed above *m/z* 211. However, using the alternating EI–CI scanning technique, the ammonia CI mass spectrum clearly identified a protonated molecular ion ($[MH]^+$) at *m/z* 339. The ions of mass 100 and 128 in the EI mass spectrum (Fig. 3) of this compound indicated that the morpholine ring system

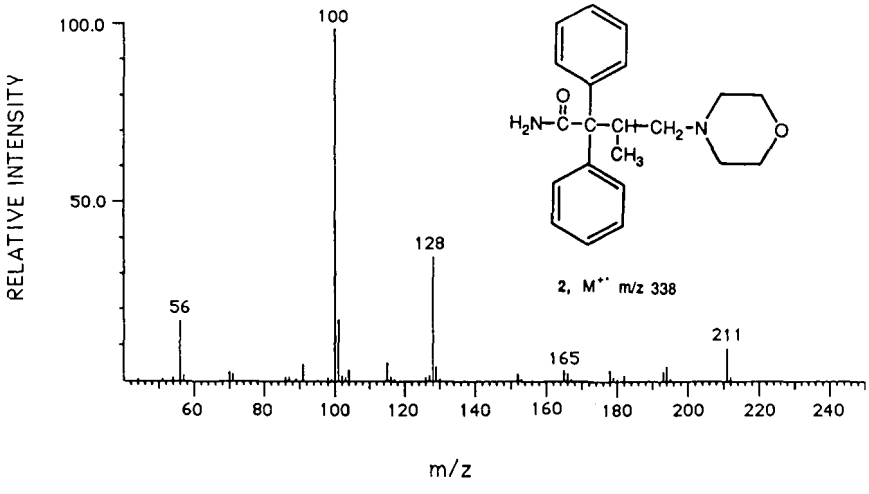

Fig. 3. EI mass spectrum (70 eV) of 2,2-diphenyl-3-methyl-4-morpholinobutyramide (**2**) corresponding to retention time 11 min 40 s in Fig. 2.

and the three carbon atoms attached to the nitrogen were present in this metabolite (see Fig. 1). The ion at *m/z* 211 in the mass spectrum of **2** (Fig. 3) corresponds in origin to that at *m/z* 265 ($[M - 127]^+$) in the mass spectrum of **1**[8] and formally corresponds to $[NH_2CO{-}CH[C_6H_5)_2]^+$ and must incorporate a hydrogen rearrangement from the N-alkylmorpholine system. A molecular weight of 338 for this metabolite indicated that 54 mass units had been eliminated from **1**. This is consistent with the assignment of structure **2** to this metabolite, and positive confirmation of this metabolite's structure was achieved by comparison with an authentic sample of **2** when an identical GC retention time and EI and CI mass spectra were obtained.

The second equine urinary metabolite of dextromoramide eluted as a broad GC peak at a retention time of 18 min 20 s (Fig. 2). Its molecular ion was identified at *m/z* 408 from the ammonia CI mass spectrum ($[MH]^+$ at *m/z* 409) and the base peak under EI conditions (Fig. 4) occurred at *m/z* 100 with a prominent ion at *m/z* 128. A significant ion was located at *m/z* 281 [*m/z* 265 in 1 (Fig. 1) plus an oxygen atom] and this product can be assigned structure **3**.

On-column methylation of the metabolites **2** and **3** was investigated in order to improve the GC characteristics of the phenol **3**. Co-injection into the hot GC injection port of MethElute and hydrolysed horse urine extract resulted in partial (**4**) and complete methylation (**5**) of the amide nitrogen in **2**. Thus two GC peaks were observed (retention times of 13 min 8 s and 13 min 15 s, respectively) and their EI mass spectra were consistent with structures **4** and **5** and had the ubiquitous fragment ions at *m/z* 100 and 128 (Fig. 1). Ions corresponding to the ion at *m/z* 211 in **2** were now located at *m/z* 225 and 239, respectively, in **4** and **5**. The ammonia CI mass spectra of **4** and **5** had their respective $(MH]^+$ ions located at *m/z* 353 and 367 consistent with these structural assignments.

The phenolic metabolite, **3**, after methylation in the GC injector with MethElute, yielded **6**, which eluted from the GC as a sharp peak with a retention time of 15 min 30 s. This product had an EI mass spectrum consistent with the fragmentation depicted in Fig. 1. The *m/z* 265 fragment in the mass spectrum of **1** was now located at *m/z* 295 but the molecular ion (*m/z* 422) was not detected. However, using ammonia CI a $[MH]^+$ ion was readily identified at *m/z* 423.

Thus the two major metabolites of dextromoramide in the horse have been

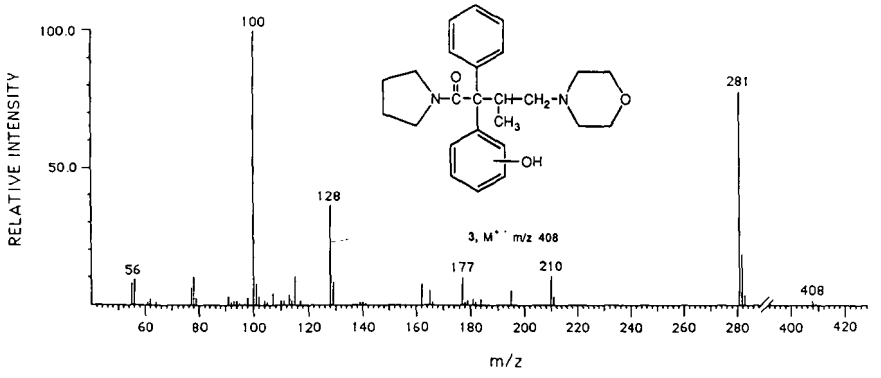

Fig. 4. EI mass spectrum (70 eV) of compound **3** corresponding to retention time 18 min 20 s in Fig. 2.

identified to have structures **2** and **3**, respectively. The ions of mass 100 and 128, using EI-MS, or of 339 and 409, using ammonia CI-MS, can be used under GC–MS conditions as a sensitive and specific method to detect these metabolites of dextromoramide in equine urine swabs. On-column methylation can also be used as additional evidence for the presence of **2** and **3** in equine urine extracts. The availability of an authenticated sample of **2** now provides the racing analyst with the necessary standard for the positive identification of dextromoramide (Palfium) in equine swabs.

ACKNOWLEDGEMENTS

We thank the Racecourse Development Committee of New South Wales for the purchase of the Kratos MS-80RFAQ mass spectrometer and DS-90 data system and for laboratory facilities. An authentic sample of 2,2-diphenyl-3-methyl-4-morpholinobutyramide (**2**) was a generous gift of Janssen Research Foundation (Beerse, Belgium). We wish to thank Mr. P. J. Ashelford for the extraction of dextromoramide from Palfium tablets.

REFERENCES

1 P. A. J. Janssen, *J. Am. Chem. Soc.*, 78 (1956) 3862.
2 K. H. Beyer, *Pharm. Ztg.*, 106 (1961) 1326.
3 A. Noirfalise and G. Mees, *J. Chromatogr.*, 31 (1967) 594.
4 T. J. Siek, *J. Forensic Sci.*, 19 (1974) 193.
5 E. Vidic and J. Schnette, *Arch. Pharm.*, 295 (1962) 342.
6 M. Attiso, *Therapie*, 14 (1959) 650.
7 B. Caddy, R. Idowu, W. J. Tilstone and N. C. Thomson, in J. S. Oliver (Editor), *Forensic Toxicology, Proceedings of the European Meeting of the International Association of Forensic Toxicologists, Glasgow, 1979*, Croom Helm, London, pp. 126–139.
8 H. Maurer and K. Pfleger, *Fresenius Z. Anal. Chem.*, 317 (1984) 42.

Journal of Chromatography, 498 (1990) 41–53
Elsevier Science Publishers B.V., Amsterdam — Printed in The Netherlands

CHROM. 22 022

CHARACTERIZATION OF POLYIMIDE SORBENTS BY USING TRACER PULSE CHROMATOGRAPHY

STEPHEN D. COOPER and EDO D. PELLIZZARI*
Research Triangle Institute, P.O. Box 12194, Research Triangle Park, NC 27709 (U.S.A.)
(First received April 18th, 1989; revised manuscript received September 22nd, 1989)

SUMMARY

A modification of tracer pulse chromatography was used to rapidly evaluate four novel polyimide sorbents for use in air sampling. This technique utilized probe molecules with different functional groups to evaluate the surface retention characteristics when the sorbents were highly loaded by these chemicals and humidity. The evaluation of the sorbents indicated the polymer subunits of each must have multiple sorption sites which is consistent with their chemical makeup. Some comparisons between the polyimides and Tenax-GC were made.

INTRODUCTION

The use of sorbents for air sampling or organic compounds has been done successfully for many years. One of the major sorbents in use is Tenax-GC (hereafter Tenax) which, when used with thermal desorption and cryofocussing in the analytical step, can allow very good sensitivity for many organic compounds[1,2]. A major advantage of Tenax in this regard is its low retention of water. This alleviates any problems from subsequent analysis steps such as obstruction of the cryofocussing trap, high mass spectrometer pressures, etc. A major disadvantage of Tenax has been the poor retention of polar organics at ambient temperatures which prevents the collection of many of the toxic and carcinogenic compounds of interest.

To improve this situation we have previously investigated polyimide sorbents that we have prepared[3] to determine their suitability for collection of a broad range of organic compounds from air including the volatile polar compounds. Among those initially tested, four polyimides were found suitable for further testing[4].

To further characterize the four polyimide sorbents, we choose to probe the competitive effects on sorption for selected organic compounds and water. By examining the competition between various organic compounds and water the surface characteristics of the sorbents can be elucidated. One approach is to use the technique of tracer pulse chromatography as developed by Parcher[5,6]. This gas chromatography (GC)–mass spectrometry (MS) technique involves continuously feeding a known, fixed concentration of an analyte into a carrier gas stream through a sorbent of interest. Once equilibration of the analyte with the sorbent is established, an injection

0021-9673/90/$03.50

of a deuterated analogue of the analyte (probe) is made. This is carried out while the sorbent is maintained at a constant temperature. The procedure is repeated for different equilibration levels of the undeuterated analogue with the sorbent. The retention times of the probe thus provide information about the capacity of the sorbent for a given compound.

The method we have employed to evaluate these sorbents is a dynamic form of the tracer pulse chromatography technique which uses a mixture of analytes instead of one analyte at a time. This approach provided the advantages of better mimicking the collection of chemicals from air and of providing faster data collection.

EXPERIMENTAL

The polyimides were synthesized in-house by using a simple reaction between pyromellitic dianhydride and the appropriate aromatic diamine[3]. The polymer resin was dried and sieved to obtain 40–60 mesh particles. The Tenax used was 40–60 mesh and was obtained from Alltech Associates–Applied Science Labs. (Deerfield, IL, U.S.A.). The deuterated organic compounds were obtained from MSD Isotopes (Montreal, Canada). All other compounds were obtained from Aldrich (Milwaukee, WI, U.S.A.). Dichlorodimethylsilane (DCDMS)-treated glass wool was obtained from Alltech.

The GC–MS–computer (COMP) instrument used was an LKB 2091 magnetic sector mass spectrometer (LKB, Bromma, Sweden) interfaced to a Varian 3700 gas chromatograph (Palo Alto, CA, U.S.A.) and a Digital Equipment PDP 11/04 computer system (Maynard, MA, U.S.A.). For later stages of the work (model compounds), a Teknivent 802 MS interface (St. Louis, MO, U.S.A.) using a Tandy 3000 microcomputer (Fort Worth, TX, U.S.A.) was used for data acquisition. A gas jet separator (Becker-Ryhage type) for the mass spectrometer was used since the column flow-rate was 10 ml/min for each sorbent. The mass spectrometer was operated in the electron impact mode under the following conditions: electron beam energy, 70 eV; accelerating voltage, 3.5 kV; trap current, 50 μA; and temperatures of ion source and Becker-Ryhage separator, 180°C. The glass columns used had dimensions sufficient to accommodate an *ca.* 80 cm × 2 mm I.D. sorbent bed and were silanized by using DCDMS. DCDMS-treated glass wool was used to plug the ends of the sorbent bed. The polyimide sorbents were used as prepared. The Tenax was extracted with methanol and pentane and then dried before use.

A diagram of the interface which generated the organic and water vapors in the helium stream is shown in Fig. 1. The flow controller and flow meter used were Tylan FC-260 and FM-360 (Carson, CA, U.S.A). The organic vapor generator was an enclosed vessel containing a mixture of the analytes for the introduction of the organic vapors into the sorbent column. The flows through the organic vapor generator and the humidifier were adjusted to provide the correct levels of organics and water vapor. The humidifier was optionally removed for experiments not involving water vapor. The gas lines from the organic vapor generator and humidifier to the GC–MS–COMP system were heated to *ca.* 100°C.

The 4-port valve allowed the interface to be operated in two modes. The initial mode of operation was with helium carrier gas valved directly to the GC–MS–COMP system; the second mode was with organics and water vapor introduced from the

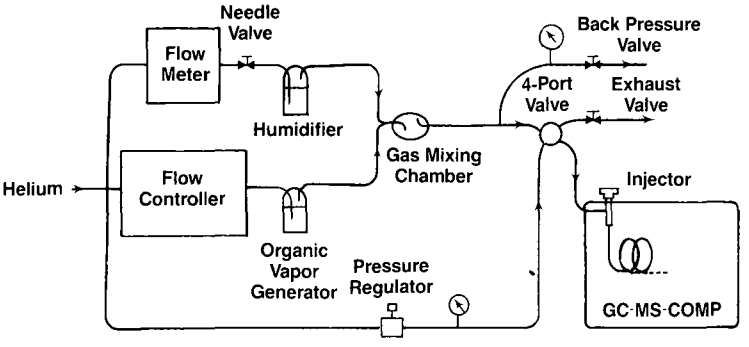

Fig. 1. Schematic of the continuous vapor introduction apparatus.

organic vapor generator and the humidifier, respectively. The pressure of the interface was maintained at 13.6 p.s.i.g. by using the back pressure valve, which was matched to the pressure regulator. The exhaust valve was set to match the flow resistance of the sorbent column.

Molecular probe studies

The actual experiments involved the use of 5 probe compounds plus water vapor. The probe compounds were ethanol, *n*-hexane, benzene, butanone, and nitromethane. These probes represent H-bonding, dispersion forces, π–π interactions and dipole interactions in a similar fashion to interactions described by McReynold's constants. This approach would most effectively provide information about the surface features of the polymer studied.

The experiments each involved five injections of a vapor mixture of the deuterated probe compounds. The deuterated compounds were: [2,2,2-$^2H_3$]-ethanol; [$^2H_{14}$]*n*-hexane; [$^2H_6$]benzene; [1,1,1,3,3-$^2H_5$]butanone and [$^2H_3$]nitromethane. The liquid mixture was prepared to provide approximately equal molar proportions of vapors. The mixture was maintained in a septum vial at 25°C. Headspace injections of this mixture consisted of *ca.* 5 μg for each compound. Injections were made at 10-min intervals starting at -10 min and ending at 30 min, where 0 min is the time at which the continuous stream of all undeuterated analytes was introduced (and optionally water vapor). The sorbent was maintained at an appropriate isothermal condition so that the most retained compound eluted approximately 30 min after injection. The 30-min period was sufficiently long to allow the changes in the retention time of the least retained compound to be evaluated. It was not so long as to cause undue band broadening of the last eluting compound. The 10-min injection interval was sufficient to evaluate changes in retention prior to an equilibrium state, therefore providing an insight into retentions on a sorbent before breakthrough of any of the frontal streams. The injection intervals (10 min) were constant to avoid minor errors due to competitions solely from the deuterated compounds. Table I shows the sorbent temperatures and the retention times of the probe compounds for each sorbent. The retention time of water was determined from its elution front.

The native (undeuterated) chemicals were also prepared as a vapor mixture for introduction into a continuously flowing stream. The organic vapor generator was

TABLE I

SORBENT TEMPERATURES AND RETENTION TIMES OF PROBE COMPOUNDS AND WATER

Probe compound	*Retention time (min)*				
	PI-119	*PI-109*	*PI-115*	*PI-149*	*Tenax*
Water	2.7	2.4	5.3	3.3	0.7
Ethanol	12.0	9.9	16.5	7.7	2.3
Nitromethane	17.6	16.5	30.8	29.6	8.0
Butanone	26.8	26.5	10.7	*ca.* 19.4	14.4
Benzene	10.9	15.7	5.1	*ca.* 13.1	28.4
n-Hexane	3.3	4.8	0.9	0.7	12.9
Temperature, °C	135	135	90	120	85

used for this and was maintained at 25°C for this group of compounds. Its operation was based on Raoult's law by using a gas stream passing through a liquid mixture of the organics. These compounds and water vapor were continuously introduced through the sorbent bed at the desired levels beginning at time $t = 0$ min of each experiment. Through a combination of eliminating the organic vapor generator, changing the organic mixture ratios, or changing the flow-rate through the humidifier (when present) various challenge conditions were created.

The organic vapor mixture that was continuously fed was nominally introduced at a level which would just show a small decrease in retention time if each chemical were introduced individually. This was accomplished by injecting larger and larger amounts of an individual compound until a retention time decrease was noted. This would imply the compound would be occupying a substantial number of the surface sites of the sorbent. This was found to be about 100 nmol/min for each compound in the vapor mixture and is the "1 ×" level used. For a 1 × experiment all organics were at this level. When added, water vapor was introduced at a level of 22 Torr, which was a higher level than for the organic compounds. This humidity level was chosen to approximate the higher ambient levels expected in actual field sampling conditions instead of being based on sorbent capacity.

The above setup essentially describes one experiment or GC–MS run. The GC–MS system was operated in the full-scan mode during the experiment. A typical experiment showing the chromatogram of the benzene front (m/z 78) and the corresponding chromatogram of the [$^2H_6$]benzene injections (m/z 84) is presented in Fig. 2.

By approaching the sorption capacity of the multi-functional sorbent with the probe molecules and water vapor (1 ×), additional loading of the sorbent with organics should show, with good sensitivity, the sorption characteristics of the polymer. This was tested by elevating the concentration of one of the organic chemicals in the continuously fed vapor mixture 10-fold to 1 μmol/min (10 ×) while maintaining the levels of the other chemicals in the mixture at 100 nmol/min (1 ×). This elevated-level experiment was conducted for each compound in separate experiments while the other compounds were continuously introduced at the nominal level (1 ×). All chemicals were also continuously introduced at 0.4 × and 0.1 × levels, to verify if the retention time reductions of the 1 × experiment were in a reasonable range, and to

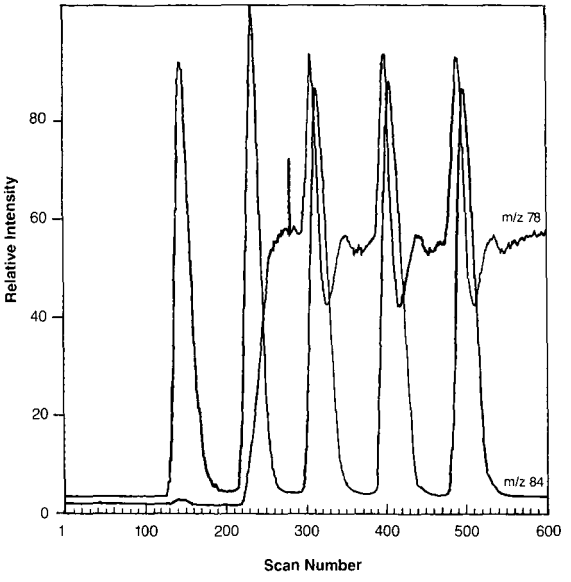

Fig. 2. Superimposed ion chromatograms showing the simultaneous elution of the benzene front (*m/z* 78) and the multiple [$^2H_6$]benzene injections (*m/z* 84) through the PI-109 polyimide sorbent.

test if changes occurred. The deuterated compounds were injected at the same levels at all times in all of the experiments, thus they did not play a role in the variable loading of the sorbents. The relative levels of the individual compounds continuously introduced are shown in Table II for reference. In the table a value of 1 indicates a feed-rate of 100 nmol/min, 10 indicates 1 μmol/min, etc. As shown, experiments were carried out by testing the overall capacity of the sorbent and the effects of humidity. Half of the experiments was carried out with humidity, though the control experiment

TABLE II

RELATIVE LEVELS OF ORGANIC VAPORS INTRODUCED INTO THE SORBENT — MOLECULAR PROBE STUDIES

These experiments were carried out with water vapor continuously fed at 22 Torr and also at 0 Torr. The level of organics is normalized so that a level of 1 indicates 100 nmol/min, 10 indicates 1000 nmol/min, etc.

Experiment	*Level of frontal loading*				
	Ethanol	*n-Hexane*	*Benzene*	*Butanone*	*Nitromethane*
Control	0	0	0	0	0
1	1	1	1	1	1
2	10	1	1	1	1
3	1	10	1	1	1
4	1	1	10	1	1
5	1	1	1	10	1
6	1	1	1	1	10
7	0.4	0.4	0.4	0.4	0.4
8	0.1	0.1	0.1	0.1	0.1

used for comparisons did not have humidity added. The control is discussed further in a later section.

Model toxic compounds

The same general procedures were followed in carrying out dynamic tracer pulse chromatography for two additional sets of model toxic compounds. These experiments with additional chemicals were carried out on the PI-119 sorbent to further characterize it and to corroborate the results by using the probe compounds.

The first set of injected compounds included [$^2H_6$]benzene, [$^2H_3$]acrylonitrile, [$^2H_4$]dichloroethane, and [$^2H_5$]ethyl acetate. Their undeuterated analogues were introduced continuously as in frontal chromatography. As before, five vapor phase injections were made of the deuterated mixture at 25°C, however, the injections were made at 8-min intervals starting at −8 min and ending at 24 min. The PI-119 sorbent was maintained at 130°C in the gas chromatograph so the most retained compound eluted within 24 min after an injection. As was conducted for the probe compounds, the organic vapor generator for continuously feeding the analytes was maintained at 25°C. The scheme for the relative levels of the continuously fed chemicals is shown in Table III. The same absolute levels for the continuously fed chemicals were used (*e.g.* "1 ×" indicates 100 nmol/min per compound, etc.). The humidity levels and all other parameters were also unchanged.

The second set of compounds included [$^2H_{22}$]*n*-decane, [$^2H_7$]*n*-propylbenzene, [$^2H_4$]*o*-dichlorobenzene, and [$^2H_5$]benzonitrile as the injected compounds, and native chemicals as the frontal streams. Five discrete injections per experiment were made, but were done at 10-min intervals as was carried out with the probe compounds. The vapor-phase injected sample was maintained at 70°C. A syringe and the septum vial of the deuterated mixture were kept in an oven, quickly loaded and injected into the GC–MS apparatus to maintain sufficient vapor pressures of the constituents. The organic vapor-phase generator for the continuous feeding of vapor was also maintained at 70°C. The GC temperature of the PI-119 sorbent was maintained at 195°C

TABLE III

RELATIVE LEVELS OF ORGANIC VAPORS INTRODUCED INTO PI-119 — MODEL TOXIC COMPOUNDS

These experiments were carried out with water vapor continuously fed at 22 Torr and also at 0 Torr. The level of organics is normalized so that a level of 1 indicates 100 nmol/min, 10 indicates 1000 nmol/min, etc.

Experiment	*Level of frontal loading*			
	Benzene	*Acrylonitrile*	*1,2-Dichloroethane*	*Ethyl acetate*
Control	0	0	0	0
1	1	1	1	1
2	10	1	1	1
3	1	10	1	1
4	1	1	10	1
5	1	1	1	10
6	0.4	0.4	0.4	0.4
7	0.1	0.1	0.1	0.1

for these experiments. The continuously fed levels used were the same as for the first set of model toxic compounds, as were the levels used for the humidity.

RESULTS AND DISCUSSION

Conceptual model of experiment

A simplified representation of the technique we employed is shown in Fig. 3. The injection of the deuterated analyte occurs at the initial time point and the front stream (of a faster eluting compound) is introduced later as indicated by "front" in this example. Other combinations of continuously fed compounds and deuterated compounds can be examined also. As indicated, a retention time decrease for the deuterated analyte may occur as a result of competition(s) with the undeuterated analyte in the frontal stream. By making an injection without a frontal stream present, a control case is generated which can be used for comparison. The retention time decrease is measured and compared to the control where no competition exists. Also, by taking account of the sweep time of the deuterated pulse, a % deviation in the retention time can be determined from $[(t'_{unk}/t'_{con}) - 1] \cdot 100$, where t' is the corrected retention time for an unknown (unk) or control (con). Corrected retention time is $t' = t - t_{sweep}$. Also, it is important that the concentration level of an analyte stream is set (nominally) just under the capacity level at which any greater sorbent loading by the analyte causes a significant reduction in its retention time. Therefore, any additional loading by the same compound, or another which competes for the same surface functional groups, will provide a much more sensitive measure of the surface effects.

Therefore, the deuterated analyte is injected before or during the frontal stream migration of the native chemicals to measure the effects of competition. It should be pointed out that using a native analyte in an injection is less desirable since a concen-

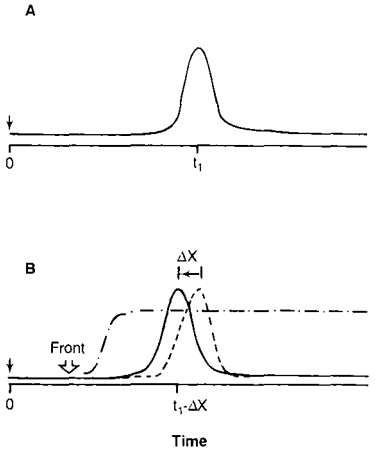

Fig. 3. Representations of the chromatography using dynamic tracer pulse chromatography. (A) The control case with a single compound injected. (B) The same compound is injected but its retention by the sorbent is affected by the front. The front is introduced after $t = 0$ and is a faster eluting compound in this example.

tration pulse does not migrate at the same rate as the actual molecules injected[7,8]. Also, as a practical matter, identification of the injected analytes is more easily accomplished.

The method we used involved 4–5 organic compounds introduced simultaneously, where each represented a different functional group. Water was optionally introduced. By pulsing (injecting) the deuterated analogues at various time points as the different frontal streams migrated, a picture of the processes in effect at the sorbent surface were seen.

Molecular probe studies

Because of the large amounts of data generated by the experiments, only selected experiments will be presented in detail. In reviewing the results for all polymers tested, including Tenax, it was quite clear that water vapor affects breakthrough volumes (BVs). BV is the flowing gas volume required to elute a compound from a sorbent bed at a given temperature. The BV curve has been typically determined in the absence of water vapor. However, at least 50% humidity is almost always present during field sampling. The BVs for some compounds were found to be over 50% lower on some of the polymers tested in the presence of humidity. This can have a substantial impact on collection efficiency if a BV is approached for a given compound of interest in the field.

The general effects of water vapor across the polyimides and Tenax are shown in Fig. 4. The effect of water vapor on the retention of ethanol on the polyimide sorbents was quite significant, while the effect was much less on Tenax. This suggests that sorption on polyimides is affected when the retention of an analyte depends on H-bonding. For Tenax the changes were less apparent. Regardless of humidity, the retention of many volatile polar compounds is poor to begin with so humidity is not of any practical consequence. Differences between the two polyimides were also observed. Overall, continuously introducing organics into the sorbent bed provided better retention for ethanol by using PI-109 when water vapor was present than when it was not present (AA *versus* BB). On the other hand a further reduction in retention for ethanol occurred by using PI-119 under the same circumstances (CC *versus* DD). For PI-109 a large decrease in retention of ethanol occurred when the water vapor was introduced alone (AA), but subsequent injections indicated small increases. This suggests that the deuterated organics from the injections themselves may be coating the surface to a certain extent, either blocking the sorption of water or aiding in sorption of other organics by serving as stationary phase. This phenomenon was not as pronounced with PI-119.

These data illustrate the utility of the technique. The apparent H-bonding in this case shows the ability of the technique to determine any functional group effects on the retention. It also provides information about other effects which may not normally be expected such as the modification of the surface characteristics by the organics. The use of multiple injections helps to observe these more subtle effects which are prior to a steady-state equilibrium.

In the experiments involving water vapor, the retentions of nitromethane can be examined across the different polymers as shown in Fig. 5. In contrast to ethanol, water vapor did not significantly affect the retention of nitromethane on Tenax. However, all of the polyimides exhibited 10–30% reductions in retention times for

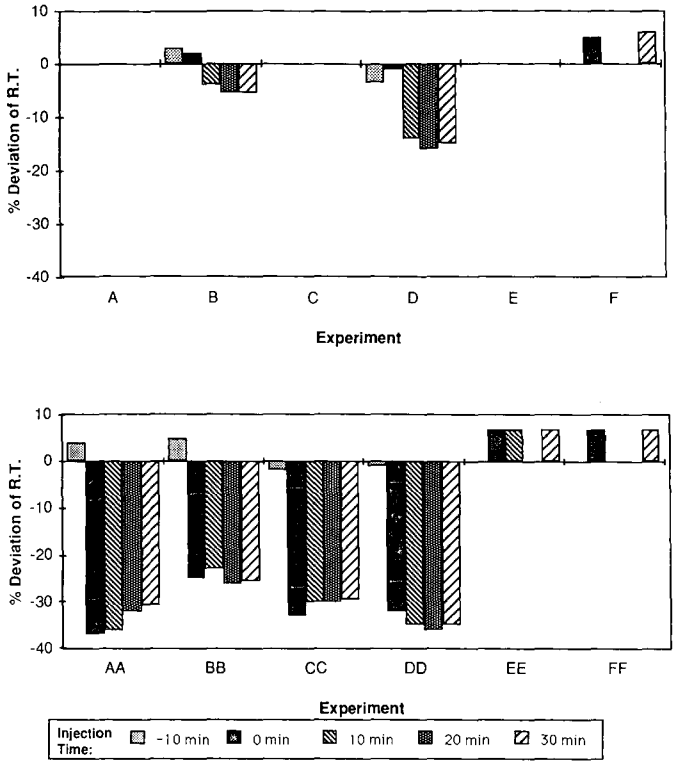

Fig. 4. Percent deviation of the retention time of [$^2H_3$]ethanol on three sorbents. Sorbents tested were: PI-109 (A,B); PI-119 (C,D); Tenax (E,F). Experiments A, C and E were cases where no organic frontal streams were introduced. Experiments, B, D and F were cases where all organic frontal streams were introduced at the 1 × level. Double letters indicate the additional presence of a water vapor frontal stream to the corresponding experiments.

nitromethane. This water vapor effect apparently was not altered upon adding the organic frontal streams for PI-115, PI-119 and Tenax, and was unchanged for PI-149. Only for PI-109 did addition of the organics change (increase) the retention of nitromethane substantially. As for ethanol on PI-109, the organic compounds in the frontal streams apparently aided in the retention of nitromethane.

The surface characteristics of the sorbents were evaluated effectively when one of the five organic frontal streams was elevated 10-fold. This provided a high loading of the sorbent with a frontal compound of a specific funtionality. Therefore, changes in retention of a deuterated probe compound would indicate competition with the elevated compound in the frontal stream for the same sites on the sorbent. In Fig. 6, the experiments on PI-119 involving each of the elevated (10 ×) frontal streams in the absence of water vapor is shown. The 0 × and 1 × experiments are also shown for reference. The retention of [$^2H_6$]benzene was not substantially affected by the increased level of hexane (B *versus* C). This suggests that the two compounds interact with different sites on the sorbent surface. An expected change in retention occurred for the frontal stream containing elevated levels of benzene as indicated by a simple

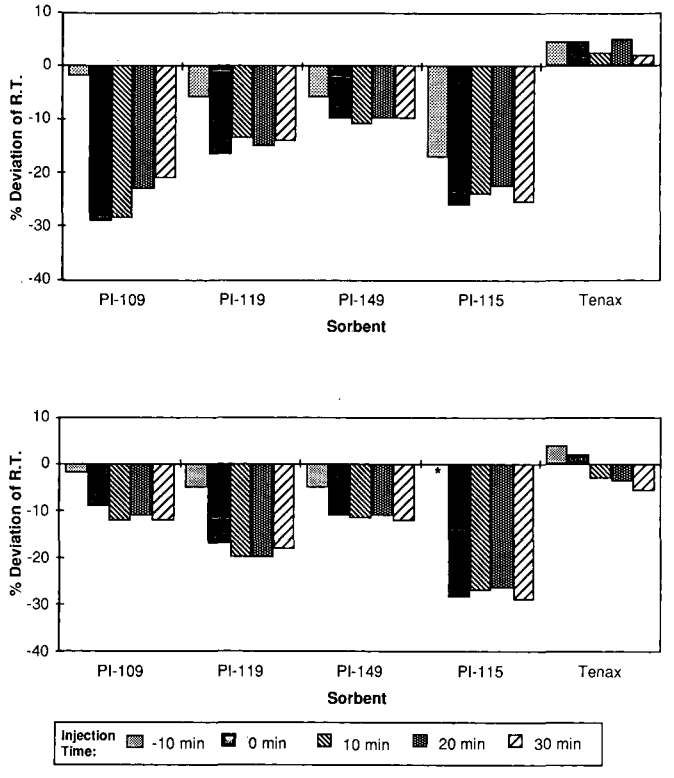

Fig. 5. Percent deviation of the retention time (R.T.) of [$^2H_3$]nitromethane in the presence of water vapor on the tested sorbents. The top frame shows experiments with no organic frontal streams introduced. The bottom frame shows experiments with 1 × level organic frontal streams introduced. * = No data.

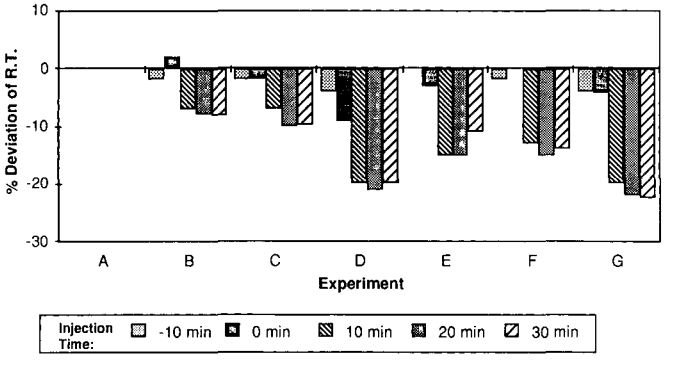

Fig. 6. Percent deviation of the retention time of [$^2H_6$]benzene without water vapor on PI-119. A = 0 × case, B = 1 × case, C = 10 × hexane case, D = 10 × benzene case, E = 10 × ethanol case, F = 10 × nitromethane case, G = 10 × butanone case.

competition for the same site. A similar effect occurred for the elevated butanone experiment which paralleled the effects observed with benzene. This may indicate one or more sites on the sorbent's molecular subunit which involve inductive (π–π) effects or dipole–dipole interactions. This is consistent with the structure of polyimides. Where ethanol and nitromethane were at elevated levels in the continuously fed fronts, some additional competitive effects with [$^2H_6$]benzene occurred, but to a lesser extent for butanone. At the 30-min injection, the elevated ethanol experiment (E) resulted in an increase in retention from the 20-min injection. This effect is probably due to a modification of the sorbent surface by the accumulated butanone based partly on the compounds' retention times. That is, this "new surface" sorbs [$^2H_6$]benzene in a manner which becomes less sensitive to the competitive effects of ethanol.

Based on these and other results, each polyimide appears to possess 2–3 different sites or functionalities which are responsible for the phenomenon of adsorption. Also, perhaps more than half of the retention characteristics are attributable to the common part of the polymer derived from pyromellitic dianhydride. This similarity in retention characteristics is indicated by the overall similarity in the retention data that was obtained throughout the experiments. The differences are clearly related to the different diamines used to synthesize the different polymers, and perhaps to the stereochemistry of the polymer subunits. Results from the 0.4× and 0.1× experiments provided only attenuated effects of the 1× case.

Model toxic compounds

These two sets of compounds were used to further evaluate the PI-119 sorbent's functional groups involved in the adsorption process. Sorbent characteristics were further probed by using many compounds with different functionalities. Some compounds such as benzonitrile have more than one functional group providing the potential for participation in adsorption by more than one mechanism.

The first set of toxics had retention times in the control experiment (without water vapor) of 15.0 min of benzene, 17.2 min for acrylonitrile, 17.6 min for 1,2-dichloroethane, and 18.6 min for ethyl acetate. By using the expression for % deviation of retention time, the data shown in Fig. 7 were generated. The data in this figure

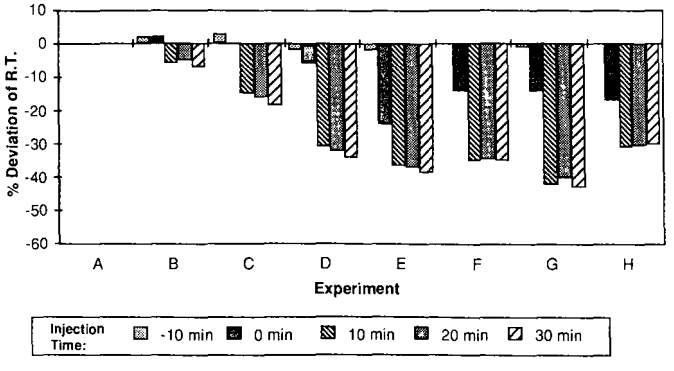

Fig. 7. Percent deviation of the retention time of [$^2H_6$]benzene without water vapor on PI-119. A = 0× case, B = 0.1× case, C = 0.4× case, D = 1× case, E = 10× benzene case, F = 10× acrylonitrile case, G = 10× dichloroethane case, H = 10× ethyl acetate case.

indicate, as in the previous figure, that chemicals which are retained longest do not *a priori* affect the retention of another chemical with a shorter retention time when more than one mechanism of sorption is operative. This is in contrast to the sorbent with only one functional site, where $\Delta H_{\text{sorption}}$ would indicate that more highly retained compounds are more successful at occupying a site. For two or more sites it is possible for one site on the sorbent subunit to be highly retentive for the most retained compound (ethyl acetate) and the other(s) to be less retentive for this compound. When 1,2-dichloroethane was continuously introduced at high levels, the weaker sites for ethyl acetate were presumably saturated while the strong site for ethyl acetate was not appreciably affected. [$^2H_6$]Benzene would be expected to be more highly retained by the sites which more weakly adsorb ethyl acetate. The net effect is an apparent irregularity in $\Delta H_{\text{sorption}}$ which is a reflection of the different operative sites.

This is also evident in Fig. 8 which demonstrates that the retention of the second set of toxics is affected by high levels of *o*-dichlorobenzene or benzonitrile. In the control experiment the retention times were 1.4 min for *n*-decane, 4.5 min for *n*-propylbenzene, 12.3 min for *o*-dichlorobenzene, and 30.4 min for benzonitrile. Water eluted at 0.7 min. On this basis, the results showed that the elevated (10×) *o*-dichlorobenzene frontal stream affected [$^2H_7$]*n*-propylbenzene, [$^2H_4$]*o*-dichlorobenzene and [$^2H_5$]benzonitrile retentions more than the elevated (10×) benzonitrile frontal stream did in the presence of water vapor. This would not occur for a monofunctional sorbent since again the magnitude of $\Delta H_{\text{sorption}}$ of the individual compounds were reversed. For [$^2H_{22}$]*n*-decane the benzonitrile frontal stream did cause the greater drop in retention time relative to the effect of the *o*-dichlorobenzene frontal stream. This is what would be expected in a simple single-site adsorption model, and may suggest this is the case of *n*-decane on the PI-119 sorbent.

CONCLUSIONS

We have demonstrated that dynamic tracer pulse chromatography provides a relatively effective means of evaluating a sorbent. The technique is particularly rele-

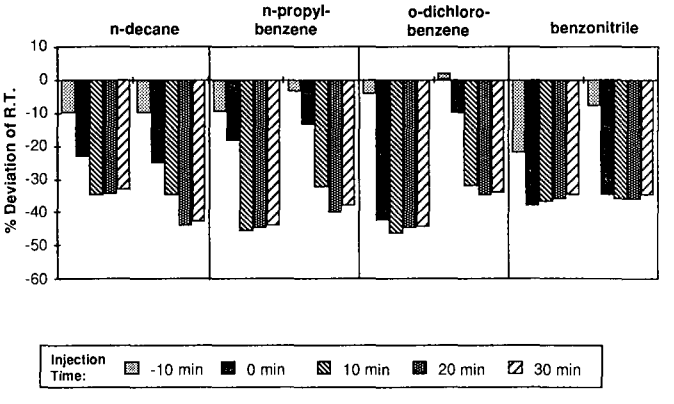

Fig. 8. Percent deviation of the retention times of the deuterated toxic compounds. The first set of bars for each compound is the elevated *o*-dichlorobenzene case with water vapor. The second set is for the elevated benzonitrile case with water vapor.

vant in that it simulates the way an air sample is collected, particularly when the sorbent is challenged by water vapor and high levels of organic compounds, which can be present at occupational levels. Water may be the only major challenging compound when sampling at environmental levels since organic levels will typically be lower.

This technique can address which functional groups of the polymer play a part in adsorption and to what extent, however, it cannot address precisely the mechanisms of adsorption or other effects due to the complexity of the elutions. The technique has also demonstrated the effect of a surface modification by organics through either coating the surface or blocking of water sorption providing some detail of the sorption process.

The information which can be gathered by this technique demonstrates the importance of humidity and high levels or organics on the BVs of a sorbent. It cannot be assumed that BVs obtained under dry conditions can be related to BVs under actual field conditions. This is most important for sorbents when retaining polar chemicals at sampling volumes which approach their BVs.

It has also been shown that the polyimides tested have good characteristics for air sampling purposes. The multifunctional polymers have tended to provide good retention volumes for a broad range of chemical classes. These polyimides do retain water more than Tenax which is a compromise for this better retention of polar organic compounds.

ACKNOWLEDGEMENTS

This work was supported by Grant R01 0H02108 from the National Institute for Occupational Safety and Health of the Centers for Disease Control.

REFERENCES

1 E. D. Pellizzari, J. E. Bunch, R. E. Berkley and J. McRae, *Anal. Lett.*, 9 (1976) 45.
2 K. J. Krost, E. D. Pellizzari, S. G. Walburn and S. A. Hubbard, *Anal. Chem.*, 54 (1982) 810.
3 E. D. Pellizzari, B. Demian, A. Schindler, K. Lam and W. Jeans, *Preparation and Evaluation of New Sorbents for Environmental Monitoring*, Vol. 1, U.S. Environmental Protection Agency, EPA 600/4-83-015A, and National Technical Information Service, Springfield, VA (PB83-195 974).
4 J. H. Raymer, S. D. Cooper and E. D. Pellizzari, in D. R. Lloyd, T. C. Ward and H. P. Schreiber (Editors), *Inverse Gas Chromatography*, American Chemical Society, Washington, DC, 1989, Ch. 20, p. 274.
5 J. F. Parcher and M. I. Selim, *Anal. Chem.*, 51 (1979) 2154.
6 J. F. Parcher, *J. Chromatogr.*, 251 (1982) 218.
7 F. Helfferich, *J. Chem. Educ.*, 41 (1964) 410.
8 J. R. Conder and C. L. Young, *Physicochemical Measurement by Gas Chromatography*, Wiley, New York, 1979, pp. 399–401.

Journal of Chromatography, 498 (1990) 55–65
Elsevier Science Publishers B.V., Amsterdam — Printed in The Netherlands

CHROM. 22 032

RELATIVE RETENTION AND COLUMN SELECTIVITY FOR THE COMMON POLAR BONDED-PHASE COLUMNS

THE DIOL-SILICA COLUMN IN NORMAL-PHASE HIGH-PERFORMANCE LIQUID CHROMATOGRAPHY

A. W. SALOTTO*, E. L. WEISER, K. P. CAFFEY, R. L. CARTY and S. C. RACINE
Department of Chemistry, Pace University, Pleasantville, NY 10570 (U.S.A.)
and
L. R. SNYDER
LC Resources, 26 Silverwood Ct., Orinda, CA 94563 (U.S.A.)
(Received July 18th, 1989)

SUMMARY

Retention data for several solutes and mobile phases composed of methylene chloride–hexane and isopropanol–hexane are reported for a diol column. These data are in agreement with a previous model of retention in normal-phase systems. These and other data from the literature have been used to characterize the selectivity of diol, cyano and amino columns for various sample types. The diol and amino columns each preferentially retain basic solutes (*e.g.*, esters, ketones) *vs.* dipolar solutes (nitro and nitrile derivatives), when compared to a cyano column. The amino column strongly retains acidic solutes.

INTRODUCTION

Although most separations using high-performance liquid chromatography (HPLC) are presently carried out under reversed-phase conditions, there is a continuing interest in the use of normal-phase chromatography[1], particularly with polar bonded-phase columns. The separation by reversed-phase HPLC of some samples may be poor, even after conditions have been optimized. Normal-phase HPLC, being based on a different retention process, often provides a greater resolution for such samples, particularly in the case of isomers[1]. In addition, many organic compounds have limited solubility in aqueous–organic mobile phases, but dissolve well in normal-phase solvents. Finally, many of the problems associated with silica[2] (*e.g.*, irreversible retention of highly polar compounds and difficulty in maintaining a constant mobile phase water content) are avoided through the use of polar bonded-phase columns.

Polar bonded-phase columns are commercially available in three common forms: cyano, diol and amino. Separation on these columns is similar in many respects

to that on silica and alumina; *i.e.*, retention involves a competition between solute and solvent molecules for sites on the adsorbent surface. Previously published studies have shown that the well-documented displacement model for alumina and silica[3] is applicable to separations on cyano[4–6], amino[6–8], diol[6] and other polar bonded-phase packings[9,10]. In this paper we will further examine the retention on a diol column of various solutes. This in turn allows us to make a comparison of column selectivity and column strength among the cyano, diol and amino columns. Some apparent anomalies for isopropanol as a polar solvent are also reported for the cyano column.

EXPERIMENTAL

A Varian 5000 programmable liquid chromatograph was used with a Rheodyne automatic injector, a 10-μl sample loop and a photometric detector. Automatic proportioning was employed for strong solvent concentrations at or above 1%.

Diol columns (25 × 0.46 cm I.D., 5-μm packing, supplied in pH 7 buffered aqueous mobile phase) were the gift of DuPont (Wilmington, DE, U.S.A.). Amino columns [25 × 0.46 cm I.D., 5-μm packing, supplied in either acetonitrile–water (75:25) or 100% hexane mobile phase] were supplied by Supelco (Bellefonte, PA, U.S.A.). Cyano columns were obtained from both Supelco [15 × 0.46 cm I.D., 5-μm packing and supplied in either acetonitrile–water (25:75) or 100% hexane mobile phase] and DuPont [15 × 0.46 cm I.D., 6-μm packing, supplied in hexane–isopropanol (96:4)]. Both the amino and cyano columns were endcapped by the manufacturers. The solvents were HPLC grade from Fisher Scientific (Pittsburgh, PA, U.S.A.) and J. T. Baker (Phillipsburg, NJ, U.S.A.). Solutes were from Aldrich (Milwaukee, WI, U.S.A.), Baker and Sigma (St. Louis, MO, U.S.A.).

The temperature of the column was maintained constant at 30°C by means of a contact heater. System pressure ranged from 20 to 140 atm depending on the solvent system used. Solvent flow was 2.00 ml/min. Sample weights were always less than 20 μg to avoid overloading of the column. Column deadtime (t_0) ranged from 1.5 to 1.7 min and *m*-nitroacetophenone was injected daily to verify reproducibility (capacity factor, k' range = $\pm 10\%$ over a one-year period).

RESULTS AND DISCUSSION

Diol column

Our interpretation of the retention data reported in this study is based upon the displacement model of retention for liquid–solid chromatography[3]. As this model is treated extensively elsewhere, only an outline of relevant aspects is discussed here. The displacement model assumes the formation of an adsorbed monolayer of solute plus solvent molecules on the surface of the stationary phase. During the course of the separation, solute and solvent molecules compete for a limited number of adsorption sites. For a homogeneous surface and the situation where solute and solvent interactions with the mobile phase essentially cancel, a fundamental relationship can be derived[3] between solute retention (k') and mobile phase strength (ε^0):

$$\log(k_2/k_1) = \alpha' A_s(\varepsilon_1^0 - \varepsilon_2^0) \quad (1)$$

Here k_1 and k_2 are k' values for the solute in mobile phases 1 and 2, α' is the adsorbent activity function for the column (assumed equal to 1.0), A_s is the molecular area of the solute, and ε_1^0 and ε_2^0 are solvent strength values (ε^0) for mobile phases 1 and 2.

Table I summarizes retention data on the diol column for fourteen solutes: twelve substituted aromatics and two polycyclic aromatics. Log k' values are given for each solute and five different mobile phase compositions [ranging from pure hexane to dichloromethane–hexane (35:65)]. Solvent strength values for these five mobile phases were determined from retention data for chrysene and perylene by means of eqn. 1 (A_s values for these non-localizing hydrocarbon solutes can be calculated from their molecular areas). Using the calculated solvent strength values for the non-polar hydrocarbons, eqn. 1 was then used to determine "experimental" A_s values for the various non-hydrocarbons of Table I. Listed in Table I are three sets of A_s values: localized, delocalized and experimental. Delocalized values of A_s correspond to actual solute molecular areas (similar to those found for adsorption on alumina[11]). The larger "localized areas" of Table I are values determined for silica as adsorbent; these A_s values reflect "site-competition delocalization"[3,10] among solute and solvent molecules as they compete for a place on the adsorbent surface. The experimental A_s values for the non-hydrocarbons of Table I fall between the localized and delocalized values for adsorption on silica and alumina, respectively. Thus, site-competition delocalization appears to be occurring on the diol column, but to a lesser extent than on silica.

The degree of site-competition delocalization occurring on the diol column can be defined in terms of an empirical parameter c, where

$$A_s = A_s(\text{alumina}) + c[A_s(\text{silica}) - A_s(\text{alumina})] \tag{2}$$

The experimental data of Table I suggest that $c = 0.7 \pm 0.1$ for the diol column. That is, site-competition delocalization effects are about 70% as important on the diol column as on unbonded silica. Eqn. 2 reflects the fact that site-competition delocalization is possible on silica but not alumina[3].

The capacity factor k_h in pure hexane as mobile phase can be determined for each of the solutes of Table I (eqn. 1), assuming that ε^0 is zero for hexane. Log k_h values are given in parentheses in Table I; the last column shows the average of these calculated values for each solute. Individual values of log k_h agree with the average within ± 0.04 units (one standard deviation).

For a mobile phase that is a binary mixture of a weaker solvent A and a stronger solvent B, solvent strength ε_{AB}^0 is given by[10]

$$\varepsilon_{AB}^0 = \varepsilon_A^0 + \{\log[N_b\, 10^{\alpha' n_b(\varepsilon_B^0 - \varepsilon_A^0)} + 1 - N_b]\}/\alpha' n_b \tag{3}$$

ε_A^0 and ε_B^0 are the solvent strengths of the pure solvents A and B respectively, N_b is the mole fraction of the stronger solvent B and n_b is the molecular area of the B solvent. Eqn. 3 can be rearranged to solve for the solvent strength of pure solvent B.

$$\varepsilon_B^0 = (1/\alpha' n_b) \log\{10^{\alpha' n_b \varepsilon_A^0}[10^{\alpha' n_b(\varepsilon_{AB}^0 - \varepsilon_A^0)} - 1 + N_b]/n_b\} \tag{4}$$

TABLE I

RETENTION DATA FOR POLYCYCLIC AROMATIC HYDROCARBONS AND SUBSTITUTED AROMATIC HYDROCARBONS

Diol-silica column, methylene chloride–hexane mobile phase.

Solute	A_s[a]			*log k' (log k_h)*					*Average log k_h*[b]
	loc	*del*	*exp*	*Methylene chloride (%, v/v)*					
				0	*5*	*10*	*20*	*35*	
Chrysene	12.3	12.3		−0.20)	−0.41	−0.521	−0.764	−1.02	
				(−0.20)	(−0.236)	(−0.186)	(−0.210)	(−0.162)	−0.218 ± 0.025
Perylene	12.8	12.8		−0.041	−0.28	−0.391	−0.682	−0.914	
				(−0.041)	(−0.099)	(−0.043)	(−0.105)	(−0.021)	−0.061 ± 0.033
1-Nitronaphthalene	15.6	9.4	13.7	−0.080	−0.24	−0.391	−0.613	−0.936	
				(−0.080)	(−0.046)	(−0.018)	(0.004)	(0.002)	−0.048 ± 0.031
1-Cyanonaphthalene	16.5	8.7	14.2	0.017	−0.16	−0.315	−0.532	−0.851	
				(0.017)	(0.041)	(0.072)	(0.108)	(0.014)	0.043 ± 0.027
2-Naphthylacetate	16.2	10.4	14.5	0.068	−0.13	−0.373	−0.544	−0.936	
				(0.068)	(0.076)	(0.087)	(0.109)	(0.075)	0.077 ± 0.009
2-Naphthaldehyde	16.4	9.2	14.2	0.076	−0.11	−0.256	−0.476	−0.799	
				(0.076)	(0.091)	(0.131)	(0.164)	(0.019)	0.099 ± 0.022
1-Naphthylacetate	16.2	10.4	14.5	0.11	−0.097	−0.284	−0.544	−0.903	
				(0.11)	(0.109)	(0.111)	(0.109)	(0.108)	0.110 ± 0.001
1-Acetonaphthalene	17.3	9.6	15.0	0.11	−0.064	−0.241	−0.476	−0.821	
				(0.11)	(0.149)	(0.167)	(0.200)	(0.225)	0.136 ± 0.036
2-Acetonaphthalene	17.3	9.6	15.0	0.21	0.017	−0.162	−0.415	−0.745	
				(0.21)	(0.230)	(0.246)	(0.260)	(0.301)	0.237 ± 0.022
1,5-Dinitronaphthalene	23.1	10.7	19.4	0.31	0.086	−0.099	−0.355	−0.712	
				(0.31)	(0.361)	(0.429)	(0.519)	(0.641)	0.405 ± 0.091
2,6-Dimethyl naphthylene dicarboxylate	24.3	12.7	20.8	0.38	0.13	−0.076	−0.360	−0.750	
				(0.38)	(0.425)	(0.490)	(0.577)	(0.704)	0.468 ± 0.086
1-Naphthyl nitrile	17.6	10.5	15.5	0.480	0.222	0.0086	−0.274	−0.750	
				(0.480)	(0.442)	(0.431)	(0.424)	(0.331)	0.444 ± 0.025
m-Nitroacetophenone	22.7	8.8	18.5	0.48	0.24	0.0086	−0.268	−0.631	
				(0.48)	(0.502)	(0.512)	(0.566)	(0.659)	0.515 ± 0.036
Benzyl alcohol	15.4	8.2	13.2	1.146	0.96	0.727	0.413	0.136	
				(1.146)	(1.147)	(1.086)	(1.008)	(1.056)	1.089 ± 0.060
ε^0_{AB}[c]				(0.000)	0.014	0.027	0.045	0.070	
ε^0_B[d]					0.096	0.100	0.100	0.109	

[a] Localized (loc) and delocalized (del) values of A_s from ref. 3; exp = experimental.

[b] Data from k' values less than −0.5 excluded.

[c] Calculated from eqn. 1, assuming $\varepsilon^0 = 0.00$ for hexane (chrysene and perylene solutes).

[d] Calculated from eqn. 4.

TABLE II

RETENTION DATA FOR STEROIDS

Diol-silica column, methylene chloride–hexane mobile phase.

Solute	*Methylene chloride (%, v/v)*	*log k'*	*ε°*	*A_s (exp)*	*A_s (calc)*[a]
4-Androstene-17-β-ol-3-one	18	1.00	0.042	27.3	25
	26	0.77	0.053		
	36	0.41	0.064		
	50	0.09	0.076		
4-Androstene-17-α-ol-3-one	18	1.21	0.042	29.9	25
	21	1.07	0.046		
	31	0.70	0.059		
	60	0.02	0.081		
Adrenosterone	13	1.22	0.033	34.0	31
	18	0.89	0.042		
	23	0.60	0.048		
	40	0.03	0.068		
Corticosterone	40	1.06	0.068	40.6	38
	47	0.81	0.073		
	57	0.54	0.080		
	81	0.05	0.092		
Prednisone	59	1.17	0.081	48.1	43
	70	0.85	0.087		
	80	0.65	0.092		
	100	0.29	0.099		

[a] According to ref. 3, assuming $c = 0.7$ (eqn. 2).

The value of n_b for dichloromethane is 4.1, from which we calculate that ε_B^0 for this solvent is equal to 0.101 ± 0.005 (one standard deviation).

Steroid solutes. In order to further verify eqn. 1 for stronger mobile phases, more highly retained solutes were necessary. Five steroids were studied at four different dichloromethane concentrations (giving k' values ranging from 1 to 20 for these solutes). Table II summarizes resulting experimental values of k', calculated values of ε_{AB}^0 (eqn. 3), experimental values of A_s (eqn. 1, slope of the log k' *versus* ε_{AB}^0 line, determined by linear regression), and calculated values of A_s (eqn. 2, $c = 0.7$). These latter values of A_s are in reasonable agreement, further verifying the applicability of eqns. 1 and 2.

The preceding analysis of experimental data for the diol column (Tables I and II) plus previously published work on the amino and cyano columns confirm the overall applicability of the displacement model (with localization effects) for polar bonded-phase systems. Separation on these polar bonded-phase columns should therefore be predictable as a function of mobile phase composition.

Column selectivity and strength

The selectivity of the cyano, diol and amino columns might be expected to parallel the acidity, basicity and dipolarity of the individual functional groups (–CN, –O–CH[OH]–CH_2OH, and –NH_2)[1], as measured by the "solvent-selectivity" tri-

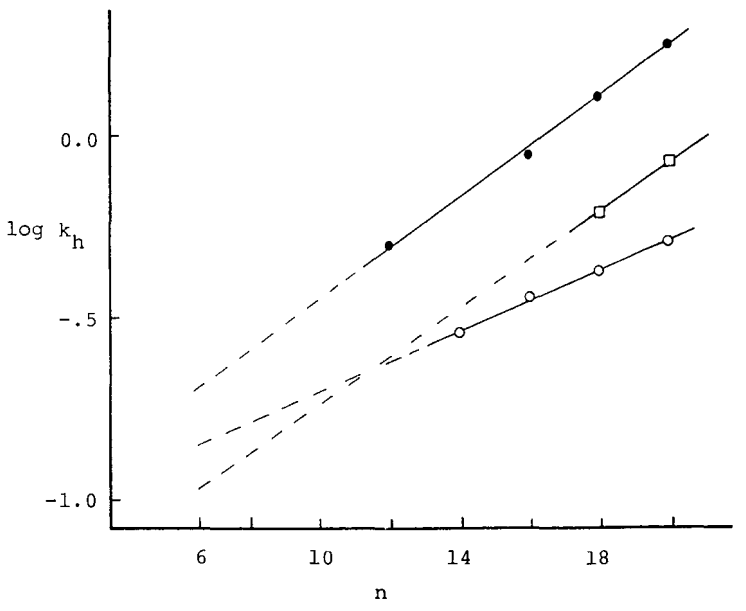

Fig. 1. Retention (log k_h) *vs.* carbon number (n) for unsubstituted aromatic hydrocarbons. Data of Table I and ref. 4. ● = amino column; ○ = cyano column; □ = diol column.

TABLE III

COMPARISONS OF FUNCTIONAL-GROUP RETENTION (ΔR_m) AND ADSORBENT ACTIVITY FUNCTIONS FOR SILICA *VS.* AMINO, DIOL AND CYANO COLUMNS

Solute	*Group X*[a]	$Q_{i(silica)}$[b]	*log* k_{hX} − *log* k_h[c]			$Q_i/\Delta R_m$[d]		
			$\Delta R_{m(amino)}$	$\Delta R_{m(diol)}$	$\Delta R_{m(cyano)}$	*Amino*	*Diol*	*Cyano*
Basic solutes								
1-Acetonaphthone	$-COCH_3$	4.69	1.06	0.87	0.69	4.42	5.39	6.80
2-Acetonaphthone		4.69	1.14	0.97	0.76	4.11	4.84	6.17
1-Naphthylacetate	$-OOCCH_3$	3.45	1.11	0.84	0.68	3.10	4.11	5.07
2-Naphthylacetate		3.45	1.10	0.81	0.59	3.14	4.26	5.85
2,6-Dimethylnaphthalene dicarboxylate	$-COOCH_3$	2.09	1.36	1.198	0.86	1.53	1.74	2.43
Acidic and dipolar								
1-Nitronaphthalene	$-NO_2$	2.77	0.81	0.68	0.64	3.44	4.07	4.33
1,5-Dinitronaphthalene		1.39	1.28	1.135	1.06	1.09	1.22	1.31
1-Cyanonaphthalene	$-CN$	3.33	0.90	0.77	0.68	3.69	4.32	4.90
1-Naphthylnitrile	$-CH_2CN$ (al)	5.27	1.48	1.17	1.01	3.56	4.50	5.22
Average						3.12	3.83	4.68
Benzyl alcohol	–OH (al)	5.6		2.08	1.36			

[a] (al) indicates aliphatic group; other groups are aromatic substituents.

[b] Group retention energy on standard silica surface (ref. 3).

[c] k_{hX} refers to k_h for substituted aromatic, k_h refers to parent unsubstituted compound.

[d] Q_i (silica)/ΔR_m (column).

angle[12]. Thus a cyano column would be expected to be more dipolar, so as to selectively retain dipolar solutes. Similarly, an amino column should be basic, and retain acidic solutes more strongly, and *vice versa* for a diol column. Previous studies suggest that these predictions are correct for the amino and cyano columns. More recently, Smith and Cooper[13] have reported that the amino and diol columns are each relatively basic, and the cyano column is essentially dipolar.

We were interested in further characterizing the selectivity of these columns toward various classes of solute molecules. For determination of column selectivity, it is necessary to compare functional-group retentions as $\log k_{hX} - \log k_h$, where k_{hX} is the capacity factor for the substituted aromatic solute and k_h is that for the parent aromatic hydrocarbon. Fig. 1 plots average values of $\log k_h$ for aromatic hydrocarbons *vs.* carbon number for the three bonded-phase columns (amino, diol and cyano). In order to determine $\log k_h$ for the parent naphthalene and benzene molecules (substituted aromatic solutes of this study and refs. 4 and 7), the lines in Fig. 1 were extrapolated to carbon numbers 10 and 6 respectively.

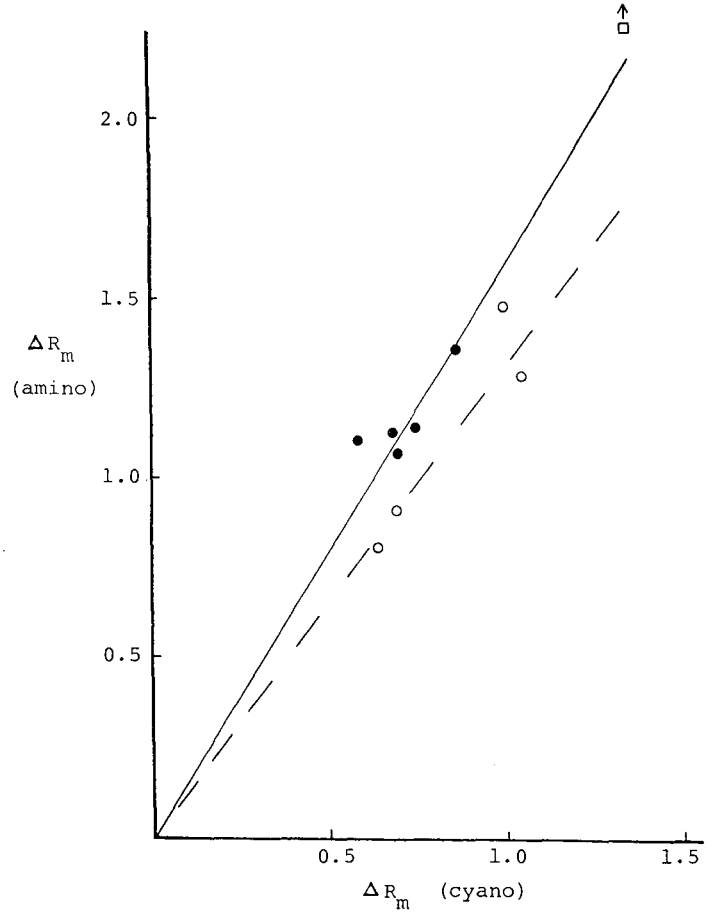

Fig. 2. Group retention values (ΔR_m) for amino *vs.* cyano columns. Regression data summarized in Table III; ——— = correlation curve for basic solutes (esters, ketones); – – – = correlation curve for dipolar solutes (nitriles and nitro compounds). ● = basic solutes; ○ = dipolar solutes; □ = benzyl alcohol.

TABLE IV

ANALYSIS OF REGRESSION LINES FROM ΔR_m DATA COMPARING AMINO, DIOL AND CYANO COLUMNS

	Slope (all solutes)	*2 × S.D.*[a]	*Slope*	
			Basic solutes[b]	*Dipolar solutes*[c]
Amino *vs.* cyano	1.4	0.127	1.60	1.32
Amino *vs.* diol	1.20	0.053	1.22	1.19
Cyano *vs.* diol	0.8	0.056	0.76	0.90

[a] Approximate 90% confidence.
[b] Esters and ketones.
[c] Nitro and nitrile compounds.

Experimental data for the cyano column are taken from our previous work[4]; data for the amino column are from the present study plus values from an earlier publication[7]; data for the diol column are from the present study. Table III summarizes group retention values, $\Delta R_m = (\log k_{hX} - \log k_h)$, for the three polar bonded-phase columns. In Figs. 2, 3 and 4, group retention values are plotted for the amino *vs.* cyano, amino *vs.* diol, and cyano *vs.* diol columns, respectively.

Linear regressions were performed on the data for all of the substituted aromatics on each column. In addition, the best straight line was obtained for the more basic compounds alone (esters and ketones), as well as for the more dipolar

TABLE V

RETENTION DATA FOR SUBSTITUTED AND UNSUBSTITUTED AROMATICS

Cyano column, 2-propanol–hexane mobile phase.

Solute	A_s	*log k'*					
		2-Propanol (%, v/v)					
		0	*0.1*	*0.2*	*0.4*	*0.8*	*1.4*
Chrysene	12.3	−0.268	−0.268	−0.276	−0.260	−0.301	−0.292
Perylene	12.8	−0.114	−0.149	−0.155	−0.167	−0.187	−0.229
Acetophenone	15.2	−0.155	−0.208	−0.215	−0.244	−0.244	−0.260
1-Cyanonaphthalene	16.5	0.000	0.000	−0.018	0.000	−0.027	0.000
Benzyl cyanide	15.5	0.230	0.204	0.204	0.204	0.176	0.176
m-Nitroacetophenone	22.7	0.342	0.301	0.279	0.279	0.255	0.230
1,3-Dinitronaphthalene	30.2	0.431	0.415	0.415	0.398	0.362	0.362
Benzyl alcohol	15.4	0.519	0.398	0.380	0.380	0.279	0.230
ε^0_{AB} [a]		(0.000)	0.002	0.002	0.002	0.004	0.004
ε^0_B [b]			0.25	0.21	0.16	0.14	0.11

[a] Calculated from eqn. 1 (benzyl alcohol data omitted).
[b] Calculated from eqn. 4.

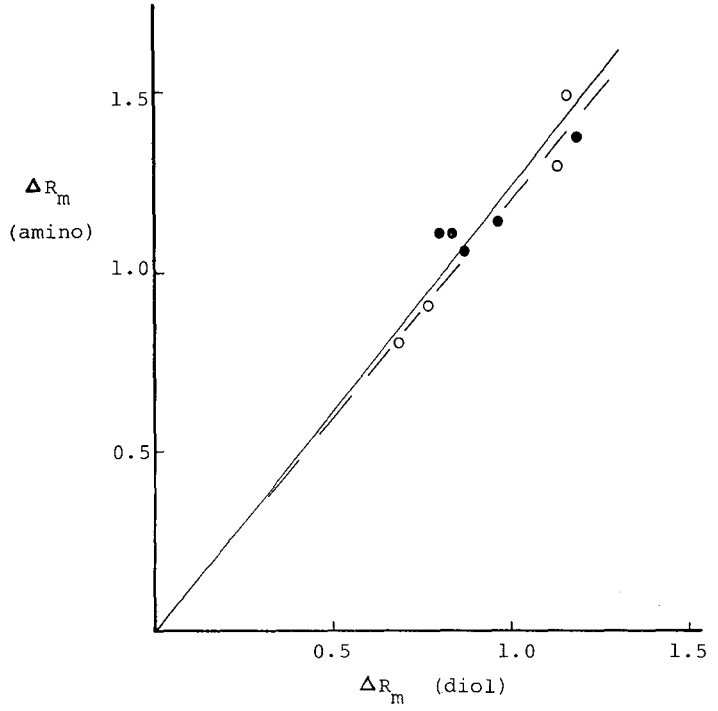

Fig. 3. Group retention values (ΔR_m) for amino *vs.* diol columns. See Fig. 2 for details.

1.8	*2.0*	*4.0*	*7.0*	*10*	*15*	*20*	*27*	*35*
−0.328	−0.357	−0.420	−0.441	−0.446	−0.509	−0.519	−0.54	−0.54
−0.260	−0.260	−0.319	−0.339	−0.370	−0.215	−0.429	−0.46	−0.47
−0.252	−0.208	−0.252	−0.362	−0.426	−0.449	−0.480	−0.52	−0.62
−0.027	−0.041	−0.076	−0.165	−0.223	−0.263	−0.308	−0.36	−0.45
0.114	0.127	0.083	0.021	−0.039	−0.104	−0.144	−0.24	−0.32
0.230	0.207	0.182	0.124	0.069	0.073	−0.034	−0.12	−0.18
0.301	0.310	0.250	0.201	0.148	0.077	0.031	−0.05	−0.10
0.079	0.030	−0.041	−0.253	−0.364	−0.427	−0.553	−0.60	−0.74
0.006	0.006	0.009	0.012	0.015	0.018	0.020	0.023	0.026
0.12	0.11	0.09	0.08	0.07	0.06	0.06	0.05	0.05

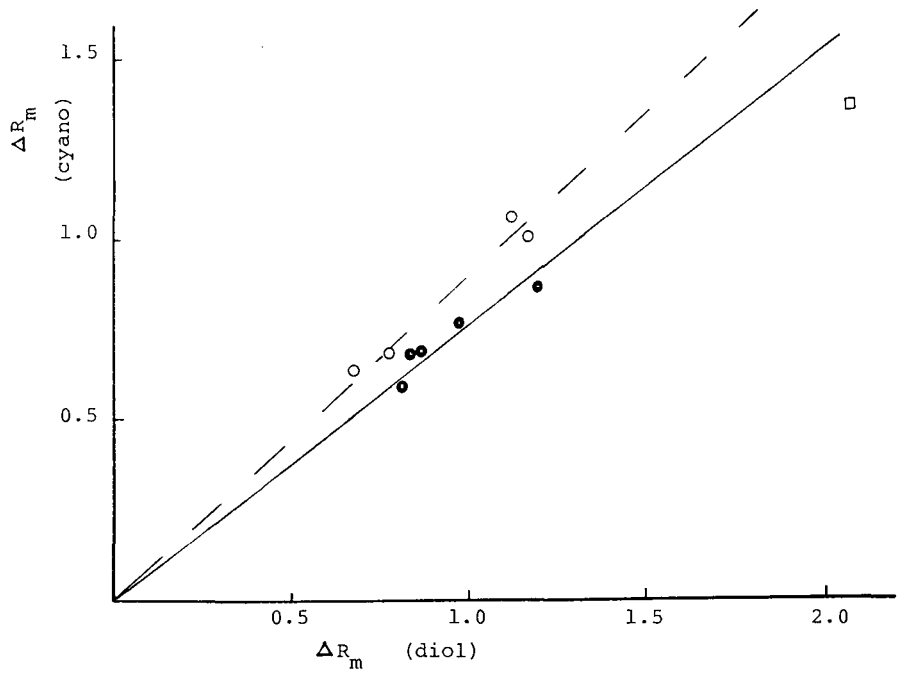

Fig. 4. Group retention values (ΔR_m) for cyano *vs.* diol columns. See Fig. 2 for details.

compounds alone (nitro and nitrile compounds)[a]. For the amino column *vs.* the cyano column (Fig. 2), there is increased retention of the more basic compounds compared with dipolar compounds (regression analysis indicates that these lines in Fig. 2 are independent, with greater than 90% confidence as summarized in Table IV).

The cyano column relative to the diol column shows increased retention of the more dipolar compounds compared with the more basic compounds (again regression analysis indicates the differences are significant to greater than 90% confidence). Finally, the amino column relative to the diol column shows greater retention of the more basic esters and ketones in comparison to the more dipolar nitro and nitrile compounds. However, these differences are less than noted above for the other columns and do not fall outside the 90% confidence limits.

On the basis of the comparisons of Table IV (summaries of Figs. 2–4), it appears that basic solutes are preferentially retained by the amino column, and dipolar solutes are preferentially retained by the cyano column, with the diol column exhibiting an intermediate behavior. However, the retention of proton donors, such as phenols and alcohols, was found by us to be strongest on the amino column. Thus the amino column gives generally stronger retention for *both* acidic and basic solutes. Our conclusions are hence in general agreement with those of Cooper and Smith[5,6,13].

Comparisons with silica. It has been noted previously (for less polar solutes and solvents) that retention on a cyano column shows similarities to retention on bare

[a] Solute basicity is best represented by the ratio β/π of ref. 14, equal to 0.5 for aromatic esters and ketones, and 0.3–0.4 for aromatic nitriles and nitrocompounds.

silica. Since the other polar bonded-phase columns correlate with retention on the cyano column, they also show similarities with silica. It is expected, however, that as the residual silanols on the bonded-phase columns are deactivated by stronger solvents, these similarities with silica will decrease.

The "strength" of a polar bonded-phase column strength *vs.* silica can be obtained by comparing the average value of $\Delta R_m = (\log k_{hX} - \log k_h)$ for that column *vs.* the average value of the group adsorption energy (Q_i) for silica (Table III). Based upon these average values, the strengths of the amino, diol and cyano columns are respectively, about 3.0-, 3.8- and 4.7-fold less than that of silica ($\alpha' = 0.7$). However, we have found significant variations in column strength from different manufacturers, and also batch-to-batch from the same supplier. In addition, we have found that column strength is critically dependent upon the solvents used in preparing the column. For example, cyano columns prepared in hexane were found to be significantly stronger than those prepared (by the manufacturer) in reversed-phase solvents. The same phenomenon has been noted with amino columns.

REFERENCES

1 L. R. Snyder, *LC, Mag. Liq. Chromatogr. HPLC*, 1 (1983) 478.
2 L. R. Snyder and J. J. Kirkland, *Introduction to Modern Liquid Chromatography*, Wiley-Interscience, New York, 2nd ed., 1979, Ch. 9.
3 L. R. Snyder, in Cs. Horváth (Editor), *High-performance Liquid Chromatography—Advances and Perspectives*, Vol. 3, Academic Press, New York, 1983, p. 157.
4 E. L. Weiser, A. W. Salotto, S. M. Flach and L. R. Snyder, *J. Chromatogr.*, 303 (1984) 840.
5 W. T. Cooper and P. L. Smith, *J. Chromatogr.*, 355 (1986) 57.
6 P. L. Smith and W. T. Cooper, *J. Chromatogr.*, 410 (1987) 249.
7 L. R. Snyder and T. C. Schunk, *Anal. Chem.*, 54 (1982) 1764.
8 W. E. Hammers, M. C. Spanjer and C. L. de Ligny, *J. Chromatogr.*, 174 (1979) 291.
9 W. E. Hammers, C. H. Kos, W. K. Brederode and C. L. de Ligny, *J. Chromatogr.*, 168 (1979) 9.
10 W. E. Hammers, A. G. M. Theeuwes, W. K. Brederode and C. L. de Ligny, *J. Chromatogr.*, 234 (1982) 321.
11 L. R. Snyder, *Principles of Adsorption Chromatography*, Marcel Dekker, New York, 1968, Ch. 8.
12 L. R. Snyder, *J. Chromatogr. Sci.*, 15 (1977) 441.
13 P. L. Smith and W. T. Cooper, *Chromatographia*, 25 (1988) 55.
14 J. H. Park, P. W. Carr, M. H. Abraham, R. W. Taft, R. M. Doherty and M. J. Kamlet, *Chromatographia*, 25 (1988) 373.

Journal of Chromatography, 498 (1990) 67–79
Elsevier Science Publishers B.V., Amsterdam — Printed in The Netherlands

CHROM. 21 966

(*S*)-*thio*-DNBTYR-A AND (*S*)-*thio*-DNBTYR-E AS CHIRAL STATIONARY PHASES FOR ANALYTICAL AND PREPARATIVE PURPOSES

APPLICATION TO THE ENANTIOMERIC RESOLUTION OF ALKYL N-ARYLSULPHINAMOYL ESTERS

L. SIRET
Laboratoire de Chimie Analytique de l'École Supérieure de Physique et Chimie Industrielles de Paris, 10 rue Vauquelin, 75231 Paris Cedex 05 (France)
A. TAMBUTÉ
Direction des Recherches et Études Techniques, Centre d'Études du Bouchet, BP No. 3, Le Bouchet, 91710 Vert-le-Petit (France)
and
M. CAUDE* and R. ROSSET
Laboratoire de Chimie Analytique de l'École Supérieure de Physique et Chimie Industrielles de Paris, 10 rue Vauquelin, 75231 Paris Cedex 05 (France)
(First received July 3rd, 1989; revised manuscript received September 5th, 1989)

SUMMARY

The enantiomeric separation of *tert.*-butyl N-arylsulphinamoyl esters, which are chiral compounds of biological interest, was investigated on three chiral stationary phases (CSPs): (*R*)-DNBPG, (*S*)-*thio*-DNBTyr-A and (*S*)-*thio*-DNBTyr-E. (*S*)-*thio*-DNBTyr-A exhibits the greatest enantiorecognition ability towards these solutes, allowing the extension of chiral separation to the preparative scale. Chiral recognition mechanisms are discussed. They involve several parameters, *e.g.*, the nature of the polar modifier used in the mobile phase, the π-basicity of the solute, the number of sites of interaction on the CSP and the steric hindrance due to the silica matrix.

INTRODUCTION

Chiral stationary phases (CSPs) derived from N-(3,5 dinitrobenzoyl)amino acids are widely used for chromatographic chiral separations on both analytical and preparative scales[1–3]. They include the well known (*R*)-DNBPG, derived from (*R*)-phenylglycine, designed by Pirkle *et al.*[4]. The wide scope of application of these CSPs probably results from the various potential sites of interactions occurring in the vicinity of the asymmetric centre. Chiral recognition mechanisms involved with these CSPs have been extensively studied[1–3], and the results indicate that small structural changes in the CSPs have significant effects on chromatographic behaviour[5–7].

Recently, we developed two novel π-acid CSPs derived from (*S*)-tyrosine[7–9]. In comparison with (*R*)-DNBPG, the original features of these CSPs result from the

0021-9673/90/$03.50

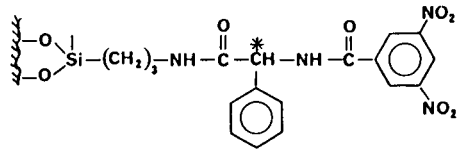

(R); CSP I [(R)-DNBPG]

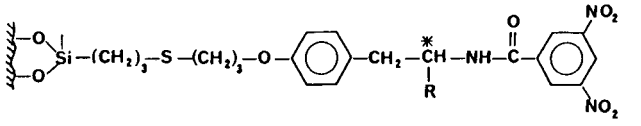

(S); CSP 2a: R = —C(=O)—O—CH$_3$ [(S)-thio-DNBTyr—E]

(S); CSP 2b: R = —C(=O)—NH—(CH$_2$)$_3$—CH$_3$ [(S)-thio-DNBTyr—A]

Fig. 1. Structure of CSPs.

grafting mode: (*S*)-tyrosine is bound to silica gel via its hydroxyl group, thus allowing the introduction of various functional groups on its carbonyl moiety *e.g.*, methyl ester [(*S*)-*thio*-DNBTyr-E] or *n*-butylamide [(*S*)-*thio*-DNBTyr-A](see Fig. 1). Both CSPs exhibit different behaviour. So far, for a few series of compounds including sulphoxides, phosphine oxides and lactams of pharmaceutical interest, we have found that (*S*)-*thio*-DNBTyr-E displays the widest range of application, whereas (*S*)-*thio*-DNBTyr-A exhibits a greater selectivity[7,8]. In comparison with (*R*)-DNBPG, which is bound to silica via an aminopropyl spacer, (*S*)-*thio*-DNBTyr-A possesses a longer spacer arm, the asymmetric centre then being removed further from the silica matrix whose steric effect is minimized. Consequently, the chromatographic behaviour of these CSPs is expected to be different. Very recently, Pirkle and Burke[10] employed the grafting mode chosen for (*S*)-*thio*-DNBTyr-A again in order to design a novel CSP.

By designing these two novel CSPs we aimed to extend the scope of application of Pirkle-type CSPs. This objective was applied to separate a family of compounds with the general formula $ArNHSOCR_1R_2COOC(CH_3)_3$, named *tert.*-butyl N-arylsulphinamoyl esters. These compounds act as specific inhibitors of coniferyl alcohol dehydrogenase (CADH), a zinc metalloenzyme involved in the lignification process of plants[11,12]. The synthesis and physico-chemical properties of these compounds were initially described by Cazaux and co-workers[13–17].

In this paper we report the direct enantiomeric separation of a series of *tert.*-butyl N-arylsulphinamoyl esters on (*R*)-DNBPG, (*S*)-*thio*-DNBTyr-A and (*S*)-*thio*-DNBTyr-E. Some insights into the chiral recognition mechanisms are also given and

the chromatographic and structural parameters that may affect them are evaluated. In addition, an example of preparative chiral chromatography is presented.

EXPERIMENTAL

Apparatus

For liquid chromatography, a modular liquid chromatograph (Gilson, Villiers-le-Bel, France) equipped with a Shimadzu C-R4A integrator (Touzart et Matignon, Vitry-sur-Seine, France), was used. The standard operating conditions were flow-rate 2 ml/min and room temperature.

Preparative chromatography was performed with a Modulprep apparatus (Jobin-Yvon, Longjumeau, France). The chiral stationary phase [200 g of (*S*)-*thio*-DNBTyr-A, $d_p = 7$ μm][7] was packed into the column (260 × 40 mm I.D.) by axial compression under 15 bar. UV detection was carried out at 254 nm with a variable-wavelength detector (190–370 nm) (Jobin-Yvon). The preparative chromatograph was operated at room temperature. The eluent inlet pressure was about 11 bar, which gave a flow-rate of *ca.* 42 ml/min.

Chiral stationary phases

The structures of the CSPs are given in Fig. 1. CSP 1 [(*R*)-DNBPG, $d_p = 5$ μm] is a Pirkle covalent column (250 × 4.6 mm I.D.) commercially available from J. T. Baker (Sochibo, Velizy-Villacoublay, France).

General procedures for the synthesis of CSP 2a and 2b derived from (*S*)-tyrosine were given in a previous paper[7]. The CSPs were obtained starting from LiChrosorb Si-60 silica gel (5 μm) (Merck, Darmstadt, F.R.G.) modified with γ-mercaptopropyltrimethoxysilane (Fluka, Buchs, Switzerland)[7]. They were packed into 150 × 4.6 mm I.D. stainless-steel columns by the classical slurry technique under 400 bar using ethanol as pumping solvent.

Mobile phase

Ethanol, isopropanol and hexane were of LiChrosolv grade (Merck) and chloroform and methylene chloride were of analytical-reagent grade (Prolabo, Paris, France).

Solutes

The structures of the *tert.*-butyl N-arylsulphinamoyl esters (**1a–d**, **2a** and **b**) are given in Table I. Samples of these compounds were given by Professor L. Cazaux (Laboratoire de Synthese et de Physicochimie Organique, Université Paul Sabatier, Toulouse, France).

RESULTS AND DISCUSSION

Chromatographic data are given in Table II. For each polar modifier, its concentration (%) in the mobile phase, the selectivity value (α) and the capacity factor for the most retained enantiomer (k'_2) are reported.

TABLE I

STRUCTURE OF TEST SOLUTES

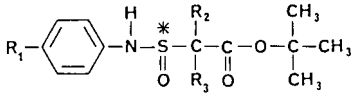

Compound	R_1	R_2	R_3
1a	NO_2	H	H
1b	CF_3	H	H
1c	Cl	H	H
1d	OCH_3	H	H
2a[a]	H	H	CH_3
2b	H	CH_3	CH_3

[a] Two asymmetric centres.

Influence of the nature of the mobile phase

Solvents were chosen according to their dominant character with regard to the selectivity parameters χ_e, χ_d and χ_n (Table III)[18]. These parameters reflect the relative ability of a solvent to act mainly as a proton acceptor (ethanol, isopropanol), a proton donor (chloroform) or a strong dipole (methylene chloride).

According to chromatographic data (Table II), polar modifiers can be classified into two groups: alcohols and chlorinated solvents. Chlorinated solvents exhibit a greater selectivity towards these solutes whereas the efficiency is higher when using alcohols, especially ethanol. This may be correlated with the fact that polar groups on CSPs are more easily solvated by alcohols than by chlorinated solvents. Therefore, CSP–solute interactions are maximized when using chlorinated solvents (higher selectivity) but the adsorption–desorption kinetics of solutes on CSPs are slower (weaker efficiency).

Improvement of the separation of solute **1d** was achieved on CSP 2b by optimizing the mobile phase composition, as reported previously for sulphoxides[19]. A ternary hexane–ethanol–chloroform mobile phase was prepared starting from hexane–ethanol (92:8, v/v; solvent A) and hexane–chloroform (50:50, v/v; solvent B) binary mixtures (Fig.2). The concave profile of the capacity factor curves is in agreement with that obtained by Pescher *et al.*[20], according to whom the following explanations can be suggested to account for this profile: (a) like the phosphine oxides studied by Pescher *et al.*, *tert.*-butyl N-arylsulphinamoyl esters are highly soluble in chloroform; and (b) ethanol molecules are strongly adsorbed on CSPs and are not easily displaced by chloroform molecules.

Starting from a hexane–ethanol binary mixture, when a small amount of chloroform is added to the mobile phase the solubility of the solute increases according to (a), whereas following (b) the chloroform displaces only a few ethanol molecules which still hinder CSP–solute interactions. Hence this leads to a decrease in k' values. This accounts for the descending left-hand part of the curve. On the other hand, starting from a hexane–chloroform binary mixture, according to (b), as soon as a few ethanol molecules are added they will be preferentially adsorbed on the CSP, making

TABLE II

SEPARATION OF *tert*-BUTYL N-ARYLSULPHINAMOYL ESTERS USING DIFFERENT POLAR MODIFIERS

% = Percentage polar modifier; k'_2 is the capacity factor of the second-eluted enantiomer, $k'_2 = (t_{R_2}/t_0) - 1$, where t_{R_2} is the retention time of the last-eluted enantiomer and t_0 the retention time of a non-retained solute. The selectivity, α, between two enantiomers is the ratio of their respective capacity factors (k'_1/k'_2). Operating conditions: flow-rate, 2 ml/min; room temperature; mobile phase, the percentage (v/v) of polar modifier in *n*-hexane is given; UV detection at 260 nm.

Polar modifier	*Solute*	*CSP 1 [(R)-DNBPG]*			*CSP 2a [(S)-thio-DNBTyr-E]*			*CSP 2b [(S)-thio-DNBTyr-A]*		
		(%)	α	k'_2	*(%)*	α	k'_2	*(%)*	α	k'_2
Ethanol	**1a**	20	NR[a]	1.97	15	NR	7.30	5	1.72	27.01
	1b	2.5	1.04	2.72	5	1.05	3.13	5	1.48	3.96
	1c	2.5	1.10	3.46	5	1.12	4.70	5	1.54	6.05
	1d	2.5	1.13	7.13	5	1.17	9.25	5	1.64	12.08
	2a	2.5	1.21	2.59	5	1.14	3.18	5	1.45	3.97
	2b	2.5	1.22	2.26	5	1.24	3.27	5	1.54	3.84
Isopropanol	**1a**	20	NR	2.76	15	NR	13.89	7	1.40	14.80
	1b	4.5	1.09	2.22	7	1.10	2.20	7	1.72	3.61
	1c	4.5	1.13	2.92	7	1.11	3.36	7	1.77	5.76
	1d	4.5	1.17	7.08	7	1.22	7.48	7	1.88	12.21
	2a	4.5	1.30	2.28	7	1.23	2.78	7	1.63	3.73
	2b	4.5	1.32	2.05	7	1.44	3.35	7	1.77	3.98
Chloroform	**1a**	50	NR	5.19	50	NR	6.43	50	1.50	11.86
	1b	20	NR	2.41	50	1.37	2.38	50	1.97	5.55
	1c	20	NR	3.31	50	1.42	3.19	50	2.04	6.28
	1d	50	1.21	7.58	50	1.45	3.66	50	2.06	5.77
	2a	30	1.23	6.38	30	1.42	5.51	30	1.82	8.45
	2b	30	1.23	6.16	30	1.64	4.47	30	1.83	5.10
Methylene chloride	**1a**	50	NR	3.22	50	1.12	7.63	50	1.54	13.15
	1b	30	NR	1.17	50	1.26	2.94	50	2.00	7.18
	1c	30	NR	2.02	50	1.28	4.14	50	2.00	8.88
	1d	30	NR	1.62	50	1.27	5.16	50	2.00	8.44
	2a	50	1.20	7.25	50	1.35	2.33	50	1.89	4.17
	2b	50	1.15	4.16	50	1.55	1.75	50	1.75	2.21

[a] NR = No resolution, $\alpha = 1$

TABLE III

SELECTIVITY PARAMETERS, AS DEFINED AND CALCULATED BY SNYDER[18] FROM SOLUBILITY DATA REPORTED BY ROHRSCHNEIDER

Values in italics indicate the dominant character of the solvent: χ_e (proton acceptor), χ_d (proton donor), χ_n (strong dipole).

Polar modifier	χ_e	χ_d	χ_n
Ethanol	*0.52*	0.19	0.29
Isopropanol	*0.55*	0.19	0.27
Chloroform	0.25	*0.41*	0.33
Methylene chloride	0.29	0.18	*0.53*

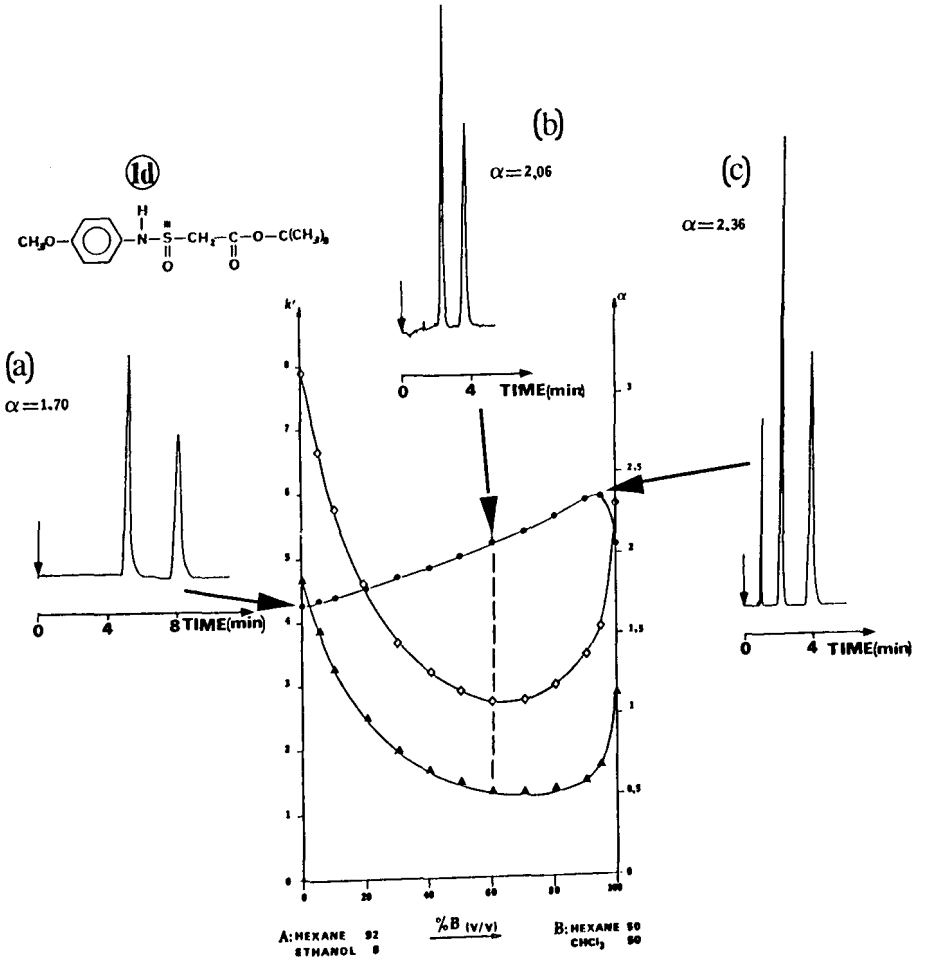

Fig. 2. Ternary optimization for compound **1d** on CSP 2b using hexane–ethanol (92:8, v/v; solvent A) and hexane–chloroform (50:50, v/v; solvent B) binary eluents. The capacity factors, k'_1 (▲) and k'_2 (◇), and the selectivity, α (●), are plotted *versus* the content of binary mixture B in the ternary mixture A–B. Flow-rate, 2 ml/min; room temperature; UV detection at 260 nm. (a) Mobile phase A 100%, $k'_1 = 4.66$, $k'_2 = 7.92$, $\alpha = 1.70$; (b) mobile phase A–B (40:60), $k'_1 = 1.30$, $k'_2 = 2.68$, $\alpha = 2.06$; (c) mobile phase A–B (5:95), $k'_1 = 1.64$, $k'_2 = 3.87$, $\alpha = 2.36$.

CSP–solute interactions more difficult and, as a consequence, decreasing the k' values (right-hand part of the curve). Consequently, the curve showing k' *versus* the ternary mixture composition passes through a minimum value corresponding to the highest resolution value per unit time (Fig. 2b).

The selectivity value shows a linear increase with increasing chloroform content with a maximum corresponding to a mobile phase containing 95% of B.

Influence of the CSP structure

According to the chromatographic data (Table II), CSP 2b exhibits the greatest selectivity towards this family of solutes. As an example, Fig. 3 shows the difference in

selectivity between the three CSPs for compound **1b** when using chloroform in the mobile phase.

CSPs 1 and 2b have the same number of potential sites of interaction. Nevertheless, in order to obtain the same retention times on these CSPs, the elution strength of the mobile phase should be weaker when using CSP 1 (see Table II). CSP–solute interactions are thus weaker on CSP 1 than on CSP 2b. The removal of the chiral centre away from the silica matrix in CSP 2b compared with CSP 1 makes the CSP 2b chiral graft more accessible to the solute. This also accounts for the weaker selectivity values observed on CSP 1 (see Fig. 4).

On the other hand, CSP 2a and CSP 2b differ only in an aliphatic amide dipole (dipole B, framed in Fig. 4) instead of an ester group. The differences in both selectivity and retention between these two CSPs may result from a CSP–solute interaction involving dipole B (acidic character) and the ester group of the solute (basic character) (see Fig. 4, interaction 3).

The elution order for compound **1d** was established on these three CSPs starting from a racemate enriched with the most retained enantiomer on CSP 2b. No inversion of elution order occurred on any CSP on changing the nature of the polar modifier of the mobile phase. This was also true on comparing CSP 2 types, whereas an inversion of elution order was observed on changing from CSP 2b to CSP 1 with

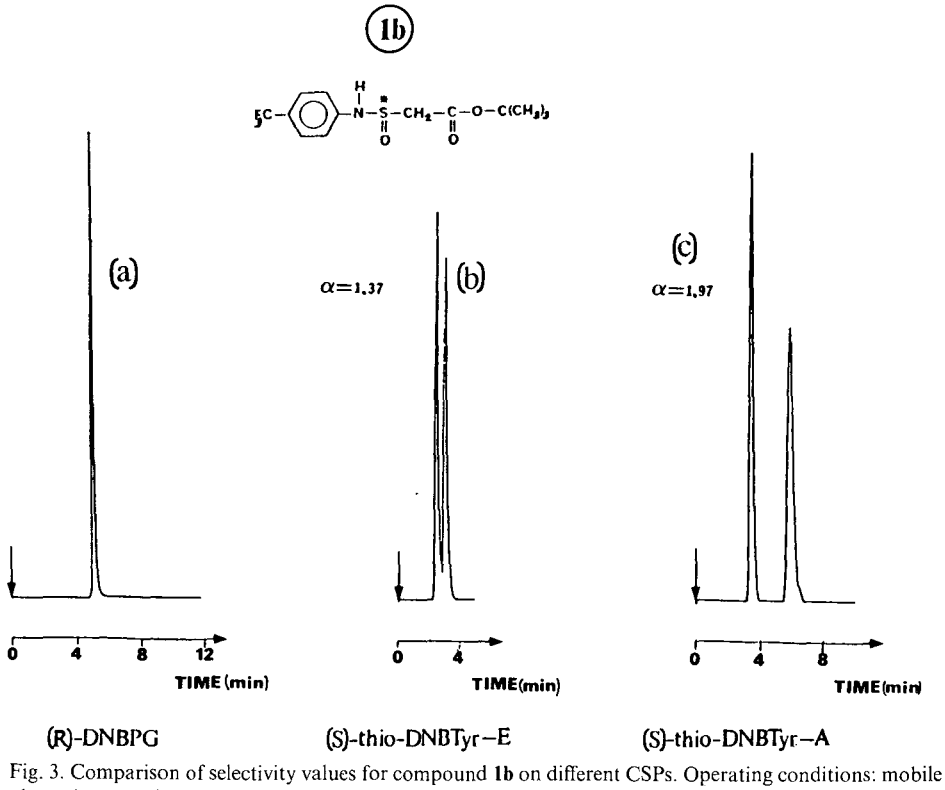

Fig. 3. Comparison of selectivity values for compound **1b** on different CSPs. Operating conditions: mobile phase, hexane–chloroform (50:50) [except for (a) (80:20)]; flow-rate, 2 ml/min; room temperature; UV detection at 260 nm.

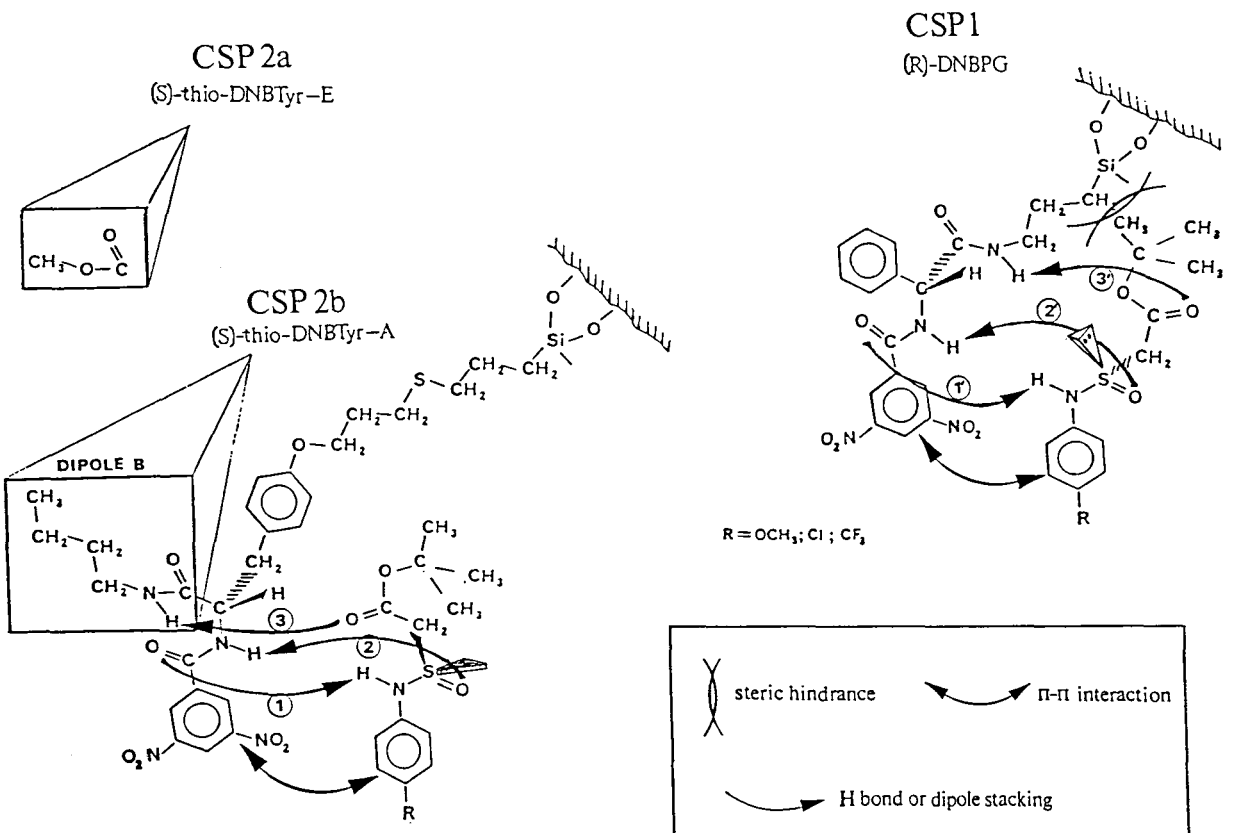

Fig. 4. Proposed chiral recognition model for compounds **1b–d**. (a) CSP 2b. The most strongly retained enantiomer is represented. (b) CSP 2a. The hydrogen bonding between the amide dipole B and the carbonyl moiety of the solute is cancelled, leading to a loss of selectivity. (c) CSP 1. Compared with CSP 2b, the CSP–solute interactions are sterically hindered by the *tert.*-butyl moiety of the solute and the silica matrix. The most retained enantiomer is opposite to that on CSP 2b according to the experimental results.

ethanol, isopropanol or chloroform (no resolution occurred for compound **1d** on CSP 1 when using methylene chloride as polar modifier).

Influence of the aromatic ring substituent

It is now well established that the π–π interaction occurring between the 3,5-dinitrobenzoyl moiety of a Pirkle-type CSP and a racemate possessing a complementary π-basic character may contribute to the chiral recognition process[1–3]. Nevertheless, this is not always the main directional attractive interaction, as the resolution of π-acid solutes on π-acid CSPs has already been reported[8,9], thus emphasizing the importance of dipole stackings and/or hydrogen bondings in the chiral recognition process.

Compounds **1a–d** differ only in the nature of their aromatic ring substituent, which can be either electron-withdrawing (NO_2, CF_3, Cl) or electron-donating (OCH_3). These substituents can be characterized by their Hammet σ_H value. The more electron-withdrawing an aromatic ring substituent is, the higher is the value assigned to it. The Hammet σ_H values given in Table IV were taken from ref. 22.

In Fig. 5 the logarithm of selectivity values of compounds **1a–d** on CSP 2b are plotted *versus* the Hammet σ_H values of their substituents. The selectivity values of compounds **1b–d** show a good linear decrease with σ_H values when using ethanol ($R = 0.9998$) or isopropanol ($R = 0.9975$). The chiral recognition mechanism probably involves a π–π interaction as the difference in energy between the two CSP–enantiomer transient complexes (represented by log α) is proportional to the π-basic character of the solute (represented by σ_H) (see Fig. 4). On the other hand, when using chlorinated solvents, the π–π interaction does not appear to be as stereoselective as with alcohols. The amide dipoles of the CSP are less solvated with chlorinated solvents, and consequently interactions involving these amide dipoles are stronger when using these solvents. It can be assumed that the π–π interaction is of lesser importance in comparison with hydrogen bonding or dipole–dipole interactions.

Compound **1a** displays a different behaviour compared to **1b–d**. The selectivity values obtained for this compound are much weaker except when using ethanol as the polar modifier (Fig. 5). Owing to the very strong electron-withdrawing effect of the nitro substituent, this compound has a π-acid character. A π-donor–acceptor interaction can no longer be considered for this compound on π-acid CSPs. Only dipole–dipole interactions, hydrogen bondings or steric effects govern the chiral recognition process. The chromatographic results are in good agreement with those obtained by Lienne *et al.*[8] on π-acid solutes: CSP 2a, which contains only one amide dipole, displays lower selectivity values than CSP 2b. From Table II, it can be inferred that

TABLE IV

HAMMET σ_H VALUES ACCORDING TO REF. 21

Solute	*Substituent*	σ_H
1a	NO_2	0.778
1b	CF3	0.551
1c	Cl	0.227
1d	OCH_3	−0.268

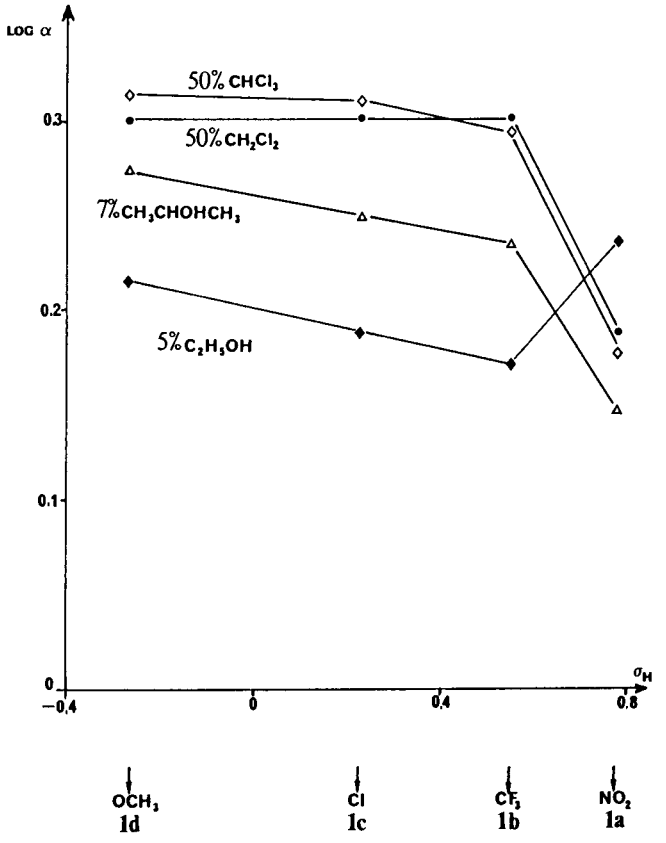

Fig. 5. Variation of log α with Hammet σ_H values for compounds **1a–d** on CSP 2b using hexane–polar modifier mobile phases.

enantiorecognition of compound **1a** is based on an interaction involving dipole B of CSP 2b.

A similar study was carried out by Wainer and Alembik[22], who studied the influence of π-basicity on the separation of aromatic amides on (*R*)-DNBPG. The results were different from those reported above because the electronegativity of the *para* substituent seemed to have very little effect on the stereoselectivity.

Influence of steric bulk at the asymmetric centre

Compounds **2a** and **2b** (Table I) differ only in the number of methyl substituents near the asymmetric centre. Table II shows that, as a general rule, they are less retained on any CSP than compounds **1a–d**. The steric hindrance due to methyl substituents probably weakens the CSP–solute **2a** and **b** interactions.

The variation of selectivity values for compounds **2a** and **b** differs with the CSP structure. According to Table II, the selectivity increases with steric hindrance on CSP 2a whereas it decreases on CSP 2b. The dipole B–solute interaction (3 in Fig. 4) is probably sterically hindered (weaker selectivity values on CSP 2b). On the other hand, steric hindrance which does not alter any CSP–solute interaction of CSP 2a

allows an increase in chiral recognition. Equivalent attractive interactions can be suggested between either the less or the most retained enantiomer and this CSP, but with regard to the less stable diastereoisomeric complex these interactions may confer an energetically disfavoured conformation on the solute enantiomer. Repulsive CSP–less retained enantiomer interactions may account for chiral discrimination.

Application to preparative-scale chromatography

Biological studies on these compounds were previously carried out using racemates as their enantiomeric separation had never been performed. By extending their analytical separation to the preparative scale, we aimed to isolate the optically pure enantiomers in order to allow biological studies to be carried out.

The high stability of this type of CSP allows their use for preparative-scale applications. A preparative separation of compound **1d** was carried out on 200 g of (*S*)-*thio*-DNBTyr-A. The mobile phase composition was determined from analytical optimization data: hexane–isopropanol (85:15, v/v) with $\alpha = 1.83$ and $k'_2 = 5.78$. The selectivity could be improved by using chlorinated polar modifiers ($\alpha = 2$), but the resolution factor was the same as with isopropanol owing to a lower efficiency. These chromatographic conditions allowed the injection of 200 mg of racemate **1d** per run.

Fig. 6 shows a preparative-scale separation of 200 mg of compound **1d**. Fractions 1 and 2 from different runs were pooled, evaporated and the final products were crystallized from hexane–diisopropyl ether. The first-eluted enantiomer was obtained with 100% enantiomeric excess (e.e.), monitored on analytical CSP 2b (Fig. 6, chromatogram 1; m.p. 107°C; $[\alpha]^{22}_D = +144°$ [c = 1, tetrahydrofuran (THF), 22°C]. The

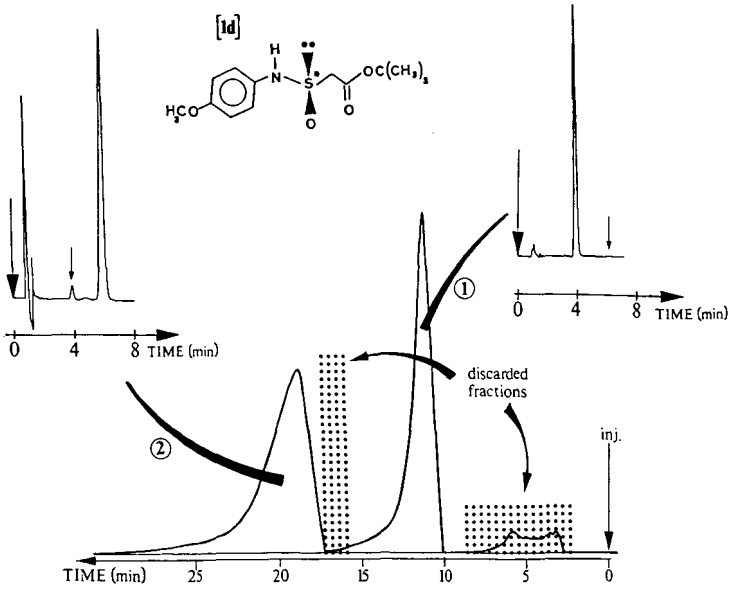

Fig. 6. Preparative-scale resolution of 200 mg of compound **1d** on 200 g of CSP 2b. Operating conditions: mobile phase, hexane–isopropanol (85:15, v/v); flow-rate, 42 ml/min; UV detection at 254 nm. The enantiomeric purity of the collected fractions was checked on an analytical column (CSP 2b). Operating conditions: mobile phase, hexane–ethanol (85:15, v/v); flow-rate, 2ml/min; UV detection at 260 nm.

most retained enantiomer was obtained with 95.8% e.e.; m.p. 102–103°C. Unfortunately, it was impossible to measure the rotatory power of this enantiomer; when it was dissolved in various solvents such as chloroform or THF, a brown precipitate rapidly appeared. For the first-eluted enantiomer, the same effect occurred but more slowly, thus allowing the determination of the rotatory power.

CONCLUSION

(*S*)-*thio*-DNBTyr-A allows the separation of the enantiomers of *tert.*-butyl N-arylsulphinamoyl esters on both analytical and preparative scales. This study shows, once again, that small changes in the chemical structure of the CSP may induce a significant enhancement of enantiorecognition ability. The binding mode of (*S*)-*thio*-DNBTyr-A allows the asymmetric centre to be away from the silica matrix, making the formation of transient CSP–bulky solute complexes easier in comparison with (*R*)-DNBPG.

The differences between alcohols and chlorinated solvents used as polar modifiers in the mobile phase may be correlated with their aptitudes to solvate amide dipoles on CSPs, thus exhibiting either a good efficiency (alcohols) or a good selectivity (chlorinated solvents).

The results also show the increase in selectivity with the π-basic character of the solute and the involvement of dipole B of (*S*)-*thio*-DNBTyr-A in the chiral recognition process. Spectroscopic studies would probably provide complementary information to the chromatographic data.

ACKNOWLEDGEMENT

The authors express their grateful thanks to Dr. L. Cazaux for the gift of the solutes which prompted us to initiate this work.

REFERENCES

1 M. Lienne, M. Caude, R. Rosset and A. Tambuté, *Analusis*, 15(9) (1987) 431.
2 J. M. Finn, in M. Zief and L. J. Crane (Editors), *Chromatographic Chiral Separations* (*Chromatographic Science Series*, Vol. 40), Marcel Dekker, New York, 1988, p. 53.
3 P. Macaudiere, M. Lienne, A. Tambuté and M. Caude, in A. M. Krstulovic (Editor), *Chiral Separation by HPLC: Applications of compounds of Pharmaceutical Interest*, Ellis Horwood, Chichester, 1989, pp. 399–445.
4 W. H. Pirkle, D. W. House and J. M. Finn, *J. Chromatogr.*, 192 (1980) 143.
5 W. H. Pirkle, A. Tsipouras and T. J. Sowin, *J. Chromatogr.*, 319 (1985) 392.
6 S. K. Yang, M. Mushtaq and P. P. Fu, *J. Chromatogr.*, 371 (1986) 195.
7 A. Tambuté, A. Bégos, M. Lienne, P. Macaudiere, M. Caude and R. Rosset, *New J. Chem.*, 13 (1989) 625.
8 M. Lienne, P. Macaudiere, M. Caude, R. Rosset and A. Tambuté, *Chirality*, 1 (1989) 45.
9 P. Macaudiere, M. Lienne, M. Caude, R. Rosset and A. Tambuté, *J. Chromatogr.*, 467 (1989) 357.
10 W. H. Pirkle and J. A. Burke, *Chirality*, 1 (1989) 57.
11 F. Sarni, C. Grand and A. M. Boudet, *Eur. J. Biochem.*, 139 (1984) 259.
12 C. Grand, F. Sarni and A. M. Boudet, *Planta*, 163 (1985) 232.
13 M. Baltas, L. Cazaux, A. De Blic, L. Gorrichon and P. Tisnes, *J. Chem. Res. Synop.* (1988) 284.
14 A. de Blic, L. Cazaux, L. Gorrichon-Guigon and M. Perry, *Synthesis*, (1982) 282.
15 M. Baltas, L. Cazaux, L. Gorrichon-Guigon, P. Maroni and P. Tisnes, *Tetrahedron Lett.*, 26 (1985) 4447.

16 M. Baltas, J. D. Bastide, A. De Blic, L. Cazaux, L. Gorrichon-Guignon, P. Maroni, M. Perry and P. Tisnes, *Spectrochim. Acta, Part A*, 41 (1985) 789.
17 M. Baltas, J. D. Bastide, L. Cazaux, L. Gorrichon-Guigon, P. Maroni and P. Tisnes, *Spectrochim. Acta, Part A*, 41 (1985) 793.
18 L. R. Snyder, *J. Chromatogr. Sci.*, 16 (1978) 223.
19 M. Lienne, M. Caude, R. Rosset, A. Tambuté and P. Delatour, *Chirality*, 2 (1989) 142.
20 P. Pescher, M. Caude, R. Rosset and A. Tambuté, *J. Chromatogr.*, 371 (1986) 159.
21 O. A. Reutov, in T. J. Katz (Editor), *Fundamentals of Theoretical Organic Chemistry*, Appleton Century Crofts, New York, 1967, p. 365.
22 I. W. Wainer and M. C. Alembik, *J. Chromatogr.*, 367 (1986) 59.

Journal of Chromatography, 498 (1990) 81–91
Elsevier Science Publishers B.V., Amsterdam — Printed in The Netherlands

CHROM. 21 996

DIRECT LIQUID CHROMATOGRAPHIC SEPARATION OF ENANTIOMERS ON IMMOBILIZED PROTEIN STATIONARY PHASES

VIII. A COMPARISON OF A SERIES OF SORBENTS BASED ON BOVINE SERUM ALBUMIN AND ITS FRAGMENTS

SHALINI ANDERSSON* and STIG ALLENMARK

**IFM/Department of Chemistry, University of Linköping, S-581 83 Linköping (Sweden) and Laboratory of Microbiological Chemistry, University of Göteborg, Guldhedsgatan 10A, S-413 46 Göteborg (Sweden)*

PER ERLANDSSON

Department of Technical Analytical Chemistry, Chemical Center, University of Lund, P.O. Box 124, S-221 00 Lund (Sweden)

and

STAFFAN NILSSON[a]

Department of Medical Chemistry 4, University of Lund, P.O. Box 94, S-221 00 Lund (Sweden)

(First received May 17th, 1989; revised manuscript received September 15th, 1989)

SUMMARY

A mixture of three peptides (M_r 38 000), obtained by enzymatic cleavage of bovine serum albumin (BSA) was isolated, immobilized to silica and used as a chiral stationary phase in liquid chromatography. A comparison of sorbents containing these fragments and intact BSA, showed that the enantioselectivity is preserved for only a limited number of compounds. Under identical mobile phase conditions, retention on the columns based on BSA fragments was also much lower than on those containing intact BSA.

The method used for immobilization has a great influence on the retentive and enantioselective properties of the sorbent obtained. When sorbents based on BSA entrapped in silica and 3-aminopropylsilica, by cross-linking with glutaraldehyde were compared under identical mobile phase conditions, the latter were generally found to give larger capacity factors and often also larger α values.

These results indicate that the increased hydrophobicity, primarily caused by the aminopropyl groups, partly contributes to the overall retention and chiral discrimination process and that the situation may be different from that in a solution of the free protein.

INTRODUCTION

The enantioselectivity exerted by biopolymers,such as proteins, has been utilized in the development of chiral stationary phases (CSPs) for use in liquid chromato-

[a] Present address: Euro-fassel AB, University Site, Ole Römersväg 12, S-223 70 Lund, Sweden.

0021-9673/90/$03.50

graphy[1]. Bovine serum albumin (BSA), immobilized to silica by various techniques[2–5], has been shown to act as a chiral discriminator for a variety of racemic organic compounds in aqueous buffers. A different approach for the immobilization of BSA has been developed, whereby derivatized silica is used for the entrapment of the protein within the silica pores by cross-linking with glutaraldehyde.

Recent investigations have indicated that only a limited number of ligand-binding sites are involved in the chiral discrimination process[6]. To gain further insight into the relationship between the solute structure and enantioselectivity, N-terminal peptic fragments (M_r 38 000) of BSA were also immobilized.

EXPERIMENTAL

Chemicals

Racemic tryptophan (**I**), kynurenine [3-(2-aminobenzoyl)-alanine] (**II**) and mandelic acid (**III**) were obtained from Sigma (St. Louis, MO, U.S.A.). Oxazepam (**IV**) and ibuprofen (**V**) were obtained from the Department of Drug Control, Biomedical Centre, Uppsala, Sweden. The synthesis of N-(2,4-dinitrophenyl)-(DNP-)aspartic acid (**VI**) was performed as described previously[7]. The sulphoxide omeprazol (**VII**) was a gift from Hässle (Mölndal, Sweden), as was warfarin (**VIII**) from Ferrosan (Malmö, Sweden). Morpholep [1-(morpholinomethyl)-3-methyl-3-phe-

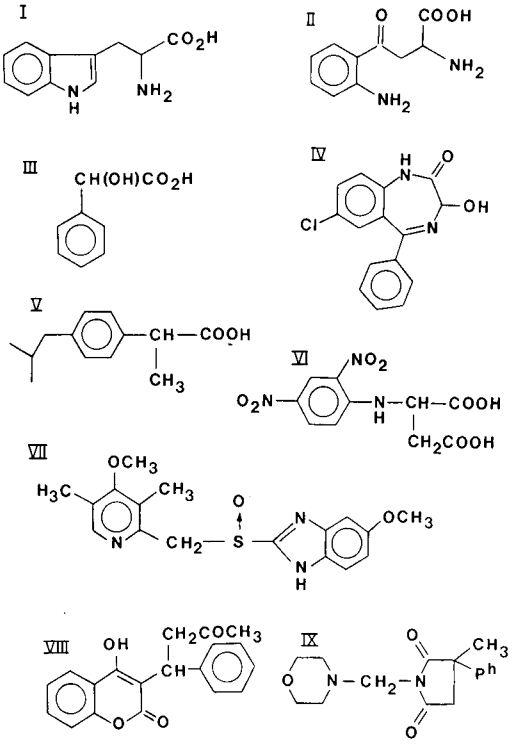

Scheme 1. Structures of the compounds investigated.

nylsuccinimide] (**IX**) was kindly provided by Dr. J. Bojarski (Krakow, Poland). The structure of compounds **I–IX** are given in Scheme 1. Benzoin and the substituted benzoins (**Xa–f**) were kindly supplied by Dr. O. Weller (University of Hamburg, F.R.G.).

Bovine serum albumin (BSA) (Art. A7030) was obtained from Sigma (St. Louis, MO, U.S.A.). The spherical silica used was from Macherey–Nagel (Düren, F.R.G.) and had a pore diameter of either 100 or 300 Å and a particle size of 5 or 7 μm.

All other chemicals and solvents were of analytical-reagent grade.

Column preparation

Four different types of BSA–silica sorbents were used: type I, Resolvosil-BSA-7 (100 Å, 7 μm; Macherey–Nagel); type II, glutaraldehyde-cross-linked BSA entrapped in silica (100 Å, 7 μm); the preparation procedure has been described previously[3]; type III, BSA cross-linked into 3-aminopropylsilica (100 Å, 7 μm) by glutaraldehyde; and type IV, BSA adsorbed on silica (300 Å, 5 μm). The last two types were also used for the immobilization of the BSA fragments (IIIF and IVF).

The protein content of the sorbents I–III was determined by elemental analysis of nitrogen and sulphur. For sorbents containing 3-aminopropylsilica only sulphur elemental analysis was performed. The analyses were performed by Mikro Kemi (Uppsala, Sweden).

Preparation of BSA–3-aminopropylsilica sorbent (type III)

Spherical silica (100 Å, 7 μm) (4.0 g) was suspended in dry toluene (80 ml) and the silane reagent 3-aminopropyltriethoxysilane (4.3 ml) was added. The reaction mixture was refluxed for 4 h, during which time the ethanol formed was continuously removed. The derivatized silica was isolated by filtration and washed successively with 100 ml each of toluene and diethyl ether before being dried at room temperature overnight *in vacuo*.

Entrapment of BSA was carried out in 0.1 *M* phosphate buffer (pH 7.0, 1% 1-propanol) by the same procedure as used for type II sorbents.

BSA fragments–aminopropylsilica sorbent (type IIIF)

Fragments of serum albumin obtained by limited proteolysis such as peptic hydrolysis suffer little chemical damage, *e.g.*, amino acid side-chains are not altered[8]. Peptides isolated from a peptic digest were purified on an ion-exchange resin (Mono Q). A fraction showing a single band with M_r 38 000, as determined by sodium dodecyl sulphate polyacrylamide gel electrophoresis (SDS-PAGE) was further purified by gel permeation (Sephadex); the detailed procedure is described elsewhere[9,10]. An amino acid sequence analysis showed that three sequences were present in the final peptide solution[10]. The three peptides were found to originate from the N-terminal half of BSA and contained mainly the same overlapping sequence. The peptide composition was found to consist of *ca.* 50% of a peptide starting with amino acid 1 (Asp) and *ca.* 25% each of peptides starting with amino acid 11 (Phe) and 49 (Phe). SDS-PAGE showed that also a small amount (*ca.* 5%) of a larger peptide (M_r 45 000) was present in the peptide solution. The peptides were collected in 50 m*M* ammonium hydrogencarbonate buffer (pH 7.8). The peptide solution was concentrated to a volume of 5 ml by ultrafiltration using a Filtron Novacell-Omegacell, diluted with 100 m*M* phosphate

buffer (pH 7.0; 1.0% 1-propanol) and reconcentrated to a volume of 3 ml (*ca.* 9 mg/ml). 3-Aminopropylsilica (200 mg) was added to the solution and the fragment immobilized by the same procedure as used for the other cross-linked sorbents.

Column packing

The columns were packed by the upward-flow packing method at a pressure of 300 bar using a stainless-steel tube *ca.* 18 ml in volume as the slurry reservoir. The slurry and packing medium was a 50 m*M* phosphate buffer containing 40% 1-propanol. The columns were then used in the liquid chromatographic system without further conditioning.

Columns with adsorbed BSA and BSA fragments (types IV and IVF)

Nucleosil (300 Å, 5 μm) was suspended in chloroform–methanol (2:1) and poured into a 75-ml packing reservoir. The upward-flow technique was used to pack the column at 300 bar. The columns were then rinsed with water followed by 50 m*M* phosphate buffer solution (pH 5.0).

A solution of the BSA (0.12 mg/ml) in 0.5 *M* phosphate buffer (pH 5.0) was pumped through the column until breakthrough was detected at 280 nm[5]. The amount of protein adsorbed on the column was found to be 60 mg/g (*ca.* 11 mg). The column was then equilibrated with the pure phosphate buffer (50 m*M*, pH 5.0).

The preparation of the adsorbed BSA fragment column was performed using the same procedure. The concentration of BSA fragments in the 50 m*M* phosphate buffer was 0.33 mg/ml and the amount of peptide immobilized was *ca.* 98 mg/g (*ca.* 18 mg)[10]. The method of calculation of the amount of BSA adsorbed has been described previously[5].

Chromatography

The chromatographic system consisted of an LKB Model 2150 pump and an ISCO Model V[4] variable-wavelength UV absorbance detector equipped with 3.5-μl (5-mm) cell. The column dimensions were either 200 × 2.1 mm I.D. or 100 × 1.6 mm I.D. and the injections were made by means of a Rheodyne Model 7125 injection valve using a 5-μl loop.

A different instrumental setup was used for chromatography on adsorbed BSA columns. A Philips PU 4003 pump and PU 4025 variable-wavelength UV detector (1 μl, 5 mm cell) together with a Rheodyne Model 7520 sample injector (0.5-μl loop) were used.

Elution was performed isocratically using 25–100 m*M* phosphate buffer containing 0–4% of 1-propanol and 0–4 m*M* octanoic acid as retention modifiers. Retention times and peak areas were determined with a Waters Model 740 electronic integrator or a Philips PM 8252 recorder interfaced with the detector.

RESULTS AND DISCUSSION

Column performance

The performances of the two columns (100 × 1.6 mm I.D.) packed with either immobilized BSA (III) or BSA fragments (IIIF) are shown in Fig. 1, which illustrates the resolution of *rac*-oxazepam (**IV**). The columns show good efficiency and peak

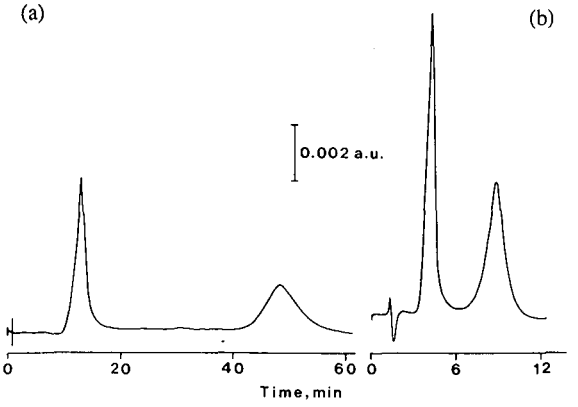

Fig. 1. Optical resolution of *rac*-oxazepam on (a) immobilized BSA (III) (k'_1 = 7.3, k'_2 = 31.7) and (b) on BSA fragment (IIIF) column (k'_1 = 1.4, k'_2 = 4.6). Mobile phase, 50 m*M* phosphate buffer (pH 7.6) containing 4% 1-propanol; flow-rate, 0.2 ml/min; UV detection 230 nm. A 25 μM solution was injected.

symmetry and the separation corresponds to a resolution factor of R_s = 5.0 and 2.6, respectively. The performance of the BSA fragment column deteriorated significantly after the use of buffers with a high alkanol content. The reason for this behaviour is not known, but one can assume that the peptides, obtained by cleavage of BSA, are less stable towards organic solvents.

Influence of the immobilization technique on retention and enantioselectivity

The existence of specific binding sites on albumin is well known, *e.g.*, for tryptophan. A specific benzodiazepine binding site on albumin has recently been postulated[6]. It is therefore plausible that the availibility of the stereospecific binding site can be affected by the immobilization technique used.

The optical resolution of oxazepam (**IV**) and omeprazol (**VII**) was performed on three different types of columns prepared under identical conditions. A selection of chromatographic data is given in Table I. It can be seen that both the resolution and

TABLE I

RESOLUTION OF RACEMIC OXAZEPAM AND OMEPRAZOL ON BSA–SILICA COLUMNS

Column dimensions, 200 × 2.1 mm I.D.; amount injected, 0.5 nmol.

Column type	*Amount of BSA*	*System*[a]	k'_1	k'_2	α	R_s
I	110	a	4.50	5.69	1.3	0.8
		b	2.69	4.00	1.5	1.4
II	190	a	9.00	28.4	3.2	4.1
		b	9.37	10.7	1.1	0.5
III	210	a	9.68	41.1	4.2	4.6
		b	7.25	17.0	2.3	3.7

[a] (a) Solute, (±)-oxazepam; mobile phase, 50 m*M* phosphate buffer (pH 7.6) containing 4% 1-propanol; flow-rate, 0.5 ml/min; UV detection at 230 nm. (b) Solute, (±)-omeprazol, mobile phase, 50 m*M* phosphate buffer (pH 5.8) containing 2% 1-propanol; flow-rate, 0.5 ml/min; UV detection at 225 nm.

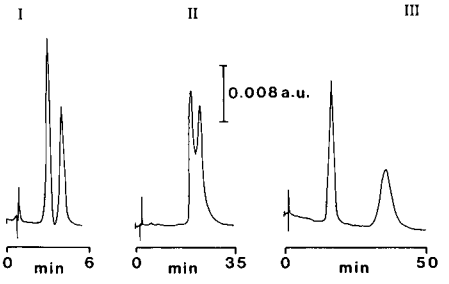

Fig. 2. Influence of the immobilization technique as shown by the optical resolution of *rac*-omeprazol on three different types (I–III) of BSA columns. Mobile phase, 50 m*M* phosphate buffer, (pH 5.8), containing 2% 1-propanol; flow-rate, 0.5 ml/min; UV detection at 225 nm. A 100-μM solution was injected.

the retention of the enantiomers of oxazepam correlate with the increased amount of entrapped BSA and increased hydrophobic character of the sorbents. However, the resolution of omeprazol shows a marked dependence on the type of column used, as illustrated in Fig. 2.

The difference between the BSA–silica type II and III sorbents is particularly well shown by their retention of acidic analytes (Table II).

The marked increase in the resolution of compounds **I** and **II** is largely due to the increased retention of the last-eluted enantiomer. The other acidic compounds and compound **VIII** show increased retention of both antipodes, resulting in less pronounced effects on the resolution.

Capacity and ligand binding of immobilized BSA fragments

The capacity of BSA–silica columns is low owing to the small proportion of the protein actually involved in the chiral recognition process. We therefore assumed that immobilization of a fragment of the protein containing some of the binding regions

TABLE II

CHROMATOGRAPHIC DATA OBTAINED WITH GLUTARALDEHYDE-CROSS-LINKED BSA COLUMNS (II AND III)

Column dimensions, 200 × 2.1 mm I.D.; amount injected, 0.5 nmol.

Compound	*Mobile phase*[a]	*Column II*			*Column III*		
		k'_1	k'_2	R_s	k'_1	k'_2	R_s
D,L-Tryptophan (**I**)	a	0.76	1.88	1.9	1.41	7.53	5.6
D,L-Kynurenine (**II**)	a	0.47	2.24	3.3	0.59	11.8	9.3
(±)-Mandelic acid (**III**)	b	3.67	6.56	1.7	11.7	18.8	3.2
Ibuprofen (**V**)	c	12.4	26.5	3.1	25.3	57.4	5.1
2,4-DNP-D,L-aspartic acid (**VI**)	a	5.85	19.0	3.7	21.1	47.1	3.5
(±)-Warfarin (**VIII**)	a	12.4	18.4	1.3	18.2	24.3	1.4

[a] Flow-rate, 0.5 ml/min; (a) 50 m*M* phosphate buffer (pH 7.6) containing 4% 1-propanol; (b) 50 m*M* phosphate buffer (pH 5.6); (c) 50 m*M* phosphate buffer (pH 8.0) containing 3% 1-propanol and 4 m*M* octanoic acid.

TABLE III

COMPARISON OF THE CAPACITY AND RESOLUTION OF (±)-BENZOIN ON COLUMNS PACKED WITH IIIF AND III

Column dimensions, 100 × 1.6 mm I.D.; solute, (±)-benzoin; mobile phase, 50 m*M* phosphate buffer, (pH 7.6) containing 4% 1-propanol; flow-rate, 0.2 ml/min; UV detection at 247 nm.

Amount injected (nmol)	*Packing*	k'_1	k'_2	η_1	η_2	α	R_s
0.125	IIIF	0.9	2.1	1.1	0.9	2.3	1.9
	III	4.1	10.2	1.2	1.0	2.5	2.8
0.50	IIIF	0.9	1.9	1.2	1.2	2.1	1.6
	III	4.0	9.7	1.0	1.4	2.4	2.5
1.00	IIIF	1.0	1.9	1.3	1.4	1.9	1.0
	III	4.0	9.6	1.1	1.4	2.4	2.4
2.50	IIIF	1.0	1.8	1.6	1.9	1.8	0.5
	III	3.9	9.0	1.2	1.7	2.3	1.7

would result in a sorbent with increased capacity owing to a higher density of chiral recognition sites. For this purpose, a study of the loading capacity of columns based on BSA (type III) or BSA fragments (type IIIF) was performed for (±)-benzoin (**Xa**). The sorbents were prepared under identical conditions.

The amount of entrapped peptide was estimated from sulphur analysis of the dried sorbent and was *ca.* 140 mg/g silica, *i.e.*, 4 μmol/g, whereas the amount of entrapped BSA was 210 mg/g (3 μmol/g).

At low concentrations there is no significant difference in the chiral recognition and overall performance of the two columns. However, as the solute concentration increases there is a marked decrease in the resolution of benzoin on the BSA fragment column (Table III). This is mainly due to the decrease in the k' value of the last-eluted isomer while the retention of the first-eluted isomer remains approximately constant. The BSA column shows a decrease in the retention of both isomers, the effect being more pronounced for the last-eluted isomer. Hence the resolution of benzoin decreases

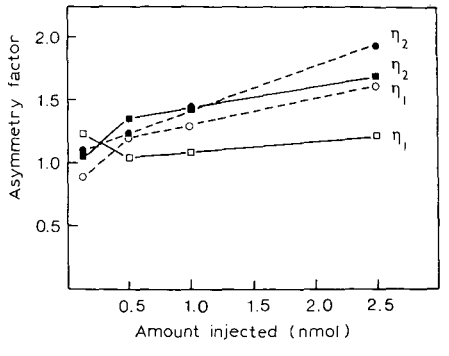

Fig. 3. Influence of sample loading on peak symmetry (η). Column: (■) type III; (●) type IIIF. Solute: (±)-benzoin. Mobile phase, 50 m*M* phosphate buffer (pH 7.6) containing 4% 1-propanol; flow-rate, 0.2 ml/min; UV detection at 247 nm.

to a lesser extent on the BSA column than on the BSA fragment column. From the asymmetry factors (η), one can also see that the column based on the intact protein has a higher column load threshold than the BSA fragment column (Fig. 3). Further, at low solute concentration, an increase in peak asymmetry is seen on the BSA column for the first-eluted enantiomer of benzoin. The reason for this behaviour is not clear, but a similar effect has been noted for N-benzoyl-D,L-alanine[3]. Theoretically, one would expect the stereoselectivity and capacity to increase owing to the increased density of stereoselective sites on the BSA fragment column; our results, however, were not in agreement with this prediction. A plausible explanation may be that the number of intact or accessible stereoselective sites in the BSA fragment column may have been reduced in a number of ways, *e.g.*, the sites may have been affected during the enzymatic cleavage or purification procedure, the stereoselective properties of the individual peptides may differ because of the small variation in the amino acid

TABLE IV

OPTICAL RESOLUTION DATA OBTAINED FOR A SERIES OF BENZOINS (**Xa–f**) ON SORBENTS IIIF AND III

Column dimension, 100 × 1.6 mm I.D.; flow-rate, 0.2 ml/min; amount injected, 125 picomol; UV detection at 254 nm.

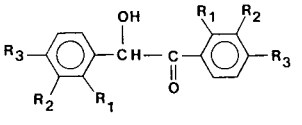

Compound	R_1	R_2	R_3	*Column type*	*Mobile phase*[a]	k'_1	k'_2	α	R_s
Xa	H	H	H	IIIF	A	1.5	3.9	2.6	2.0
				IIIF	B	1.1	2.6	2.4	1.9
				III	B	5.1	13.1	2.6	2.8
Xb	F	H	H	IIIF	A	2.6	2.6	1.0	
				IIIF	B	1.5	1.5	1.0	
				III	B	6.0	8.0	1.3	0.9
Xc	H	F	H	IIIF	A	4.2	5.8	1.4	0.6
				IIIF	B	2.0	2.7	1.4	0.4
				III	B	10.9	16.7	1.5	1.6
Xd	H	H	F	IIIF	A	2.3	2.9	1.3	0.4
				IIIF	B	1.7	1.7	1.0	
				III	B	6.7	10.7	1.6	1.6
Xe	Cl	H	H	IIIF	A	11.0	11.0	1.0	
				IIIF	B	7.8	7.8	1.0	
				III	B	23.2	28.1	1.2	0.8
Xf	H	H	Cl	IIIF	A	19.5	23.3	1.2	
				IIIF	B	10.1	10.1	1.0	
				III	B	55.1	83.7	1.5	2.0
				III	C	4.8	5.9	1.2	1.0

[a] Mobile phase: 50 m*M* phosphate buffer (pH 8.3) containing (A) 0%, (B) 4% and (C) 20% 1-propanol.

sequence of the three peptides, or the immobilization procedure is not optimal for the peptides.

The resolving power of the immobilized BSA fragments was lost for a number of compounds, *e.g.*, tryptophan, kynurenine and warfarin, which indicates that the binding sites for these compounds have been lost or otherwise affected. This is consistent with the proposed location of the binding site for tryptophan and warfarin reported by Peters[11], *i.e.*, in the C-terminal part of the BSA molecule. However, it was possible to separate certain uncharged, aromatic compounds, *i.e.*, oxazepam (**IV**), morpholep (**IX**) and benzoins (**X**), on the BSA fragment column. The large α-value for oxazepam is in agreement with the highly stereospecific benzodiazepine binding site postulated by Müller[6]. A decrease in the retention was found for all compounds, indicating the elimination of interactions not contributing to the chiral recognition.

A series of benzoins were resolved on the two different types of columns (Table IV). Introduction of substituents on the aromatic rings has an unfavourable effect on the enantioseparation of benzoins, particularly with the peptide column. Further, the position of the substituents in the isomers has a significant effect on the resolution and the smallest α-values were found for the *ortho*-substituted isomers. Fig. 4 illustrates the resolution of compound **Xd**. The large increase in the retention of benzoins on changing the halogen atom from F to Cl is difficult to explain, but these results are consistent with our earlier studies on the resolution of a series of racemic barbiturates[12].

To investigate the possible adverse effect of cross-linking on the availibility of the enantiomer-discriminating binding sites, a comparison of sorbents prepared by cross-linking and by adsorption of the protein or peptide was performed (Table V). It was found that the same compounds were resolvable on both types of peptide-containing sorbents.

The higher BSA content and the increased hydrophobicity of the cross-linked sorbents gave an increased retention of the solutes investigated and, in most instances, increased the enantioseparation. Columns III and IIIF show a similar trend in the k' values when the pH of the mobile phase is changed from 6.0 to 7.5. However, compared with the BSA column (IV), the adsorbed fragment column (IVF) shows the opposite retention behaviour in the case of oxazepam and warfarin on increasing the pH. The reason for this chromatographic behaviour is not known.

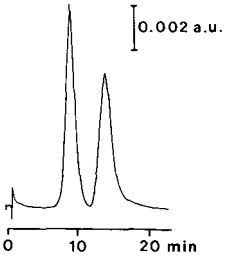

Fig. 4. Enantiomers of fluoro-substituted benzoin (**Xd**) separated on type III sorbent. Mobile phase, 50 m*M* phosphate buffer (pH 8.3) containing 4% 1-propanol; flow-rate, 0.2 ml/min; UV detection at 254 nm. A 25-μM solution was injected.

TABLE V

INFLUENCE OF IMMOBILIZATION TECHNIQUE FOR BSA FRAGMENTS ON THE OPTICAL RESOLUTION OF A SERIES OF COMPOUNDS

Column dimensions, 100 × 1.6 mm I.D.; mobile phase, 50 m*M* phosphate buffer; flow-rate, 0.2 ml/min amount injected, 125 pmol.

Compound	*pH*	*Chiral stationary phase*							
		III		*IV*		*IIIF*		*IVF*	
		k'_1	α	k'_1	α	k'_1	α	k'_1	α
D,L-Tryptophan (**I**)	6.0	2.1	1.6	0.28	1.2	1.3	1.0	0.23	1.0
	7.5	2.3	7.8	0.32	7.2	1.4	1.0	1.17	1.0
D,L-Kynurenine (**II**)	6.0	1.2	1.9	0.24	1.3	0.89	1.0	0.24	1.0
	7.5	1.6	14.5	0.29	13.0	1.09	1.0	0.26	1.0
Oxazepam (**IV**)	6.0[a]	7.4	4.9	3.1	2.0	1.9	3.1	1.9	1.3
	7.5[a]	10.6	4.8	2.6	2.0	2.7	3.0	2.1	1.5
(±)-Warfarin (**VIII**)	6.0[a]	24.9	1.5	3.3	1.5	6.4	1.0	1.0	1.0
	7.5[a]	22.7	1.6	3.4	1.5	5.1	1.0	0.29	1.0
Morpholep (**IX**)	6.0	1.7	2.0	0.91	1.3	1.2	1.4	0.75	1.3
	7.5	1.3	1.1	0.54	1.0	0.93	1.0	0.32	1.0
(±)-Benzoin (**Xa**)	6.0[a]	3.6	2.6	1.2	1.3	1.8	2.5	0.66	1.2
	7.5[a]	6.4	2.5	1.5	1.4	4.0	2.4	0.82	1.7

[a] Mobile phase contained 2% 1-propanol.

The retention behaviour of oxazepam was also dependent on the technique used for the immobilization of BSA. The cross-linked sorbent (III) showed increasing k' values with increasing pH whereas the opposite was true for the adsorbed BSA column (IV). A possible reason for this behaviour could be that the orientation of the adsorbed protein molecule is such that the binding site for oxazepam is affected in a different manner on increasing the pH. Earlier results using adsorbed BSA columns show certain differences in the chiral discrimination of sulphoxides. Omeprazol and 2-methylsulphinylbenzoic acid could not be resolved on adsorbed BSA–silica columns, which indicates that the binding sites for these compounds are no longer available[5]. No resolution of omeprazol was achieved on columns containing BSA fragments (IIIF and IVF).

An advantage of the adsorption immobilization technique, however, lies in its simplicity, which makes it suitable for the preparation of CSPs for semi-preparative purposes.

ACKNOWLEDGEMENTS

This work was supported by grants from the Swedish Natural Science Research Council, the Crafoord Foundation, Lund, the Royal Physiographical Society of Lund and the Lars Hierta Memorial Foundation.

REFERENCES

1 S. Allenmark, in A. M. Krstulovic (Editor), *Chiral Separations by HPLC: Applications to Pharmaceutical Compounds*, Ellis Horwood, Chichester, 1989, p. 285.
2 S. Allenmark, B. Bomgren and H. Borén, *J. Chromatogr.*, 264 (1983) 63.
3 R. A. Thompson, S. Andersson and S. Allenmark, *J. Chromatogr.*, 465 (1989) 263.
4 M. Aubel and L. B. Rogers, *J. Chromatogr.*, 392 (1987) 415.
5 P. Erlandsson, L. Hansson and R. Isaksson, *J. Chromatogr.*, 370 (1986) 475.
6 W. E. Müller. in I. W. Wainer and D. E. Drayer (Editors), *Drug Stereochemistry, Analytical Methods and* Stereochemistry, Marcel Dekker, New York, 1988, p. 227.
7 S. Allenmark and S. Andersson, *J. Chromatogr.*, 351 (1986) 231.
8 R. G. Reed, R. C. Feldhoff, O. L. Clute and T. Peters, Jr., *Biochemistry*, 14 (1975) 4578.
9 P. Erlandsson and S. Nilsson, presented at the *11th International Symposium on Column Liquid Chromatography, Amsterdam, 1987.*
10 P. Erlandsson and S. Nilsson, *J. Chromatogr.*, 482 (1989) 35.
11 T. Peters Jr., *Adv. Protein Chem.*, 37 (1985) 161.
12 S. Allenmark, S. Andersson and J. Bojarski, *J. Chromatogr.*, 436 (1988) 479.

Journal of Chromatography, 498 (1990) 93–104
Elsevier Science Publishers B.V., Amsterdam — Printed in The Netherlands

CHROM. 21 947

MOLECULAR WEIGHT DISTRIBUTION OF ASPEN LIGNINS FROM CONVENTIONAL GEL PERMEATION CHROMATOGRAPHY, UNIVERSAL CALIBRATION AND SEDIMENTATION EQUILIBRIUM

M. E. HIMMEL*, K. TATSUMOTO and K. GROHMANN
Applied Biological Sciences Section, Biotechnology Research Branch, Solar Fuels Research Division, Solar Energy Research Institute, 1617 Cole Blvd., Golden, CO 80401 (U.S.A.)
and
D. K. JOHNSON and H. L. CHUM
Chemical Conversion Branch, Solar Fuels Research Division, Solar Energy Research Institute, 1617 Cole Blvd., Golden, CO 80401 (U.S.A.)
(First received December 27th, 1988; revised manuscript received July 11th, 1989)

SUMMARY

Molecular weight distributions of ball-milled, organosolv, alkali-extracted/mild acid-hydrolyzed and alkali-extracted/steam-exploded aspen lignins in tetrahydrofuran were compared using conventional gel permeation chromatography (GPC), universal calibration and sedimentation equilibrium. Molecular weight averages reported in the literature from universal calibration for the four low-molecular-weight lignins agreed more closely with values found in this study from sedimentation equilibrium experiments than from conventional GPC. This result supports the suggestion that these acetylated lignins fit universal calibration.

INTRODUCTION

Lignins are complex, cross-linked phenylpropane polymers that compose, with cellulose and other carbohydrates, the cell wall structural members of living plants. They constitute 15–25% of the dry weight of material found in hardwoods[1–3]. Further progress in understanding the macromolecular properties of lignins now requires a reliable method for determining the molecular weights (MW) and molecular weight distributions (MWD) in a solvent that minimizes solute–solute, solute–solvent and solute–column interactions. Important contributions have been made using packed-bed and high-performance size-exclusion chromatography (HPSEC) in both neat and mixed organic solvents with underivatized[4–6] and methylated, silylated or acetylated lignins[7–13], and in aqueous sodium hydroxide with underivatized lignins[14–17], but a chromatographic system that performs optimally has not been reported. Tetrahydrofuran (THF), however, works well in minimizing solute–column and solute–solute interactions and, although limited in its ability to solubilize lignins over a wide range of MW, is suitable for use with polystyrene–divinylbenzene (*e.g.*, μStyragel) column packing materials[18]. Hydrophilic, high-dielectric solvents such as form-

0021-9673/90/$03.50

amide[19], dimethyl sulfoxide (DMSO)[20] and dimethylformamide (DMF)[21] solubilize higher-MW underivatized lignins, yet perform poorly with μStyragel packing materials because of excessive bead instability[18]. Chromatography in DMF also results in extreme sensitivity to solute–column interaction.

Two commercial detectors introduced recently have greatly extended the capability of SEC, the real-time differential viscometer (DV) and the low-angle laser light-scattering (LALLS) photometer. On-line viscometric detectors allow the determination of unknown polymer MWs using the principle of universal calibration[22–26]. On-line LALLS detectors and software systems apply Debye theory as improved by Zimm and Stockmayer[27]to find MWs and the root mean square radii for unknown polymers. These methods allow the real-time calculation of "true" MWs for unknown polymers from SEC and have been reviewed extensively[28–31]. An important limitation of LALLS is that values of the change in refractive index with solute concentration (dn/dc) for the polymer in a pure solvent must be precisely known and problems arise when polymers are heterogeneous in composition with respect to MW, because dn/dc will then also vary with MW.

This paper reports the first direct comparison of results from MWD analyses using conventional GPC, universal calibration via HPSEC–DV and sedimentation equilibrium for four acetylated hardwood lignins in THF. The lignin samples were obtained from aspen (*Populus tremuloides*) wood meal by ball milling, steam explosion followed by alkaline extraction, organosolv pulping and dilute sulfuric acid hydrolysis followed by sodium hydroxide extraction.

EXPERIMENTAL

Chemicals and standards

All chemical and HPSEC eluents were obtained from J. T. Baker (Phillipsburgh, NJ, U.S.A.), Fisher Scientific (Pittsburgh, PA, U.S.A.) and Aldrich (Milwaukee, WI, U.S.A.). The MW standards used to calibrate the three column system were obtained from American Polymer Labs. (Mentor, OH, U.S.A.) [polybutadienes (narrow MWD), poly-α-methylstyrenes (narrow MWD), poly(methyl methacrylates) (broad MWD)] and Polymer Labs. (Shropshire, U.K.) [polystyrenes (narrow MWD) and poly(methyl methacrylates) (narrow MWD)]. Two synthetic polymers prepared by anion-initiated polymerizations of a quinone methide (QMa) according to the procedure of Chum *et al.*[32] were treated as intermediate-MW lignin models.

Lignin samples

Ball-milled (BM) aspen lignin was prepared following the procedure of Lundquist *et al.*[33]. Alkali-extracted/steam-exploded (AESE) aspen lignin samples were prepared from steam-exploded wood pulp as described by Chum *et al.*[12]. Alkali-extracted/acid hydrolysis (AH/NaOH) lignin samples were prepared by subjecting aspen wood flour to a 1-hour cook at 120°C in 0.025 *M* sulfuric acid[34] and mixing the clarified supernatant with 1% (w/w) NaOH at 25°C with a Waring blender. The organosolv (OS) lignin was prepared from the liquor obtained by extracting aspen wood flour with methanol–water (70:30, v/v)[35]. Lignin samples were acetylated following the method of Gierer and Lindeberg[36]. Lignin samples were stored frozen during the study.

Chromatographic system

The chromatographic system used to evaluate conventional GPC analysis consisted of a Hewlet-Packard Model 1090M liquid chromatograph equipped with a Hewlett-Packard Model 1037A high-sensitivity refractive index (RI) detector and a Hewlett-Packard Model 1040A diode-array detector using signals at 260 nm with a band width of 80 nm. The column system was composed of three 30 × 7.8 mm I.D. columns (Beckman μSpherogel of pore size 10 000, 1000 and 500 Å) connected in series in order of increasing pore size. Narrow MWD standards (see *Chemicals and standards*) were used to obtain a linear calibration graph from $1 \cdot 10^6$ to 500 daltons. Lignin samples were injected at a concentration of 1.0 mg/ml with an autoinjector setting of 225 μl. Experimental data were reduced to statistical molecular weight averages using the Hewlett-Packard Chromatography Software with GPC upgrade.

Partial specific volume determination

Densities and apparent partial specific volumes of lignin samples in THF were determined using a Mettler/Paar Model DMA60 six-place precision digital density meter equipped with a DMA602 measuring cell. During measurement the sample temperature was controlled to within ±0.005°C using a Cascade Systems thermal circulator. The experimental protocol and instrument calibration followed a procedure described by Elder[37]. Air-free, deionized water was prepared just prior to use following the procedure of Wagenbreth and Blanke[38]. Lignin samples were prepared in THF at a concentration of 3 mg/ml by weighing to ±0.0005 mg; samples at concentrations of 1.5 and 0.75 mg/ml were prepared by serial dilution. All samples were prepared and analyzed in duplicate. Five measurements were taken for each sample when the time-lapse measurement reached equilibrium. Weighted-average values for these measurements were used for the density calculations.

Analytical ultracentrifugation

Sedimentation equilibrium studies were performed on a Beckman Model E ultracentrifuge equipped with RTIC temperature control and electronic speed control. Acetylated lignin samples at a concentration of *ca.* 1.8 mg/ml were normally allowed to reach equilibrium at 15 000, 30 000 and 40 000 rpm at 20°C. Rayleigh interference fringe patterns were recorded on Kodak Spectroscopic IIG film and analyzed on a Nikon Model V12 microcomparator equipped with a Nikon digital x–y stage. To improve the quality of the interference fringes at higher rotor speeds, the instrument light source was fitted with a polarizing filter[39] and the cell was assembled with sapphire windows, custom-cut window gaskets of polyamide sheet stock (0.013 cm thickness) and window liners of polyaramide sheet stock (0.025 cm thickness). To maintain a leak-free cell for THF solutions, special center-piece gaskets were cut from 0.010-cm thick Kel-F (3M) sheet stock.

Although double-sector center-pieces molded from Kel-F (currently unavailable from Beckman) deformed at elevated rotor speeds in the presence of THF and were therefore unsuitable for extended sedimentation equilibrium runs, they could be scribed as necessary to form a synthetic boundary center-piece. The short-duration, low rotor speed of the synthetic boundary forming experiment, necessary to find the initial solute concentration, c_0, was acceptable for THF exposure.

The right-hand cell sector was filled with 0.02 ml of FC-43 fluorocarbon and

0.120 ml of sample and the left-hand sector was filled with 0.160 ml of HPLC-grade THF. Synthetic boundary experiments for c_0 determinations used 0.120 ml of sample and 0.360 ml of THF in the right- and left-hand sectors, respectively.

Theory of universal calibration

The concept of universal calibration, as introduced by Benoit *et al.*[22], is based on the Einstein viscosity law:

$$[\eta] = \nu N \upsilon_h / M \tag{1}$$

This equation relates the hydrodynamic volume, υ_h, of a macromolecule of molecular weight M to its intrinsic viscosity, $[\eta]$, in cm^3/g; N is Avogadro's number and ν is a shape factor developed by Simha[40]. Also, as $[\eta]$ can be expressed as a function of the form $[\eta] = AM^x$, the familiar relationship,

$$[\eta] = K'M^a \tag{2}$$

first expressed by Mark[41] and Houwink[42] in the 1940s, was found. Here K' and a are the Mark–Houwink constants and are specific to a polymer–solvent–temperature system[43].

The principal of universal calibration is based on eqn. 1, which predicts that all molecules having the same value of $[\eta]M$ would have the same value of υ_h. Also, if υ_h is the parameter that uniquely determines the elution volume, V_e, these molecules should have the same elution volume. Universal calibration, then, permits the calculation of M for polymers of unknown structure from column elution data, without a knowledge of the Mark–Houwink constants, using a set of calibrated columns for which a calibration graph of $[\eta]M$ versus V_e (found using well characterized polymer standards) is known. Sources of error in this approach arise from both experimental SEC limitations and theoretical considerations[44,45].

Theory of sedimentation equilibrium

The expressions that describe the equilibrium concentration of solutes in the ultracentrifuge cell have been derived from both classical thermodynamics and material transport theory[46]. Svedberg[47,48] derived expressions from both approaches and showed that identical results can be found from both methods for ideal solutions. An equation that was found suitable for application of Rayleigh interference optics to ultracentrifuge data[49], assuming solution ideality, is

$$M_{app} = \{2RT/[(1-\bar{\upsilon}\rho)\omega^2]\}\,(\mathrm{d}\ln c/\mathrm{d}r^2) \tag{3}$$

where c is concentration in fringes, r is the radial distance from the center of rotation in cm, T is time, $\bar{\upsilon}$ is the partial specific volume, ρ is the density of the solution, ω is the angular velocity of the rotor and R is the gas constant.

For homogeneous systems, plots of ln c versus r^2 yield straight lines. In general, systems indicating polydispersity show upward-sloping curves of ln c versus r^2 and non-ideal systems show downward-sloping curves[50]. Also important in determining the MWD of polydisperse polymers, although seldom applied, is multiple rotor speed

analysis. This method, developed by Fujita[51] and improved by Osterhoudt and Williams[52] and Scholte[53], permits the description of the total MWD of a sample of high polydispersity from MW data collected at multiple rotor speeds for various heights in the sample fluid column. Unfortunately, this method has not been translated directly for use with data collected with the interference optical system reported in this study[54].

Calculation of sedimentation equilibrium results

The Raleigh interference fringe photographs are aligned in the microcomparator and analyzed by the methods described by Chervenka[55] and Richards and Schachman[50]. The total weight-average molecular weight is estimated by the "conservation of mass" method first described by Lansing and Kraemer[56] and later developed by Richards *et al.*[57] and others. Here, a specific and limited form of eqn. 3 is used:

$$M_{app} = \{2RT/[(1-\bar{v}\rho)\omega^2]\}\,(c_b - c_m)/[c_o(r_b^2 - r_m^2)] \quad (4)$$

where c_b, c_m and c_o represent the concentration of solute in fringes at the upper fluid meniscus, at the cell bottom (sample fluid column bottom–FC-43 interface) and in the original sample before loading, respectively. Values given in r, radial distance in rotor coordinates (cm), define these points in the cell. Further, we have assumed that at the 1–2 mg/ml solute concentrations used in this study we can assume ideal behavior in THF and therefore the data presented were collected at one concentration only.

RESULTS AND DISCUSSION

Chromatographic methods

The aspen wood lignin samples chosen for this study were prepared by organosolv, steam explosion, dilute acid hydrolysis and ball-milling procedures. Fig. 1 and 2 show the elution profiles of these four lignin samples using refractive index (RI) and UV detection, respectively. In comparison, elution profiles obtained with UV detection indicated minor variances with the RI curves at early elution (*e.g.*, high MW) for all samples analyzed. These differences in the tail of the elution envelope, which probably reflect different dependences of absorptivity on molecular weight for the two detection methods, may result in the differences in M_z calculated from these data and shown in Table I.

Table I also illustrates the results of applying "conventional GPC" analysis to the four lignin samples. A sensitive UV detector permitted the chromatograms to be recorded at low loadings (0.22 mg per injection). The values of the number-average (M_n), weight-average (M_w) and z-average (M_z) molecular weight obtained proved to be consistent with those reported by other laboratories[7–10] where a μStyragel (or similar) gel system in THF was used. The general trend shown by these data was the similarity in M_w between all the acetylated aspen lignins tested except the ball-milled lignin, which had a higher M_w. The polydispersities probably ranged within experimental error, *i.e.*, 3.2 (RI detection) for ball-milled aspen lignin to 4.8 (UV detection) for the steam-exploded lignin. The synthetic quinone methide-derived polymers were considerably narrower in polydispersity (near 1.5).

We recently reported[58] the use of universal calibration to analyze the MWD of

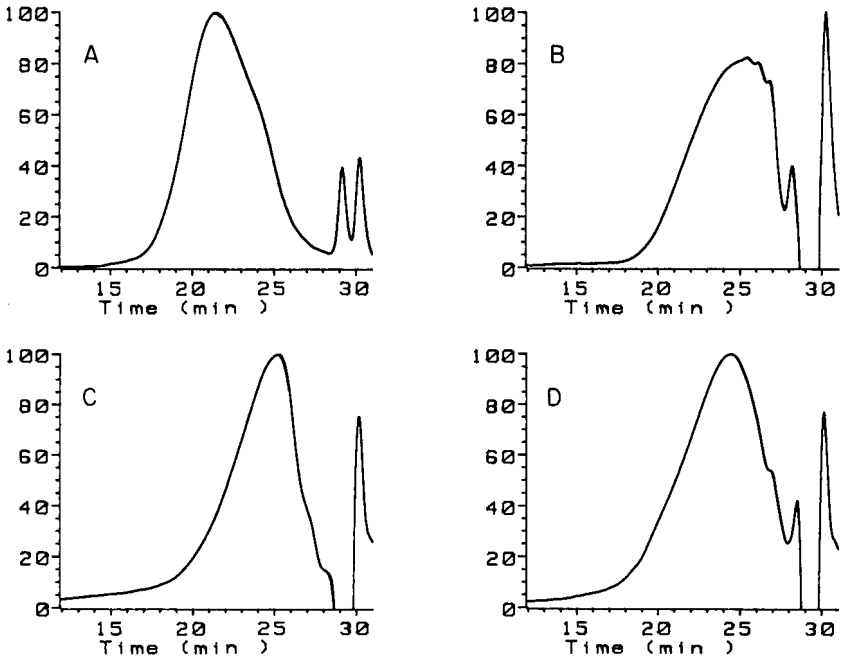

Fig. 1. High-performance size-exclusion chromatography of four acetylated aspen lignin preparations: (A) ball-milled; (B) organosolv; (C) alkali-extracted/dilute acid-hydrolyzed; and (D) alkali-extracted/steam-exploded. Elution curves were obtained with a refractive index detector and displayed in normalized amplitude with the Hewlett-Packard Chromatography Software. Multiple positive and negative peaks near the total column elution volume (28–31 min) reflect elution of non-polymeric compounds and injection solvent and were not included in the MWD analysis. The sample loading was 0.22 mg per injection.

four acetylated aspen lignins and two quinone methide-derived polymers identical with those used here. Table II compares the molecular weight averages found for these polymers in that earlier study, using a Viscotek HPSEC–DV detector, with values found in this study by conventional GPC. The relative ordering of the values found by HPSEC–DV is very similar to those from conventional GPC (Table II), with ball-milled aspen lignin showing the highest molecular weight averages. However, the values of M_n from conventional GPC range from identical within experimental error (AESE) to values that are 35% smaller than those from universal calibration (OS and AH/NaOH), to values from GPC that are half of those from universal calibration (ball-milled and model polymers). The values of M_w are 20–40% smaller by conventional GPC for AESE, OS, AH/NaOH and ball-milled aspen lignin and are a factor of two smaller for the model polymers. There is a systematic difference in M_z of a factor of *ca.* 2 from the averages of conventional GPC and universal calibration, with the GPC values always being larger (lignins) and smaller (model polymers) by the same factor. This may indicate a detector- or software-based bias (in both GPC and HPSEC–DV data systems), as the placement of baselines on the original chromatographic data is especially critical in calculating the high-molecular-weight-sensitive M_z values. The polydispersities are the same within experimental

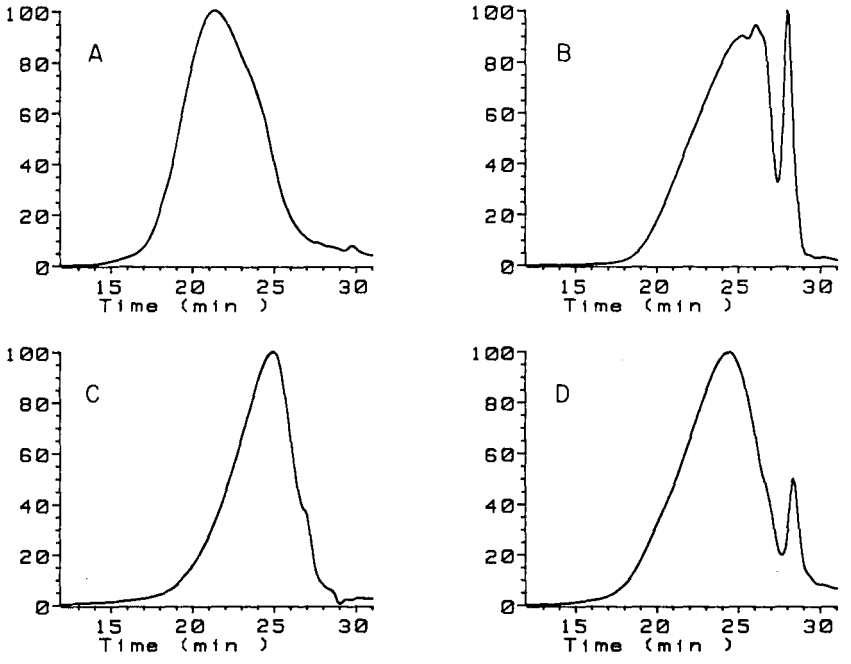

Fig. 2. High-performance size-exclusion chromatography of the acetylated lignins shown in Fig. 1. Elution curves were obtained with a UV detector at 260 nm and the sample loading was 0.22 mg per injection.

TABLE I

MWDs OF ACETYLATED ASPEN LIGNINS AND LIGNIN MODEL POLYMERS

From conventional GPC at different loadings and detection systems. GPC in THF at 20° with UV detection at 260 nm and a band width of 80 nm for low loadings, and 270 nm with a band width of 10 nm for the higher loadings. Low loadings were produced from solutions of 1.0 mg/ml and injections of 225 μl; high loadings were produced from solutions of 8.0 mg/ml with the same injection volume.

Sample[a]	*Loading (mg)*	M_n		M_w		M_z		M_w/M_n	
		UV	*RI*	*UV*	*RI*	*UV*	*RI*	*UV*	*RI*
AESE	0.22	1200	1300	5600	5100	88000	44000	4.7	3.9
AESE	1.7	1300	1400	6300	5900	110000	62000	4.8	4.2
OS	0.22	680	880	2800	2800	28000	9500	4.1	3.2
OS	1.7	610	840	2800	3400	64000	52000	4.6	4.0
AH/NaOH	0.22	1100	1100	4600	3700	120000	43000	4.2	3.4
AH/NaOH	1.7	1100	1200	4500	4300	95000	62000	4.1	3.6
BM	0.22	2800	3000	12000	12000	130000	120000	4.3	4.0
BM	1.7	3000	3100	10000	10000	58000	55000	3.3	3.2
QM 34	0.25	3710	--	5070	--	6320	--	1.4	--
QM 33	0.25	3930	--	7350	--	10170	--	1.9	--

[a] Acetylated lignins: alkali-extracted/steam-exploded, AESE; organosolv, OS; alkali-extracted/dilute acid-hydrolyzed, AH/NaOH; and ball milled, BM. QM indicates quinonemethide-derived model polymers.

TABLE II

MWDs OF ACETYLATED ASPEN LIGNINS AND MODEL COMPOUNDS: COMPARISON OF VALUES FROM UNIVERSAL CALIBRATION WITH AVERAGE VALUES FROM CONVENTIONAL GPC

Sample	*Loading (mg)*	M_n	M_w	M_z	M_v	M_w/M_n
AESE[a]	1	1100	7300	34 500	3300	6.7
AESE[a]	2	1900	7100	27 000	–	3.7
From GPC[b]	1.7	1400	5900	62 000	–	4.2
OS[a]	1	1300	5200	16 000	3200	4.0
OS[a]	2	1000	4400	18 000	–	4.4
From GPC[b]	1.7	840	3400	52 000	–	4.1
AH/NaOH[a]	1	2200	8100	38 000	4600	3.7
AH/NaOH[a]	2	1300	6600	34 000	–	5.0
From GPC[b]	1.7	1200	4300	62 000	–	3.6
BM[a]	1	3600	17300	46 800	11500	4.7
BM[a]	2	9000	22000	47 000	–	2.4
From GPC[b]	1.7	3100	10000	55 000	–	3.2
QM 34[a]	0.25	8700	10300	12 400	9900	1.1
From GPC[b]	0.25	3710	5070	6 320	–	1.4
QM 33[a]	0.25	14700	16700	20 000	16000	1.1
From GPC[b]	0.25	3930	7350	10 170	–	1.9

[a] Universal calibration values from Himmel *et al.*[58]. Obtained in THF at 20°C with RI detection and Unical 2.71 software (Viscotek). For high loadings, injections (250 μl) were made from 8 mg/ml stock solutions. For low loadings, injections (250 μl) were made from 4 mg/ml stock solutions.

[b] From RI detection values in Table I.

error for all lignin samples. In contrast, the polydispersities found for the quinone methide-derived polymers by universal calibration are near 1.1.

Sedimentation equilibrium

Values of the partial specific volume for the acetylated AESE, organosolv, AH/NaOH and ball-milled aspen lignins in THF found with the Mettler–Paar mechanical oscillator were 0.689, 0.665, 0.656 and 0.657 ml/g, respectively. Interestingly, these values are very similar to that of 0.663 ml/g found for unacetylated kraft lignin in dilute NaOH by McNaughton *et al.*[59]. These values were used to calculate a series of molecular weight averages for the lignin samples at various rotor speeds using the conservation of mass method (eqn. 5). Table III shows the results of these experiments at lignin concentrations of 1.8 mg/ml.

The issue of rotor speed variance and its impact on "intrinsic" M_w requires further discussion. Early work by Fujita[51] and Adams[60] clearly indicated the need to examine polydisperse samples at a wide range of ultracentrifuge rotor speeds. As the centrifugal force (proportional to ω^2) is increased on the cell and sample fluid column, the apparent distribution of components in the sample changes as heavier fractions sediment to the cell bottom (or lie close to this position). Work by Scholte[53] improved Fujita's early methods so that widely polydisperse polymers could be fully analyzed by extrapolation to zero rotor speed. Unfortunately, Scholte's work contributed precise methods for analysis of schlieren patterns only. Our work was per-

TABLE III

MWDs OF ACETYLATED ASPEN LIGNINS FROM PRELIMINARY SEDIMENTATION EQUILIBRIUM IN THF AS A FUNCTION OF ROTOR SPEED

Lignin concentrations were 1.8 mg/ml. The values obtained at the lowest rotor speed are considered to be the best approximation for M_w by sedimentation equilibrium and should be used for comparison with values in Tables I and II.

Sample	*Rotor speed (rpm)*	$M_{w,app}$
AESE	15 000	9100
	30 000	5400
OS	15 000	8000
	30 000	3100
	40 000	2300
AH/NaOH	15 000	9000
	30 000	4900
BM	15 000	10600
	20 000	10200
	30 000	5200
	40 000	2400

formed with the Rayleigh interference optical system so that more dilute solutions could be studied [schlieren optical analysis requires solute concentrations in the range 3–6 mg/ml]. Such extrapolations are not yet possible with our present data. We can, however, infer from Scholte's work that values found for apparent M_w at low rotor speeds (*i.e.*, 15 000 rpm) lie near to, and slightly lower than, the intrinsic M_w for the sample. In this paper we shall consider these values for $M_{w,app}$ obtained at 15 000 rpm to be a good approximation of M_w. Future work must focus on the development of the theory necessary to perform the extrapolation of interference optical data to both zero solute concentration and zero rotor speed.

CONCLUSIONS

Reconciliation of internal data

The approach outlined here is certainly not new in philosophy, yet we have employed instrumentation and methodologies both very old and very new to this problem. Historically, the task of bringing together multiple disciplines to the problem of polymer MWD analysis has been slow. Early work (1948) by Wales[61] and Wales *et al.*[62] attempted to reconcile results from intrinsic viscosity, sedimentation equilibrium and osmometric experiments for polydisperse materials (polystyrenes) in organic solvents. In 1970, Sokolov *et al.*[63] performed little known but landmark work in which approach-to-equilibrium methods were used to describe lignin in a variety of solvents. Also important were the contributions of Pla and Robert[64–66], who gathered hydrodynamic data from viscometry, sedimentation velocity and GPC on spruce lignins in THF. They showed that spruce lignins exhibit typical behavior from plots of log M versus log $[\eta]$ indicative of branched polymers. Kraft lignin MWDs in sodium hydroxide have also been extensively studied more recently using short-column sedimentation equilibrium by Sarkanen and co-workers[15,17]. Such examples of multidisciplinary examination of lignin MDWs are limited, however.

One important aspect of this study was that all lignin samples, sample handling, column calibration standards, mobile phase (THF) and chromatographic column sets used for all experiments (including those from ref. 58) were the same. Hence significantly greater control of experimental variables resulting from laboratory-specific differences in these conditions and instrumentation was achieved. This consideration renders the differences shown in Tables I and II meaningful.

Although evidence exists that concentration effects may be important with even acetylated lignins in THF, increasing the column loadings from 0.25 to 1 mg seems unlikely to be the cause of the differences shown in Table II. These data identify poor sensitivity as a more general and pressing problem in state-of-the-art, SEC-based "absolute" MW analysis. From our work, the limiting value for sample loading appears to be near 0.1 mg per injection for conventional GPC (RI detector) and 1 mg per injection for HPSEC–DV. Loadings for HPSEC–LALLS are commonly reported[31] to be between 0.2 and 1 mg per injection. An increase in sensitivity of one order of magnitude would be highly valuable and should be an area of focus for suppliers of SEC detection equipment. For comparison, the non-SEC-based method, sedimentation equilibrium equipped with Rayleigh interference optics or UV scanning, has a detection limit of *ca.* 1 or 0.1 mg/ml, respectively. The SEC elution of polymers (lignins) at concentrations many orders of magnitude below this can, of course, be achieved by UV detection, but calculations are then limited to only conventional GPC methods.

In this study we compared the results from three hydrodynamic approaches to unknown polymer MW determination. Conventional GPC analysis from polystyrene-calibrated columns produced the lowest MW estimates for the four lignins and quinone-methide-derived polymers. Universal calibration methodology led to higher MW estimates (1.5–2.5 fold) than conventional GPC, and sedimentation equilibrium produced values for apparent MW that were similar to those from universal calibration. This result is not surprising, because conventional GPC examines the elution of a calibration series ordered on the basis of effective hydrodynamic volume, not MW. A similar result was recently found by Wooten *et al.*[67] in a study of the M_w found for "resole" phenolic resins in 0.1 *M* NaOH by conventional GPC and sedimentation equilibrium, where the M_w from the latter was five times greater than that from GPC. Universal calibration, however, relies on the conservation of the relationship between the hydrodynamic volume ($[\eta]M$) and elution volume for a specific column set throughout a wide range of polymer chemistries and sizes. Indeed, finding higher apparent MWs from universal calibration than from GPC is consistent with the concept of lignin being a branched polymer (*e.g.*, a branched polymer of higher MW may occupy the same hydrodynamic volume as a linear polymer). The ultimate conclusion of this study is that the low-MW, acetylated aspen lignins examined appear to fit universal calibration; however, comparison with data from LALLS (if possible) and from a refinement of sedimentation equilibrium analysis performed at multiple rotor speeds should eventually confirm or disprove this conclusion.

ACKNOWLEDGEMENTS

The authors thank Dr. Russ Middaugh for providing access to the Mettler–Paar density meter and Mr. Greg Noll for technical support. They thank Drs. E. Glen

Richards and Simo Sarkanen for many valuable discussions concerning the application of sedimentation equilibrium to this problem. This work was funded by the Biochemical Conversion Program at the DOE Biofuels and Municipal Waste Technology Division.

REFERENCES

1 F. E. Brauns and D. A. Brauns, *The Chemistry of Lignin*, Academic Press, New York, 1960.
2 K. V. Sarkanen and C. H. Ludwig (Editors), *Lignins, Occurrence, Formation, Structure, and Reactions*, Wiley-Interscience, New York, 1971.
3 K. V. Sarkanen, in B. L. Browning (Editor), *The Chemistry of Wood*, R. E. Krieger, Huntington, 1975.
4 R. H. Marchessault, S. Coulombe, T. Hanai, H. Morikawa and D. Robert, *Can. J. Chem.*, 60 (1982) 2372.
5 F. J. Kolpak, D. J. Cietek, W. Fookes and J. J. Call, *J. Appl. Polym. Sci., Polym. Sci. Symp.*, 31 (1983) 491.
6 M. E. Himmel, K. K. Oh, D. W. Sopher and H. L. Chum, *J. Chromatogr.*, 267 (1983) 249.
7 O. Faix, W. Lange and O. Beinhoff, *Holzforschung*, 34 (1980) 174.
8 O. Faix, W. Lange and E. C. Salud, *Holzforschung*, 35 (1981) 3.
9 W. Lange, W. Schweers and O. Beinhoff, *Holzforschung*, 35 (1981) 119.
10 D. Meier, O. Faix and W. Lange, *Holzforschung*, 35 (1981) 247.
11 W. Lange, O. Faix and O. Beinhoff, *Holzforschung*, 37 (1983) 63.
12 H. L. Chum, D. K. Johnson, M. P. Tucker and M. E. Himmel, *Holzforschung*, 41 (1987) 97.
13 J. Pellinen and M. Salkinoja-Salonen, *J. Chromatogr.*, 328 (1985) 299.
14 W. J. Connors, S. Sarkanen and J. L. McCarthy, *Holzforschung*, 34 (1980) 80.
15 S. Sarkanen, D. C. Teller, J. Hall and J. L. McCarthy, *Macromolecules*, 14 (1981) 426.
16 S. Tirtowidjojo, *M.S. Dissertation*, University of Washington, Seattle, 1984.
17 S. Sarkanen, D. C. Teller, C. R. Stevens and J. L. McCarthy, *Macromolecules*, 17 (1984) 2588.
18 W. W. Yau, J. J. Kirkland and D. D. Bly, *Modern Size Exclusion Chromatography: Practice of Gel Permeation and Gel Filtration Chromatography*, Wiley, New York, 1979.
19 W. Brown and S. I. Falkehag, *Nature (London)*, 214 (1967) 410.
20 B. D. Bogomolov, O. M. Sokolov, G. G. Kochergina and I. I. Rudakova, *Sovrem. Metody Issled. Khim. Lignina*, (1970) 41.
21 W. G. Glasser, P. C. Barnett, P. C. Muller and K. V. Sarkanen, *J. Agric. Food Chem.*, 31 (1983) 921.
22 H. Benoit, Z. Grubisic, P. Rempp, D. Decker and J. G. Zilliox, *J. Chim. Phys.*, 63 (1966) 1507.
23 L. Letot, J. Lesec and C. Quivoron, *J. Liq. Chromatogr.*, 3 (1980) 427.
24 F. B. Malihi, C. Kuo, E. Koehler, T. Provder and A. F. Kah, in T. Provder (Editor), *Size Exclusion Chromatography—Methodology and Characterization of Polymers and Related Materials*, Vol. 245, American Chemical Society, Washington, DC, 1984, p. 281.
25 M. G. Styring, J. E. Armonas, and A. E. Hamielec, *J. Liq. Chromatogr.*, 10 (1987) 783.
26 M. E. Himmel and P. G. Squire, in P. Dubin (Editor), *Aqueous Size Exclusion Chromatography*, Elsevier, Amsterdam, 1988, pp. 3–22.
27 B. H. Zimm and W. H. Stockmayer, *J. Chem. Phys.*, 17 (1949) 1301.
28 A. E. Hamielec, A. C. Ouano and L. L. Nebenzahl, *J. Liq. Chromatogr.*, 1 (1978) 527.
29 S. H. Agarwal, R. F. Jenkins and R. S. Porter, *J. Appl. Polym. Sci.*, 27 (1982) 113.
30 J. Roovers, N. Hadjichristidis and L. J. Fetters, *Macromolecules*, 16 (1983) 214.
31 R. C. Jordan, S. F. Silver, R. D. Sehon and R. J. Rivard, in T. Provder (Editor), *Size Exclusion Chromatography—Methodology and Characterization of Polymers and Related Materials*, Vol. 245, American Chemical Society, Washington, DC, 1984, p. 295.
32 H. L. Chum, D. K. Johnson, P. D. Palasz, C. Z. Smith and H. P. Utley, *Macromolecules*, 20 (1987) 2698.
33 K. Lundquist, R. Ohlsson and R. Simonson, *Sven. Papperstidn.*, 78 (1975) 30.
34 K. Grohmann, R. Torget and M. E. Himmel, *Biotechnol. Bioeng. Symp.*, 17 (1986) 135.
35 H. L. Chum, D. K. Johnson, M. Ratcliff, S. Black, H. A. Schroeder and K. Wallace, in *Proceedings of the International Symposium on Wood and Pulping Chemistry*, Canadian Pulp and Paper Association, Vancouver, 1985, pp. 223–227.
36 J. Gierer and O. Lindeberg, *Acta Chem. Scand.*, 34 (1980) 161.

37 J. T. Elder, *Methods Enzmol.*, 61 (1979) 12.
38 H. Wagenbreth and W. Blanke, *PTB-Mitt.*, 6 (1971) 412.
39 A. T. Ansevin, D. E. Roark and D. A. Yphantis, *Anal. Biochem.*, 34 (1970) 237.
40 R. Simha, *J. Phys. Chem.*, 44 (1940) 25.
41 H. Mark, *Der feste Körper*, Hirzel, Leipzig, 1938, p. 103.
42 R. Houwink, *J. Prakt. Chem.*, 157 (1941) 15.
43 Z. Gallot-Grubisic, P. Rempp and H. Benoit, *J. Polym. Sci.*, 5 (1967) 753.
44 E. F. Cassassa, *Macromolecules*, 9 (1976) 182.
45 R. P. Frigon, J. K. Leypoldt, S. Uyeji and L. W. Henderson, *Anal. Chem.*, 55 (1983) 1349.
46 A. Fick, *Ann. Phys. Chem.*, 94 (1855) 59.
47 T. Svedberg, *Z. Phys. Chem.*, 121 (1926) 65.
48 T. Svedberg, *Kolloid-Z.*, 36 (1925) 53.
49 H. K. Schachman, *Ultracentrifugation in Biochemistry*, Academic Press, New York, 1959.
50 E. G. Richards and H. K. Schachman, *J. Phys. Chem.*, 63 (1959) 1578.
51 H. Fujita, *Mathematical Theory of Sedimentation Analysis*, Academic Press, New York, London, 1962, pp. 344–354.
52 H. W. Osterhoudt and J. W. Williams, *J. Phys. Chem.*, 69 (1965) 1050.
53 T. G. Scholte, *J. Polym. Sci.*, 6 (1968) 91.
54 H. Fujita, in P. J. Elving and J. D. Winefordner (Editors), *Chemical Analysis*, Vol. 42, Wiley, New York, 1975, p. 344.
55 C. H. Chervenka, *Anal. Chem.*, 38 (1966) 356.
56 W. D. Lansing and E. O. Kraemer, *J. Am. Chem. Soc.*,57 (1935) 1369.
57 E. G. Richards, D. C. Teller and H. K. Schachman, *Biochemistry*, 7 (1968) 1054.
58 M. E. Himmel, K. Tatsumoto, K. K. Oh, K. Grohmann, D. K. Johnson and H. L. Chum, in S. Sarkanen and W. Glasser (Editors), *Lignin: Properties and Materials*, Vol. 397, American Chemical Society, Washinton, DC, 1989, pp. 82–99.
59 J. G. McNaughton, W. Q. Yean and D. A. I. Goring, *Tappi*, 50 (1967) 548.
60 E. T. Adams, *Proc. Natl. Acad. Sci. U.S.A.*, 51 (1964) 509.
61 M. Wales, *J. Phys. Colloid Chem.*, 52 (1948) 235.
62 M. Wales, J. W. Williams, J. O. Thompson and R. H. Ewart, *J. Phys. Colloid Chem.*, 52 (1948) 983.
63 O. M. Sokolov, B. D. Bogomolov and N. D. Babikova, *Sovrem. Metody Issled. Khim. Lignina*, (1970) 22.
64 F. Pla and A. Robert, *Cellul. Chem. Technol.*, 8 (1974) 3.
65 F. Pla and A. Robert, *Cellul. Chem. Technol.*, 8 (1974) 11.
66 F. Pla and A. Robert, *Holzforschung*, 38 (1984) 37.
67 A. L. Wooten, M. L. Prewitt, T. Sellers and D. C. Teller, *J. Chromatogr.*, 345 (1988) 371.

Journal of Chromatography, 498 (1990) 105–111
Elsevier Science Publishers B.V., Amsterdam — Printed in The Netherlands

CHROM. 22 009

USE OF HIGH-PERFORMANCE SIZE-EXCLUSION CHROMATOGRAPHY FOR THE SEPARATION OF POLIOVIRUS AND SUBVIRAL PARTICLES

ANDRÉ FORIERS*
Department of Medical and Special Biochemistry, Vrije Universiteit Brussel, Laarbeeklaan 103, B-1090 Brussels (Belgium)
and
BART ROMBAUT and ALBERT BOEYÉ
Department of Microbiology and Hygiene, Vrije Universiteit Brussel, Laarbeeklaan 103, B-1090 Brussels (Belgium)
(First received April 11th, 1989; revised manuscript received August 22nd, 1989)

SUMMARY

The size-dependent separation of viral and subviral particles in the range 10^5–10^7 daltons was undertaken by high-performance liquid chromatography. A combination of Ultrahydrogel 2000 and 1000 size-exclusion columns, equilibrated and developed with Tris buffer (pH 7.4), was used to fractionate extracts of cells infected with radiolabelled poliovirus. Poliovirions (30 nm) and subviral particles (20 nm) were separated according to size with full retention of their biological activities. Procapsids (same size as virions, but devoid of RNA) could not be separated from virions. Sample recoveries as determined with radiolabelled material constantly exceeded 70%. The method was successfully applied to the separation of viral and subviral particles from complex mixtures.

INTRODUCTION

Previous work with soft size-exclusion columns (Sepharose-type support materials) provided a relatively high resolving capacity for macromolecules, but typically required long elution times, as the gel matrix did not withstand the high pressures required for increased flow-rates. Moreover, relatively large amounts of material were required. The resolution of proteins according to their molecular mass has made rapid advances after the introduction of rigid, small-diameter silica-based gels, covalently bonded with hydrophilic compounds. Owing to their improved efficiency (narrower peak widths, higher plate counts), permeability and surface properties, the performance of these gels exceeded that of the soft gels, with typically a 100-fold reduction in separation times[1].

Ultrahydrogel columns (Waters–Millipore, Milford, MA, U.S.A.), which are cross-linked hydroxylated polymers with some residual carboxyl functionality, have been recommended for separating a variety of biological polymers[2]. The molecular mass calibration graphs of these columns are similar to those of the TSK-PW col-

0021-9673/90/$03.50

TABLE I

PHYSICAL PARAMETERS OF VIRIONS, PROCAPSIDS AND 14S SUBUNITS

Species of particles	*Molecular mass*[a]	*Sedimentation value*[a,b]	*Diameter (nm)*[c]	*Elution volume (ml)*[d]
Virions	$8.25 \cdot 10^6$	160S	29	17.4
Procapsids	$5.85 \cdot 10^6$	65S	29	17.4
14S subunits	$4.80 \cdot 10^5$	14S	20	19.6

[a] From ref. 12.
[b] From ref. 13.
[c] From ref. 11.
[d] Using a Ultrahydrogel 2000 + 1000 column combination at a flow-rate of 0.2 ml min^{-1}.

umns manufactured by TosoHaas (Philadelphia, PA, U.S.A.)[2–4], which were successfully applied to the separation of polysaccharides, large enzymes, viruses, ribosomes, DNA, RNA, etc.[5,6] (we chose the Ultrahydrogel material for reasons of economy).

The study of poliovirus morphogenesis requires the separation of viral precursor particles and their assembly products (Table I). Until now, this separation could only be achieved by sucrose gradient ultracentrifugation[7]. We present here an alternative methodology, *i.e.*, the size-dependent separation of virions and subviral particles by size-exclusion high-performance liquid chromatography (HPLC) using a combination of Ultrahydrogel columns.

EXPERIMENTAL

Preparation of radiolabelled extracts of poliovirus-infected cells[8,9]

HeLa cells in suspension (10^7 ml^{-1}) were infected with Mahoney (serotype 1) poliovirus at an input multiplicity of 100 plaque-forming units per cell, and 25 μCi ml^{-1} [^{35}S]methionine were added after 3 h, *i.e.*, after host cell protein synthesis was completely shut-off. The cells were collected 2.5 h later by centrifugation and resuspended to a density of $2 \cdot 10^8$ cells ml^{-1} in RSB buffer (10 m*M* Tris, 10 m*M* NaCl, 1.5 m*M* $MgCl_2$, HCl to pH 7.4). They were freeze–thawed three times and cleared of debris and nuclei by low-speed centrifugation. The supernatant was stored at −80°C until use.

Preparation of radiolabelled poliovirons and subviral particles[8,9]

Radiolabelled virions, procapsids and 14S subunits were prepared as described. Briefly, a radiolabelled poliovirus-infected cell extract (as described above) was submitted to ultracentrifugation in a sucrose density gradient (prepared in RSB). The radioactivity profile was determined, and the 160S virions, 65S procapsids and 14S subunits were collected and stored at −80°C in 50 000 cpm aliquots. The characteristics of the three species of particles are described in Table I.

High-performance liquid chromatography

High-performance size-exclusion chromatography was carried out at 4°C in an LKB 2203 Minicoldlab refrigerated system (Pharmacia LKB, Bromma, Sweden) on

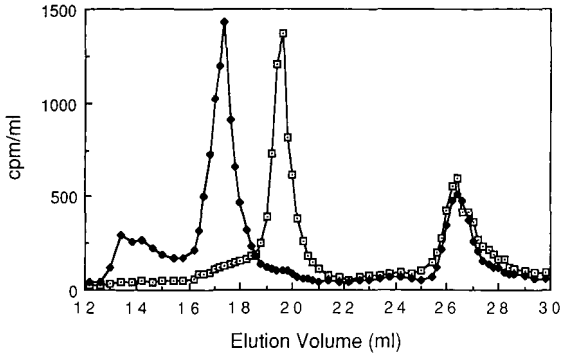

Fig. 1. Elution profile of ^{35}S-labelled 14S viral particles on Ultrahydrogel 2000 + 1000 at 0.2 ml min^{-1} before (□) and after (■) incubation for 20 min at 37°C.

Ultrahydrogel 2000 and Ultrahydrogel 1000 columns (300 × 7.5 mm I.D.) (Waters–Millipore), reported to have polyethylene oxide separation ranges of $5 \cdot 10^4$–$5 \cdot 10^6$ and $5 \cdot 10^3$–$1 \cdot 10^6$ daltons, respectively. Samples were applied with a heparin syringe using a 7000-p.s.i. injection valve (Valco Instruments, Houston, TX, U.S.A.) and a 250-μl loop. The columns were attached to a Waters Model M 45 pump, equilibrated and eluted with RSB of pH 7.4 (filtered with 0.45-μm filter). In all experiments an operating flow-rate of 0.2 ml min^{-1} was used. According to Swergold and Rubin[10], flow-rates exceeding 0.2 ml min^{-1} reduce the efficiency of this type of column. The low back-pressure (40–60 p.s.i.) exhibited by these columns allowed their use in tandem for more efficient separations. The column effluent was monitored at 277 nm with an LKB Uvicord S detector, and collected with an LKB fraction collector. A portion of each eluate fraction was mixed with scintillation liquid to determine the radioactivity profile, using a 1218 Rackbeta liquid scintillation counter and Rackbeta Plot program (LKB).

The total permeation volume (V_t) of the columns was determined from the elution of [^{35}S]methionine (Table II). As no test material of a size sufficient for complete exclusion was available, the total exclusion volume (V_0) was inferred from the sharp rise in absorbance observed when the largest particles were eluted, as illustrated in Fig. 1.

TABLE II

EXCLUDED AND TOTAL VOLUMES OF ULTRAHYDROGEL COLUMNS

Volumes determined at a flow-rate of 0.2 ml min^{-1}.

Column	V_0 *(ml)*	V_t *(ml)*
Ultrahydrogel 2000	6.06	13.52
Ultrahydrogel 1000	5.94	12.67
Ultrahydrogel 2000 + 1000	12.00	26.20

RESULTS

Table I gives a survey of the poliovirus-related particles, the separation of which was attempted. Procapsids, which lack RNA, have a much lower (65S) sedimentation coefficient than virions (160S), and can easily be separated by ultracentrifugation. On the other hand, they have the same size (29 nm). When tested in size-exclusion chromatography using Ultrahydrogel 2000 and 1000 columns mounted in series, both species of particles yielded a single main radioactivity peak (Fig. 2) with an elution volume of 17.4 ml. This result confirms that separation was exclusively according to size.

The third species of poliovirus-related particles is the 14S subunit. These particles measure 20 nm in diameter, to a thickness of 6–7 nm[11]. As expected, 14S subunits eluted separately from virions, with an elution volume of 19.6 ml (Fig. 3).

As the chromatographic separation of poliovirus-related particles was intended as an aid for the study of poliovirus assembly, it was important to learn whether the 14S subunits could be separated from the empty capsids, into which they are known to assemble spontaneously at 37°C[7,12]. Therefore, a sample of 14S material was incubated at 37°C for 20 min, with a control sample being kept in the cold. Both samples were then analysed by HPLC. Fig. 1 shows the results; the control 14S subunits eluted at 19.6 ml as previously observed, whereas those which were allowed to assemble into empty capsids eluted at 17.4 ml, the characteristic elution volume of virions and procapsids. Obviously, the size-exclusion HPLC method allows us to follow the progress of the assembly reaction.

An unfractionated extract of poliovirus infected HeLa cells (see Experimental) was chromatographed. The poliovirus infection is known to cause a complete shut-off of host protein synthesis. Therefore, only viral proteins and particles were radiolabelled in the extract. The radioactivity and absorbance profiles are illustrated in Fig. 4. The radioactivity profile showed four peaks, as follows.

(i) The material eluting at 17.4 ml, corresponded to virions and procapsids. This identification was confirmed by ultracentrifugation of the eluate peak fraction (Fig. 5a) and also by antigenicity determination (presence on N1 and N2 epitopes; results not shown).

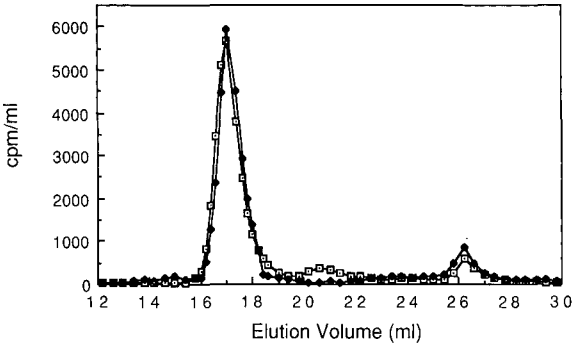

Fig. 2. Elution profile of ^{35}S-labelled virions (□) and procapsids (■), eluted as in Fig. 1.

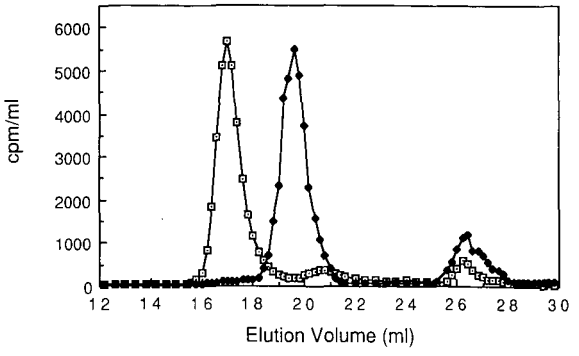

Fig. 3. Elution profile of ^{35}S-labelled virions (□) and 14S subunits (■), eluted as in Fig. 1.

(ii) Similarly, the material eluting at 19.6 ml consisted of 14S subunits (Fig. 5b); as expected, these particles had N1 and H epitopes (not shown).

(iii) The bulk of the radioactivity eluted as an asymmetric peak around 24.5 ml; this elution volume suggested a molecular weight close to 20 kilodaltons. The radioactive material was not precipitable by trichloroacetic acid and presumably consisted of [^{35}S]methionine-loaded tRNA; this tentative identification was confirmed by the similar elution pattern of purified tRNA (Fig. 6).

(iv) The material eluting at 26.2 ml was presumably free [^{35}S]methionine, as this elution volume corresponded to the total volume of the combined columns (300 × 7.5 mm × 2).

The absorbance profile shown in Fig. 4 was remarkable in that some UV-absorbing components eluted past the total volume of 26.2 ml (Table II), indicating that the columns may not function solely in the exclusion mode, but may retain some components by hydrophobic interaction with the gel matrix.

Only a minor decrease in resolution was noted when the volume of the injected mixture was increased from 5 to 100 μl. When the injection volume was further increased to 250 μl, the resolution was significantly decreased as far as the total protein content (shown by the absorbance profile) is concerned. However, the sep-

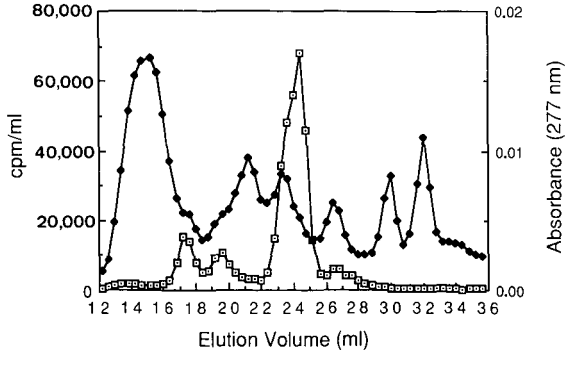

Fig. 4. Elution profile of an extract of infected HeLa cells eluted as in Fig. 1. (□) Radioactive ^{35}S profile in cpm ml^{-1}; (■) absorbance monitored at 277 nm.

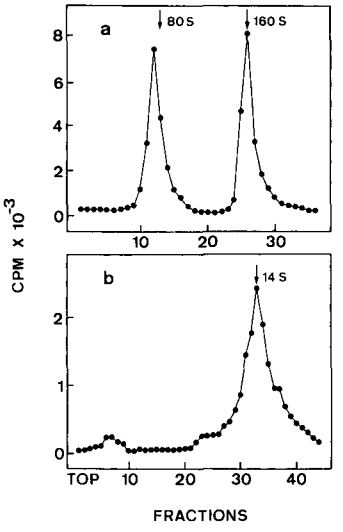

Fig. 5. Sucrose gradient ultracentrifugation of size-exclusion eluate fractions. Two of the fractions shown in the elution profile in Fig. 4 were collected: (a) peak fraction at 17.4 ml and (b) peak fraction at 19.6 ml. Sample a (50 000 cpm) was layered onto a 15–30% sucrose gradient and centrifuged for 5.5 h at 110 000 g_{av} in an MSA 30.6 rotor. Sample b (20 000 cpm) was layered onto a 5–20% gradient and centrifuged for 21 h at 82 000 g_{av} in an MSA 30.3 rotor. Vertical arrows indicate location of 14S subunits, virions (160S) and artificial empty capsids (80S) in control tubes.

aration of the radioactive products (only viral products are radiolabelled, owing to the host shut-off) remained unmodified. At the rate of 0.2 ml min^{-1}, the elution profile of the various viral components was highly reproducible. This was verified in 20 runs, which yielded a precision in retention time of 0.1% (data not shown).

Recovery of input radioactivity, studied using either microgram amounts of [^{35}S]methionine-labelled purified particles or unfractioned cell extracts, always exceeded 70%.

The viability of poliovirus was unaffected by the chromatographic process. In an experiment with ^{35}S-labelled virus, 75% of the input radioactivity and 70% of the

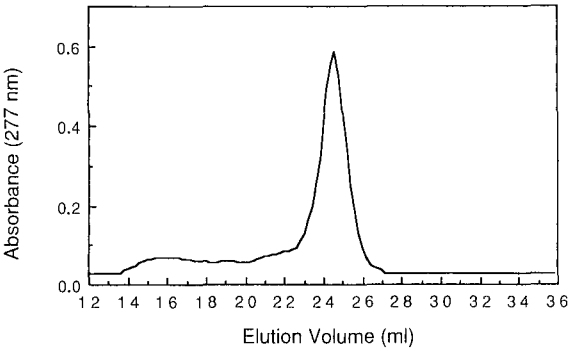

Fig. 6. Elution profile of 100 μg of tRNA (Sigma, St. Louis, MO, U.S.A.) eluted as in Fig. 1.

infectivity (plaque-forming units) were recovered from the virus peak; in other words, the specific infectivities of the recovered and input virus were essentially the same.

DISCUSSION

As demonstrated by Ollivon *et al.*[6], size-exlusion HPLC allows the quantitation and recovery of viral products with a much better resolution than could be achieved with conventional materials. The present results demonstrate that the combination of Ultrahydrogel 2000 and 1000 columns is suitable for the purification and characterization of viral and subviral particles up to $8 \cdot 10^6$ daltons. The 14S subunit, a crucial intermediate in the morphogenetic pathway of poliovirus, can easily be separated from the larger particles (naturally occuring procapsids, empty capsids and virions).

The process entails less than a 30% loss of input material and does not cause denaturation of virions (retention of infectivity) or 14S subunits (retention of assembly activity). Each run requires approximately 3 h; however, as no material is eluted during the first hour, new injections can be made every 2 h without interference with the previous sample. In comparison, sucrose gradient ultracentrifugation typically requires 5–21 h (Fig. 5), although it allows the simultaneous analysis of up to six samples.

As a preparative tool, size-exclusion HPLC has two major advantages over sucrose gradient ultracentrifugation: the eluate fractions are free of sucrose and even relatively small subviral particles, such as 14S subunits, are completely free of [^{35}S]methionine. In sucrose gradient ultracentrifugation, 14S material is always contaminated by free labelled amino acids, owing to their fast diffusion. The removal of either sucrose or free amino acids then requires a dialysis, which often entails losses of labelled material. In conclusion, size-exclusion HPLC on Ultrahydrogel columns is a useful alternative to sucrose gradient ultracentrifugation for the separation of viral and subviral particles, such as those involved in poliovirus morphogenesis.

ACKNOWLEDGEMENTS

The authors are grateful to Monique De Pelsmacker and Alfons De Rees for their excellent technical assistance. This study was supported by the Fonds voor Geneeskundig Wetenschappelijk Onderzoek (Belgium). One of us (B.R.) is a Senior Research Assistant of the National Fund for Scientific Research.

REFERENCES

1 S. Rokushika, T. Ohkawa and H. Hatano, *J. Chromatogr.*, 176 (1979) 456.
2 R. Nielson, *J. Anal. Purif.*, 2 (1987) 57.
3 Y. Kato, H. Sasaki, M. Aiura and T. Hashimoto, *J. Chromatogr.*, 153 (1978) 546.
4 T. Hashimoto, H. Sasaki, M. Aiura and Y. Kato, *J. Chromatogr.*, 160 (1978) 301.
5 M. E. Himmel and P. G. Squire, *J. Chromatogr.*, 210 (1981) 443.
6 M. Ollivon, A. Walter and R. Blumenthal, *Anal. Biochem.*, 152 (1986) 262.
7 B. Rombaut, R. Vrijsen and A. Boeyé, *Virology*, 153 (1986) 137.
8 B. Rombaut, R. Vrijsen and A. Boeyé, *J. Gen. Virol.*, 66 (1985) 303.
9 B. Rombaut, R. Vrijsen and A. Boeyé, *Arch. Virol.*, 76 (1983) 289.
10 G. D. Swergold and C. S. Rubin, *Anal. Biochem.*, 131 (1983) 295.
11 S. Onodera, J. J. Cardamone, Jr. and B. A. Phillips, *J. Virol.*, 58 (1986) 610.
12 J. R. Putnak and B. A. Phillips, *Microbiol. Rev.*, 45 (1981) 287.
13 B. Rombaut, R. Vrijsen, P. Brioen and A. Boeyé, *Virology*, 122 (1982) 215.

Journal of Chromatography, 498 (1990) 113–128
Elsevier Science Publishers B.V., Amsterdam — Printed in The Netherlands

CHROM. 22 043

MODELLING SINGLE-COMPONENT PROTEIN ADSORPTION TO THE CATION EXCHANGER S SEPHAROSE® FF

GRAHAM L. SKIDMORE, BRENDA J. HORSTMANN and HOWARD A. CHASE*
Department of Chemical Engineering, University of Cambridge, Pembroke Street, Cambridge CB2 3RA (U.K.)
(First received May 5th, 1989; revised manuscript received September 29th, 1989)

SUMMARY

The equilibrium and kinetic characteristics of the adsorption of bovine serum albumin (BSA) and lysozyme to the strong cation exchanger S Sepharose FF have been determined. The rates of protein adsorption have been compared to two different models, the first being based on a single lumped kinetic parameter, whilst the second model considers the individual transport processes occurring prior to the adsorption reaction, that is taking into account diffusion across the liquid film surrounding individual particles and also the diffusion within the ion-exchanger particle itself. It was found that the adsorption of lysozyme to S Sepharose FF, in both batch, agitated tanks and in packed beds was consistent with both models. In the case of BSA however, the agitated tank adsorption profile was consistent only with the pore diffusion model and neither model correctly predicted the latter part of the breakthrough profile observed in packed-bed experiments.

INTRODUCTION

Ion-exchange adsorbents have found widespread use in the purification of proteins, both in the laboratory and in the production plant, since the introduction in 1956 of the first ion exchanger spcifically designed for proteins[1]. This has recently been highlighted in a study by Bonnerjea *et al.*[2] which showed that ion exchangers were used in 75% of all the published purification protocols that they examined. This widespread use of ion exchangers is due to their versatility, relative cheapness and their acceptance by the regulatory authorities in the production of pharmaceutical proteins. This is in contrast to affinity adsorbents which, although they result in good resolution, are limited to one protein or group of proteins, are expensive and their use is currently questioned by regulatory bodies.

We have been studying the adsorption of proteins to ion exchangers to investigate how different properties of the ion exchangers affect their adsorption performance, and with the aim of producing simple models of the purification process to assist in process design. Previous studies examined how the properties of different anion exchangers, such as functional groups and the particle matrix, affected

0021-9673/90/$03.50

performance[3]. In this paper we have obtained experimental data for the binding of bovine serum albumin (BSA) and lysozyme to the strong cation exchanger S Sepharose FF. These results have been compared to the results calculated from two different models of the adsorption process. The characteristics of the adsorption of each protein to the ion exchanger were determined by several different types of experiment. The equilibrium capacity of S Sepharose FF for each of the proteins was established by determining adsorption isotherms. However, the adsorption of protein by an ion exchanger is not an instantaneous event and mass transfer effects must also be considered. The dynamic approach to equilibrium was therefore examined by studying the rate of uptake of protein in a shaken vessel. Finally the adsorption of protein to packed beds of S Sepharose FF was studied by determining breakthrough profiles. The completion of these studies provided a characterised system which was then used as the basis for studies of the simultaneous adsorption of BSA and lysozyme to S Sepharose FF from a solution containing both proteins. These studies will be reported in a following paper[4].

THEORY

An equilibrium model

When discussing protein adsorption to ion exchangers, the adsorbent is frequently considered as consisting of functional groups the charge of which is balanced by associated counter-ions, whilst the protein molecule is considered to exist in an ionized state in solution. On adsorption to an ion exchanger, a protein molecule displaces the counter-ions which were previously associated with the charged groups of the ion exchanger. For an ion exchanger equilibrated with monovalent counter-ions, this process can be represented by an equilibrium of the form:

$$A \cdot nI + P^n \rightleftharpoons A \cdot P + nI \tag{1}$$

where A represents the adsorption site on the ion exchanger, I represents the counter-ions, P the protein molecule and n the number of charges involved in the interaction per adsorbed protein molecule. If the change in bulk-fluid concentration of the counter-ion I is small as a result of protein adsorbing to the ion exchanger, as is the case when buffered solutions containing I are used, then equilibrium 1 may be simplified to:

$$A + P \underset{k_{-1}}{\overset{k_1}{\rightleftharpoons}} A \cdot P \tag{2}$$

and hence the rate of change of the adsorbed protein concentration is given by:

$$\frac{dq}{dt} = k_1 c(q_m - q) - k_{-1} q \tag{3}$$

where c is the soluble protein concentration, k_1 and k_{-1} are the adsorption and desorption rate constants respectively, q is the adsorbed protein concentration, q_m the maximum protein capacity of the ion exchanger and t represents time.

At equilibrium eqn. 3 equates to zero and hence:

$$q^* = \frac{c^* q_m}{c^* + \frac{k_{-1}}{k_1}} \tag{4}$$

where the superscript * denotes values when equilibrium has been established between solid and liquid phases. Substituting $K_d = k_{-1}/k_1$ into eqn. 4 gives:

$$q^* = \frac{c^* q_m}{c^* + K_d} \tag{5}$$

where K_d is the dissociation constant of the protein–ion-exchanger complex. Eqn. 5 is the form of the Langmuir adsorption isotherm that we have previously used to describe the adsorption of BSA to anion exchangers[3]. The Langmuir isotherm is used frequently to describe the adsorption of proteins to various adsorbents, including ion exchangers, for example Leaver[5], Chase[6] and Annesini and Lavecchia[7]. Rearranging eqn. 5 gives the linear form of:

$$\frac{c^*}{q^*} = \frac{K_d}{q_m} + \frac{c^*}{q_m} \tag{6}$$

from which the dissociation constant, K_d and the maximum protein capacity of the ion exchanger, q_m, can be calculated by least squares linear regression analysis.

The approach to equilibrium—models of the uptake of protein

Kinetic rate constant model. We have previously used a kinetic rate constant model, based on a single "lumped" adsorption rate constant, to describe the adsorption of proteins to affinity adsorbents[8]. The model takes an empirical approach to the adsorption process and assumes that all the rate limiting processes can be represented by kinetic rate constants. In such an approach, the rate of mass transfer of protein to the adsorbent is assumed to be described by eqn. 3 above. For batch adsorption in a stirred tank, the protein concentration in solution at time t is given by the analytical solution of eqn. 3, namely:

$$c = c_0 - \frac{v}{V}\left[\frac{(b+a)\left(1 - \exp\left\{-\frac{2av}{V}k_1 \cdot t\right\}\right)}{\left(\frac{b+a}{b-a}\right) - \exp\left\{-\frac{2av}{V}k_1 \cdot t\right\}}\right] \tag{7}$$

where

$$a^2 = b^2 - \left(\frac{c_0 \cdot V}{v}\right)q_m \tag{8}$$

$$b = \frac{1}{2}\left(\frac{c_0 \cdot V}{v} + q_m + \frac{K_d V}{v}\right) \tag{9}$$

and c_0 is the initial liquid phase protein concentration, v is the volume of ion exchanger present and V the volume of liquid external to the ion exchanger.

If it is assumed that the effects of axial dispersion are negligible then eqn. 3 can also be solved analytically to describe adsorption in packed columns, first performed by Thomas[9] for classical ion exchange processes and adapted by Chase[8] for the adsorption of proteins to affinity adsorbents.

Film and pore diffusion model. A more rigorous approach to modelling the adsorption process is to consider the different steps that occur during protein uptake. These are commonly defined as transport through the liquid film surrounding the adsorbent particles, diffusion within the pores of the adsorbent and finally the adsorption reaction itself. We have recently shown that the affinity adsorption of immunoglobulin G to protein A immobilised on agarose matrices is described well by a combination of surface-film resistance and porous-diffusion resistance[10]. Such a model might also be expected to account for the rates of protein adsorption to ion exchangers. The following assumptions are used as the basis for the construction of the model:

(1) The adsorbent is made of a porous material, into which the solute must diffuse, in a manner described by an effective pore diffusivity, D. D is assumed to be independent of concentration and is based on the porosity of the particle towards small molecules, rather than the actual extent to which molecules of a particular protein can penetrate the particle.

(2) Mass transfer to the surface of the adsorbent is governed by a film model characterised by a mass transfer coefficient, k_f.

(3) Surface reaction between the adsorbate and an adsorption site is described by a reversible second order reaction. Adsorption is isothermal, and its equilibrium behaviour can be represented by the Langmuir equation. Surface diffusion in which adsorbate moves directly between adsorption sites without interim desorption into the liquid phase is assumed to occur at a negligible rate and hence a term to describe this process is not thought appropriate.

(4) The adsorbent particles are spherical, with uniform size and density, and the functional groups of the ion exchanger are distributed evenly throughout the interior of the particle.

(5) Axial dispersion, D_x, is negligible in packed bed simulations.

For diffusion of protein in the liquid within the ion exchanger particle, the point concentration of protein, c_i, is given by:

$$\varepsilon\frac{\partial c_i}{\partial t} = \varepsilon D\left(\frac{\partial^2 c_i}{\partial r^2} + \frac{2\partial c_i}{r\partial r}\right) - (1-\varepsilon)\frac{\partial q_i}{\partial t} \tag{10}$$

where ε is the particle porosity, q_i the point concentration of adsorbed protein and r the radial coordinate within the ion-exchanger particle. The particle porosity was determined from a knowledge of the solids content of the adsorbent. S Sepharose FF is formulated from 6% agarose and hence the particle porosity was taken as being 0.94.

The rate of mass transfer through the external film relates the bulk liquid concentration, c, to the concentration in the pore liquid at the surface of the particle. The expression is:

$$\left.\frac{\partial c_i}{\partial r}\right|_{r=R} = \left.\frac{k_f}{D\varepsilon}(c - c_i)\right|_{r=R} \tag{11}$$

At the centre of the particle

$$r = 0 \qquad \frac{\partial c_i}{\partial r} = 0 \tag{12}$$

If a second order rate of surface reaction is assumed then the rate of change of adsorbed protein concentration is given by eqn. 3 above. At equilibrium this gives a form of the Langmuir equation with maximum capacity q_m and dissociation constant $K_d = k_{-1}/k_1$, eqn. 5 above.

For adsorption and desorption in a stirred tank, the rate of change of bulk concentration of protein, c, is given by:

$$\frac{dc}{dt} = -\left(\frac{3vk_f}{RV}\right)(c - c_i)\bigg|_{r=R} \tag{13}$$

The correlation used to estimate the liquid film mass transfer coefficient, k_f, of protein to the adsorbent particles in stirred tank experiments was that given by Geankoplis[11].

$$k_f = \frac{2D_{AB}}{d} + 0.31\left(\frac{\mu}{\rho D_{AB}}\right)^{-\frac{2}{3}}\left(\frac{\Delta\rho\mu g}{\rho^2}\right)^{\frac{1}{3}} \tag{14}$$

where ρ is the particle density, $\Delta\rho$ is the density difference between the adsorbent particle and the liquid, μ is the liquid viscosity and g is the gravitational constant. The molecular diffusivity of lysozyme and BSA in free aqueous solution, D_{AB}, was estimated using the semi-empirical equation of Polson[12]:

$$D_{AB} = 9.4 \cdot 10^{-15}\frac{T}{\mu(M_A)^{\frac{1}{3}}} \tag{15}$$

where M_A is the relative molecular mass of A and T is the absolute temperature. Taking 14 500 and 66 300 as the relative molecular masses of lysozyme and BSA respectively, gives molecular diffusion coefficients in acetate buffer, D_{AB}, of $1.2 \cdot 10^{-10}$ m^2/s and $7.3 \cdot 10^{-11}$ m^2/s respectively.

For adsorption in a packed bed, the equation of continuity in the mobile phase is given by:

$$D_x\frac{\partial^2 c}{\partial x^2} - l\frac{\partial c}{\partial x} - R_i = \frac{\partial c}{\partial t} \tag{16}$$

where x is the axial coordinate in the bed, l the interstitial velocity of liquid in the bed and R_i is rate of interface mass transfer. The rate expression is:

$$R_i = \frac{3}{R}\frac{(l - \varepsilon_b)}{\varepsilon_b} D\frac{\partial c_i}{\partial r}\bigg|_{r=R} \tag{17}$$

where ε_b is the porosity of the packed bed. Using data from molecular-exclusion experiments performed with very high-molecular-weight dextran, the porosity of packed beds of S Sepharose FF was taken to be 0.35.

At each point in the column, the concentration outside the fluid film is related to the liquid phase concentration at the surface of the particle by:

$$k_f(c - c_i)\Big|_{r=R} = \varepsilon D \frac{\partial c_i}{\partial r}\Big|_{r=R} \tag{18}$$

To estimate k_f in a packed bed, the following correlation of Foo and Rice[13] was used:

$$Sh = 2 + 1.45 Re^{\frac{1}{2}} Sc^{\frac{1}{3}} \tag{19}$$

where $Sh = k_f d/D_{AB}$, $Re = u\rho d/\mu$, $Sc = \mu/(\rho D_{AB})$, u is the superficial velocity of liquid flow through the column and d is the mean particle diameter.

EXPERIMENTAL

Materials

BSA and lysozyme (EC 3.2.1.17) were obtained from Sigma (Poole, U.K.), catalogue numbers A-3912 and L-6876, respectively. BSA has a relative molecular mass of 66 300 daltons[14] and an isoelectric point (p*I*) of pH 4.7 (ref. 15), whilst lysozyme has a relative molecular mass of 14 500 daltons[16] and a p*I* of pH 11.1 (ref. 17). The choice of these two proteins was largely determined by cost considerations as the capacity of ion exchangers (commonly in the range 50–100 mg protein per ml of ion exchanger) meant that gram quantities of pure proteins were required for these studies.

All solutions were buffered with 0.1 *M* sodium acetate–acetic acid, pH 5. Sodium acetate, acetic acid and sodium chloride were all laboratory grade reagents. S Sepharose FF was a gift from Pharmacia LKB (Uppsala, Sweden). Known volumes of ion exchanger were obtained by allowing a suspension of the ion exchanger to settle in a measuring cylinder overnight and then adjusting the liquid volume to equal that of the settled ion exchanger. Aliquots of a known volume of a 50:50 (v/v) suspension were then obtained by the use of a Gilson Pippetman automatic pipette.

Adsorption isotherms

Isotherms for the adsorption of each protein to S Sepharose FF were determined in batch experiments. A known volume of a 50:50 (v/v) suspension of ion exchanger in buffer was added to each of a series of flasks containing known volumes of buffered protein solution at different concentrations. The flasks were incubated overnight in a shaking water bath at 25°C to allow equilibrium to be established. The ion exchanger was then allowed to settle under gravity for approximately 30 min and the resulting supernatant was filtered before determining the equilibrium concentration of protein in the soluble phase by UV spectrophotometry. The amount of protein adsorbed to the S Sepharose FF was then calculated by mass balance.

Kinetics of batch adsorption

The rate of adsorption of protein to a suspension of S Sepharose FF was determined in experiments in which the soluble phase protein concentration of a batch system was continuously monitored. This was achieved by recycling the liquid phase; the liquid was first passed through a 2-μm HPLC pump inlet filter to prevent removal of suspended S Sepharose FF from the reaction vessel and then through a continuous flow UV spectrophotometer before return to the experimental vessel. The reaction vessel was incubated and agitated in a shaking water bath maintained at 25°C. A typical experiment consisted of 25 ml of buffer containing protein at a concentration of 2 mg/ml. In order to achieve a rapid response time the volume of the recycle was kept as small as possible (approximately 1 ml) and the solution was pumped at a flow-rate of 7 ml/min. Experiments were commenced by the addition of 0.5 ml of a 50:50 (v/v) suspension of S Sepharose FF. The output from the UV spectrophotometer was connected to a chart recorder, and the protein concentration in the liquid phase at selected times was determined from the chart recorder trace and reference to calibration data. The protein concentrations were normalised by dividing the concentration c, at time t, by the protein concentration at time zero, c_0.

Frontal analysis

Breakthrough curves were determined in order to evaluate packed bed performance. All column experiments were performed with 2 ml (settled volume) of ion exchanger packed in a chromatography column, 1 cm diameter (0.785 cm^2 cross-sectional area), mounted vertically. It was found that the volume of ion exchanger used gave a bed height of 2.2–2.3 cm, equivalent to a packed volume of approximately 1.75 ml. All experiments were performed at a volumetric flow-rate of 1 ml/min (superficial velocity 1.27 cm/min) and flow was always in an upward direction. Protein was applied to the beds at a concentration of 1 mg/ml (c_0) and the optical density at 280 nm of the outlet stream was recorded. For the determination of breakthrough curves, the beds were loaded until the protein concentration in the outlet stream equalled, or was approaching, that of the inlet stream, c_0. At the end of the adsorption phase protein was eluted from S Sepharose FF with 1 *M* sodium chloride in 0.1 *M* acetate buffer. Data were plotted in the form of normalised concentration, c/c_0, of the outlet stream against the amount of protein applied. Time zero was taken as the point at which the adsorbate solution first entered the bed.

Computer simulations

The equations of the kinetic rate constant model were solved using programs written in BASIC running on a BBC microcomputer[8]. The governing differential equations of the film and pore diffusion model were solved using a finite difference method using the University of Cambridge IBM 3084 mainframe computer as described previously[10].

RESULTS

Adsorption isotherms

The isotherms for the adsorption of BSA and lysozyme to S Sepharose FF in 0.1 *M* sodium acetate buffer, pH 5 are shown in Fig. 1. The experimental data for both

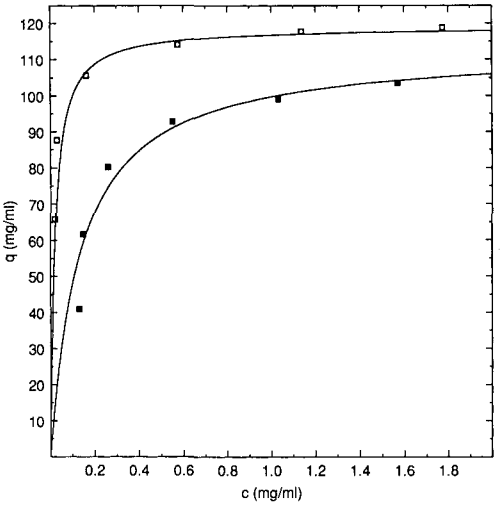

Fig. 1. Adsorption isotherms for the binding of lysozyme (□) and BSA (■) to S Sepharose FF in 0.1 *M* acetate buffer, pH 5 at 25°C. The data are plotted as mg protein adsorbed per ml S Sepharose FF against mg/ml protein in solution. The Langmuir constants were determined by linear regression and are presented in Table I.

proteins fitted well to a Langmuir isotherm and the characteristic parameters K_d and q_m are shown in Table I. The adsorption capacities of the adsorbents are based on the volume that the adsorbent would occupy when packed in a bed. The maximum capacities for the two proteins are similar when compared on a mass basis but the dissociation constants are only similar when compared on a molar basis.

Kinetics of adsorption in a stirred tank

The experimental data for the rates of protein adsorption in a stirred tank were compared with the two models described above; namely the kinetic rate constant model and the film and pore diffusion model. In each model there was only a single unknown parameter describing the rate of protein adsorption and the value of this parameter could be determined by finding the best fit to the experimental data. With the kinetic rate constant model, a simulation of the rate of protein adsorption was made using eqn. 7. The only unknown parameter was the apparent rate constant, k_1 as values of the isotherm parameters q_m and K_d were taken to be those determined in the batch isotherm experiments described above and the other parameters were known from the conditions of the experiment. k_{-1} is given simply by $K_d \cdot k_1$ since the ratio of the reverse to the forward rate constant is the dissociation constant. The simulation was run with a variety of values of the unknown parameter k_1 and the value of this parameter was thus determined as the value that gave the best fit to the experimental curve. Similarly for the pore and diffusion model, simulations of the rate of protein adsorption were made by solving eqns. 11–14 for a variety of values of the only unknown parameter D. Again the value of D was taken to be that value which gave the best fit to the experimental curve.

The agreement between the simulations and the experimental uptake curve is

TABLE I

VALUES OF K_d, q_m, k_1, k_f AND D FOR THE ADSORPTION OF BSA AND LYSOZYME TO S SEPHAROSE FF

	K_d $(mg\ ml^{-1})$	K_d (M)	q_m $(mg\ ml^{-1})$	q_m $(mol\ l^{-1})$	k_1 $(ml\ mg^{-1}\ s^{-1})$	k_1 $(l\ mol^{-1}\ s^{-1})$	k_f[a] $(m\ s^{-1})$	k_f[b] $(m\ s^{-1})$	D $(m^2\ s^{-1})$
Lysozyme	0.019	$1.3 \cdot 10^{-6}$	120	$8.4 \cdot 10^{-3}$	$1.7 \cdot 10^{-3}$	23.88	$8.0 \cdot 10^{-6}$	$8.1 \cdot 10^{-6}$	$5.0 \cdot 10^{-11}$
BSA	0.133	$2.0 \cdot 10^{-6}$	113	$1.7 \cdot 10^{-3}$	$5.0 \cdot 10^{-4}$	33.15	$5.0 \cdot 10^{-6}$	$5.6 \cdot 10^{-6}$	$8.5 \cdot 10^{-12}$

[a] Values obtained from the correlation for stirred tanks (eqn. 14).
[b] Values obtained from the correlation for packed beds (eqn. 19).

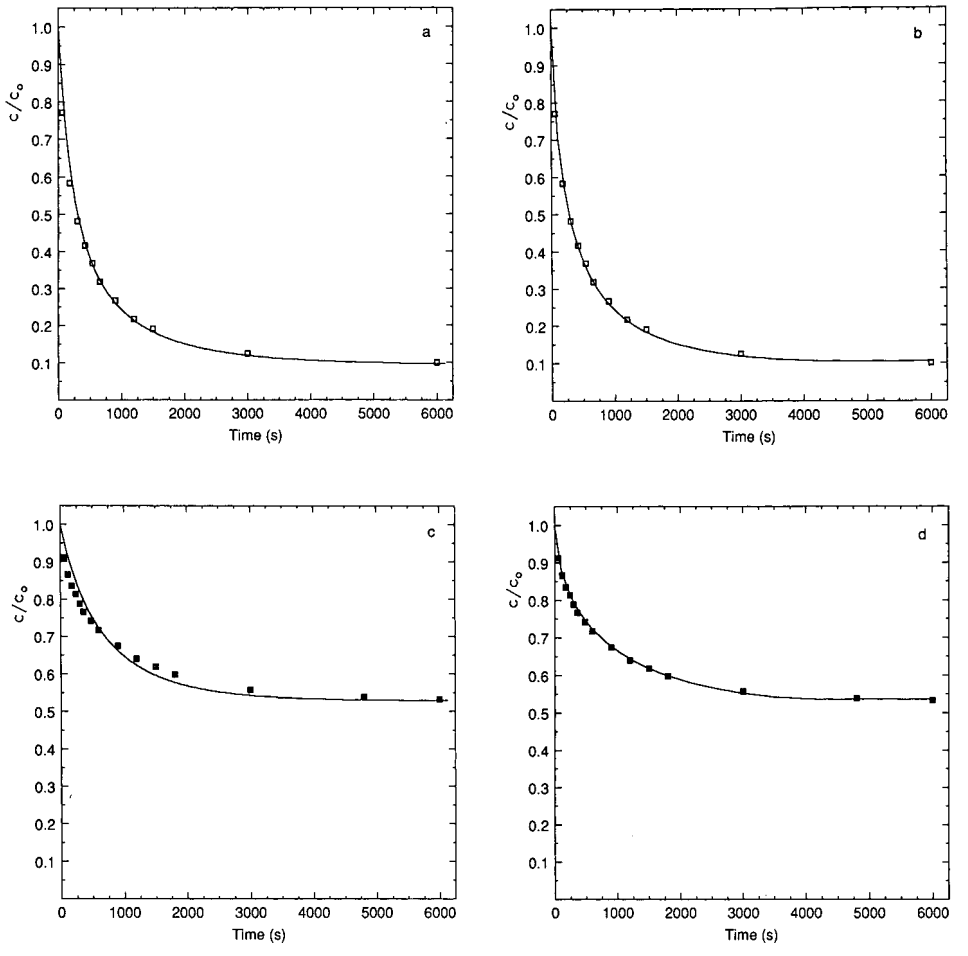

Fig. 2. Batch adsorption profiles for the uptake of lysozyme (□) and BSA (■) by S Sepharose FF in suspension in agitated vessels. The solid lines were calculated by solution of the appropriate equations describing the adsorption profiles for the two models discussed in the text. (a) The adsorption of lysozyme and the adsorption profile predicted by the kinetic rate constant model. (b) The adsorption of lysozyme and the adsorption profile predicted by the film and pore diffusion model. (c) The adsorption of BSA and the adsorption profile predicted by the kinetic rate constant model. (d) The adsorption of BSA and the adsorption profile predicted by the film and pore diffusion model. The parameters used in the calculations are listed in Table I.

shown in Fig. 2. Table I shows the best fit values for the rate constant, k_1, for the kinetic rate constant model and the effective diffusivity, D, for the film and pore diffusion model. It was possible to obtain equally good fits to both models for the adsorption of lysozyme (Fig. 2a and b) but the uptake profile for the adsorption of BSA fitted better to the pore and film diffusion model (Fig. 2d). When the latter system was compared with the kinetic rate constant model (Fig. 2c), it was not possible to find a value of the unknown parameter, k_1, that was appropriate throughout the entire time course of adsorption.

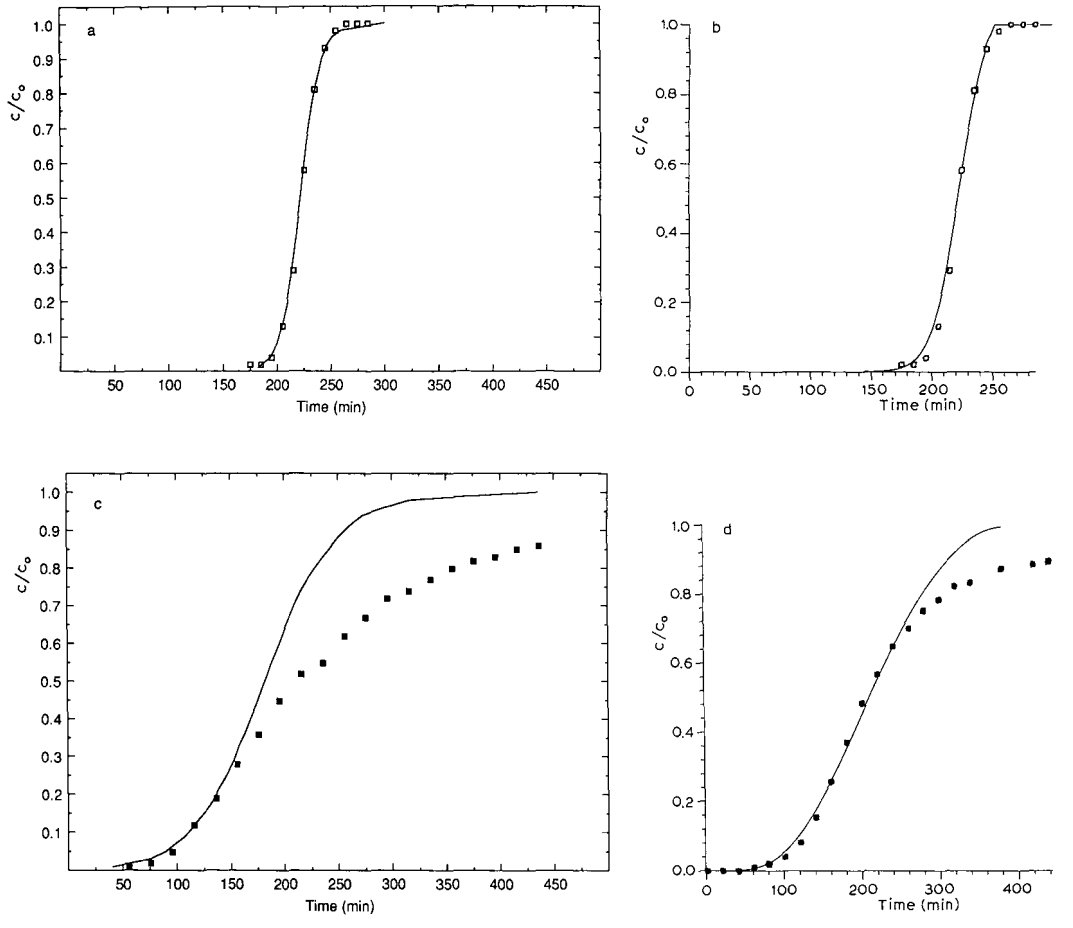

Fig. 3. Breakthrough profiles for the adsorption of lysozyme (□) and BSA (■) to S Sepharose FF in packed beds. The beds used were 1 cm diameter and 2.3 cm high. All flow-rates were 1 ml/min in an upward direction and protein solutions at a concentration of 1 mg/ml. The solid lines were calculated by solution of the appropriate equations describing the adsorption profiles in packed beds for the two models discussed in the text. (a) The adsorption of lysozyme and the adsorption profile predicted by the kinetic rate constant model. (b) The adsorption of lysozyme and the adsorption profile predicted by the film and pore diffusion model. (c) The adsorption of BSA and the adsorption profile predicted by the kinetic rate constant model. (d) The adsorption of BSA and the adsorption profile predicted by the film and pore diffusion model. The parameters used in the calculations are listed in Table I with the exception of (d) in which the value of q_m used was 130 mg/ml.

Frontal analysis

Frontal analysis experiments were performed to see whether the two models of protein adsorption that had been used to model uptake in a stirred tank could also describe adsorption in a packed bed. The experimental breakthrough curves are shown in Fig. 3. The figure also shows the curves predicted by the two models using the values of the equilibrium and rate parameters determined in the isotherm and batch uptake experiments. However, the values of k_f used in the film and pore diffusion model were

those appropriate for adsorption in a packed bed and were estimated from the correlation given above (eqn. 19).

For lysozyme, it was found that both models gave a good fit to the experimental breakthrough curve using the parameters derived from batch experiments (Fig. 3a and b). However, neither model gave a precise fit to the breakthrough curve obtained with BSA (Fig. 3c and d). The experimental curve for the latter system was very asymmetric and approached the inlet concentration very slowly. Indeed, it appeared that the equilibrium capacity of the bed for BSA was greater than that predicted from the adsorption isotherm experiments. A value for the apparent maximum capacity in fixed bed uptake was not able to be determined by integrating the area above the breakthrough curve as the outlet concentration had not risen completely to the inlet value by the end of those experiments. Both models failed to predict the later stages of breakthrough correctly although the film and pore diffusion model did predict some degree of asymmetry to the shape of the curve and a good fit to the earlier stages of adsorption was obtained. The best fit with this model was obtained if the value of q_m used in the simulations was increased from the value found in batch uptake experiments (113 mg/ml) to 130 mg/ml. Attempts were also made to obtain better fits to the experimental data by varying the values of the rate parameters from those obtained from the batch uptake experiments. Hence, with the kinetic rate constant model, simulations were carried out with other values of k_1 and other values of D were used in the film and pore diffusion model. However, in both cases, it was not possible to obtain better fits to the top end of the curve without resulting in a lack of fit to the earlier part of the experimental curve. This approach to obtain a better fit was thus abandoned as it was considered better to retain an accurate description of the early part of the breakthrough curve. Possible reasons for the poor fit to the latter stages of the breakthrough curve for BSA adsorption are discussed in detail below.

DISCUSSION

The Langmuir isotherm has been successfully used to describe the adsorption of both BSA and lysozyme to the cation exchanger S Sepharose FF in single component experiments. This is consistent with our studies of the adsorption of BSA to anion exchangers in which a Langmuir isotherm was also found to be appropriate[3]. The values of the dissociation constant, K_d, for the adsorption of the two proteins to S Sepharose FF are similar in molar terms, a somewhat surprising observation as the pH used in this study, pH 5, was very close to the isoelectric point of BSA and the molecule would have been carrying a net negative charge of -2 (ref. 18). As such it may be expected that the protein would only bind weakly to an anion exchanger and not at all to a cation exchanger such as S Sepharose FF. In fact there was a considerable degree of BSA adsorption to S Sepharose FF, indicating that although the net charge of the molecule may be negative, there must be an asymmetric distribution of charges on the molecule such that a considerable degree of positive charge is present in one region[18] which may interact with the negatively charged sulphonic groups present in S Sepharose FF. Kopaciewicz *et al.*[19] have reported similar studies in which a number of proteins, including BSA were found to bind to ion exchangers at pH values at which the net charge carried by the proteins was the same as that carried by the functional group on the ion exchanger. In molar terms, the maximum capacity of S Sepharose FF

for lysozyme is several times greater than for BSA. A possible reason for this is the smaller size of the lysozyme molecule which could have two effects. Firstly more molecules of lysozyme than BSA may be able to fit onto a given surface area and secondly the smaller lysozyme molecule will be able to penetrate regions of the ion-exchanger particles which are too restricted for the larger BSA molecule to enter, this being the working principle behind molecular exclusion separation methods.

The use of the Langmuir isotherm to describe protein adsorption has recently been criticised by Velayudhan and Horváth[20]. They point out that a consideration of the nature of adsorption of proteins to many adsorbents, including ion exchangers, indicates that proteins do not bind at individual, independent sites, one of the assumptions of the theoretical derivation of the Langmuir isotherm, but that multivalent attachment involving several functional groups on both the protein and the adsorbent occurs. Such multivalent adsorption has been demonstrated by several authors in different systems, including ion exchangers. Gosling[21] for example, has demonstrated the expulsion of 10–15 moles of chloride for every mole of BSA that was adsorbed to a diethylaminoethyl (DEAE) derivatised ion-exchange material. Velayudhan and Horváth[20] also point out that the Langmuir isotherm can not account for changes in protein retention with changes in salt concentration. However, many authors have found that experimental protein-adsorption data from a variety of different systems can be described by a Langmuir type isotherm and constants derived from it can be used in models of the dynamic processes of protein adsorption, as demonstrated in this paper. Whilst accepting its limitations, the Langmuir isotherm remains therefore, a simple and useful tool which can be used to help in the study of protein adsorption and to compare and contrast different ion exchangers.

Two different models, both utilising equilibrium constants derived from the Langmuir isotherm, have been used to describe protein-adsorption profiles in stirred tanks. The shapes of the predicted curves were compared to experimental data for each of the proteins being studied. In the case of lysozyme the kinetic rate constant model gave a curve which followed closely the experimental adsorption profile throughout the whole period of the experiment. A similar fit could not be obtained to the adsorption profile of BSA. A possible reason for the relatively poor fit of the BSA adsorption data to the kinetic rate constant model is that diffusion of BSA within the S Sepharose FF particles is severely hindered and hence adsorption of BSA may occur initially in the outer regions of particles. As the diffusion paths are short, adsorption appears to take place rapidly whilst later phases of adsorption, which must take place deeper in the particle as the outer regions are filled, are thus much slower than the initial rate. The lysozyme molecule, being smaller than BSA, is able to penetrate the particles more easily and adsorption could be occurring at a more even rate throughout the whole adsorption period. The resulting lysozyme adsorption profile is a shape that can be successfully described by the kinetic rate constant model. This hypothesis could be further investigated by performing a series of experiments in which the adsorption process is stopped at different time points, followed by visualising the location of the adsorbed protein within the adsorbent particle.

The fits of the film and pore diffusion parameter model are very close to the experimental data for both proteins. In the case of lysozyme the experimental data fitted this model slighter better than the kinetic rate constant model. As expected, for both proteins, the values of the effective pore diffusion coefficient, D, were found to be

lower than the calculated molecular diffusion coefficients in free solution, D_{AB}. The ratios of the molecular diffusivity in free solution, D_{AB}, to the effective diffusivity in the adsorbent particle, D are 2.4 for lysozyme and 8.6 for BSA, which provides strong evidence that the diffusion of BSA within the particle is more restricted than for the smaller lysozyme molecule. The ability to get excellent agreement between theoretical and experimental profiles for both proteins suggests that the film and pore diffusion model can be used successfully to predict the rates of adsorption of proteins to ion exchangers in mixed tank situations.

Both the kinetic rate constant model and the film and pore diffusion model predict breakthrough curves very close to the experimental points obtained for lysozyme. Both the sharpness of the curve and its symmetry is mirrored in each of the calculated curves. The reasons why BSA behaved anomalously in the fixed bed experiments are not known. The ion exchanger had a greater capacity for BSA when loaded in a packed bed mode than had been predicted from isotherms that were the result of stirred tank experiments. This additional capacity appeared to be characterised by slow adsorption kinetics as evidenced by the slow rise in the value of c/c_0 during the later part of the breakthrough curve. The time–concentration profile seen by the adsorbent is much different in packed bed and stirred tank experiments and this may partially explain the difference observed. It is well established that BSA can form dimers in solution[22] and it is possible that the high local concentrations of BSA that are present when this protein is adsorbed to the ion exchanger, and the constant flow of fresh BSA solution in packed bed experiments, may promote the formation of dimers. If this were the case, the apparent additional adsorption capacity may be the result of multi-layer binding of BSA molecules to molecules that are already adsorbed. Indeed when BSA eluted from S Sepharose FF was analysed by molecular exclusion chromatography two peaks were observed. The retention volume of the peaks suggested the presence of BSA monomer and dimer forms, indicating that dimer formation was occurring in the packed bed. Although there was evidence for some dimers in the fresh, unadsorbed solutions, the concentration of the dimer in the eluted protein was much enhanced.

The results presented here illustrate the use of two different models to describe the adsorption of proteins to the strong cation exchanger S Sepharose FF. In the case of lysozyme both models predicted accurately the observed adsorption profiles in mixed tanks and in packed beds. The predictions from both models of BSA adsorption were not as accurate as those of lysozyme adsorption, however, the apparent agreement may be sufficient for most design purposes. Although it is recognised that the kinetic rate constant model is a gross simplification of the actual adsorption process, it may be a useful method for the prediction of the adsorption of proteins to ion exchangers, given its simplicity and the small amount of computing power required in contrast to the more rigorous film and pore diffusion model. Similar studies with an affinity adsorption system involving the adsorption of immunoglobulin G to agarose based affinity adsorbents showed that only the film and pore diffusion model described the experimental data accurately[10].

SYMBOLS

A adsorption site on the ion exchanger
c soluble protein concentration
c_i point concentration of protein
c_0 initial, or inlet liquid phase protein concentration
d mean particle diameter
D effective pore diffusivity
D_{AB} molecular diffusivity in free solution
D_x axial dispersion coefficient
g gravitational constant
I counter-ion
k_1 adsorption rate constant
k_{-1} desorption rate constant
k_f liquid film mass transfer coefficient
K_d dissociation constant for the protein–ion-exchanger complex
l interstitial velocity of liquid in the bed
M_A relative molecular mass of A
n the number of charges involved in the interaction between an adsorption site and a single protein molecule
P protein molecule
q concentration of protein adsorbed to the ion exchanger
q_i point concentration of adsorbed protein
q_m maximum protein capacity of the ion exchanger
r radial coordinate of ion exchanger particle
R radius of ion exchanger particle
R_i rate of interface mass transfer
t time
T absolute temperature
u superficial velocity of liquid flow through the column
v volume of ion exchanger
V volume of liquid external to the ion exchanger
x axial coordinate of packed bed
ε porosity of ion exchanger particle
ε_b porosity of packed bed
μ liquid viscosity
ρ particle density

Superscript
* value when system is at equilibrium

ACKNOWLEDGEMENTS

The authors would like to thank the Science and Engineering Research Council for financial support. They are also grateful to Pharmacia LKB Biotechnology AB, Uppsala, Sweden, for the provision of experimental materials and equipment.

REFERENCES

1 E. A. Peterson and H. A. Sobers, *J. Am. Chem. Soc.*, 78 (1956) 751.
2 J. Bonnerjea, S. Oh, M. Hoare and P. Dunnill, *Biotechnology*, 4 (1986) 954.
3 G. L. Skidmore and H. A. Chase, in M. Streat (Editor), *Ion Exchange for Industry*, Ellis Horwood, Chichester, 1988, p. 520.
4 G. L. Skidmore and H. A. Chase, *J. Chromatogr.*, submitted for publication.
5 G. Leaver, *Ph.D. Thesis*, University of Wales, Swansea, 1984.
6 H. A. Chase, in D. Naden and M. Streat (Editors), *Ion Exchange Technology*, Ellis Horwood, Chichester, 1984, p. 400.
7 M. C. Annesini and R. Lavecchia, *Chem. Biochem. Eng. Q.*, 1 (1987) 89.
8 H. A. Chase, *J. Chromatogr.*, 297 (1984) 179.
9 H. Thomas, *J. Am. Chem. Soc.*, 66 (1944) 1664.
10 B. J. Horstmann and H. A. Chase, *Chem. Eng. Res. Des.*, 67 (1989) 243.
11 C. J. Geankoplis, *Transport Processes and Unit Operations*, Allyn and Bacon, Boston, MA, 2nd. ed., 1983.
12 A. Polson, *J. Phys. Colloid Chem.*, 54 (1950) 649.
13 S. C. Foo and R. G. Rice, *AIChE J.*, 21 (1975), 1149.
14 T. Peters and R. G. Reed, in T. Peters and I. Sjöholm (Editors), *FEBS 11th Meeting, Volume 50, Colloquium B9, Albumin: Structure, Biosynthesis, Function*, Pergamon Press, Oxford, 1978, p. 11.
15 R. M. C. Dawson, D. C. Elliot, W. H. Elliot and K. M. Jones, *Data for Biochemical Research*, Oxford University Press, Oxford, 1974.
16 A. Fersht, *Enzyme Structure and Mechanism*, Freeman, Reading, 1977, p. 330.
17 T. Imoto, L. N. Johnson, A. C. T. North, D. C. Phillips and J. A. Rupley, in P. D. Boyer (Editor), *The Enzymes*, Vol. 7, Academic Press, New York, 2nd ed, 1972, p. 665.
18 J. P. van der Wiel and J. A. Wesselingh, presented at *NATO Advanced Study Institute, Vimeiro, Portugal, July 17–29, 1988.*
19 W. Kopaciewicz, M. A. Rounds, J. Fausnaugh and F. E. Regnier, *J. Chromatogr.*, 266 (1983) 3.
20 A. Velayudhan and Cs. Horváth, *J. Chromatogr.*, 443 (1988) 13.
21 I. S. Gosling, *Ph.D. Thesis*, University of Wales, Swansea, 1985.
22 J. F. Foster, in V. M. Rosenoer, M. Oratz and M. A. Rothschild (Editors), *Albumin Structure, Function and Uses*, Pergamon Press, Oxford, 1977, p. 53.

Journal of Chromatography, 498 (1990) 129–135
Elsevier Science Publishers B.V., Amsterdam — Printed in The Netherlands

CHROM. 21 953

SEPARATION OF METHYL-SUBSTITUTED BENZ[*c*]ACRIDINES BY CATION-EXCHANGE HIGH-PERFORMANCE LIQUID CHROMATOGRAPHY

KUNIHIRO KAMATA*
Tokyo Metropolitan Research Laboratory of Public Health, 24-1, Hyakunincho 3-chome, Shinjuku-ku, Tokyo 169 (Japan)
and
NOBORU MOTOHASHI
Meiji College of Pharmacy, Yato-cho, Tanashi, Tokyo 188 (Japan)
(Received April 18th, 1989)

SUMMARY

High-performance liquid chromatography on an ion-exchange column for the separation of methyl-substituted benz[*c*]acridines was investigated. A cation-exchange column (Partisil 10 SCX) was used with acetonitrile–0.001 *M* $(NH_4)_2HPO_4$ as the mobile phase. The retention times depended on the composition of the mobile phase. An elution order depending on the pK_a values was established.

INTRODUCTION

Methyl-substituted benz[*c*]acridines (BAcs) are widespread environmental pollutants[1–6] and are well known for their carcinogenic and mutagenic characteristics[7–10]. Therefore, there is considerable interest in their qualitative and quantitative analysis in complex mixtures.

Methods for the determination of BAcs using paper chromatography[11,12], thin-layer chromatography[1–4,13–16] and gas–liquid chromatography[15,17–23] have been reported. Recently, in order to improve the sensitivity and specificity, high-performance liquid chromatography (HPLC) methods have been developed[5,6,15,22,24–29]. In many of these studies, both reversed-phase (RP)[5,6,15,22,24–26,28] and normal-phase (NP) HPLC were used[22,24,25,29]. Very little work, however, has been done on the determination of BAcs by ion-exchange HPLC[27]. This technique is particularly suitable for the separation and determination of polar compounds that are not separated by RP- or NP-HPLC. In this study, the separation of BAcs by cation-exchange HPLC (CE-HPLC) was investigated.

EXPERIMENTAL

Materials

Twelve BAcs were synthesized according to the literature[30–36] and purified as

0021-9673/90/$03.50

described in a previous paper[15]: benz[*c*]acridine (1), 7-methylbenz[*c*]acridine (2), 8-methylbenz[*c*]acridine (3), 9-methylbenz[*c*]acridine (4), 10-methylbenz[*c*]acridine (5), 11-methylbenz[*c*]acridine (6), 5,7-dimethylbenz[*c*]acridine (7), 7,9-dimethylbenz[*c*]acridine (8), 7,10-dimethylbenz[*c*]acridine (9), 7,11-dimethylbenz[*c*]acridine (10), 7,9,10-trimethylbenz[*c*]acridine (11) and 7,9,11-trimethylbenz[*c*]acridine (12).

A 100 μg/ml stock solution of BAcs in methanol was prepared and diluted as required.

The reagents (analytical-reagent grade) and solvents (HPLC-grade) were obtained from Wako (Osaka, Japan).

Chromatographic apparatus and conditions

The HPLC apparatus consisted of a JASCO Model BIP-I pump (Japan Spectroscopic, Tokyo, Japan), a Rheodyne (Berkeley, CA, U.S.A.) Model 7125 injector equipped with a 20-μl loop, a JASCO Model 860-CO column oven and a JASCO UVIDEC-100 III spectrophotometer. The HPLC columns used were strong cation exchangers: (1) Partisil 10 SCX (10 μm, 250 × 4.6 mm I.D.) (Whatman, Clifton, NJ, U.S.A.) and (2) TSKgel SP-2SW (5 μm, 250 × 4.6 mm I.D.) (TOSOH, Tokyo, Japan). Various proportions of acetonitrile–$(NH_4)_2HPO_4$ buffer and methanol–$(NH_4)_2HPO_4$ buffer were used as mobile phases and were filtered through Millipore membrane filters (0.45 μm) and degassed under vacuum prior to use. The sample injected was 2 μl of a methanol solution containing 10 ng of each BAc. Separations were carried out at a flow-rate of 1.0 ml/min and a column oven temperature of 40°C.

Elution patterns were monitored at 280 nm. The results were evaluated with a Shimadzu Chromatopac CR-3A digital integrator.

RESULTS AND DISCUSSION

The composition of the mobile phase (percentage of water, salt concentration, nature of the buffer and pH) had a strong influence on the quality of the CE-HPLC separation. The optimum mobile phase composition was chosen for each column to give the best separation of the BAcs and to detect as many as possible of the components in one injection. The column efficiency was checked by making injections of a mixture of BAcs dissolved in methanol. Isocratic elution was used.

The solvent systems finally chosen were acetonitrile–0.001 *M* $(NH_4)_2HPO_4$ (adjusted to pH 3.0 with phosphoric acid) (60:40, v/v) and methanol–0.001 *M* $(NH_4)_2HPO_4$ (pH 3.0) (70:30, v/v) for the Partisil 10 SCX column and acetonitrile–0.01 *M* $(NH_4)_2HPO_4$ (pH 3.0) (50:50, v/v) and methanol–0.01 *M* $(NH_4)_2HPO_4$ (pH 3.0) (65:35, v/v) for the TSKgel SP-2SW column. The retention times of BAcs using either acetonitrile–$(NH_4)_2HPO_4$ or methanol–$(NH_4)_2HPO_4$ as eluent are given in Table I and the chromatograms are shown in Figs. 1 and 2. The HPLC patterns of BAcs on the Partisil 10 SCX and TSKgel SP-2SW columns were very similar to each other and also to that obtained previously by NP-HPLC[22]. The resolution of BAcs was considerably better using the Partisil 10 SCX than the TSKgel SP-2SW column. The former column was particularly useful for separating compounds 3 and 4, which could not be sufficiently separated on the TSKgel SP-2SW column. With respect to the retention time of BAcs on the Partisil 10 SCX column, acetonitrile–$(NH_4)_2HPO_4$ was better than methanol–$(NH_4)_2HPO_4$ (Fig. 1).

TABLE I

HPLC RETENTION TIMES OF BAcs

Mobile phase: (A) acetonitrile–0.001 *M* $(NH_4)_2HPO_4$ (pH 3.0) (60:40); (B) methanol–0.001 *M* $(NH_4)_2HPO_4$ (pH 3.0) (70:30); (C) acetonitrile–0.01 *M* $(NH_4)_2HPO_4$ (pH 3.0) (50:50); (D) methanol–0.01 *M* $(NH_4)_2HPO_4$ (pH 3.0) (65:35).

Compound	pK_a[a]	*Retention time (min)*			
		Partisil 10 SCX column		*TSKgel SP-2SW column*	
		A	*B*	*C*	*D*
1	2.80	9.8	10.7	13.0	14.8
2	3.55	24.4	29.8	28.1	34.9
3	3.12	12.4	14.0	16.5	19.7
4	3.11	12.0	13.6	16.4	19.6
5	3.37	17.9	20.6	22.4	26.9
6		3.1	3.5	5.3	9.8
7	3.68	26.5	34.3	32.0	44.2
8	3.70	28.3	36.9	33.0	47.0
9	3.91	37.9	52.2	40.4	62.6
10		3.8	4.7	6.0	11.3
11	4.25	41.2	60.6	46.2	84.0
12		4.2	5.5	6.4	12.1

[a] pK_a values taken from ref. 37.

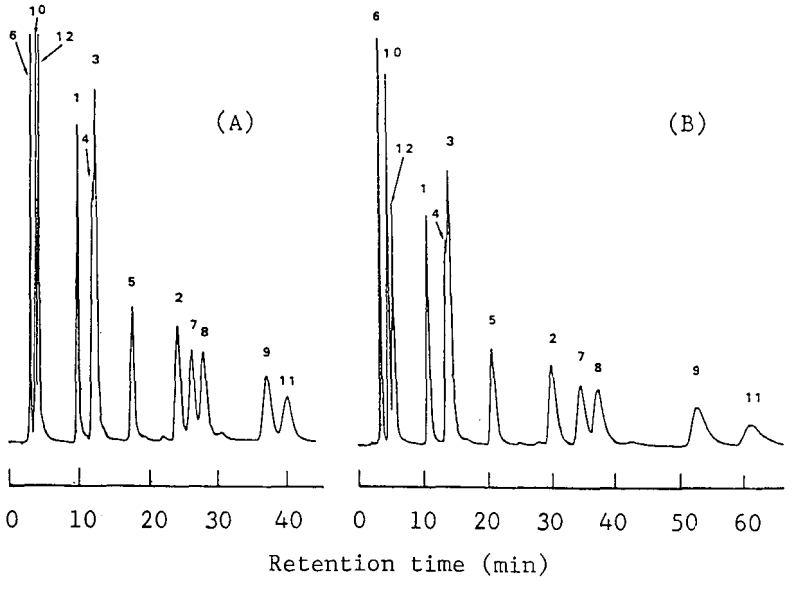

Fig. 1. Separation of twelve BAcs on a Partisil 10 SCX column. Mobile phase: (A) acetonitrile–0.001 *M* $(NH_4)_2HPO_4$ (pH 3.0) (60:40); (B) methanol–0.001 *M* $(NH_4)_2HPO_4$ (pH 3.0) (70:30).

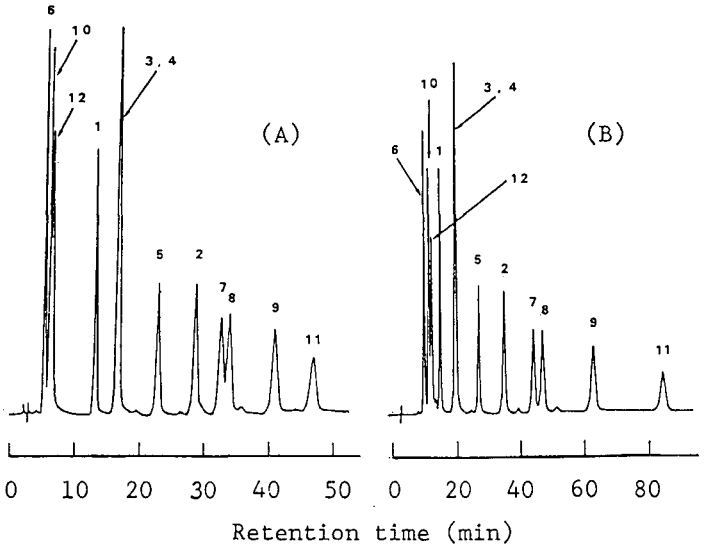

Fig. 2. Separation of twelve BAcs on a TSKgel SP-2SW column. Mobile phase: (A) acetonitrile–0.01 *M* $(NH_4)_2HPO_4$ (pH 3.0) (50:50); (B) methanol–0.01 *M* $(NH_4)_2HPO_4$ (pH 3.0) (65:35).

The influence of organic solvent concentration, buffer concentration and mobile phase pH on the chromatographic characteristics of BAcs was systematically examined and the results are shown in Figs. 3–5. The retention time increased with

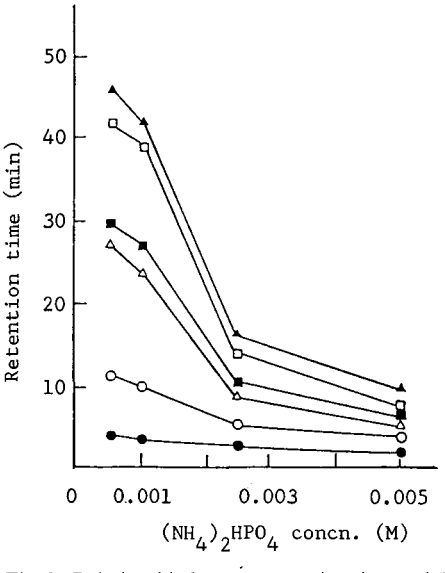

Fig. 3. Relationship between retention time and $(NH_4)_2HPO_4$ concentration in the mobile phase. Column Partisil 10 SCX; eluent, acetonitrile–$(NH_4)_2HPO_4$ (60:40), adjusted to pH 3.0 with phosphoric acid; flow-rate, 1.0 ml/min. Compounds: (○) = 1; (●) = 2; (□) = 6; (■) = 7; (△) = 9; (▲) = 11.

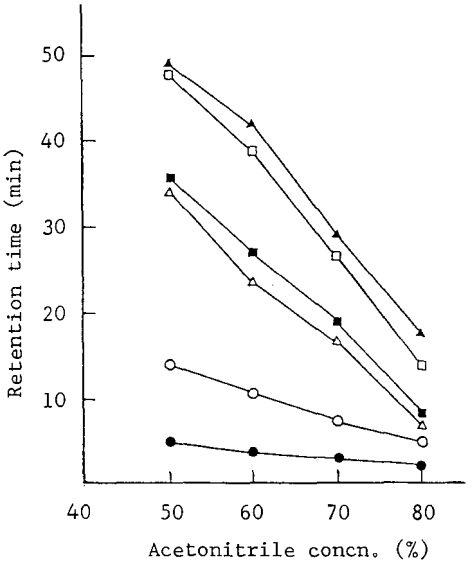

Fig. 4. Relationship between retention time and acetonitrile concentration in the mobile phase. Column, Partisil 10 SCX; eluent, acetonitrile–0.001 *M* $(NH_4)_2HPO_4$, adjusted to pH 3.0 with phosphoric acid; flow-rate, 1.0 ml/min. Symbols as in Fig. 3.

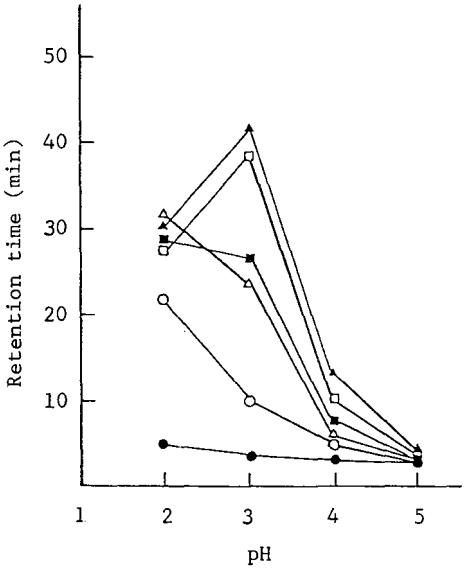

Fig. 5. Relationship between retention time and pH of mobile phase. Column, Partisil 10 SCX; eluent, acetonitrile–0.001 *M* $(NH_4)_2HPO_4$ (60:30), adjusted to various pH values with phosphoric acid; flow-rate, 1.0 ml/min. Symbols as in Fig. 3.

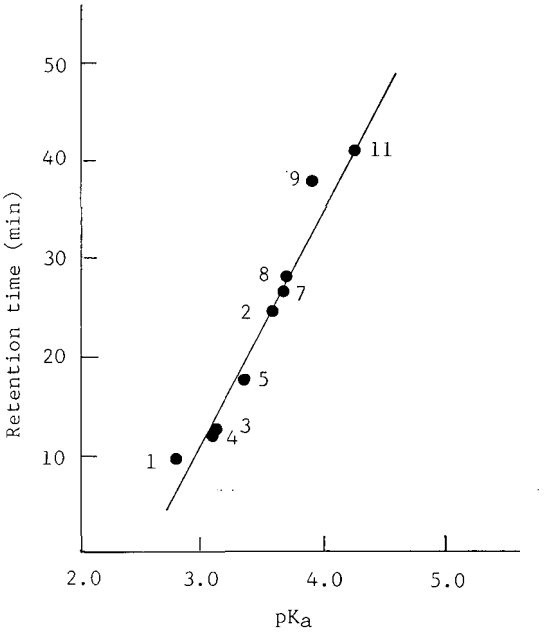

Fig. 6. Relationship between pK_a and retention times of BAcs on a Partisil 10 SCX column. Mobile phase, acetonitrile–0.001 *M* $(NH_4)_2HPO_4$ (pH 3.0) (60:40); flow-rate, 1.0 ml/min.

decreasing concentration of organic solvent and buffer and was sensitive to pH. The optimum pH for separating BAcs was 3.0.

The relationship between pK_a and retention time on the Partisil 10 SCX column using acetonitrile–0.001 *M* $(NH_4)_2HPO_4$ (pH 3.0) (60:40) as the mobile phase was linear (correlation coefficient 0.975), as shown in Fig. 6.

Previous investigations showed that the HPLC of BAcs provides satisfactory results[22]. Excellent separations of BAcs were obtained by a combination of RP-HPLC and NP-HPLC. Using the individual techniques, however, BAcs were not well separated. RP-HPLC did not give a good separation of compounds 7, 8 and 9, and in NP-HPLC compounds 6, 10 and 12 were eluted close to the solvent peak. These compounds were completely separated using CE-HPLC. In conclusion BAcs were separated in a relatively short time by CE-HPLC.

REFERENCES

1 E. Sawicki, T. W. Stanley and W. C. Elbert, *Occup. Health Rev.*, 16 (1964) 8.
2 E. Sawicki, S. P. McPherson, J. W. Stanley, J. E. Meeker and W. C. Elbert, *Int. J. Air Water Pollut.*, 9 (1965) 515.
3 C. R. Engel and E. Sawicki, *J. Chromatogr.*, 31(1967) 109.
4 T. W. Stanley, M. J. Morgan and E. M. Grisby, *Environ. Sci. Technol.*, 2 (1968) 699.
5 P. Maschlet, M. A. Bresson, S. Beyne and G. Mouvier, *Analusis*, 13 (1985) 401.
6 T. Yamauchi and T. Handa, *Environ. Sci. Technol.*, 21 (1987) 1177.
7 A. Lacassagne, N. P. Buu-Hoi, R. Dauel and F. Zajdela, *Adv. Cancer Res.*, 4 (1956) 315.
8 H. R. Glatt, H. Schwind, F. Zajela, A. Croisy, P. C. Jecquignon and F. Oesch, *Mutat. Res.*, 6 (1976) 307.
9 D. Niculescu-Duvas, T. Craescu, M. Tugulea, A. Croisy and P. C. Jacquignon, *Carcinogenesis*, 2 (1981) 269

10 R. P. Deutsch-Wenzel, H. Brune and G. Grimmer, *Cancer Lett.*, 20 (1983) 97.
11 A. M. Luly and K. Sakodynsky, *J. Chromatogr.*, 19 (1965) 624.
12 S. Caroli and M. Lederer, *J. Chromatogr.*, 21 (1968) 333.
13 E. Sawicki, T. W. Stanley, J. D. Pfaff and W. C. Elbert, *Anal. Chim. Acta*, 31 (1964) 359.
14 E. Sawicki, W. C. Elbert and T. W. Stanley, *J. Chromatogr.*, 17 (1965) 120.
15 N. Motohashi and K. Kamata, *Yakugaku Zasshi*, 103 (1983) 795.
16 K. Kamata and N. Motohashi, *J. Chromatogr.*, 396 (1987) 437.
17 D. Brocco, A. Cimmino and M. Possanzini, *J. Chromatogr.*, 84 (1973) 371.
18 M. Pailer and V. Hlozek, *J. Chromatogr.*, 128 (1976) 163.
19 I. Ignatiadis, J. M. Schmitter and G. Guiochon, *J. Chromatogr.*, 246 (1982) 23.
20 J. M. Schmitter, I. Ignatiadis and G. Guiochon, *J. Chromatogr.*, 248 (1982) 203.
21 P. Burchill, A. A. Herod, J. P. Mahon and E. Pritchard, *J. Chromatogr.*, 265 (1983) 223.
22 K. Kamata and N. Motohashi, *J. Chromatogr.*, 319 (1985) 331.
23 G. Grimmer, K.-W. Naujack and G. Dettharn, *Toxicol. Lett.*, 35 (1987) 117.
24 M. Dong and D. C. Locke, *J. Chromatogr. Sci.*, 15 (1977) 32.
25 H. Colin, J.-M. Schmitter and G. Guiochon, *Anal. Chem.*, 53 (1981) 625.
26 L. J. Boux, C. M. Ireland, D. J. Wright, G. M. Holder and A. J. Ryan, *J. Chromatogr.*, 227 (1982) 149.
27 D. A. Hougen, M. J. Peak, K. M. Suhrbier and V. C. Stamoudls, *Anal. Chem.*, 54 (1982) 32.
28 L. A. D'Avla, M. Colin and G. Guiochon, *Anal. Chem.*, 55 (1983) 1019.
29 A. H. Siouffi, M. Righezza and G. Guiochon, *J. Chromatogr.*, 368 (1986) 189.
30 N. P. Buu-Hoi, R. Roger and M. Hubert-Habart, *J. Chem. Soc.*, (1965) 1082.
31 F. Ullmann and A. La Torie, *Chem. Ber.*, 37 (1904) 2922.
32 I. Y. Postovskii and B. N. Lundion, *J. Gen. Chem. USSR*, 10 (1940) 71.
33 N. P. Buu-Hoi, *J. Chem. Soc.*, (1949) 670.
34 N. P. Buu-Hoi and L. Lecocq, *C.R. Acad. Sci.*, 218 (1944) 794.
35 N. P. Buu-Hoi, *J. Chem. Soc.*, (1946) 792.
36 J. V. Braum and P. Wolff, *Chem. Ber.*, 55 (1922) 3675.
37 T. Okano, T. Horie, N. Motohashi, Y. Watanabe and Y. Nishimiya, *Gann*, 66 (1975) 529.

Journal of Chromatography, 498 (1990) 137–144
Elsevier Science Publishers B.V., Amsterdam — Printed in The Netherlands

CHROM. 21 956

STUDIES ON IODINATED COMPOUNDS

V. REVERSED-PHASE HIGH-PERFORMANCE LIQUID CHROMATOGRAPHIC DETERMINATION OF IODIDE WITH CYCLODEXTRIN-CONTAINING MOBILE PHASES

MASAHIRO MIYASHITA and SABURO YAMASHITA*
Department of Clinical Chemistry, Hoshi College of Pharmacy, 2-4-41 Ebara, Shinagawa-ku, Tokyo 142 (Japan)
(First received February 6th, 1989; revised manuscript received August 16th, 1989)

SUMMARY

α-, β-, γ- and dimethyl-β-cyclodextrin (CD) were used as mobile phase additives in a reversed-phase high-performance liquid chromatographic determination of iodide (I^-). The retention of I^- was decreased by the addition of CDs in mobile phases composed of hexyl-, heptyl- or octylammonium phosphate. The decrease in the retention was influenced by the molecular species and the concentration of CDs. Using 2 m*M* heptylammonium phosphate (pH 4.0) containing 2 m*M* β-CD as the mobile phase, determination of I^- was performed with a UV detector at 226 nm. Good linearity of the calibration graphs and good reproducibility of repeated determinations were obtained for I^- in the range 25 pmol (3.2 ng) to 12.5 nmol (1.6 μg).

INTRODUCTION

Reversed-phase high-performance liquid chromatography (RP-HPLC) has been widely used for the determination of iodide (I^-)[1–3]. Often alkylammonium salts are added to the mobile phase consisting of water–organic solvent mixtures, as ion-pairing reagents to increase the retention of I^- on the non-polar stationary phase. The retention of I^- is influenced and controlled by various mobile phase parameters such as molecular species and concentration of ion-pairing reagents, pH, ionic strength and content of organic modifiers[3–5].

Recently, host–guest interactions, using crown ethers (CEs) or cyclodextrins (CDs) as hosts, have been applied to the RP-HPLC separation of various solutes. Many compounds have been separated selectively on the basis of selective interactions of CEs or CDs with solutes. The host–guest interactions can also be utilized as a novel retention-controlling factor for the RP-HPLC separation of I^-. CEs, which are cyclic polyethers, are known to form complexes with metal ions and primary alkylammonium ions. We previously applied the CE, 18-crown-6, to the separation of I^- and found that the retention of I^- was increased by the addition of 18-crown-6 to mobile

0021-9673/90/$03.50

phases composed of primary alkylammonium phosphates because of complex formation of CE with ion-pairing reagents[6].

CDs, which are homologous series of cyclic oligosaccharides with glucose units joined by α-1,4-linkages, are known to form inclusion complexes with various guest compounds[7]. The inclusion phenomena have been applied to the separation of positional isomers of aromatic compound[8–10] and the resolution of racemic compounds into enantiomers[11–13] by using CDs as mobile phase additives in RP-HPLC. However, the use of CDs for the separation of I^- has not previously been attempted.

This paper reports the application of CDs as mobile phase additives for the separation and determination of I^-. The aim of this study was to establish a novel RP-HPLC method for I^- based on the inclusion interaction of CDs, controlling the retention behaviour.

EXPERIMENTAL

Apparatus

The HPLC equipment consisted of a Model 6000A pump, a U6K universal injector (Waters Assoc., Milford, MA, U.S.A.), a Model NS-310A variable-wavelength UV detector (Nippon Seimitsu Kagaku, Tokyo, Japan) and a Model VP-6511W pen recorder (Matsushita Communication, Yokohama, Japan). The HPLC column was a radial compression separation system with a Radial-Pak Novapak C_{18} (4 μm) cartridge (100 mm × 5 mm I.D.) (Waters Assoc.). UV spectra were measured on a Model 100-50 double-beam spectrophotometer with a Model 200 recorder (Hitachi, Tokyo, Japan).

Chemicals

All reagents were of commercial guaranteed grade. Potassium iodide (KI) was obtained from Wako (Osaka, Japan) and CDs from Nakarai (Kyoto, Japan). Deionized, distilled water was used to prepare the mobile phases.

Mobile phases

Alkylammonium phosphate solutions were prepared by dissolving alkylamines in water and adjusting to the desired pH with phosphoric acid. After dissolving CDs in the alkylammonium phosphate solutions, all mobile phases were filtered through a 0.45-μm filter and degassed prior to use.

Procedure

HPLC was performed at room temperature (*ca.* 20°C). The flow-rate of the mobile phase was 1.0 ml/min. The detection wavelength was set at 226 nm. The retention of I^- was determined by injecting 5 μl of KI standard solution ($1 \cdot 10^{-4}$ *M* in water). The capacity factor, k', of I^- was calculated using the equation $k' = (V - V_0)/V_0$, where V is the retention volume of I^- and V_0 is the hold-up volume of the column. The hold-up volume of the column was obtained from the retention volume of nitrate ion after injection of sodium nitrate using 60% acetonitrile as the mobile phase.

RESULTS AND DISCUSSION

Effect of addition of CDs

The capacity factor of I^- was investigated by using three molecular species of 2 m*M* alkylammonium phosphate (pH 4.0) solutions containing 2 m*M* α-CD, β-CD, γ-CD, 2,6-di-O-methyl-β-CD (DM-β-CD) or no CDs as mobile phases. The results are given in Table I and the typical chromatograms are shown in Fig. 1.

TABLE I

EFFECT OF CD IN THE MOBILE PHASE ON CAPACITY FACTOR OF I^-

Mobile phase: 2 m*M* alkylammonium phosphate (pH 4.0) containing 2 m*M* CD.

Ion-pairing reagent[a]	*CD*				
	None	*α-CD*	*β-CD*	*γ-CD*	*DM-β-CD*
Hexylammonium	5.10	3.33	3.33	3.90	0.96
Heptylammonium	12.18	6.68	7.82	7.94	2.05
Oxtylammonium	26.68	14.63	16.15	20.79	5.10

[a] Added as phosphate salts.

In all instances, the retention of I^-, which was influenced by the ion-pairing reagent used, was decreased by the addition of any CD to the mobile phase. The magnitude of the decrease in retention was dependent on the molecular species of CD; the decrease in retention was greater when a CD having a small condensation number of glucose units was used (γ-CD < β-CD < α-CD) or when a CD having methylated glucose units was used (β-CD < DM-β-CD).

Retention mechanism of I^-

It is interesting to consider the retention mechanism of I^- with the CD-containing mobile phases in combination with the model of ion-pair chromatography. However, many different models of ion-pair chromatography have been proposed[14]. Here we adopt the dynamic ion-exchange model to explain the retention mechanism of I^-. According to this model, the retention of I^- in mobile phase systems without CDs is governed mainly by the following two important equilibria: (1) sorption of ion-pair-

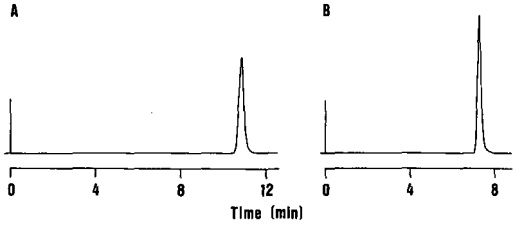

Fig. 1. High-performance liquid chromatograms of I^-. Mobile phase: (A) 2 m*M* heptylammonium phosphate (HAP, pH 4.0) and (B) 2 m*M* HAP (pH 4.0) containing 2 m*M* β-CD. For other conditions, see Experimental.

ing reagent (alkylammonium ion) and counter ion (phosphate ion) on the surface of a non-polar stationary phase and (2) ion exchange of I^- with the counter ion. Moreover, when CDs are added to the mobile phase, interactions of the CDs with the mobile phase component, I^- and the stationary phase, etc., further complicate the chromatographic equilibria. CDs, which are toroidal-shaped molecules having a relatively hydrophobic cavity, form inclusion complexes with various guest molecules in the cavity. Therefore, in the dynamic ion-exchange model, the retention of I^- in CD-containing mobile phase systems will be considerably influenced by the formation of inclusion complexes between CDs and ion-pairing reagents or CDs and I^-.

The formation of the inclusion complexes between part of the CDs and the ion-pairing reagents used in this study was suggested by the work of Miyajima *et al.*[15] They reported that α-CD and β-CD form 1:1 inclusion complexes with hexyl-, heptyl- and octylammonium salts (chlorides) in aqueous solutions. When the CDs form complexes with alkylammonium (AA) phosphates in a mobile phase, the AA–CD complexes function as ion-pairing reagents. The hydrophobicity of the newly formed ion-pairing reagents is lower than that of the original reagents because the AAs are included in the CD cavity by van der Waals and hydrophobic interactions, whereas the outside of the CD molecules is hydrophilic. Hence the concentration of the ion-pairing reagents on the surface of a non-polar stationary phase is decreased when CD-containing mobile phases are used, and the retention of I^- is decreased. The dependence of the retention of I^- on the molecular species of CD is attributed to the differences in stability, which depend on the cavity size of the CDs, the alkyl chain length of AAs and the hydrophobicity of the AA–CD complexes formed. However, the decrease in the retention of I^- observed on using γ-CD-containing mobile phases is not explained by the decrease in the hydrophobicity of the ion-pairing reagents, because γ-CD does not form inclusion complexes with hexyl-, heptyl- and octylammonium salts[15].

On the other hand, α-, β- and γ-CDs also form inclusion complexes with I^- in aqueous solutions[16]. When the CDs form complexes with I^- in a mobile phase, the I^-–CD complexes function as anionic solutes. The ionic nature of the newly formed solutes is weaker than that of the original solutes, because the charge of I^- is shielded by the complex formation with CDs. Therefore, the ionic interaction of the anionic solutes with cationic ion-pairing reagents on the stationary phase is decreased when CD-containing mobile phases are used, and the apparent retention of I^- is decreased. The dependence of the retention of I^- on the molecular species of CD is attributed to the differences in stability, which depend on the cavity size of CDs and the ionic nature of the I^-–CD complexes formed.

It has not been reported whether DM-β-CD forms inclusion complexes with alkylammonium salts and I^-. However, the marked decrease in the retention of I^- observed when using DM-β-CD-containing mobile phases is noteworthy and requires a different retention mechanism. The methylation of CDs brings about changes in chemical and physical properties, *e.g.*, the hydrophobicity of methylated CDs is increased significantly and the adsorption of methylated CDs on the stationary phase is not negligible[17]. When DM-β-CD is adsorbed on the non-polar octadecyl stationary phase, the DM-β-CD–octadecyl complex functions as a stationary phase. The polarity of the newly formed stationary phase is greater than that of the original phase, because the polarity of the secondary phase, which is formed by DM-β-CD, is higher

than that of the primary phase, which is formed by octadecyl, in the stationary phase. Hence the concentration of the ion-pairing reagents on the surface of stationary phase is decreased when DM-β-CD-containing mobile phases are used and the retention of I^- is then decreased.

In this manner, the interaction of CDs with ion-pairing reagents, I^- and stationary phase may be demonstrated. As a result, we conclude that the retention of I^- with CD-containing mobile phase would be decreased by the combined effect of these interactions of CDs.

Effect of pH of mobile phase

The dependence of the capacity factor of I^- on the mobile phase pH was investigated by using 2 m*M* HAP solution (pH 3.0–7.0) containing 2 m*M* CD or without a CD as mobile phases. The pH of the HAP solution was not altered by the addition of CDs. Under these pH conditions, it is assumed from the pK_a of heptylamine (10.65) that the heptylammonium added as an ion-pairing reagent exists in the fully dissociated form. The results (k' profiles) are shown in Fig. 2 as a function of the mobile phase pH.

The maximum retention of I^- was observed at pH 4.0 when a mobile phase without CDs was used, and similar results were also obtained when α-, β- or γ-CD-containing mobile phases were used. Therefore, it is considered that the addition of these CDs to the mobile phase affects the magnitude of the retention of I^-, but does not affect the retention *vs.* pH profiles.

On the other hand, the retention of I^- was almost independent of the mobile phase pH when a DM-β-CD-containing mobile phase was used.

Effect of concentration of CDs

The dependence of capacity factor of I^- on the CD concentration in the mobile phase was investigated by using 2 m*M* HAP (pH 4.0) containing 0–5 m*M* CDs as mobile phases. The results are shown in Fig. 3 as a function of the CD concentration.

In all instances, the retention of I^- decreased with increasing CD concentration. This behaviour may be caused by promotion of the formation of inclusion complexes between CDs and heptylammonium or CDs and I^-, and the adsorption of DM-β-CD on the stationary phase with increasing CD concentration.

The complexation ratio of the CDs with heptylammonium or I^- (CD:heptylammonium or CD:I^-) will be assumed to be 1:1[15,16]. However, other complexation

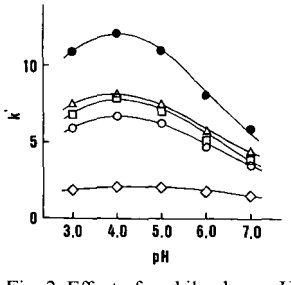

Fig. 2. Effect of mobile phase pH on the capacity factor of I^-. Mobile phase: 2 m*M* HAP containing 2 m*M* (○) α-CD, (□) β-CD, (△) γ-CD or (◇) DM-β-CD or (●) no CDs.

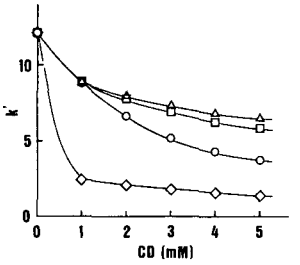

Fig. 3. Effect of CD concentration on the capacity factor of I^-. Mobile phase: 2 m*M* HAP (pH 4.0) containing (○) α-CD, (□) β-CD, (△) γ-CD or (◇) DM-β-CD.

ratios will not be negligible. In general, the relationship between solute retention and CD concentration in mobile phase gives an estimate of the complexation ratio of CD with the solute[18]. However, such an estimate was established on the basis that a CD interacts solely with the solute to form an inclusion complex in the chromatographic system. In our chromatographic system, it will be difficult to assume a definite ratio of complexation of the CDs with I^-, because multiple interactions of the CDs with I^-, the ion-pairing reagent or the stationary phase take place. Moreover, it is difficult to assume a ratio of complexation of the CDs with the ion-pairing reagent from the present results.

Determination of I^-

The determination of I^- was performed with a UV detector using 2 m*M* HAP (pH 4.0) containing 2 m*M* β-CD as a mobile phase. The UV spectral characteristics of I^- in the various solutions with or without CDs are given in Table II. There were almost no differences in the spectra, so the detection wavelength was set at 226 nm.

Calibration graphs for I^- were prepared by injecting 10 μl of various concentrations of KI standard solutions at three detector sensitivities. The results are given in Table III.

The calibration graphs exhibit good linearity between amount of I^- and peak height over the range of 25 pmol (3.2 ng) to 12.5 nmol (1.6 μg). The detection limit of I^- was 0.5 pmol (64 pg) (signal-to-noise ratio = 3, 0.005 a.u.f.s.).

The reproducibility of peak heights was examined by repeated analyses (n = 10) of 0.1, 1.0 and 10 nmol of I^- at 0.01, 0.1 and 1.0 a.u.f.s., respectively. The relative

TABLE II

UV SPECTRAL CHARACTERISTICS OF I^- IN VARIOUS SOLUTIONS

Solution	λ_{max} *(nm)*	*Molar absorptivity, ε* *(10^4 l mol^{-1} cm^{-1})*
Water	226	1.40
2 m*M* HAP (pH 4.0)	226	1.42
2 m*M* HAP (pH 4.0) containing 2 m*M* α-CD	226	1.40
2 m*M* HAP (pH 4.0) containing 2 m*M* β-CD	226	1.38
2 m*M* HAP (pH 4.0) containing 2 m*M* γ-CD	226	1.39
2 m*M* HAP (pH 4.0) containing 2 m*M* DM-β-CD	226	1.37

TABLE III
REGRESSION LINES OF THE CALIBRATION GRAPHS FOR I^-

Detector sensitivity (a.u.f.s.)	*Amount of I^- (nmol)*	*Regression line*[a]	*Correlation coefficient*
0.01	0.025– 0.125	$y = 111x + 0.034$	0.9988
0.1	0.25 – 1.25	$y = 11.8x - 0.018$	0.9996
1.0	2.5 –12.5	$y = 1.06x + 0.310$	0.9999

[a] y = Peak height (cm); x = I^- (nmol).

standard deviations of the peak heights were 1.43% (0.1 nmol), 1.35% (1.0 nmol) and 0.89% (10 nmol).

The effect of other halogen ions on the determination of I^- was examined by injecting solutions containing 1 nmol of I^- with or without various amounts of other halogen ions. The results are given in Table IV. It was found that I^- could be determined without any interference in the presence of up to a 100-fold excess of the other halogen ions. On the other hand, I^- could not be determined quantitatively in the presence of a 1000-fold excess of the other halogen ions because the peak heights of I^- were markedly lower, with peak broadening.

TABLE IV
EFFECT OF OTHER HALOGEN IONS ON THE DETERMINATION OF I^-

Halogen ion (with I^-)	*Added as*	*Amount added (nmol)*	*Recovery*[a] *(%)*	*Error (%)*
None	–	–	100.0	0.0
F^-	KF	10	100.3	+0.3
		100	99.7	−0.3
		1000	53.2	−46.8
Cl^-	KCl	10	99.5	−0.5
		100	100.2	+0.2
		1000	47.8	−52.2
Br^-	KBr	10	100.4	+0.4
		100	99.4	−0.6
		1000	41.0	−59.0

[a] Peak height of 1 nmol of I^- = 100%. Values are averages of five determinations.

CONCLUSIONS

The retention characteristics and determination of I^- by RP-HPLC were investigated using mobile phases containing CDs. It was found that the CDs decrease the retention of I^- and the determination of I^- is not affected by the presence of CDs in the mobile phase. The decreasing effect of the retention of I^- may be the result of the formation of inclusion complexes between CDs and ion-pairing reagents or CDs and I^-, and by the adsorption of CDs on the stationary phase changing its original nature.

It is necessary to decrease the retention of I^- in ion-pair RP-HPLC to obtain a reasonable analysis time, as the retention is relatively high in conventional RP-HPLC. The present method represents a useful technique with a simple modification of the mobile phase in conventional RP-HPLC.

REFERENCES

1 W. J. Hurst, K. P. Snyder and R. A. Martin, Jr., *J. Liq. Chromatogr.*, 6 (1983) 2067.
2 M. Miyashita, K. Kaji, Y. Seyama and S. Yamashita, *Chem. Pharm. Bull.*, 32 (1984) 2430.
3 H. Nagashima and K. Nakamura, *J. Chromatogr.*, 324 (1985) 498.
4 N. E. Skelly, *Anal. Chem.*, 54 (1982) 712.
5 R. Vespalec, J. Neca and M. Vrchlabsky, *J. Chromatogr.*, 286 (1984) 171.
6 M. Miyashita and S. Yamashita, *J. Liq. Chromatogr.*, 9 (1986) 2143.
7 M. L. Bender and M. Komiyama, *Cyclodextrin Chemistry*, Springer, Berlin, 1978.
8 T. Sakai, Y. Ninuma, S. Yanagihara and K. Ushio, *J. Chromatogr.*, 276 (1983) 182.
9 D. Sybilska, J. Debowski, J. Jurczak and J. Zukowski, *J. Chromatogr.*, 286 (1984) 163.
10 J. Zukowski, D. Sybilska and J. Jurczak, *Anal Chem.*, 57 (1985) 2215.
11 J. Debowski, D. Sybilska and J. Jurczak, *J. Chromatogr.*, 237 (1982) 303.
12 J. Debowski, J. Jurczak and D. Sybilska, *J. Chromatogr.*, 282 (1983) 83.
13 Y. Nobuhara, S. Hirano and Y. Nakanishi, *J. Chromatogr.*, 258 (1983) 276.
14 W. R. Melander and C. Horvath, in M. T. W. Hearn (Editor), *Ion-Pair Chromatography*, Marcel Dekker, New York, 1985, Ch. 2, p. 27.
15 K. Miyajima, M. Ikuto and M. Nakagaki, *Chem. Pharm. Bull.*, 35 (1987) 389.
16 J. P. Diard, E. Saint-Aman and D. Serve, *J. Electroanal. Chem.*, 189 (1985) 113.
17 M. Tanaka, T. Miki and T. Shono, *J. Chromatogr.*, 330 (1985) 253.
18 D. W. Armstrong, F. Nome, L. A. Spino and T. D. Golden, *J. Am. Chem. Soc.*, 108 (1986) 1418.

Journal of Chromatography, 498 (1990) 145–157
Elsevier Science Publishers B.V., Amsterdam — Printed in The Netherlands

CHROM. 22 018

DETERMINATION OF BENZIMIDAZOLE ANTHELMINTICS IN MEAT SAMPLES

A. M. MARTI[a], A. E. MOOSER*[,b] and H. KOCH
Swiss Federal Veterinary Office, Berne (Switzerland)
(First received June 14th, 1988; revised manuscript received September 20th, 1989)

SUMMARY

A procedure for the detection of eight benzimidazole anthelmintics in meat samples using high-performance liquid chromatography is described. The limits of detection are in the range 20–50 μg/kg with a recovery of 66–87%. Chromatography is performed on an octadecylsilane column using mobile phases of acetonitrile–water with an ion-pair reagent, with UV detection. For verification of positive results, the drug substances are derivatized to methyl or pentafluorobenzyl derivatives suitable for detection by gas chromatography–mass spectrometry in the electron-impact or positive or negative chemical-ionization mode.

INTRODUCTION

Benzimidazoles are of importance as anthelmintics. As some members of this class of drugs have shown embryotoxic properties with some animal species, the analysis of residues was of major interest. Also, for the establishment and control of tolerance values a method for monitoring residues of benzimidazoles in meat was necessary. There have been many reports of the detection of particular benzimidazoles in plasma, serum, body fluids[1–4] and tissues[5–9] using high-performance liquid chromatography (HPLC) with UV or fluorescence detection. At present no method is available for the determination and subsequent verification of all benzimidazoles registered in Switzerland (see Fig. 1) in a single procedure. Methods for the detection of benzimidazoles and related compounds by gas chromatography (GC) and verification of the results by GC–mass spectrometry (GC–MS) have been described for thiabendazole (**7**) as the pentafluorobenzoyl derivative[10], the tetramethylsilyl derivative, which decomposes to the isocyanate[11], the methyl derivative[12] or the pentafluorobenzyl derivative[13]. Many methods have been developed for the determination of the carbamate pesticides[13–15], which are related to the "carbamate-type" benzimidazoles (see Fig. 1).

[a] Part of the Thesis of A.M.M.; present address: Veterinaria AG, Zürich, Switzerland.
[b] Address for correspondence: Swiss Federal Veterinary Office, Schwarzenburgstrasse 161, CH-3097 Liebefeld, Switzerland.

0021-9673/90/$03.50

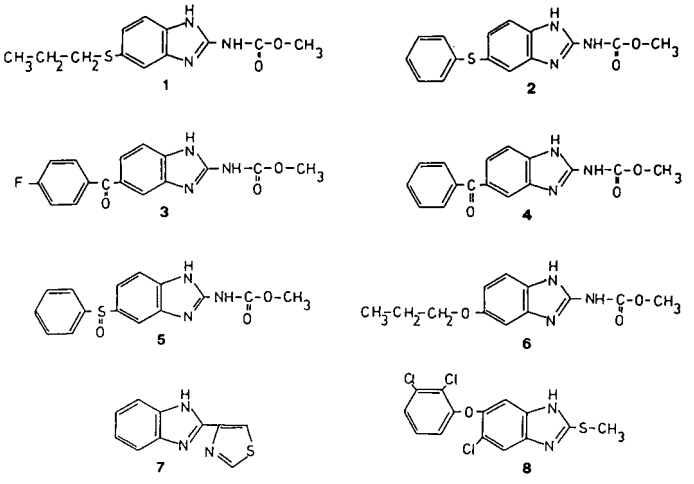

No.	DCI name	Chemical name
1	Albendazole	Methyl 5-propylthio-2-benzimidazolecarbamate
2	Fenbendazole	Methyl 5-phenylthio-2-benzimidazolecarbamate
3	Flubendazole	Methyl 5-(4-fluorobenzoyl)-2-benzimidazolecarbamate
4	Mebendazole	Methyl 5-benzoyl-2-benzimidazolecarbamate
5	Oxfendazole	Methyl 5-phenylsulfinyl-2-benzimidazolecarbamate
6	Oxibendazole	Methyl 5-propoxy-2-benzimidazolecarbamate
7	Thiabendazole[a]	2-(4-Thiazolyl)benzimidazole
8	Triclabendazole	5-Chloro-6-(2,3-dichlorophenoxy)-2-methylthiobenzimidazole

Fig. 1. Benzimidazoles investigated. DCI stands for denominatio communis internationalis, *i.e.* international non-proprietary name. [a] No longer registered in Switzerland.

In this paper, an HPLC method is described, which was tested with different tissue and blood samples, including samples from pigs treated with fenbendazole (**2**).

EXPERIMENTAL

Instrumentation

The HPLC system consisted of a Hewlett-Packard (Palo Alto, CA, U.S.A.) 1081B isocratic solvent-delivery system, a Hewlett-Packard 79841/2 injector and autosampler, an Uvikon 722LC variable-wavelength spectrophotometric detector (Kontron, Zurich, Switzerland) and a Hewlett-Packard Model 3390A reporting integrator. The column was a Hewlett-Packard RP-18 (5 μm) type (200 × 4.6 mm I.D.), connected to a Kontron RP-18 Presat precolumn (40 × 4.6 mm I.D.) of particle size 25–40 μm.

The GC system was a Carlo Erba (Milan, Italy) HRGC 5160 gas chromatograph with a split–splitless injector and an NPD 40 nitrogen–phosphorus detector or a Perkin-Elmer (Norwalk, CT, U.S.A.) Sigma-2000 gas chromatograph with a split–splitless injector, a nitrogen–phosphorus detector and a Perkin-Elmer LCI100 computing integrator. GC was performed using OV-1-CB fused-silica capillary

columns (10 m × 0.25 mm I.D.; film thickness 0.25 μm; chemically bonded) (Macherey, Nagel & Co., Düren, F.R.G.) and helium as the carrier gas (flow-rate *ca.* 1 ml/min) with temperature programming (60°C for 0.5 min, increased from 60 to 150°C at 30°C/min and from 150 to 300°C at 6°C/min). The injector temperature was 270°C and the detector was set at 350°C. The injection mode was splitless with an injection volume of 1 μl.

The GC–MS system consisted of a Finnigan-MAT (San Jose, CA, U.S.A.) 5100 quadrupole GC–MS system, equipped with an interchangeable electron-impact–chemical-ionization (EI–CI) ion source and an INCOS data system with the PPINICI option. GC was performed on a DB-1 fused-silica column (30 m × 0.25 mm I.D.; film thickness 0.25 μm; chemically bonded) (J&W Scientific, Folsom, CA, U.S.A.) with helium as the carrier gas (flow-rate *ca.* 1 ml/min). The injector temperature and temperature program were as described above, the interface oven temperature was set at 300°C and the injection volume was 1 μl. The operating conditions for the mass spectrometer were as follows: direct interface, ionization voltage 70 eV, source temperature 250°C, mass range 50–750 amu, scan rate 480 amu/s, source pressure reading in positive or negative CI mode 1.6 mbar (reactant gas methane) and manifold pressure 10^{-7} bar.

Chemicals

The chemicals used were iodomethane (Fluka, Buchs, Switzerland), methane of 99.995% (v/v) purity (Carbagas, Berne, Switzerland), pentafluorobenzyl bromide (α-bromo-2,3,4,5,6-pentafluorotoluene) (Fluka), pentanesulphonate solution (PIC reagent B5) (Waters Assoc., Milford, MA, U.S.A.), phosphorus pentaoxide (Sicca-pent) (Merck, Darmstadt, F.R.G.), Sep-Pak C_{18} cartridges (Waters Assoc.), Sep-Pak Florisil cartridges (Waters Assoc.) and triethylamine (Fluka). Solvents such as acetone, acetonitrile, chloroform, dichloromethane, ethyl acetate, hexane, methanol and tetrahydrofuran were of Merck LiChrosolv or analytical-reagent grade. The reference substances albendazole, fenbendazole, flubendazole, mebendazole, oxfendazole, oxibendazole, thiabendazole and triclabendazole were kindly provided by the manufacturers.

Detection by HPLC

Operating conditions. Under normal conditions, mobile phase 1 (see Table I) was used; in order to detect or determine oxfendazole (**5**) in certain extracts mobile phase

TABLE I

MOBILE PHASES USED IN HPLC

Mobile phase No.	*Components*[a]	*Proportions (v/v)*
1	Acetonitrile–methanol–ion pair mixture	35:35:30
2	Acetonitrile–ion pair mixture	50:50
3	Acetonitrile–ion pair mixture–water	43:45:12

[a] Ion pair mixture: aqueous solution of 0.01 *M* pentasulphonate (PIC-B5) and 0.5% (m/v) triethylamine, adjusted to pH 3.5 with acetic acid (100%).

2 or 3 was used. When special matrix-dependent problems arose, these mobile phases were also used.

The mobile phase was filtered through a 0.45-μm filter (HVLP; Millipore, Bedford, MA, U.S.A.), degassed and pumped at a rate of 1.0 ml/min. The detector wavelength was set at 298 nm, the column temperature was ambient and the injection volume was 10 μl.

Standard solutions. Stock standard solutions of 10 mg of each of the benzimidazoles in 20 ml of methanol or tetrahydrofuran were prepared by dissolution with heating or in an ultrasonic bath. Working standard solutions were prepared by suitable dilution of the stock solutions with acetonitrile.

Extraction procedure. A 10-g amount of ground tissue was homogenized with 20 ml of acetonitrile in a Polytron mixer (Kinematica, Littau, Switzerland). The suspension was centrifuged at 4000 rpm (2.2 *g*) for 5 min and the supernatant was removed and saved (extract 1). The residue was treated again in the same manner with 12 ml of acetonitrile and 3 ml of water (extract 2). Extract 1 was defatted with 50 ml of hexane in a separating funnel, then extract 2 was treated in the same manner with the same hexane. The acetonitrile phases were pooled, and subsequently 20 ml of hexane and 3 g of sodium chloride were added and the mixture was vigorously stirred and centrifuged at 4000 rpm (2.2 *g*) for 10 min. Three phases of saturated sodium chloride solution, acetonitrile and hexane were formed, of which the hexane phase was discarded. Then 10 ml of dichloromethane were added and the mixture was stirred and centrifuged in the same way as above. The acetonitrile phase (the upper layer) was removed, dried over sodium sulphate and evaporated with a vacuum evaporator (Rotavapor; Büchi, Flawil, Switzerland) at 40°C to a volume of 0.5–0.2 ml, the sodium sulphate being rinsed with 3 ml of acetonitrile. The extract was pipetted onto a Sep-Pak C_{18} cartridge that had previously been rinsed with 10 ml of methanol and 10 ml of acetonitrile. The benzimidazoles were eluted with 3 ml of acetonitrile and the solution was collected in a conical vial and evaporated with a stream of nitrogen at 40°C to a volume of 0.2 ml. The extract was then pipetted onto a Sep-Pak Florisil cartridge that had previously been conditioned with chloroform–methanol–triethylamine (90:10:1, v/v/v). The benzimidazoles were eluted with 10 ml of the same mixture, collected in a conical centrifuge tube and evaporated to dryness with a stream of nitrogen at 40°C. The residue was dissolved in 0.5 ml of the appropriate mobile phase for HPLC (normally phase 1), treated in an ultrasonic bath for 5 min and centrifuged at 4000 rpm (2.2 *g*) for 10 min. The clear solution was transferred into a 2-ml HPLC autosampler vial and submitted to HPLC analysis.

The extraction procedure is summarized schematically in Fig. 2.

Chromatography. Aliquots (10 μl) of sample and standard solutions were injected by means of the autosampler. The amount of the benzimidazoles was determined by means of external standards.

Detection and confirmation by GC and GC–MS

Operating conditions. These are described under *Instrumentation.*

Standard solutions. The standard solutions were prepared by dilution of the appropriate stock solutions of the benzimidazoles with acetone. Aliquots were submitted directly to the derivatization procedure as described below.

Extraction procedure. The extraction procedure is described under *Detection by*

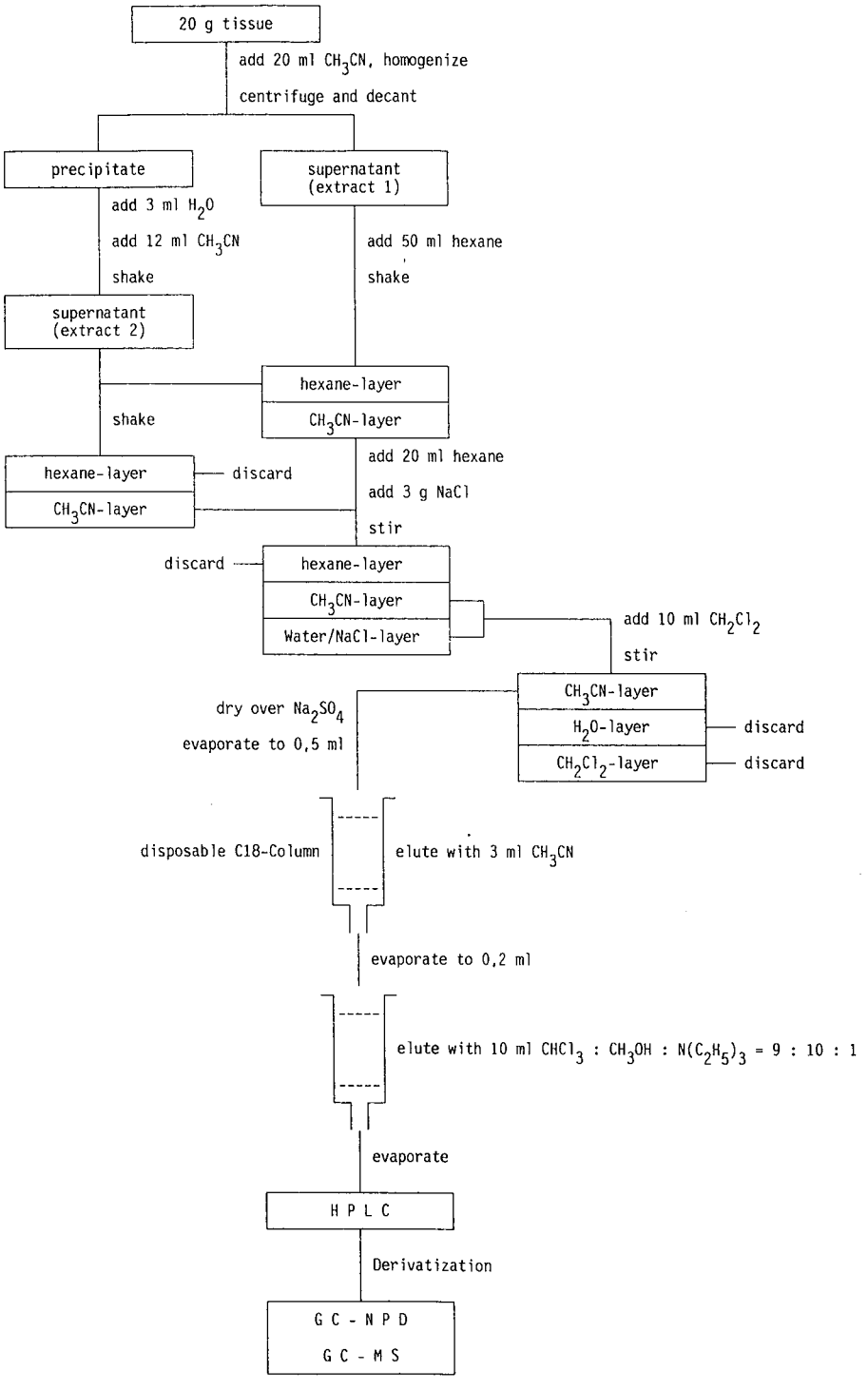

Fig. 2. Extraction procedure.

HPLC. After the final cleaning step, the eluate is evaporated to dryness in a conical vial under a stream of nitrogen and submitted to the derivatization reaction.

As an alternative, the HPLC sample solution was evaporated in the same way and the vial dried *in vacuo* (20 mbar) over phosphorus pentaoxide at 40°C in an oven (TO-50; Büchi) for 8 h. The residue was dissolved in 2 ml of acetone and filtered through a microfiltration apparatus (13 mm diameter HVHP microfilters, 0.45-μm pore size; Swinny Filter Holder, Millipore). The solution was then submitted to derivatization.

Derivatization procedures. To prepare methyl derivatives, the residue was dissolved in 2 ml of acetone and 30 μl of an aqueous 30% (m/v) sodium carbonate solution and 50 μl of a 10% (v/v) solution of methyl iodide in acetone were added. The mixture was shaken on a Vortex mixer, the reaction vial was well sealed and the mixture was heated in a paraffin bath at 60°C for 30 min. After cooling, the mixture was evaporated to dryness with a gentle stream of nitrogen. To the residue, 1 ml of ethyl acetate and 1 ml of water were added, the mixture was shaken on a Vortex mixer and the ethyl acetate phase was removed. The extraction was repeated with two portions of 1 ml of ethyl acetate. The combined ethyl acetate solutions were evaporated to 0.1 ml by a stream of nitrogen after drying over sodium sulphate. A 1-μl volume of this solution was injected into the GC system.

For pentafluorobenzyl derivatives, the procedure was the same as for the methyl derivatives except that 50 μl of a 1% (v/v) pentafluorobenzyl bromide solution were used instead of the methyl iodide solution.

Chromatography. A 1-μl volume of the sample solution was injected in the splitless mode. The needle of the syringe was a long type (7 cm). The temperature programme is described under *Instrumentation.*

RESULTS AND DISCUSSION

Detection by HPLC

For the detection of the benzimidazoles in tissues containing large amounts of interfering substances such as liver or kidney, a laborious clean-up was necessary; the use of acetonitrile for the extraction resulted in a recovery of better than 50% in all instances. Acidic extraction procedures did not result in better recoveries. The extraction and defatting step caused a loss of a few percent of the substances. The high content of matrix substances in the resulting sample solution required the application of further clean-up steps such as chromatography on disposable reversed-phase and Florisil cartridges. Experiments with preparative thin-layer chromatography resulted in a severe loss of sample substance and an increase in interferences in HPLC caused by the extraction of plate-derived substances. For muscle tissues the chromatographic clean-up on the Florisil cartridge may be omitted. It did not seem that the benzimidazoles form conjugates in large amounts; recovery studies were performed on tissue samples from a pig administered a therapeutic dose of fenbendazole (**2**). The samples were treated with β-glucuronidase in conjunction with arylsulphatase (Glusulase; Boehringer, Mannheim, F.R.G.) or by simple hydrolysis with acids and the contents of treated and untreated samples were determined by HPLC; the results showed no difference.

The HPLC separation with the ion-pair reagent pentasulphonate at pH 3.5 was

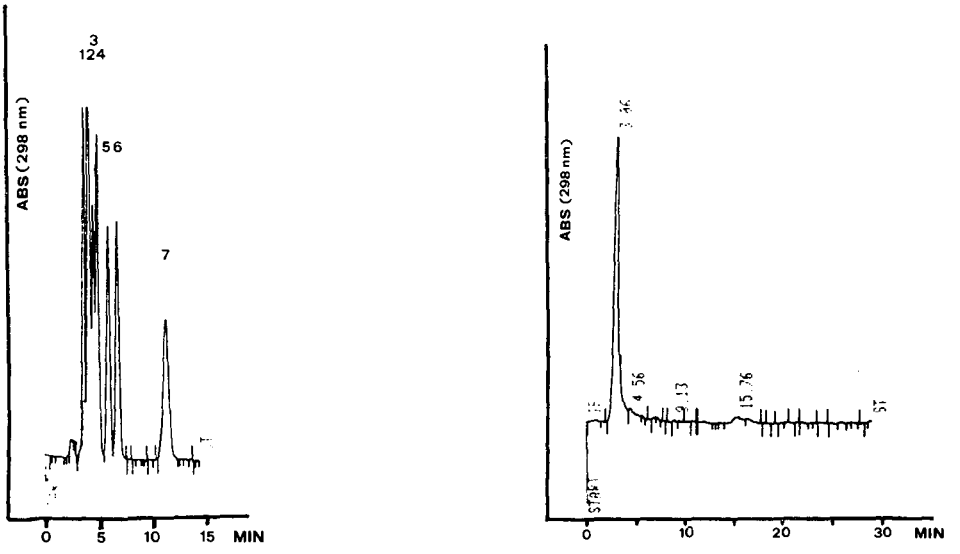

Fig. 3. Chromatogram of standard solution of (1) oxfendazole, (2) thiabendazole, (3) mebendazole, (4) flubendazole/oxibendazole, (5) albendazole, (6) fenbendazole and (7) triclabendazole obtained using mobile phase 1. Injected amounts: 100 ng of each substance in 10 μl. Absorbance range setting: 0.5 a.u.f.s.

Fig. 4. Chromatogram of typical extract of an unfortified muscle of a pig obtained using mobile phase 1. Injection volume: 10 μl (sample solution: 500 μl, corresponding to 10 g of sample). Absorbance range setting: 0.05 a.u.f.s.

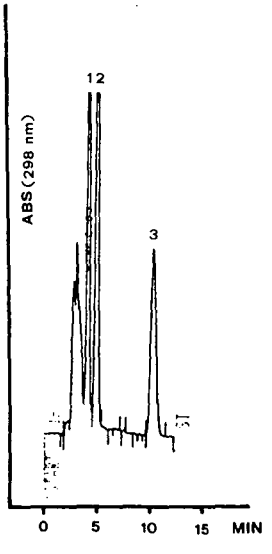

Fig. 5. Chromatogram of typical extract of muscle of a pig after administration of fenbendazole obtained using mobile phase 2. Peaks: (1) fenbendazole (0.5 mg/kg); (2) sulphone metabolite (1 mg/kg); (3) oxfendazole, another metabolite of fenbendazole (1.4 mg/kg). Injection volume: 10 μl (sample solution: 500 μl, corresponding to 10 g of sample). Absorbance range setting: 0.05 a.u.f.s.

TABLE II

TYPICAL RETENTION TIMES ON AN RP-18 COLUMN

Benzimidazole	*Retention time (min)*		λ_{max} *(nm)*[a]	ε *(l mol^{-1} cm^{-1})*[a]
	Mobile phase 1	*Mobile phase 2*		
Oxfendazole (**5**)[b]	3.7	3.9	295	18 200
Thiabendazole (**7**)	4.2	4.6	301	24 200
Mebendazole (**4**)	4.8	5.8	314	14 100
Flubendazole (**3**)	4.9	6.2	312	14 600
Oxibendazole (**6**)	5.1	6.3	297	13 500
Albendazole (**1**)	6.3	8.5	297	12 400
Fenbendazole (**2**)	7.2	10.4	297	14 700
Triclabendazole (**8**)	12.4	20.0	306	19 100

[a] Measured in methanol.
[b] In mobile phase 3: 4.8 min.

the most suitable for the detection of all eight benzimidazoles in one step; ion-suppression systems resulted in longer retention times, poorer separations and considerable tailing of the peaks. The mobile phases described allow the benzimidazoles to be identified and determined in tissue samples, but a baseline separation of the eight benzimidazoles was not achieved. Mobile phase 1 was used for routine analysis and screening. For the verification of oxfendazole (**5**) in liver and kidney samples, mobile phase 2 was used; a better separation from interfering matrix peaks was not possible. Mobile phase 3 was used for the quantification of oxfendazole (**5**) in liver and kidney.

UV detection of the benzimidazoles at 298 nm was used, and the UV spectra show two maxima at about 250 and 300 nm (see Table II). The more intense maxima at 250 nm were not suitable for detection because of self-absorption of the mobile phases. In order to improve the detection limit, fluorescence emission could be used, but only for albendazole (**1**), oxibendazole (**6**) and thiabendazole (**7**) was a gain in sensitivity in

TABLE III

TYPICAL RECOVERIES FOR A CONCENTRATION RANGE OF 0.1 mg/kg

Contents in spiked samples of 10 g each determined by HPLC.

Benzimidazole	*Recovery (%)*[a]		
	Liver	*Kidney*	*Muscle*
Albendazole (**1**)	71 (4.1)	74 (3.9)	71 (5.7)
Fenbendazole (**2**)	87 (3.6)	86 (4.2)	77 (3.5)
Flubendazole (**3**)	70 (7.8)	74 (2.8)	73 (5.8)
Mebendazole (**4**)	65 (5.1)	72 (3.8)	66 (11.6)
Oxfendazole (**5**)	45 (7.6)	39 (4.4)	80 (6.6)
Oxibendazole (**6**)	75 (6.9)	79 (4.0)	70 (8.2)
Thiabendazole (**7**)	66 (4.4)	66 (2.2)	66 (5.5)
Triclabendazole (**8**)	74 (5.3)	71 (2.9)	72 (2.8)

[a] Relative standard deviations (%) (n = 4) in parentheses.

relation to UV detection obtained; unequal excitation and emission wavelengths rendered the test suitable for only one substance in one chromatographic run.

In the region of 0.1 mg/kg, the recoveries obtained were 66–87% with a relative standard deviation of 3–11%. High relative standard deviations were obtained for liver samples containing large amounts of interfering substances (see Table III).

The detection limits were in the range 20–50 μg/kg, depending on the matrix (for the standard solutions, 1–4 ng per injection, determined on the basis of a signal-to-noise ratio of 1:3). The quantification was accomplished by integration of the peak areas and using external standards. If the detection involved all eight benzimidazoles, an internal standard could not be used. Linear regression was determined within the range 10–200 ng. For typical chromatograms see Figs. 3–5.

Detection by GC and GC–MS

As the benzimidazoles are basic and exhibit low volatility, a derivatization procedure was inevitable. Only thiabendazole (**7**) and triclabendazole (**8**) are accessible by direct GC, although with a high detection limit.

Of the derivatization reactions generally used in the GC determination of substances with amino functions, we chose acylation with trifluoroacetic anhydride, heptafluorobutyric anhydride, N-methyltrifluoroacetamide and pentafluorobenzoyl chloride and alkylation with methyl iodide and pentafluorobenzyl bromide.

Nose *et al.*[10] described the acylation of thiabendazole with pentafluorobenzoyl chloride for GC with electron-capture detection (ECD). We tried the same derivatization with the present benzimidazoles, but only for thiabendazole (**7**) was a derivative detectable; triclabendazole (**8**) and the benzimidazoles of the carbamate type (**1–6**) yielded no results. Although in HPLC and thin-layer chromatography reaction products could be recognized, the derivatives of these substances decomposed during GC. Cline *et al.*[14] and Tjan and Jansen[13] obtained similar results with chemically related carbamate pesticides.

For this reason, we applied the Claisens carbonate alkylation method[16] using the reagents cited above for all eight benzimidazoles. Tjan and Jansen[13] described a similar procedure for the determination of thiabendazole (**7**) and carbamate fungicides in fruits.

Although the detection of the pentafluorobenzyl derivatives by ECD could be very sensitive, we used thermionic nitrogen–phosphorus detection (NPD), as it is less affected by impurities in the matrices. As shown by GC–MS (see below), for the benzimidazoles of the carbamate type (**1–6**) the N,N′-dialkyl derivatives were always obtained. If two tautomeric forms are possible, the derivatives always appeared as two well separated peaks. Figs. 6–8 show typical chromatograms for liver, kidney, tissue and blood samples. On a non-polar capillary column, *e.g.*, of the OV 1-type, the alkyl derivatives normally appear in the following order: thiabendazole (**7**), oxibendazole (**6**), albendazole (**1**), triclabendazole (**8**), fenbendazole (**2**), flubendazole (**3**), mebendazole (**4**) and oxfendazole (**5**). The peaks of these derivatives appeared in a region of the chromatogram in which no interference from matrix peaks occurred.

Verification was accomplished by comparison with external standards on two or more chromatographic systems. As the derivatives undergo decomposition during the injection and chromatography owing to the high temperatures needed, quantitative determinations were not possible by GC.

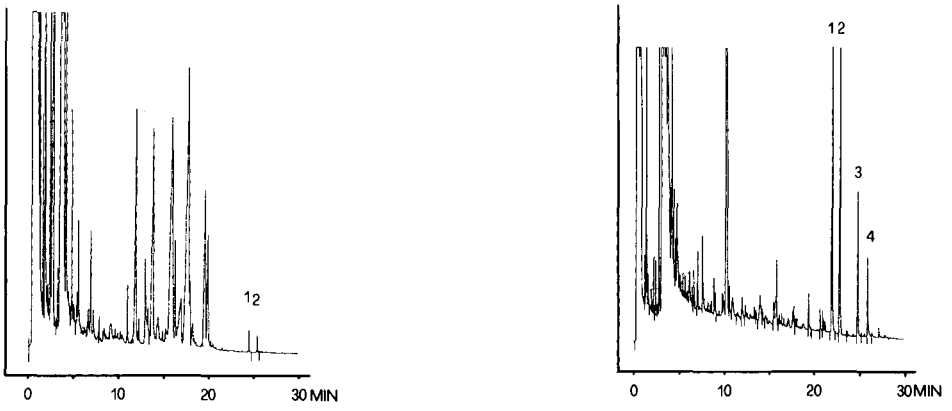

Fig. 6. Typical chromatogram of a liver sample spiked with 0.1 mg/kg mebendazole, obtained with NPD. Peaks 1 and 2 are pentafluorobenzyl derivatives.

Fig. 7. Typical chromatogram of a kidney sample from a pig administered with fenbendazole, obtained with NPD. Peaks: 1 and 2, pentafluorobenzyl derivatives of fenbendazole; 3 and 4, pentafluorobenzyl derivatives of the sulphone metabolite of fenbendazole.

The derivatives were more useful for verification by GC–MS. With the methyl derivatives, the electron-impact (EI) mass spectra of each of the derivatives exhibit a series of a few ions. Generally, the molecular ion appears as the base peak. Then a characteristic fragmentation of the benzimidazoles of the carbamate type (**1**–**6**) is the loss of the neutral mass 59, corresponding to the carbamic acid methyl ester moiety, the resulting fragment appearing as an abundant ion, often as the base peak. The derivative of triclabendazole (**8**) shows the typical isotopic composition of four molecular ions corresponding to the isotopic combinations of three chlorine atoms.

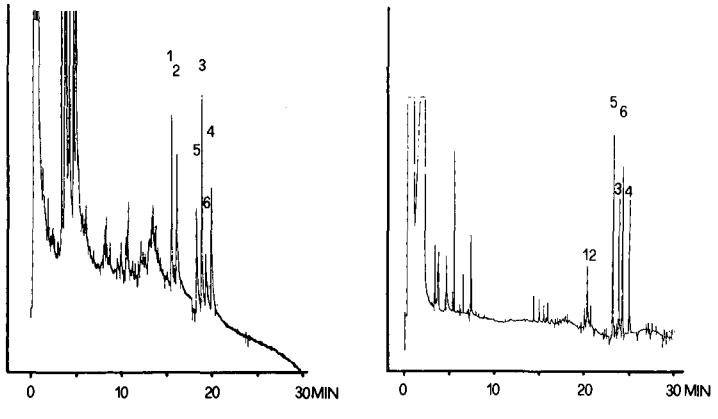

Fig. 8. Chromatograms of muscle tissue (left) and blood (right) from a pig administered fenbendazole, obtained using NPD. Methyl derivatives: 1, 2, of fenbendazole; 3, 4, of a sulphone metabolite; 5, 6, of oxfendazole, also appearing as a metabolite.

TABLE IV

ELECTRON-IMPACT (EI) AND POSITIVE-ION (PICI) AND NEGATIVE-ION (NICI) CHEMICAL-IONIZATION MASS SPECTRA [*m/z* VALUES (RELATIVE INTENSITIES)]

Benzimidazole	*Methyl derivatives: EI spectra*	*Pentafluorobenzyl derivatives*		
		EI spectra	*PICI spectra*	*NICI spectra*
Albendazole	293 (100%) M^+ 234 (32%) 192 (45%) 72 (19%) 59 (23%)	625 (100%) M^+ 566 (25%) 444 (15%) 181 (86%)	654 (13%) 626 (100%) 446 (32%) 182 (75%) 181 (77%)	444 (100%)
Fenbendazole	327 (100%) M^+ 268 (91%) 59 (38%)	659 (100%) M^+ 600 (27%) 478 (36%) 181 (63%) 59 (33%)	688 (13%) 660 (100%) 480 (18%) 182 (24%) 181 (17%)	478 (100%)
Flubendazole	341 (65%) M^+ 282 (100%)	673 (22%) M^+ 614 (23%) 181 (90%) 123 (100%) 59 (30%)	702 (13%) 674 (100%) 494 (19%) 182 (44%) 181 (50%)	492 (100%)
Mebendazole	323 (63%) M^+ 264 (100%) 246 (23%) 159 (23%) 105 (44%) 77 (76%) 59 (27%)	655 (34%) M^+ 596 (30%) 181 (79%) 105 (100%) 77 (81%) 59 (26%)	684 (15%) 656 (100%) 476 (16%) 182 (64%) 181 (64%)	474 (100%)
Oxfendazole	343 (57%) M^+ 327 (37%) 295 (64%) 266 (75%) 250 (30%) 236 (100%) 159 (73%) 72 (76%) 59 (79%)	675 (28%) M^+ 659 (16%) 627 (4%) 600 (6%) 181 (100%) 59 (43%)	704 (7%) 676 (100%) 660 (17%) 85 (25%) 73 (20%) 57 (65%)	494 (100%) 478 (82%)
Oxibendazole	277 (100%) M^+ 235 (27%) 234 (31%) 218 (27%) 176 (98%)	609 (79%) M^+ 550 (24%) 508 (11%) 428 (17%) 386 (35%) 181 (100%) 59 (23%)	638 (16%) 610 (100%) 568 (8%) 430 (9%) 182 (14%) 181 (11%)	428 (100%)
Thiabendazole	215 (100%) M^+ 187 (31%) 156 (23%) 155 (24%) 77 (41%)	381 (100%) M^+ 362 (65%) 303 (27%) 214 (43%) 181 (54%) 90 (66%)	410 (24%) 382 (100%) 202 (46%) 182 (38%) 181 (27%)	200 (100%)
Triclabendazole	372/374/376/378 M^+ (75/67/24/8%) 339/341/343/345 (100/67/24/6%)	538/540/542/544 M^+ (45/42/14/3%) 357/359/361/363 (42/58/28/2%) 181 (100%)	567/569/571/573 (8/9/3/1%) 539/541/543/545 (97/100/59/7%) 359/361/363/365 (19/17/6/2%) 182 (21%) 181 (17%)	357/359/361/363 (100/98/37/5%)

The loss of the neutral mass of 33 (probably HS) leads to an analogous isotopic pattern of prominent peaks, including the base peak.

The relatively simple spectra of these derivatives with their few, abundant heavy fragments are suitable for EI–MS in the scan- or fragmentation mode (MID, SIM).

Although the pentafluorobenzyl derivatives are chromatographically less suitable than the methyl derivatives, because the molecular mass often reaches high values, they are very useful in detection by chemical ionization (CI) MS techniques, *e.g.*, for pulsed positive ion–negative ion chemical ionization.

In EI–MS, the benzimidazoles of the carbamate type (**1–6**) produce a set of prominent ions, including the molecular ion (most abundant), the fragment of *m/z* 181, corresponding to the pentafluorotropylium ion, a fragment formed by the loss from the molecular ion of neutral mass 59, which is similar to the fragmentation pattern of the methyl derivatives, and a less abundant ion arising from the loss of the pentafluorobenzyl moiety, $[M - 181]^+$. The fragment of *m/z* 181 often appears as the base peak, a fact that renders these EI spectra unsuitable for the fragmentation MS (MID, SIM), the ion of *m/z* 181 also being ubiquitous in the matrix spectra.

The positive-ion CI (PICI) spectra show as a common feature the quasimolecular ion $[M + 1]^+$ as the base peak and an ion $[M + 29]^+$, typical of PICI using methane as the reactant gas. The pentafluorotropylium ion (*m/z* 181) and the protonated analogue (*m/z* 182) are also of important abundance. The derivative of triclabendazole (**8**) shows the characteristic isotopic profiles for the quasimolecular ion $[M + 1]^+$, the ion $[M + 29]^+$ and the probably protonated fragment resulting from the loss of the pentafluorobenzyl moiety, $[M - 180]^+$.

The negative-ion CI (NICI) spectra result in a single abundant fragment $[M - 181]^-$. This fragmentation has its counterpart in the removal of the pentafluorobenzyl moiety in the PICI spectra; the fragmentation seems to follow an ion-pair mechanism.

The EI- and CI-MS results are summarized in Table IV.

Practical application

In order to verify that the methods do indeed work, a pig was fed 15 mg of fenbendazole (**2**) per kg body weight in the feed, and was slaughtered 24 h after the application. Fenbendazole and two metabolites were found in the tissues (Table V,

TABLE V

RESIDUES IN THE TISSUES OF A TREATED PIG

Benzimidazole	*Concentration (ppm)*[a]		
	Liver (n = 3)	*Kidney (n = 3)*	*Muscle*[b] *(n = 9)*
Fenbendazole (**2**)	12.50 (2.9)	2.83 (4.4)	0.44 (7.5)
Oxfendazole (**5**)	0.17 (30.6)	n.d.[c]	1.34 (8.5)
Sulphoxide metabolite	4.12 (1.5)	2.00 (5.2)	1.14 (7.1)

[a] Relative standard deviations (%) in parentheses.
[b] Samples were taken from different muscles.
[c] Not detected.

Fig. 5). The metabolites were identified as the sulphoxide metabolite, which corresponds to oxfendazole (**5**), and the sulphone metabolite.

To check the practical routine application of the methods, the tissues (muscle, kidney, liver) from 43 normal slaughtered pigs and 25 forced slaughtered cattle were examined. No residues of benzimidazoles were found. The analysis showed that the described method is routinely practicable.

CONCLUSION

The method described here is suitable for detecting and verifying the benzimidazole anthelmintics albendazole, fenbendazole, flubendazole, mebendazole, oxfendazole, oxibendazole, thiabendazole and triclabendazole in tissue samples with a detection limit of 20–50 μg/kg. The verification of the results is performed by GC–MS or GC–NPD methods using the methyl or pentafluorobenzyl derivatives of the drugs.

ACKNOWLEDGEMENTS

We thank Miss B. Gampp and Mr. M. Sievi for technical assistance.

REFERENCES

1 K. Alton, J. Patrick and J. McGuire, *J. Pharm. Sci.*, 68 (1979) 880.
2 G. Karlaganis, G. J. Münst and J. Bircher, *J. High Resolut. Chromatogr. Chromatogr. Commun.*, (1979) 141.
3 M. T. Watts, V. A. Raisys and L. A. Bauer, *J. Chromatogr.*, 230 (1982) 79.
4 J. A. Bogan and S. Marriner, *J. Pharm. Sci.*, 69 (1980) 422.
5 K. Frgalova, *Cesk. Hyg.*, 27 (1982) 102.
6 M. Petz, *Z. Lebensm.-Unters.-Forsch.*, 180 (1984) 267.
7 R. Malisch, *Z. Lebensm.-Unters.-Forsch.*, 182 (1986) 385.
8 R. Malisch, *Z. Lebensm.-Unters.-Forsch.*, 183 (1986) 253.
9 R. Malisch, *Z. Lebensm.-Unters.-Forsch.*, 184 (1987) 467.
10 N. Nose, S. Kobayashi, A. Tanaka, A. Hirose and A. Watanabe, *J. Chromatogr.*, 130 (1977) 410.
11 W. VandenHeuvel, J. Wood, M. Di Giovanni and R. Walker, *J. Agric. Food Chem.*, 25 (1977) 386.
12 A. Tanaka and Y. Fujimoto, *J. Chromatogr.*, 117 (1976) 149.
13 G. Tjan and J. Jansen, *J. Assoc. Off. Anal. Chem.*, 62 (1979) 769.
14 S. Cline, A. Felsot and L. Wei, *J. Agric. Food Chem.*, 29 (1981) 1087.
15 H. Haase, W. Heidemann and H. Rüssel, *Fresenius' Z. Anal. Chem.*, 318 (1984) 111.
16 W. Dünges, *Prächromatographische Mikromethoden*, Hüthig, Heidelberg, 1980.

Journal of Chromatography, 498 (1990) 159–168
Elsevier Science Publishers B.V., Amsterdam — Printed in The Netherlands

CHROM. 22 012

PARTIAL PURIFICATION OF GLUCOSE 6-PHOSPHATE DEHYDROGENASE AND PHOSPHOFRUCTOKINASE FROM RAT ERYTHROCYTE HAEMOLYSATE BY PARTITIONING IN AQUEOUS TWO-PHASE SYSTEMS

CRISTINA DELGADO, M. CRISTINA TEJEDOR and JOSE LUQUE*
Departamento de Bioquimica y Biologia Molecular, Universidad de Alcala de Henares, 28871 Alcala de Henares, Madrid (Spain)
(First received February 13th, 1989; revised manuscript received September 20th, 1989)

SUMMARY

Glucose 6-phosphate dehydrogenase shows a high partition coefficient in poly(ethylene glycol)–dextran aqueous two-phase systems in comparison with those for 6-phosphogluconate dehydrogenase, phosphofructokinase and the bulk of proteins present in rat erythrocyte haemolysates. As a consequence, fractions highly enriched in glucose 6-phosphate dehydrogenase can be obtained after multiple partitions in the above systems with a counter-current distribution procedure. Phosphofructokinase shows a high affinity for Cibacron Blue and, as a result, the enzyme can be extracted in the top phase of poly(ethylene glycol)–dextran systems containing Cibacron Blue–poly(ethylene glycol) (affinity systems). The efficiency for the purification of the enzymes by partitioning is increased up to 10-fold when enzyme-rich fractions, obtained by precipitation with poly(ethylene glycol), are used instead of original haemolysate. The recovery of enzyme activities is near 100% in both instances.

INTRODUCTION

The principle of partitioning has been applied to the fractionation of a mixture of proteins with the development of aqueous two-phase systems formed by either two hydrophilic polymers, poly(ethylene glycol) (PEG) and dextran, or a polymer (PEG) and salt[1–3]. The high water content of the phases, the low interfacial tension between them and the protective effect exerted by the polymers make these systems very mild toward labile macromolecules[1–3]. The ease, speed and economy of the methodology involved in aqueous two-phase systems have been emphasized[4–6]. Further, as the partition coefficient of the protein and the properties which determine it share an exponential relationship, partitioning in aqueous two-phase systems allows fractionations of proteins which are not currently available by other methods[1,7].

Partitioning of proteins in standard biphasic systems depends on the concentration and molecular weight of the polymers, the concentration and type of salt and pH[1–3]. By manipulation of these parameters, single partition experiments can be used to direct a protein selectively towards the desired phase[1–3]. Using this approach,

0021-9673/90/$03.50

preparations of proteins free from nucleic acids[8] and the separation of proteins from nucleic acids and polysacharides[9] have been achieved.

The partition coefficient (K) of the target protein is not always different enough from that of the bulk proteins to allow an efficient separation with a single extraction. The separation may then be achieved by using a multiple partition procedure such as counter-current distribution[1,2]. Alternatively, the introduction in one of the phases of a ligand with a selective affinity for the target protein gives rise to affinity-partitioning systems, in which the protein is directed towards that phase[10–12]. The triazine dye Cibacron Blue F3GA (Cb) covalently linked to PEG (PEG–Cb) has been used as an affinity ligand for the selective extraction of phosphofructokinase from bakers' yeast into the top phase of a PEG–dextran system[13,14]. The use of these affinity systems for multiple partitions with the counter-current distribution procedure has provided a high-resolution methodology for the fractionation of glycolytic enzymes from yeast extract[15–16].

In this paper, we report the partitioning behaviour of glucose 6-phosphate dehydrogenase (E.C. 1.1.1.49, G6PD), 6-phosphogluconate dehydrogenase (E.C. 1.1.1.44, 6PGD) and phosphofructokinase (E.C. 2.7.1.11, PFK) from rat erythrocytes in both standard and affinity PEG–dextran two-phase systems. The aim of the work was to design an experimental protocol for the extraction of these enzymes by using partitioning in aqueous two-phase systems which allows the extraction of enzymes under very mild conditions. Our group is interested in the study of regulatory enzymes in the glucolytic and pentose–phosphate pathways in eryhtrocytic cells[17,18]. A first extraction step for phosphofructokinase and glucose 6-phosphate dehydrogenase by precipitation with PEG[19] was employed to improve the efficiency of the partitioning step.

EXPERIMENTAL

Chemicals

PEG (M_r 6000) and Cibacron Blue F3GA were obtained from Serva (Heidelberg, F.R.G.), dextran T-500 from Pharmacia (Uppsala, Sweden), nucleotides (sodium salts of ATP, NADH and NADP), dithioerythritol, glucose 6-phosphate, 6-phosphogluconate, fructose 6-phosphate and coupling enzymes from Boehringer (Mannheim, F.R.G.), EDTA (disodium salt) from Sigma (St. Louis, MO, U.S.A.) and Tris, 2-mercaptoethanol and all other chemicals (analytical-reagent grade) from Merck (Darmstadt, F.R.G.).

Preparation of the haemolysate

Anesthetized male Wistar rats weighing 180–200 g were decapitated and whole blood was collected in heparinized tubes and centrifuged (400 g, 10 min) to separate the plasma. Red cells were washed three times with 0.9% sodium chloride solution and freed from leucocytes and platelets by removing the top layer of cells after centrifugation. Subsequently, the red cells were lysed by mixing with an equal volume of a hypotonic solution containing 2.7 mM EDTA and 0.7 mM 2-mercaptoethanol. The mixture was frozen and thawed twice and finally centrifuged (15000 g, 30 min) to remove stroma. All these steps were carried out at 4°C.

Preparation of fractions enriched in phosphofructokinase and glucose 6-phosphate dehydrogenase

Enriched fractions were obtained by mixing one volume of haemolysate (total protein about 20 mg/ml) with one volume of a solution of 12% (w/w) PEG made up in 96 m*M* potassium phosphate buffer (pH 6) (for the precipitation of phosphofructokinase) and 170 m*M* sodium acetate buffer (pH 5) (for the precipitation of glucose 6-phosphate dehydrogenase). The buffers contained 10 m*M* EDTA and 1 m*M* 2-mercaptoethanol. The mixtures of PEG and haemolysate were kept in an ice-bath for 30 min and then centrifuged (5000 *g*, 10 min). The supernatants were discarded and the pellets redissolved in 1 volume of 25 m*M* sodium phosphate buffer (pH 7) containing 5 m*M* EDTA and 0.5 m*M* 2-mercaptoethanol[17].

Preparation of Cibacron Blue–poly(ethylene glycol)

This substituted polymer was prepared as described by Johansson[12]. In brief, 50 g of PEG were dissolved in 100 ml of water and the solution was heated in a water-bath at 80°C, then 5 g of Cibacron Blue F3GA and 2 g of sodium hydroxide were added and the mixture was stirred for 2 h at 80°C. Solid sodium phosphate was added to adjust the pH of the mixture to 7. The PEG–Cb was extracted with five portions of 150 ml of chloroform and the pooled organic extracts were dried with anhydrous sodium sulphate and filtered through a Whatman GF/A paper. The dark-blue solid was recovered by evaporation of the solvent under reduced pressure. The excess of Cibacron Blue was eliminated by ion-exchange chromatography with DEAE-cellulose (DEAE-52; Servacel, Heidelberg, F.R.G.). The PEG–Cb was eluted from the column with 2 *M* potasium chloride. The dye–polymer was finally extracted with chloroform and the solvent removed by evaporation.

Single partitioning

Systems of 4 g were prepared in 10-ml graduated tubes by weighing 0.4 g of sample and appropriate amounts of distilled water and the following stock solutions: 40% (w/w) PEG, 20% (w/w) dextran (standardized by polarimetry) and 0.25 *M* sodium phosphate buffer (pH 7) containing 2.5 m*M* EDTA and 25 m*M* 2-mercaptoethanol. A ratio of 1.5:1 (w/w) of dextran to PEG was maintained in all the systems to obtain two-phase systems in which the volume ration of the top to the bottom phases was close to 1. After mixing by 30–40 inversions the mixtures were left to settle at 4°C until complete separation of the phases was achieved. Aliquots from the top and bottom phases were then analysed for protein concentration and enzymic activities.

The affinity systems were prepared as above but using a 40% (w/w) stock solution of PEG containing 6% of PEG–Cb. This substituted polymer was prepared as described by Johansson and Joelsson[6].

The partition coefficient, *K*, is defined as the ratio between the enzyme activities or total protein concentrations in the top and bottom phases of the systems. The percentage of protein in the top phase of the systems was calculated from the partition coefficient and volume ratio values as described by Johansson[12]. The concentration of polymers in the systems is always expressed by weight.

Counter-current distribution

Counter-current distribution (CCD) was carried out in a two-phase system formed by 5% PEG–7.5% dextran, 50 m*M* sodium phosphate buffer (pH 7), 0.5 m*M* EDTA and 5 m*M* 2-mercaptoethanol. The two-phase system (normally 250 g) was prepared by mixing the required amounts of the above stock solutions and distilled water. Once the top and bottom phases had separated at 4°C, they were stored at 4°C.

An automatic thin-layer counter-current distribution apparatus (Bioshef TLCCD MK3; University of Sheffield, Sheffield, U.K.) with a distribution rotor formed by two circular plates (60 cavities) was used[20]. Cavities 4–60 each received an equal volume (0.765 ml) of the bottom and top phases. Cavities 1–3 each received an equal volume (0.765 ml) of the bottom and top phases of a "biphasic system containing sample" prepared immediately before use from the same stock solutions as the bulk system but replacing the distilled water for the sample. A distribution run consisted of 57 partitions. Each partition step was composed of a 20-s shaking time followed by a 6-min settling time and a transfer of the top phase to the next right bottom phase by means of a displacement of the top rotor plate. The experiment was carried out at 4°C. After completion, the contents of each cavity were diluted with 1 ml of 25 m*M* sodium phosphate (pH 7), 0.25 m*M* EDTA and 5 m*M* 2-mercaptoethanol (to convert the system into one phase) and collected in plastic tubes. Aliquots from each alternate cavity were assayed for total protein or enzymic activities.

Enzyme and total protein assays

Enzymic activities were measured in a double-beam spectrophotometer (Kontron Uvikon 810) at 37°C.

Glucose 6-phosphate and 6-phosphogluconate dehydrogenases were measured by using a double-step assay. The first cuvette contained 50 m*M* Tris–HCl pH 7.5, 1 m*M* EDTA, 0.5 m*M* NADP, 0.6 m*M* glucose 6-phosphate and 0.6 m*M* 6-phosphogluconate. From the linear increase in the absorbance due to NADPH (340 nm), activities of both enzymes were obtained. In the second step, glucose 6-phosphate was omitted and the activity of only 6-phosphogluconate dehydrogenase was obtained. The activity of glucose 6-phosphate dehydrogenase was then calculated by the difference in activities between the first and second steps.

Phosphofructokinase activity was measured by the linear decrease in NADH absorbance (340 nm) in a test mixture containing 100 m*M* Tris–HCl (pH 7.1), 0.3 m*M* EDTA, 3 m*M* magnesium chloride, 90 m*M* potassium chloride, 0.15 m*M* NADH, 1.5 m*M* dithiothreitol, 1 m*M* phosphate, 3 m*M* fructose 6-phosphate, 9 m*M* glucose 6-phosphate, 1.5 m*M* ATP, 0.1 U/ml fructose diphosphate aldolase, 6 U/ml triose phosphate isomerase and 0.5 U/ml glycerol 3-phosphate dehydrogenase.

Total protein concentration was measured by the Coomassie Brilliant Blue assay[21], which is not subject to any interference from either PEG or dextran in the samples[2].

RESULTS AND DISCUSSION

Partitioning in standard systems

Partition coefficients of glucose 6-phosphate dehydrogenase, 6-phosphogluconate dehydrogenase, phosphofructokinase and total protein from rat erythrocyte

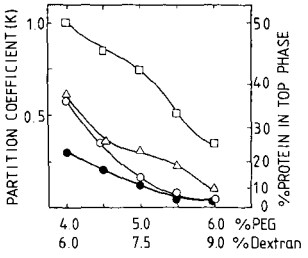

Fig. 1. Influence of the concentration of polymers on the partition coefficient of (□) glucose 6-phosphate dehydrogenase, (△) 6-phosphogluconate dehydrogenase, (○) phosphofructokinase and (●) total proteins from rat erythrocyte haemolysate in PEG–dextran aqueous two-phase systems. All systems were buffered with 50 m*M* sodium phosphate (pH 7) containing 0.5 m*M* EDTA and 5 m*M* 2-mercaptoethanol. The percentage of protein in the top phase is also shown for a system with phases of equal volumes.

haemolysate in two-phase systems with concentrations varying from 4% to 6% PEG and from 6% to 9% dextran have values lower than one (Fig. 1), *i.e.*, partition favours the dextran-rich bottom phase. In all instances, the increase in the concentration of both polymers in the system leads to a decrease in *K*. These two features have been described as a general behaviour for the partitioning of proteins[1,2].

The partition coefficient of glucose 6-phosphate dehydrogenase is higher than those for 6-phosphogluconate dehydrogenase, phosphofructokinase and the bulk of proteins, all of which show a similar behaviour in any of the biphasic systems used (Fig. 1). This fact will be exploited partially to purify the enzyme by counter-current distribution.

Partitioning in affinity systems

Partition coefficients of phosphofructokinase, glucose 6-phosphate and 6-phosphogluconate dehydrogenases in affinity PEG (PEG–Cb)–dextran systems are, in general, higher (Fig. 2a) than in the relevant standard systems (Fig. 1). This fact reflects an interaction between the Cb molcule and each of the three enzymes. The total protein shows similar partition coefficients in affinity (Fig. 2a) and standard

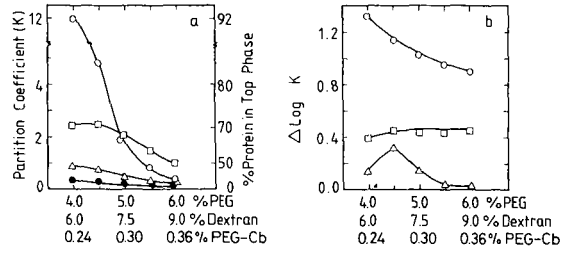

Fig. 2. (a) Partition coefficient of (□) glucose 6-phosphate dehydrogenase, (△) 6-phosphogluconate dehydrogenase, (○) phosphofructokinase and (●) total protein from rat erythrocyte haemolysate in aqueous two-phase systems with increasing concentrations of PEG, dextran and PEG–Cb. Other conditions as in Fig. 1. (b) Change in the logarithm of the partition coefficient of (□) glucose 6-phosphate dehydrogenase, (△) 6-phosphogluconate dehydrogenase and (○) phosphofructokinase in whole haemolysate between affinity and standard systems.

biphasic systems (Fig. 1). In all instances, the partition coefficient decreases with increase in the concentration of polymers.

The affinity partitioning effect due to the presence of Cb in the system is given by the increase in the logarithm of the partition coefficient in affinity systems (Fig. 2a) with respect to that in standard systems (Fig. 1). Results thus calculated ($\Delta \log K$) are shown in Fig. 2b. 6-Phosphogluconate dehydrogenase shows the lowest affinity for the ligand, the affinity being totally prevented when the concentration of polymers is increased above 5.5% (0.33%) PEG (PEG–Cb)–8.25% dextran. Glucose 6-phosphate dehydrogenase shows an intermediate affinity for Cibacron Blue with a $\Delta \log K$ value of about 0.45 in any of the systems (Fig. 2b). Phosphofructokinase shows the highest value of $\Delta \log K$ in all the systems, reflecting a higher affinity of the phosphofructokinase for Cibacron Blue. In spite of the concentration of PEG–Cb being raised, an increase in the concentration of polymers in the systems leads to a decrease in $\Delta \log K$ for phosphofructokinase. It seems, therefore, that the effect due to the increase in the concentration of PEG and dextran which directs the protein towards the bottom phase[2,12] is stronger than the affinity effect promoted by PEG–Cb which should direct the protein to the top phase.

Phosphofructokinase was partially extracted by precipitation with PEG and its partition coefficient was measured in standard and affinity two-phase systems (Fig. 3a). Again, the partition coefficient of the phosphofructokinase is higher in affinity than in standard systems. Moreover, in all the affinity systems the K values for the phosphofructokinase in the enriched fraction are higher than those for the enzyme in the whole haemolysate. This result indicates than the interaction of phosphofructokinase with Cibacron Blue is reduced by a higher amount of other proteins in the haemolysate which, in competing for the ligand, decreases the concentration of free ligand. This result emphasizes the importance that the presence of other proteins may have in the affinity partitioning effect of a selected protein. Therefore, when applying affinity partitioning to the purification of a protein from a crude extract, it should be

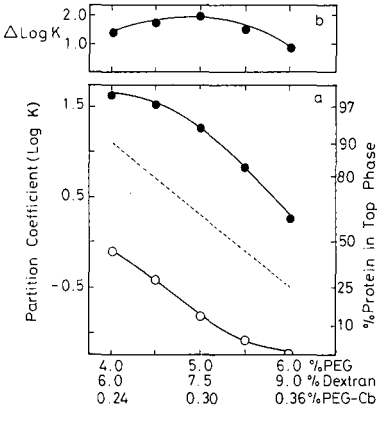

Fig. 3. (a) Partition coefficient of phosphofructokinase from a PFK-enriched fraction in (○) standard and (●) affinity systems with increasing concentrations of PEG, dextran and PEG–Cb. The broken line represents the partition coefficient of phosphofructokinase from the whole haemolysate in affinity systems. Other conditions as in Fig. 1. (b) Change in the logarithm of the partition coefficient of phosphofructokinase in the enriched fraction between affinity and standard systems.

taken into account that the presence of other proteins that interact with the ligand may reduce the yield of protein in the affinity phase.

In contrast to the $\Delta \log K$ observed for phosphofructokinase in the whole haemolysate, that for phosphofructokinase in the enriched fraction (Fig. 3b) increases when the concentration of the polymers in the system is increased to 5% (0.3%) PEG (PEG–Cb)–7.5% dextran. Such an increase in $\Delta \log K$ (Fig. 3b) seems to be consistent with the increase in $\Delta \log K$ found by Johansson[2,12] when purified bakers' yeast phosphofructokinase was partitioned in biphasic systems containing increasing concentrations of PEG, PEG–Cb and dextran. Further increases in the concentration of the polymers lead to reductions in this affinity effect (Fig. 3b), as observed in the whole haemolysate.

Application of partitioning in aqueous two-phase systems in purification schedules for phosphofructokinase and glucose 6-phosphate dehydrogenase

The highest affinity of phosphofructokinase for PEG–Cb and the high partition coefficient of glucose 6-phosphate dehydrogenase in standard systems allow experimental protocols for their partial purification to be designed. The similar behaviour of 6-phosphogluconate dehydrogenase and the total proteins in either standard or affinity systems does not lead to an enrichment of this enzyme under any of the conditions studied.

TABLE I

TWO-STEP PROCEDURES FOR THE EXTRACTION OF GLUCOSE 6-PHOSPHATE DEHYDROGENASE AND PHOSPHOFRUCTOKINASE FROM RAT ERYTHROCYTE HAEMOLYSATE INVOLVING PRECIPITATION WITH POLY(ETHYLENE GLYCOL) AND PARTITIONING IN AQUEOUS TWO-PHASE SYSTEMS

Enzyme	*Step*	*Procedure*	*Fraction Collected*	*Yield (%)*[a]	*Purification Factor*[b]
Phosphofructokinase	1	Precipitation, 6% PEG, pH 6	Pellet	80	8
	2	Affinity partitioning[c]	Top phase	95	10
		Overall result		75	80
Glucose 6-phosphate dehydrogenase	1	Precipitation, 6% PEG, pH 5	Pellet	90	5
	2	Counter-current distribution[d]	Tubes 22–36	70	8
		Overall result		60	40

[a] Percentage of enzymic units recovered in each step with respect to those in the fraction subjected to the procedure.

[b] Ratio between specific activities in the fraction collected and the fraction subjected to the procedure.

[c] The system used is formed by 5% (w/w) PEG, 7.5% (w/w) dextran in 25 m*M* sodium phosphate buffer (pH 7) containing 0.25 m*M* EDTA and 2.5 m*M* 2-mercaptoethanol. 6% of the total PEG is PEG–Cb.

[d] The system used is formed by 5% (w/w) PEG, 7.5% (w/w) dextran in 50 m*M* sodium phosphate buffer (pH 7) containing 0.5 m*M* EDTA and 5 m*M* 2-mercaptoethanol.

Phosphofructokinase. The enzyme is first precipitated from the haemolysate by addition of 6% PEG at pH 6. As previously reported[19], the pellet thus obtained contains 80% of the original phosphofructokinase with a specific activity eight times higher (Table I).

The second step involves extraction of the phosphofructokinase in the top phase of the system formed by 5% (0.3%) PEG (PEG–Cb)–7.5% dextran. In this system the highest value for the log K is obtained (Fig. 3b) and it provides the best compromise between yield and purification factor. The top phase of this system contains 95% of the enzyme present in the enriched pellet (Fig. 3a) with a specific activity ten times higher (Table I). The net result is 75% of the original phosphofructokinase (95% of 80%) with a specific activity 80 times higher (10 times 8) (Table I).

This extraction of phosphofructokinase can be completed within 2 h. Partitioning in affinity two-phase systems appears to be a suitable purification method as the activity of the enzyme is not destroyed during the procedure. The preliminary precipitation of the phosphofructokinase with PEG leads to a higher yield of the enzyme in the top phase (see Fig. 3a) and also a higher enrichment, *i.e.*, a higher efficiency of the affinity systems.

Glucose 6-phosphate dehydrogenase. In the biphasic system formed by 5% PEG–7.5% dextran, in which the greatest difference between the partition coefficient for glucose 6-phosphate dehydrogenase and the total proteins is found, 43% of the enzyme appears in the top phase with a content of only 10% of the total protein (Fig. 1), *i.e.*, 4-fold enrichment. To improve such a low enrichment in glucose 6-phosphate dehydrogenase, multiple partition steps with Albertsson's counter-current distribution procedure were then analysed (Fig. 4). A recovery of more than 90% of the total activity introduced in the distribution rotor is obtained for the three enzymes.

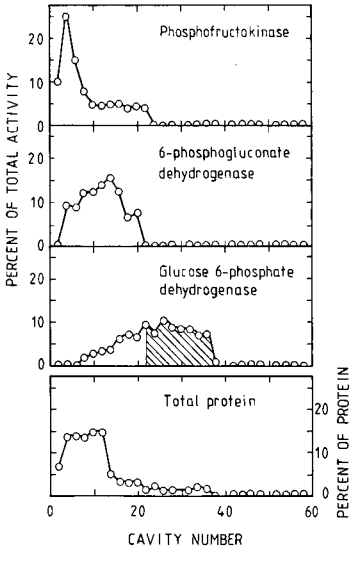

Fig. 4. Distribution profiles of total protein, phosphofructokinase, 6-phosphogluconate dehydrogenase and glucose 6-phosphate dehydrogenase obtained by counter-current distribution of rat erythrocyte haemolysate. The fractions highly enriched in G6PD are emphasized.

Distribution profiles for phosphofructokinase, 6-phosphogluconate dehydrogenase and total proteins are located towards the left-hand side of the distribution train, between cavities 1 and 20, in agreement with the low partition coefficients found in single-tube experiments (Fig. 1). Glucose 6-phosphate dehydrogenase shows a distribution profile between cavities 10 and 36. This location to the right of the other proteins was expected from the higher partition coefficient found for this enzyme in single-tube experiments (Fig. 1). The spreading of the peak could be due to the presence of isoenzymes differing in their K values.

For purification purposes, fractions 22–36 contain 70% of the original glucose 6-phosphate dehydrogenase and only 10% of the total protein. This means that a 7-fold enrichment in glucose 6-phosphate dehydrogenase with a yield of 70% has been achieved.

Glucose 6-phosphate dehydrogenase present in the enriched fraction (see Experimental) has a distribution profile located similarly (data not shown) to that for the enzyme in the total haemolysate (Fig. 4). Again, fractions 22–36 contains 70% of the enzyme introduced in the distribution rotor with a specific activity eight times higher. As the enriched fraction had 90% of the enzyme present in the haemolysate with an activity five times higher[19] (Table I), the net result of the whole procedure is 60% (70% of 90%) of the original enzyme with an activity increased 50-fold (8 times 5) (Table I).

This two-step procedure can be completed within 8 h and the enzyme is not inactivated during the manipulation. This is a further example of the ease and speed of the methodology involved in partitioning in aqueous two-phase systems.

ACKNOWLEDGEMENT

This work was supported by grants from the Comision Asesora de Investigacion Cientifica y Technica (Spain).

REFERENCES

1 P.-A. Albertsson, *Partition of Cell Particles and Macromolecules*, Wiley, New York, 3rd ed., 1985.
2 G. Johansson, in H. Walter, D. Brooks and D. Fisher (Editors), *Partitioning in Aqueous Two-Phase Systems, Theory, Methods, Uses and Applications to Biotechnology*, Academic Press, New York, 1985, pp. 161–226.
3 H. Hustedt, K. H. Kroner and M.-R. Kula, in H. Walter, D. Brooks and D. Fisher (Editors), *Partitioning in Aqueous Two-Phase Systems, Theory, Methods, Uses and Applications to Biotechnology*, Academic Press, New York, 1985, pp. 529–587.
4 B. Mattiasson, *Trends Biotechnol.*, 1 (1983) 16–20.
5 H. Hustedt, K. H. Kroner, V. Menge and M.-R. Kula, *Trends Biotechnol.*, 3 (1985) 139—144.
6 G. Johansson and M. Joelsson, *Biotechnol. Bioeng.*, 27 (1985) 621–625.,
7 D. E. Brooks, K. A. Sharp, and D. Fisher, in H. Walter, D. E. Brooks and D. Fisher (Editors), *Partitioning in Aqueous Two-Phase Systems, Theory, Methods, Uses and Applications to Biotechnology*, Academic Press, New York, 1985, pp. 11–84.
8 T. Okazaki and A. Kornberg, *J. Biol. Chem.*, 239 (1964) 259–268.
9 M.-R. Kula, K. H. Kroner and H. Hustedt, *Adv. Biochem. Eng.*, 24 (1982) 73–118.
10 S. D. Flanagan and S. H. Barondes, *J. Biol. Chem.*, 250 (1975) 1484–1489.
11 K. H. Kroner, A. Cordes, A. Schelper, M. Morr, A. F. Buckmann and M.-R. Kula, in T. C. J. Gribnau, J. Visser, and R. J. F. Nivard (Editors), *Affinity Chromatography and Related Techniques*, Elsevier, Amsterdam, 1982, pp. 491–501.
12 G. Johansson, *Methods Enzymol.*, 104 (1984) 356–364.

13 G. Kopperschlager and G. Johansson, *Anal. Biochem.*, 124 (1982) 117–124.
14 G. Johansson, G. Kopperschlager and P.-A. Albertsson, *Eur. J. Biochem.*, 131 (1983) 589–594.
15 G. Johansson, M. Andersson and H.-E. Akerlund, *J. Chromatogr.*, 298 (1984) 483–493.
16 G. Johansson and M. Andersson, *J. Chromatogr.*, 291 (1984) 175–183.
17 M. Pinilla and J. Luque, *Mol. Cell. Biochem.*, 15 (1977) 219–223.
18 M. C. Tejedor, A. Ramirez and J. Luque, *Biochem. Int.*, 9 (1984) 577–586.
19 M. C. Tejedor, C. Delgado, A. Rubio and J. Luque, *Biosci. Rep.*, 6 (1986) 395–401.
20 T. E. Treffry, P. T. Sharpe, H. Walter and D. E. Brooks, in H. Walter, D. E. Brooks and D. Fisher (Editors), *Partitioning in Aqueous Two-Phase Systems, Theory, Methods, Uses and Applications to Biotechnology*, Academic Press, New York, 1985, pp. 132–148.
21 M. N. Bradford, *Anal. Biochem.*, 72 (1976) 248–254.

Journal of Chromatography, 498 (1990) 169–178
Elsevier Science Publishers B.V., Amsterdam — Printed in The Netherlands

CHROM. 22 042

IMPROVED HIGH-SPEED COUNTER-CURRENT CHROMATOGRAPH WITH THREE MULTILAYER COILS CONNECTED IN SERIES

II. SEPARATION OF VARIOUS BIOLOGICAL SAMPLES WITH A SEMI-PREPARATIVE COLUMN

YOICHIRO ITO* and HISAO OKA

Laboratory of Technical Development, National Heart, Lung, and Blood Institute, National Institutes of Health, Building 10, Room 5D12, Bethesda, MD 20892 (U.S.A.)

and

YUE WEI LEE

Research Triangle Institute, Chemistry and Life Sciences, P.O. Box 12194, Research Triangle Park, NC 27709 (U.S.A.)

(First received June 27th, 1989; revised manuscript received September 28th, 1989)

SUMMARY

The semipreparative capability of the newly developed high-speed counter-current chromatograph equipped with a set of three multilayer coils has been demonstrated in separations of a variety of biological samples including triterpenoic acids, indole auxins, bacitracin, flavonoids and tetracycline derivatives, each with a suitable two-phase solvent system. The sample quantities ranging from 50 to 500 mg were efficiently separated within a few hours. The separation of tetracycline derivatives was remarkably improved by adding ammonium acetate to the solvent system.

INTRODUCTION

The newly developed high-speed counter-current chromatography (HSCCC) system eliminates the use of a counterweight by integrating a set of three multilayer coils symmetrically mounted on the rotary frame to increase the partition efficiency and sample loading capacity of the system. The above design also provides a perfect balance of the centrifuge system, once the hydrodynamic equilibrium is established in the separation column. In Part I[1], the potential capability of the present apparatus has been demonstrated in separation of 2,4-dinitrophenyl (DNP) amino acids with a solvent system composed of chloroform–acetic acid–0.1 *M* hydrochloric acid (2:2:1, v/v/v).

This paper describes the applications of this new apparatus in semipreparative separation of various biological samples with two-phase solvent systems covering a broad range of polarity.

0021-9673/90/$03.50

EXPERIMENTAL

Apparatus

The principle of the design and function of the apparatus has been described in detail in Part I[1]. Fig. 1 shows the apparatus which is equipped with three multilayer coils connected in series with flow tubes to make up a total capacity of 400 ml.

Each multilayer coil was prepared from a single piece of about 70 m long × 1.6 mm I.D. polytetrafluoroethylene (PTFE) tubing with a standard wall thickness (0.4 mm) (Zeus, Raritan, NJ, U.S.A.) wound onto a holder hub measuring 7.5 cm in diameter. A total of nine layers of coils were formed between a pair of flanges spaced 5 cm apart, resulting in about 200 helical turns with a total capacity of about 135 ml. The β value ($\beta = r/R$, where r is the distance from the axis of the holder to the coil and R the distance between the holder axis and the central axis of the centrifuge) ranges from 0.5 at the internal terminal to 0.75 at the external terminal. In order to prevent dislocation of the multilayer coil on the holder, innermost layer of the coil was glued onto the hub with silicone rubber adhesive while a sheath of heat-shrinkable vinyl tubing was applied over the entire multilayer coil and the peripheral portion of each flange. Three multilayer coils are serially connected with 0.85 mm I.D. thick wall (0.46 mm) PTFE tubing as described in Part I.

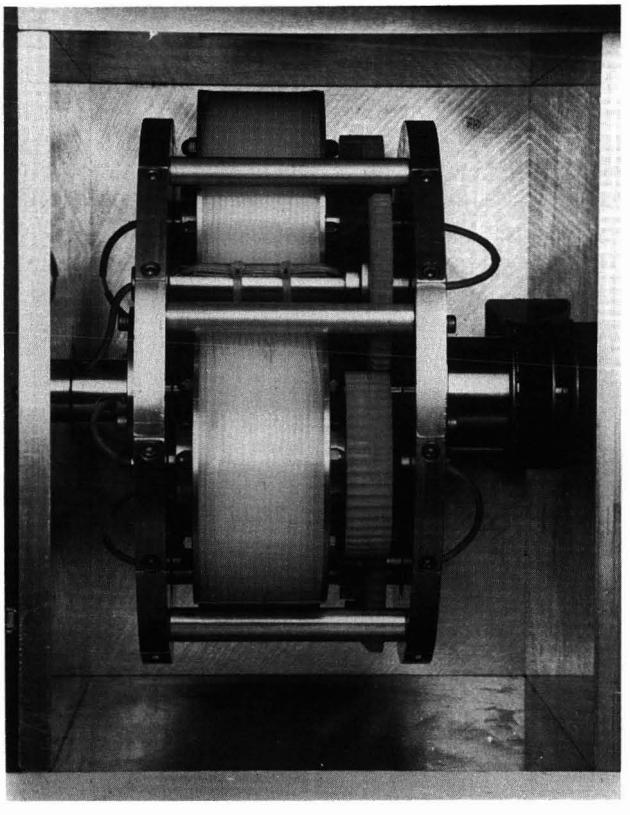

Fig. 1. Photograph of the apparatus.

Reagents

Organic solvents, including *n*-hexane, chloroform, ethyl acetate, *n*-butanol and methanol, were glass-distilled chromatographic grade and obtained from Burdick & Jackson Labs., Muskegon, MI, U.S.A. USP 95% ethanol was obtained from Warner-Graham, Cockeysville, MD, U.S.A. Ammonium acetate was of reagent grade and purchased from Fisher Scientific, Fair Lawn, NJ, U.S.A.

Indole-3-acetamide (IA), indole-3-acetic acid (IAA), indole-3-butyric acid (IBA), indole-3-acetonitrile (IAN), bacitracin, oxytetracycline (OTC), chlortetracycline (CTC) and doxycycline (DC) were all reagent grade and obtained from Sigma, St. Louis, MO, U.S.A. The crude triterpenoic acids were obtained from the extract of *Boswellia carterii* (Burseraceae). Sea buckthorn (*Hippophae rhamnoides*) ethanol extract dried powder was obtained from China by the courtesy of Professor Tian-You Zhang, Beijing Institute of New Technology Application, Beijing, China.

Preparation of two-phase solvent systems and sample solutions

Six pairs of two-phase solvent systems used in the present study are listed in Table I in the increasing order of polarity. Each solvent mixture was thoroughly equilibrated in a separatory funnel by repeating vigorous shaking and degassing several times at room temperature, and the two phases were separated shortly before use.

For the present study, the following five samples were selected: triterpenoic acids, indole auxins, flavonoids in a crude sea buckthorn ethanol extract, commercial bacitracin, and tetracycline derivatives as listed in Table I. Triterpenoic acids were separated with a two-phase solvent system composed of *n*-hexane–95% ethanol–water (6:5:2, v/v/v), and the sample solution was prepared by dissolving 500 mg of the crude triterpenoic acids in 5 ml of the upper phase of the above solvent system. Indole auxins were separated with a two-phase solvent system composed of *n*-hexane–ethyl acetate–methanol–water (1:1:1:1, v/v). The sample solution was prepared by dissolving 100 mg of a sample mixture consisting of 10 mg of IA and 30 mg each of IAA, IBA and IAN in 2 ml of the upper non-aqueous stationary phase. A crude sea buckthorn ethanol extract was separated with a two-phase solvent system composed of chloroform–methanol–water (4:3:2, v/v/v). The sample solution was prepared by first dissolving 100 mg of the dried powder in 1.5 ml of methanol, and then adding 2 ml of chloroform and 1 ml of distilled water to adjust the phase composition. The total sample volume was 4.5 ml consisting of about equal volumes of the upper and the lower phases. The bacitracin was separated with a two-phase solvent system composed of chloroform–95% ethanol–water (5:4:3, v/v/v) and 100 mg of the sample were dissolved in 1 ml of the lower non-aqueous phase. The tetracycline derivatives were separated with two different solvent systems, *i.e.*, ethyl acetate–*n*-butanol–water (2:3:5, v/v/v) and ethyl acetate–*n*-butanol–0.25 *M* ammonium acetate (1:1:2, v/v/v), and for each solvent system sample solution was prepared by dissolving a total 50 mg quantity of the mixture consisting of 10 mg of OTC, 20 mg of CTC and 20 mg of DC in 5 ml of the phase mixture.

Separation procedure

The HSCCC separations were performed according to the standard preparative CCC method, as described elsewhere[1,2], in the following manner. In each separation,

TABLE I

SUMMARY OF EXPERIMENTAL CONDITIONS

Sample	*Amount (mg)*	*Solvent system*		*Mobile phase*	*Flow-rate (ml/h)*	*Revolution (rpm)*	*Pressure (p.s.i.)*	*Retention (%)*
Triterpenoic acids	500	*n*-Hexane	6	Lower aqueous	180	1200	90	70.0
		95% Ethanol	5					
		Water	2					
Indole auxins								
Indole-3-acetamide	10	*n*-Hexane	1	Lower aqueous	600	1250	260	57.4
Indole-3-acetic acid	30	Ethyl acetate	1					
Indole-3-butyric acid	30	Methanol	1					
Indole-3-acetonitrile	30	Water	1					
Flavonoids		Chloroform	4	Lower non-aqueous	360	1250	130	51.3
(see buckthorn ethanol extract)	100	Methanol	3					
		Water	2					
Bacitracin	50	Chloroform	5	Lower non-aqueous	360	1250	170	49.1
		95% Ethanol	4					
		Water	3					
Tetracycline derivatives								
Oxytetracycline	10	Ethyl acetate	2	Lower aqueous	300	1250	80	59.2
Chlortetracycline	20	*n*-Butanol	3					
Doxycycline	20	Water	5					
Oxytetracycline	10	Ethyl acetate	1	Lower aqueous	360	1250	90	64.0
Chlortetracycline	20	*n*-Butanol	1					
Doxycycline	20	0.25 *M* Ammonium acetate	2					

the column was first entirely filled with the stationary (upper) phase. This was followed by injection of sample solution through the sample port. Then, the mobile (lower) phase was introduced into the column in a head-to-tail elution mode, while the apparatus was run at the desired speed of 1200 to 1250 rpm. The effluent from the outlet of the separation column was continuously monitored with an LKB Uvicord S at the suitable wavelength and fractionated with an LKB fraction collector. After the separation was completed, the centrifugation was stopped and the column contents were collected into a graduated cylinder to measure the volume of the stationary phase retained in the column. This was done by connecting the inlet of the separation column to a pressured nitrogen line (*ca.* 100 p.s.i.) while the column was rotated at 200–300 rpm in the tail to head elution mode to accelerate the collection process. Then, the column was washed by pumping about 100 ml of ethanol at 10 ml/min while it was rotated at 100–200 rpm in the tail-to-head elution mode. Finally, the column was emptied and dried by passing nitrogen pressured at *ca.* 100 p.s.i.

Analysis of fractions

The fractions collected in each separation were subjected to spectrophotometric analysis to obtain an elution curve. An aliquot of each fraction was mixed with a known volume of methanol or water (used when the effluent is an aqueous phase containing salt) and the absorbance was determined at the suitable wavelengths (210 nm for triterpenoic acids, 250 nm for bacitracin, 260 nm for flavonoids, 280 nm for indole auxins and 350 nm for tetracycline derivatives) with a Zeiss PM6 spectrophotometer.

For indentification, peak fractions of triterpenoic acids and bacitracin components (A and F) were further separated by high-performance liquid chromatography (HPLC) and retention times compared to those of known samples. These HPLC analyses were performed by using a set of Shimadzu HPLC system (Shimadzu, Kyoto, Japan) consisting of a variable-wavelength UV detector (Model SPD-6A), a constant-flow pump (Model LC-6A) with a manual injector kit and a recording data processor (Model C-R5A). A Capcell Pak C_{18} column (15 × 0.46 cm I.D., type AG) (Shiseido, Tokyo, Japan) was employed. The HPLC analysis of triterpenoic acids was performed by isocratic elution of the mobile phase composed of methanol–distilled water (95:5, v/v) at a flow-rate of 1.5 ml/min and the effluent was monitored at 210 nm. Bacitracin fractions were similarly analyzed with a mobile phase composed of methanol and 0.04 *M* Na_2HPO_4 (pH 9.4) at a flow-rate of 1 ml/min and the effluent was monitored at 234 nm.

The peaks for isorhamnetin and quercetin in the flavonoid separation were identified previously by comparing the retention times to those obtained from the pure compounds[3].

RESULTS AND DISCUSSION

Preparative capability of the present HSCCC system was demonstrated in separations of five sets of samples with suitable two-phase solvent systems having a wide range of polarity. Separations were performed under optimized experimental conditions, as summarized in Table I, where experiments were arranged in the increasing order of polarity of the solvent system used for separation.

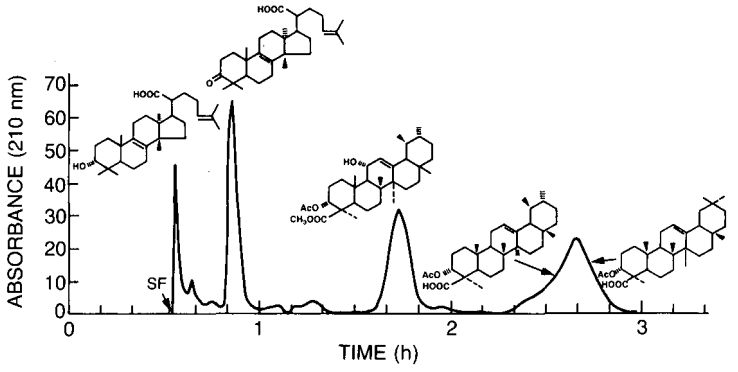

Fig. 2. Chromatogram of triterpenoic acid obtained from the present HSCCC system. See Table I for experimental conditions. Ac = Acetyl; SF = solvent front.

Fig. 2 shows a chromatogram of triterpenoic acids obtained with a two-phase solvent system composed of *n*-hexane–95% ethanol–water (6:5:2, v/v/v) at a flow-rate of 3 ml/min, using a lower aqueous phase as the mobile phase. A total of 500 mg of the crude sample was efficiently separated in multiple peaks within 3 h of elution. Four triterpenoic acids corresponding to peaks 1 to 4 were further separated and retention lines compared to known triterpenoic acids by HPLC analysis.

Fig. 3 shows a chromatogram of indole auxins obtained with a two-phase solvent system composed of *n*-hexane–ethyl acetate–methanol–water (1:1:1:1, v/v) using the lower aqueous phase as the mobile phase. Four components with a total weight of 100 mg of the synthetic mixture were well resolved in symmetrical peaks and eluted out within 1 h. The partition efficiency of each peak was estimated according to the following conventional gas chromatographic formula:

$$N = (4R/W)^2 \tag{1}$$

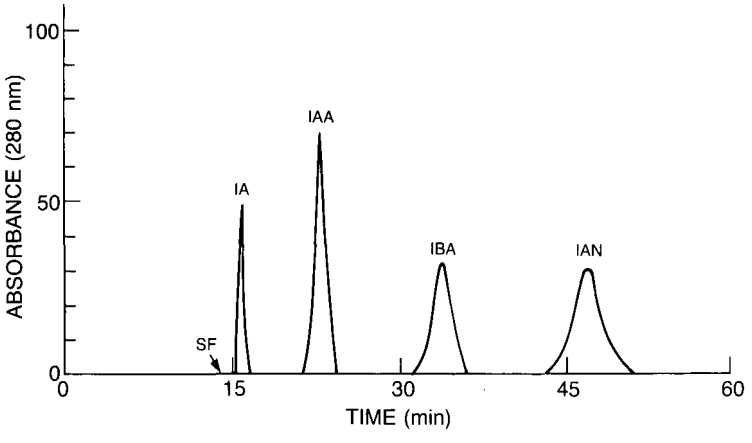

Fig. 3. Chromatogram of indole auxins obtained from the present HSCCC system. Peaks: IA = indole-3-acetamide; IAA = indole-3-acetic acid; IBA = indole-3-butyric acid; IAN = indole-3-acetonitrile. See Table I for experimental conditions.

where N denotes the partition efficiency expressed in terms of theoretical plates (TP); R, the retention time or volume referred to the peak maximum; and W, the peak width expressed in the same unit as R. The results gave high partition efficiencies ranging from 3500 TP for the first peak to 1200 TP for the fourth peak.

Fig. 4 shows the separation of a commercial bacitracin sample with a two-phase solvent system composed of chloroform–95% ethanol–water (5:4:3, v/v/v) by eluting the lower non-aqueous phase at a high flow-rate of 6 ml/min. A total 100 mg quantity of the bacitracin sample was separated in 2 h. Bacitracin A was found in the major peak which showed a high purity as indicated by HPLC analysis of the peak fraction.

Flavonoids in a crude ethanol extract of sea buckthorn were separated with a two-phase solvent system composed of chloroform–methanol–water (4:3:2, v/v/v) with the lower non-aqueous phase used as the mobile phase. Fig. 5A shows a chromatogram of the flavonoids which revealed one major peak of isorhamnetin and several minor peaks including the quercetin peak. The partition efficiency of the major peak was computed as 2150 TP. Fig. 5B illustrates a similar chromatogram obtained from a commercial high-speed CCC centrifuge of 10 cm revolution radius equipped with a single multilayer coil column of 1.6 mm I.D. and a 280 ml capacity[3]. The separation was performed with the same solvent system under the similar operational conditions except at a lower flow-rate of 3 ml/min and at a lower revolutional speed of 800 rpm. The partition efficiency computed from the isorhamnetin peak was 800 TP. Comparison between these two chromatograms (Fig. 5A and B); revealed that the present system yields more efficient separation in a shorter elution time. A near three-fold increase in partition efficiency in the present model is attributable to various factors such as the increased column length (about 1.5 times that in the existing model), reduced helical diameter, and higher revolutional speed (1200 rpm *vs.* 800 rpm).

Fig. 6A and B show chromatograms of three tetracycline derivatives, oxytetracycline (10 mg), chlortetracycline (20 mg) and doxycycline (20 mg), obtained with

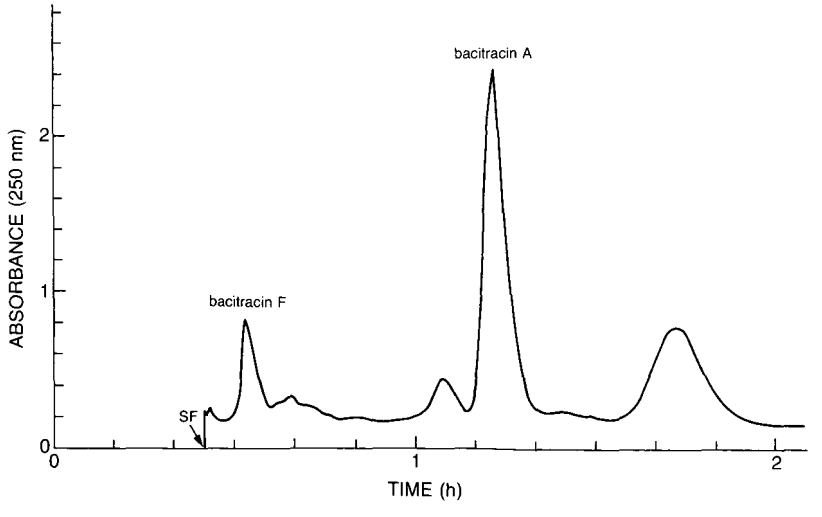

Fig. 4. Chromatogram of bacitracin components obtained with the present HSCCC system. See Table I for experimental conditions.

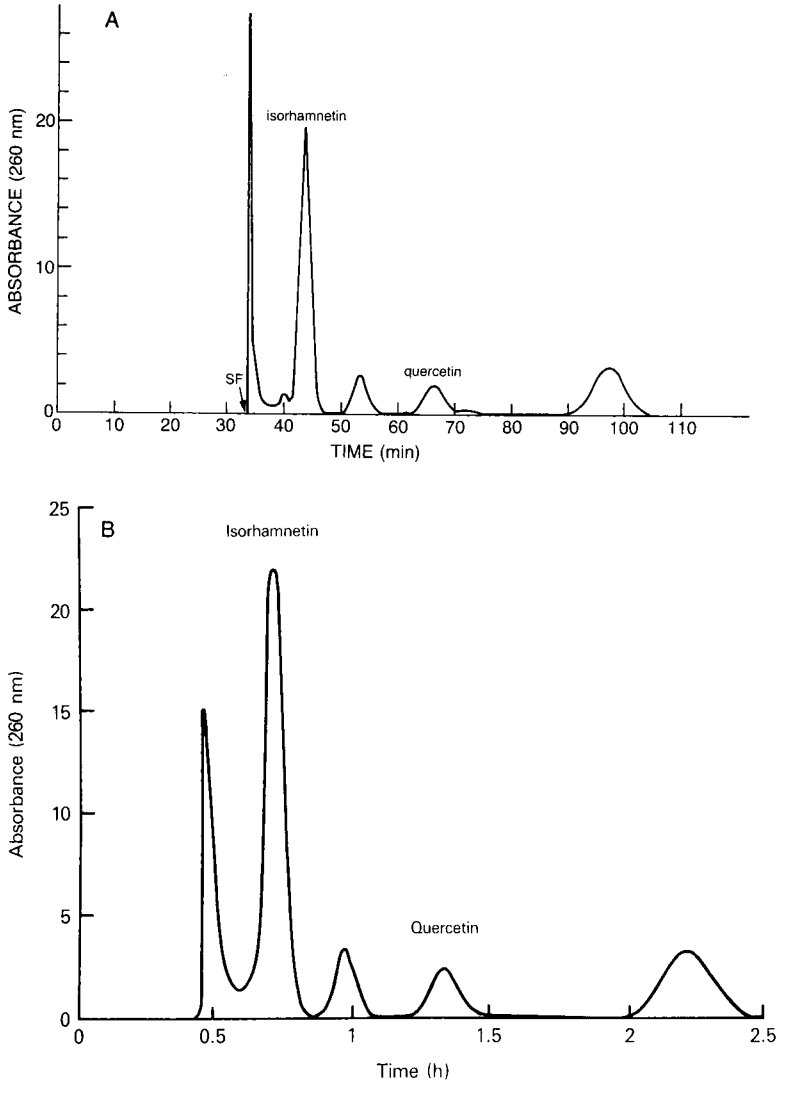

Fig. 5. Separation of flavonoids in a crude ethanol extract of sea buckthorn (*Hippophae rhamnoides*) obtained from two different high-speed CCC instruments. (A) Chromatogram obtained with the present HSCCC system. See Table I for experimental conditions. (B) Chromatogram obtained with a commercial apparatus[3]. Experimental conditions are described in the text.

two different solvent systems, *i.e.*, ethyl acetate–*n*-butanol–water (2:3:5, v/v/v) (chromatogram A) and ethyl acetate–*n*-butanol–0.25 *M* ammonium acetate (1:1:2, v/v/v) (chromatogram B). Both separations were performed under similar operational conditions except for a minor difference in the applied flow-rate which was 5 ml/min for A and 6 ml/min for B. Nevertheless, these two chromatograms revealed a striking difference in peak resolution while the relative retention times of the three peaks remain fairly similar. Chromatogram A shows broad peaks, especially for the second and the

third which were only partially resolved. The partition efficiencies computed for the three peaks revealed an extremely low value in the second peak, *i.e.*, 430 TP for the first peak, 38 TP for the second peak and 144 TP for the third peak. In chromatogram B, the separations were remarkably improved, especially in the second and the third peak which are completely resolved by disclosing a shoulder and a fairly well resolved minor peak between them. Partition efficiencies are much improved for the second and the third peaks, *i.e.*, 340 TP for the first peak, 690 TP for the second peak, and 380 TP for the third peak.

The drastically broad peaks of CTC and DC observed in Fig. 6A cannot be explained on the basis of molecular interactions between two different species[4] because each component, if chromatographed separately, reproduces the broad but fairly symmetrical peak at the original location. The possibility of the molecular

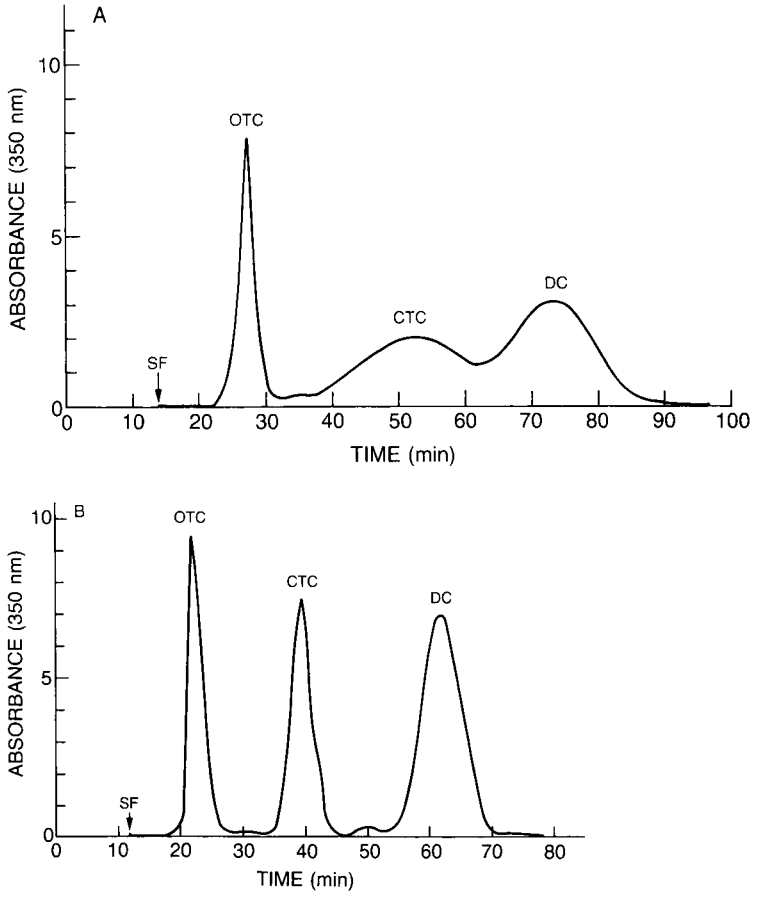

Fig. 6. Separation of tetracycline derivatives obtained by the present HSCCC system with two different solvent systems. (A) Chromatogram obtained with the ethyl acetate–*n*-butanol–water (2:3:5, v/v/v) solvent system. (B) Chromatogram obtained with the ethyl acetate–*n*-butanol–0.25 *M* aqueous ammonium acetate (1:1:2, v/v/v) solvent system. Peaks: OTC = oxytetracycline; CTC = chlortetracycline; DC = doxycycline. See Table I for experimental conditions.

interaction within a single species is also unlikely because molecular aggregation usually causes a skewed peak as often observed in peptide separation.

Although an addition of ammonium acetate to the solvent system remarkably improved the separation, partition efficiencies computed from the obtained chromatogram range from 300 to 700 TP, which are still much lower than those obtained from separations of other samples described earlier. It is conceivable that once the mechanism of the salt effect is fully understood, the partition efficiencies in tetracycline derivative separation may be further improved by selecting an optimum combination of salt and solvent system.

The overall experimental results described above successfully demonstrated excellent capability of the present HSCCC system in semipreparative separations of various biological samples ranging in quantity from 50 to 500 mg. The partition efficiency of the present system may be further increased by the use of smaller I.D. columns. For gram-quantity preparative separations, the column capacity can be increased by mounting larger I.D. columns on wider column holders.

REFERENCES

1 Y. Ito, H. Oka and J. L. Slemp, *J. Chromatogr.*, 475 (1989) 219.
2 Y. Ito, *CRC Crit. Rev. Anal. Chem.*, 17 (1986) 65.
3 T.-Y. Zhang, X. Hua, R. Xiao and S. Kong, *J. Liq. Chromatogr.*, 11 (1988) 233.
4 D. J. Wilson, *Sep. Sci. Technol.*, 22 (1987) 1835.

Journal of Chromatography, 498 (1990) 179–190
Elsevier Science Publishers B.V., Amsterdam — Printed in The Netherlands

CHROM. 21 998

STUDY OF THE LIPOPHILIC CHARACTER OF XANTHINE AND ADENOSINE DERIVATIVES

I. R_M AND LOG *P* VALUES

G. L. BIAGI*, M. C. GUERRA, A. M. BARBARO and S. BARBIERI
Istituto di Farmacologia, Università di Bologna, Via Irnerio 48, 40126 Bologna (Italy)
M. RECANATINI
Dipartimento di Scienze Farmaceutiche, Università di Bologna, Bologna (Italy)
P. A. BOREA
Istituto di Farmacologia, Università di Ferrara, Ferrara (Italy)
and
M. C. PIETROGRANDE
Dipartimento di Chimica, Università di Ferrara, Ferrara (Italy)
(First received August 1st, 1989; revised manuscript received September 18th, 1989)

SUMMARY

The R_M values of a series of xanthine and adenosine derivatives were measured using silicone reversed-phase thin-layer chromatographic (TLC) and C_{18} reversed-phase high-performance TLC systems. The two series of data were well correlated. Both were compared with experimental log *P* and calculated CLOGP values. For xanthine derivatives a good linear relationship was shown between the R_M values from the two chromatographic systems and the log *P* or CLOGP data. For adenosine derivatives the CLOGP values had to be corrected in order to fit the data to the same equation. The TLC data proved to be reliable parameters for describing the lipophilic properties of the test compounds.

INTRODUCTION

Purine (I) and its derivatives xanthine (2,6-dioxopurine), adenine (6-aminopurine) and guanine (2-amino-6-oxopurine) are the parent compounds of several very important classes of biologically active chemicals. Purine and guanine derivatives, such as 6-mercaptopurine and 6-thioguanine, are potential anticancer agents[1]. Allopurinol is an isomer of hypoxanthine (6-oxopurine), which decreases uric acid production by inhibiting xanthine oxidase[1].

The pharmacological actions of the classical natural methylxanthines, such as caffeine, theobromine and theophylline, and a few other synthetic derivatives, such as etofylline and enprofylline, are well known, *e.g.*, stimulation of the central nervous system, tachycardia, bronchodilatation and increased diuresis[1]. Inhibition of phosphodiesterase was postulated as the mechanism by which xanthines elicit these effects.

0021-9673/90/$03.50

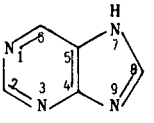

(I)

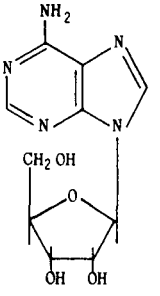

(II)

Recently, the role of xanthines as antagonists of adenosine binding emerged as an alternative explanation for these effects. In fact, in recent years, several important roles for adenosine (II) in the control of many physiological processes have been delineated, *e.g.*, vasodilatation, cardiodepressant effects, relaxation of smooth muscle, stimulation of steroidogenesis in adrenal cells, depression of the central nervous system and inhibition of neurotransmitters release[2]. From a biochemical point of view, adenosine inhibits adenylate cyclase via a high-affinity receptor and activates adenylate cyclase via a low-affinity receptor. These receptors, called A_1 and A_2, respectively, show different profiles for activation by adenosine analogues[3]. The limited use of drugs acting on the adenosine system is mainly due to the lack of seleçtivity, which is typical of these drugs, and to the numerous sites of action of adenosine throughout the body. Studies on quantitative structure–activity relationships have been reported for xanthine derivatives in the above mentioned pharmacological areas. Silipo and co-workers[4–6] studied the inhibition of xanthine oxidase and other enzymes by 9-phenylguanines. The bronchodilator activity of 6-mercaptoxanthines was investigated by Bowden and Wooldridge[7]. Lien *et al.*[8] examined the phosphodiesterase inhibition and cytotoxicity of xanthine analogues. Olaru and Simon[9,10] investigated the inhibition of human erythrocytic ipoxanthine phosphoribosyltransferase. Hamilton *et al.*[11] analysed the influence of several physico-chemical parameters on the adenosine A_1 receptor affinity of a series of 8-phenylxanthines. Neiman and Quinn[12,13] studied the activity against adenocarcinoma CA755 and the acute toxicity in mice of a series of 2,6-mono- and disubstituted purines.

In the above-mentioned papers, the lipophilic character, which was shown to affect variously the different biological activities, was expressed by means of the Hansch π values and only a very few log P values were measured and reported[11]. Gaspari and Bonati[14] were the first to study the correlation between the experimental octanol–water partition coefficients and the high-performance liquid chromatographic (HPLC) retention data of 18 xanthine derivatives. They also found some correlations between the lipophilicity of xanthines and their pharmacokinetic parameters in rats.

Walther and co-workers[15,16] determined the HPLC log k' values of a series of substituted xanthines and compared them with the log P values calculated by means of the Rekker's fragmental method. The differences between the two lipophilicity indexes were attibuted to the conformational behaviour of the compounds. They found that

lipophilicity plays a role in determining the phosphodiesterase inhibition of N-7-unsubstituted compounds.

Despite these more recent contributions, there is still a lack of experimental data describing the lipophilicity of xanthine and adenosine derivatives. In view of a QSAR study dealing with adenosine receptors binding, the main purpose of this work was to study the lipophilic character of a number of adenosine and xanthine derivatives. The lipophilic character was expressed by means of the R_M values obtained from reversed-phase silicone thin-layer chromatography (silicone RP-TLC) and C_{18} high-performance TLC (C_{18} RP-HPTLC). The R_M values were compared with calculated and experimental octanol–water log P values. A further purpose of this work was to show the usefulness of the R_M values in checking the reliability of calculated log P values.

EXPERIMENTAL

Chemicals

Xanthine and adenosine derivatives 8–42 were purchased from RBI (Natick, MA, U.S.A.); compounds 1–7 and 43 were obtained from Sigma (St. Louis, MO, U.S.A.). All other chemicals and solvents were of analytical-reagent or HPLC grade. In the following we shall refer to any purine derivative as xanthines and to any nucleoside as adenosines or guanosines.

Determination of R_M values by silicone RP-TLC

The details of the reversed-phase chromatographic technique were described previously[17]. Glass plates measuring 20 × 20 cm were coated with silica gel GF_{254} in the usual manner. In order to obtain a better control of the pH of the stationary phase, the slurry of silica gel GF_{254} was obtained with 0.09 or 0.36 M sodium hydroxide solution or 0.09 M hydrochloric acid when the pH of the mobile phase had to be 7.0, 9.0 or 1.2, respectively. A non-polar stationary phase was obtained by impregnating the silica gel GF_{254} layer with silicone DC 200 (350 cS) from Applied Science Labs., (State College, PA, U.S.A.). The impregnation was carried out by developing the plates in a 5% silicone solution in diethyl ether. Eight plates could be impregnated in a single chromatographic chamber containing 200 ml of the silicone solution. The plates were left in the chamber for 12 h, *i.e.*, for several hours after the silicone solution had reached the top of the plates.

The mobile phases, saturated with silicone, were aqueous buffers alone or mixed with various amounts of acetone. Glycine buffer at pH 9.0 and sodium acetate–Veronal buffer (1/7 M) at pH 7.0 were used. The R_M values of compounds 4, 8, 22 and 27 were also measured at pH 1.2 (glycine buffer). Two plates were developed simultaneously in a chromatographic chamber containing 200 ml of mobile phase. The test compounds were dissolved in 0.1 M sodium hydroxide solution, water or acetone (1–2 mg/ml), and 1 μl of solution was spotted randomly on the plates in order to avoid any systematic error. The developed plates were dried and the spots detected under UV light (254 nm). The R_M values were calculated by means of equation $R_M = \log[(1/R_F) - 1]$.

Determination of R_M values by C_{18} RP-HPTLC

The HPTLC determinations were carried out on Whatman KC18F plates[18]. A Camag (Berlin, F.R.G.) Nanomat was used to spot the compounds on the plates (about 100 nl of each compound solution). The solutes were detected under UV light (254 nm). Solvent mixtures of methanol–phosphate buffer at pH 7.0 were used. A mobile phase at pH 1.2 was used for compounds 4, 8, 22 and 27. The methanol concentration ranged from 30 to 80%.

Octanol–water partition coefficients

Most of the log P values in Table I were calculated by means of the CLOGP program developed by the Pomona College group[19]. The experimental log P values of compounds 1, 2, 3, 4, 9, 12, 15 and 30 were taken from the STARLIST file of the Pomona College database[20]. The log P of guanosine (compound 43) was measured in our laboratory using the classical shake-flask method[21]. For the adenosine derivatives a log P value was calculated by adding a correction factor to the CLOGP value of each compound. This was obtained by averaging the difference between the experimental and the CLOGP values of adenosine and guanosine:

$$\log P_{\text{adenosine}} - \text{CLOGP}_{\text{adenosine}} = -1.23-(-3.51) = 2.28$$

$$\log P_{\text{guanosine}} - \text{CLOGP}_{\text{guanosine}} = -1.85-(-4.42) = 2.57$$

$$\bar{x} = 2.42$$

RESULTS

R_M values from silicone RP-TLC

In the first step the R_M values of most of the compounds in Table I were measured with a mobile phase represented by the Veronal buffer at pH 7.0, alone or mixed with various amounts of acetone. RP-TLC showed that for each compound there was a linear relationship between R_M values and a certain range of acetone concentrations in the mobile phase. The equations of the straight lines were used to calculate a theoretical R_M value at 0% acetone in the mobile phase. The intercepts of the equations are reported in Table I to represent the theoretical R_M values at 0% acetone. These extrapolated R_M values at 0% could be considered as a measure of the partitioning of the compounds between an aqueous buffer and the hydrophobic stationary phase, *i.e.*, in a standard system where all the compounds could be compared on the basis of their lipophilic character. At acetone concentrations higher than 12% all the compounds tended to migrate with the solvent front. Therefore, the equations were calculated by means of the R_M values obtained at acetone concentrations only up to 12%. The only exceptions were compounds 18, 23 and 29, which were much more lipophilic and did not migrate at 0% acetone. Their extrapolated R_M values were calculated from higher ranges of acetone concentrations in the mobile phase.

However, in the present instance, except for compounds 18, 23 and 29, all the compounds migrated in a reliable way even at 0% acetone. Therefore, in Table I both the experimental and the extrapolated R_M values are reported for 33 compounds. The

TABLE I
LIPOPHILICITY INDICES OF XANTHINES AND ADENOSINES

No.	*Compound*	$R_{M\ exp.}$ *(pH 7.0)*	$R_{M\ extrap}$ *(pH 7.0)*	$R_{M\ exp.}$ *(pH 9.0)*	$R_{M\ C_{18}}$ *(pH 7.0)*	*Log P*
	Xanthines:					
1	Purine	0.25	–	−0.37	0.50	−0.58[b] −0.37[c]
2	Adenine	0.35	–	−0.01	0.83	−0.33[b] −0.09[c]
3	Guanine	−0.08	–	−0.44	–	−1.28[b] −0.91[c]
4	Xanthine	−0.72 0.02[a]	–	−0.81	−0.13 0.57[a]	−1.65[b] −0.73[c]
5	1-Methylxanthine	−0.30	–	−0.83	0.42	−1.25[b]
6	3-Methylxanthine	−0.08	–	−0.63	0.40	−1.00[b]
7	7-Methylxanthine	−0.12	–	−0.83	0.26	−1.32[b]
8	1,3-Dimethyluric acid	−0.73 −0.08[a]	−0.71	–	0.60[a]	–
9	Theophylline (1,3-dimethylxanthine)	0.38	0.33	−0.20	1.19	−0.05[b] −0.02[c]
10	1,7-Dimethylxanthine (paraxanthine)	0.39	0.35	−0.24	1.06	−0.92[b]
11	1,9-Dimethylxanthine	−0.21	−0.21	−0.41	0.28	−0.92[b]
12	Theobromine (3,7-dimethylxanthine)	0.26	0.22	0.04	0.92	−0.67[b] −0.78[c]
13	3,9-Dimethylxanthine	0.04	−0.01	0.02	0.50	−0.67[b]
14	7,9-Dimethylxanthine	−0.73	−0.76	–	−0.46	–
15	Caffeine (1,3,7-trimethylxanthine)	0.79	0.77	0.61	1.54	0.26[b] −0.07[c]
16	Thiocaffeine	1.14	1.15	0.97	2.14	–
17	3-Isobutyl-1-methylxanthine	1.03	1.05	0.31	2.36	1.41[b]
18	1,3-Diethyl-8-phenylxanthine	–	1.45	0.78	2.95	3.10[b]
19	3-Propylxanthine (enprofylline)	0.35	0.29	−0.10	1.29	0.05[b]
20	7-Propylxanthine	0.25	0.23	−0.13	1.07	−0.26[b]
21	9-Propylxanthine	0.04	0.09	−0.35	0.65	−0.26[b]
22	1,3-Dipropyl-8-(*p*-sulphophenyl)xanthine	1.12 –	1.11 1.57[a]	0.10	2.51 3.18[a]	2.31[b]
23	1,3-Dipropyl-8-(2-amino-4-chlorophenyl)xanthine	–	2.24	0.92	3.57	4.05[b]
24	7-(β-Hydroxyethyl)theophylline (etofylline)	0.39	0.35	0.11	0.86	−1.20[b]
25	7-(β-Chloroethyl)-theophylline	1.03	1.00	0.74	1.70	0.50[b]
26	8-Phenyltheophylline	1.11	1.11	0.60	2.08	2.05[b]
27	8-(*p*-Sulphophenyl)-theophylline	0.15 0.52[a]	0.00	−0.52	1.26 1.50[a]	0.19[b]
28	8-Cyclopentyltheophylline	1.03	1.06	0.77	2.55	2.16[b]
29	8-Cyclopentyl-1,3-dipropylxanthine	–	1.94	1.05	3.61	4.28[b]
	Adenosines					
30	Adenosine	0.24	0.26	0.36	0.42	−3.51[b] −1.23[c]
31	2-Chloroadenosine	0.19	0.15	0.41	0.66	−2.76[b] −0.34[d]

(Continued on p. 184)

TABLE I *(continued)*

No.	*Compound*	$R_{M\ exp.}$ *(pH 7.0)*	$R_{M\ extrap}$ *(pH 7.0)*	$R_{M\ exp.}$ *(pH 9.0)*	$R_{M\ C_{18}}$ *(pH 7.0)*	*Log P*
32	2-Phenylaminoadenosine	0.96	0.97	1.22	1.83	−0.55[b] 1.87[d]
33	6-Methyladenosine	0.41	0.28	0.51	0.80	−2.78[b] −0.36[d]
34	6-Cyclopentyladenosine	1.12	1.18	1.08	2.29	−1.31[b] 1.11[d]
35	6-Cyclohexyladenosine	1.14	1.16	1.02	2.44	−0.75[b] 1.67[d]
36	6-Phenyladenosine	0.96	0.96	1.16	1.86	−0.80[b] 1.62[d]
37	6-Phenylethyladenosine	1.30	1.30	1.20	2.94	−0.68[b] 1.74[d]
38	6-(2-Phenylisopropyl)-adenosine	1.34	1.31	1.38	2.87	−0.37[b] 2.05[d]
39	6-Benzyladenosine	0.93	0.92	0.89	1.98	−1.08[b] 1.34[d]
40	5′-N-Methylcarboxamido-adenosine	0.41	0.34	0.41	0.72	−3.62[b] −1.20[d]
41	5′-N-Ethylcarboxamido-adenosine	0.67	0.61	0.82	1.13	−3.09[b] −0.67[d]
42	5′-N-Cyclopropylcarbox-amidoadenosine	0.89	0.90	0.55	2.02	−3.26[b] −0.84[d]
43	Guanosine	−0.38	–	−0.83	−0.16	−4.42[b] −1.85[c]
44	1-Methylisoguanosine	−0.33	−0.39	−0.20	0.08	–

[a] Measured at pH 1.2.
[b] CLOGP.
[c] Experimental log *P* in octanol–water.
[d] Calculated log *P* values (see text).

very good correlation between the experimental and extrapolated R_M values is described by the equation

$$R_{M\ exptl} = 0.036\ (\pm\ 0.010) + 0.972\ (\pm\ 0.013)\ R_{M\ extrap}$$
$$(n = 33;\ r = 0.997;\ s = 0.043;\ F = 5523;\ P < 0.005) \qquad (1)$$

The intercept and slope, very close to 0 and 1 respectively, show the validity of the extrapolation technique. Because of eqn. 1, in the second step of our work the R_M values of compounds 1–7 and 43 were measured with a mobile phase represented only by the buffer and therefore their extrapolated R_M values were not available for Table I. Further, a mobile phase at pH 1.2 (glycine buffer) was also used for compounds 4, 8, 22 and 27 in order to measure the R_M value of their non-ionized form.

The above mobile phase of pH 7.0 was chosen on the basis of the ionization profiles of the test compounds. Owing to their structure, the xanthine derivatives are amphoteric compounds that exhibit acidic and basic ionization constants; substituents

on different positions of the heterocyclic ring may variously affect the pK_a values[22]. However, basic pK_a values <4 and acidic pK_a values >9 are reported for the most representative compounds of this class[23]. Xanthine ($pK_a = 7.4$), 1,3-dimethyluric acid (uric acid: $pK_a = 5.4$), 1,3-dipropyl-8-(*p*-sulphophenyl)xanthine ($pK_a < 2$) and 8-(*p*-sulphophenyl)theophylline (1,3-diethyl analogue: $pK_a < 2$) are exceptions, showing "stronger" acidic properties[11,22,23]. The purine nucleosides appear to be even weaker acids than the 9-unsubstituted purines, whereas their basic properties are similar to those of the above-mentioned group (adenosine has basic $pK_a = 3.58$, acidic $pK_a = 12.5$). At pH 7.0 most of the compounds we examined should therefore be non-ionized or ionized to only a very small extent.

In order to illustrate this point, the R_M values of all the compounds in Table I (except compound 8) were also measured at pH 9.0 by means of a glycine buffer without the addition of acetone. The data reported in Table I show that at pH 9.0 compounds 18, 23 and 29 also migrated in a reliable way without the addition of acetone to the mobile phase. In contrast, it was not possible to measure reliable R_M values for compounds 8 and 14 as these migrated with the solvent front. In any event at pH 9.0 all the xanthine derivatives are characterized by longer migrations, *i.e.*, lower R_M values, which means that ionization occurred at some extent, according to their acidic pK_a values. The relationship between the R_M values of xanthine derivatives at pH 7.0 and those at pH 9.0 is described by

$$R_{M\ pH\ 7.0} = 0.481\ (\pm\ 0.057) + 1.079\ (\pm\ 0.100)\ R_{M\ pH\ 9.0}$$
$$(n = 27;\ r = 0.907;\ s = 0.298;\ F = 116.7;\ P<0.005) \qquad (2)$$

If all the derivatives had the same pK_a value, one should have obtained an equation characterized by an intercept higher than 0 and a slope equal to 1, *i.e.*, very close to eqn. 2. However, the standard deviation is rather high, suggesting that not all the compounds are equally affected by the increased pH of the chromatographic system.

In contrast, for the series of adenosine derivatives an increase in pH did not seem to have any significant influence on their chromatographic migration. This behaviour might be explained by considering the higher acidic pK_a value of adenosine (and presumably of the adeonsine derivatives), which prevents the ionization of the compounds even under strongly basic conditions. The only exception is guanosine, which shows a lower R_M value at pH 9.0. In fact, guanosine has a lower acidic pK_a of 9.2[8], which should induce ionization at pH 9.0. The relationship between the R_M values at pH 7.0 and 9.0 is described by the equation

$$R_{M\ pH\ 7.0} = -0.062\ (\pm\ 0.092) + 1.027\ (\pm\ 0.105)\ R_{M\ pH\ 9.0}$$
$$(n = 14;\ r = 0.943;\ s = 0.168;\ F = 96.15;\ P<0.005) \qquad (3)$$

which was calculated with the exclusion of guanosine. The intercept and slope are very close to 0 and 1, respectively. As a consequence of its pK_a value, guanosine could be incorporated into eqn. 2 as shown by the following equation, calculated with 28 compounds:

$$R_{M\ pH\ 7.0} = 0.482\ (\pm\ 0.055) + 1.076\ (\pm\ 0.094)\ R_{M\ pH\ 9.0}$$
$$(n = 28;\ r = 0.913;\ s = 0.292;\ F = 130.5;\ P<0.005) \qquad (2a)$$

In conclusion, eqns. 2 and 3 show that at pH 7.0 both xanthine and adenosine derivatives are mainly in their non-ionized form, except compounds 4, 8, 22 and 27. Therefore, in any subsequent correlation the R_M values at pH 7.0 or 1.2 (compounds 4, 8, 22 and 27) were used.

R_M values from C_{18} RP-HPTLC

The chromatographic work carried out at pH 7.0 with Whatman KC18F plates showed the usual linear relationship between R_M values and methanol concentrations for each compound. The compounds did not migrate without the addition of methanol to the mobile phase. The equations of the straight lines yielded the extrapolated R_M values at 0% methanol (Table I). The relationship between the silicone RP-TLC (R_M) and C_{18} RP-HPTLC ($R_{M\,C_{18}}$) data for the xanthine and adenosine derivatives at pH 7.0 or 1.2 is shown in Fig. 1 and described by

$$R_M = -0.272\ (\pm\ 0.040) + 0.610\ (\pm\ 0.023)\ R_{M\,C_{18}}$$
$$(n = 43;\ r = 0.972;\ s = 0.154;\ F = 706.8;\ P<0.005) \qquad (4)$$

The very good correlation coefficient explains 94% of the variance in the silicone RP-TLC R_M values.

Although in silicone RP-TLC acetone was added to the mobile phase and in C_{18} RP-HPTLC methanol was used, the R_M values are very well correlated. In previous papers it was shown that the extrapolated R_M values were very similar whether one used acetone or methanol in the mobile phase[24,25]. Therefore, the present data seem to confirm that the nature of the organic solvent added to the mobile phase does not

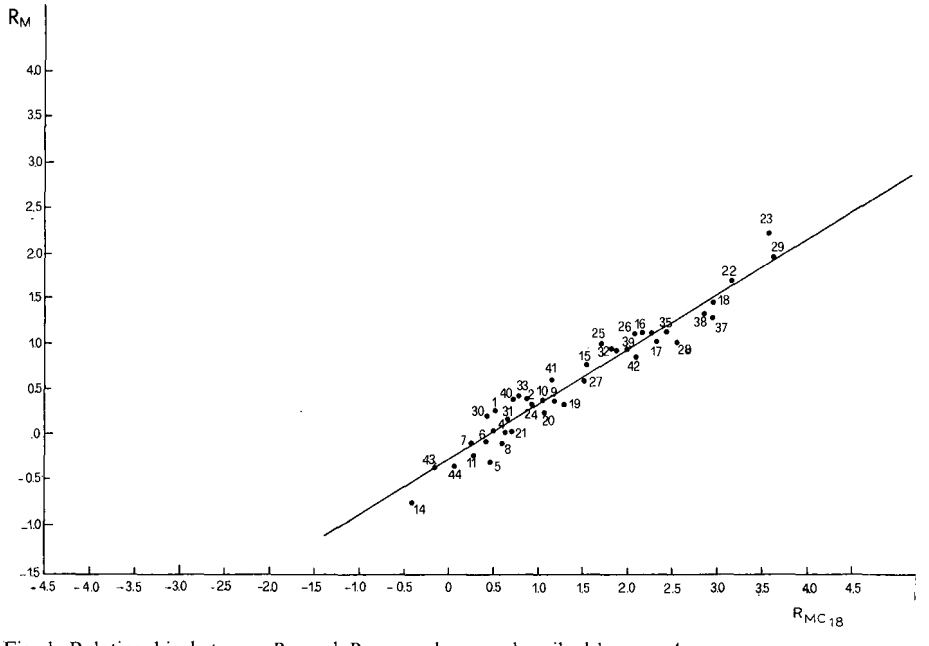

Fig. 1. Relationship between R_M and $R_{M\,C_{18}}$ values, as described by eqn. 4.

affect the results in a qualitative way. An intercept lower than zero is due to the difference in the stationary phase. The C_{18} RP-HPTLC system seems to be more lipophilic. In fact, both xanthine and adenosine derivatives have higher $R_{M\,C_{18}}$ values. A slope lower than 1 is due to the narrower range of the silicone RP-TLC R_M values. It can be also pointed out that the extrapolated C_{18} RP-HPTLC R_M values are very well correlated with the silicone RP-TLC experimental R_M values. This again indicates the reliability of the extrapolation technique.

Log P values

The experimental log *P* values of caffeine, theophylline, theobromine, guanine, xanthine, purine and adenine, and also the CLOGP values of these and other xanthines derivatives, are reported in Table I. The relationship between the R_M values at pH 7.0 or 1.2 and the log *P* values is described by eqn. 5, which was calculated with the CLOGP values, or the experimental log *P* values when available (compounds 1, 2, 3, 4, 9, 12 and 15). Eqn. 5 and all the subsequent equations in this section are given in Table II.

Owing to the acceptable agreement between the CLOGP and experimental log *P* values for the above seven compounds, eqn. 5 does not change when calculated with the CLOGP values for all the 26 xanthine derivatives.

In the series of the adenosine derivatives there is a striking difference between the experimental log *P* and the CLOGP values of adenosine and guanosine. In fact, an equation calculated with the CLOGP values or the experimental log *P* values, when available (compounds 30 and 43), yielded a very low correlation coefficient (r = 0.523). Therefore, eqn. 6 was calculated by means of the CLOGP values of all the adenosine derivatives, showing a much better correlation coefficient.

The regression coefficient of eqn. 6 is not much different from that of eqn. 5, and eqns. 5 and 6 describe two almost parallel straight lines. However, the two correlations cannot be combined in one equation, because of the much higher intercept of eqn. 6. This is due to the very low CLOGP values for the adenosine derivatives as calculated by the CLOGP program. As described under Experimental, a log *P* value was calculated for each of the twelve adenosines for which an experimental log *P* value was

TABLE II

CORRELATION EQUATIONS BETWEEN R_M AND LOG *P* VALUES

Equation	*a*	*b*	*n*	*r*	*s*	*F* (*P*<0.005)	*Eqn. No.*
$R_M = a + b \log P$	0.423 (±0.044)	0.390 (±0.027)	26	0.947	0.221	209.8	5
	1.360 (±0.125)	0.306 (±0.050)	14	0.868	0.255	36.58	6
	0.620 (±0.072)	0.305 (±0.052)	14	0.861	0.261	34.46	7
	0.490 (±0.041)	0.367 (±0.026)	40	0.916	0.250	199.4	8
	0.468 (±0.037)	0.376 (±0.023)	39	0.935	0.224	257.6	13
$R_{M\,C_{18}} = a + b \log P$	1.184 (±0.061)	0.609 (±0.036)	25	0.962	0.294	283.0	9
	2.784 (±0.247)	0.592 (±0.100)	14	0.863	0.503	35.13	10
	1.348 (±0.140)	0.595 (±0.101)	14	0.862	0.507	34.75	11
	1.243 (±0.062)	0.604 (±0.040)	39	0.929	0.379	232.4	12
	1.202 (±0.053)	0.622 (±0.033)	38	0.952	0.315	348.9	14

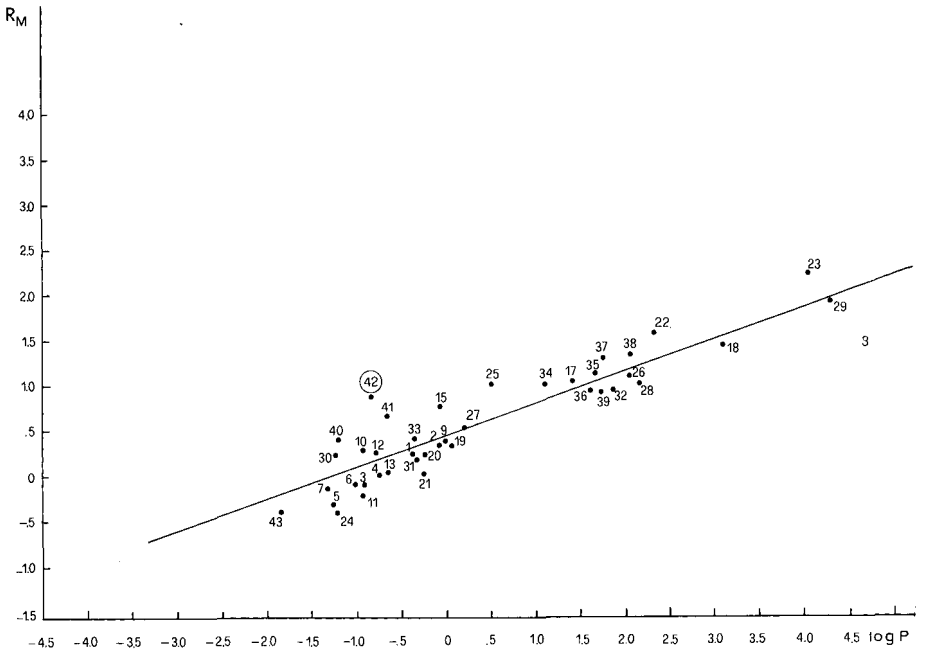

Fig. 2. Relationship between R_M and log P values, as described by eqn. 13 (compound 42 was not used in calculating the equation).

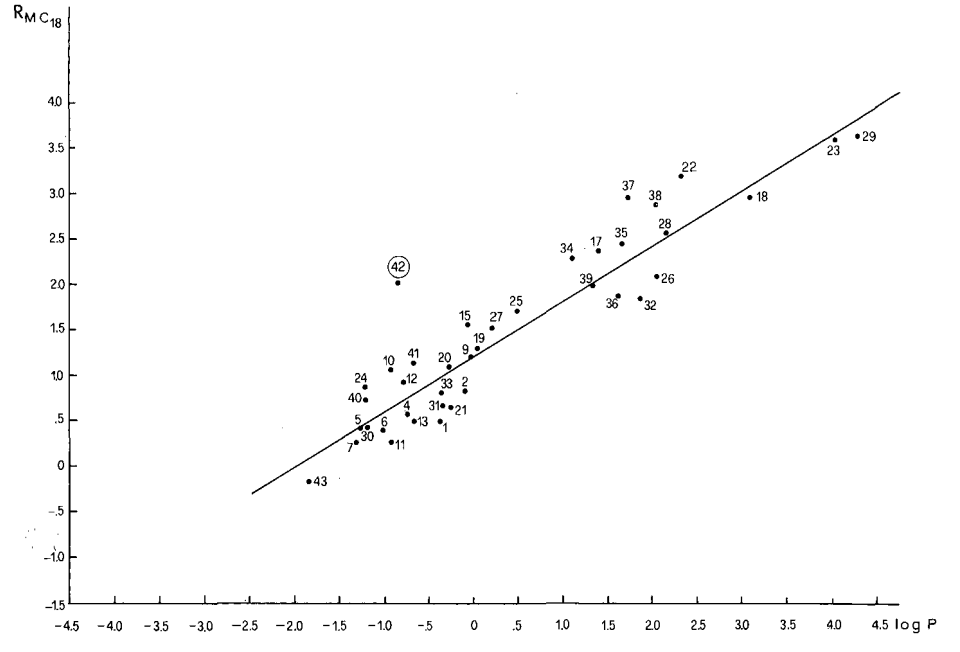

Fig. 3. Relationship between $R_{M\,C_{18}}$ and log P values, as described by eqn. 14 (compound 42 was not used in calculating the equation).

not available. The relationship described by eqn. 7 between the R_M values and the calculated (compounds 31–42) or experimental (compounds 30 and 43) log P values for the adenosine derivatives is closer to that described by eqn. 5 for the xanthine derivatives. Finally, eqns. 5 and 7 were incorporated into eqn. 8.

Following the same procedure that led to eqns. 5–8, the corresponding eqns. 9–12 were calculated using the same log P values and the $R_{M\ C_{18}}$ instead of the R_M values.

Eqns. 8 and 12 are shown graphically in Figs. 2 and 3. From the plots it can be seen that in both equations compound 42 is an outlier. When it is excluded, eqns. 13 and 14 are obtained. The reason why compound 42 has to be excluded from eqns. 13 and 14 might be that the carboxamido group in the sugar moiety can interact via hydrogen bonding with free OH groups of the stationary phases. This hypothesis is supported by the fact that in the silicone RP-TLC system the same behaviour, although at a lesser extent, is shown also by the analogous compounds 40 and 41.

DISCUSSION AND CONCLUSIONS

The results show a very good correlation between the R_M values from two different chromatographic systems. It is interesting that the correlation described by eqn. 4 holds over a wide range of lipophilicity. This justifies our confidence in the use of chromatographic data as lipophilic parameters.

At the same time, the very good correlations described by enqs. 5 and 9 show that the calculated CLOGP value of the xanthine derivatives is a reliable lipophilic index for these compounds. In fact, eqns. 5 and 9 were calculated using the experimental log P values for seven compounds and the CLOGP values for the remaining derivatives.

In the adenosine series the CLOGP values could not be used with the experimental log P values in the same equation. A correction had to be made in order to allow the calculation of eqns. 8 and 12 and also eqns. 13 and 14. In fact, the CLOGP program does not correctly estimate the partition coefficient of nucleosides. The program might not be able to take into account interactions between the purine ring and the sugar moiety. On the other hand, a disadvantageous aspect of the silicone RP-TLC and C_{18} RP-HPTLC systems is the interaction with the stationary phases causing the deviation of compound 42 from eqns. 8 and 12. As a final remark, it is pointed out that Gaspari and Bonati[14] and Walther and co-workers[15,16] did not obtain very good correlations when they considered their whole series of derivatives. In contrast, the present R_M and $R_{M\ C_{18}}$ values allowed two structurally different series of compounds, such as xanthines and adenosines, to be combined in one equation. Work is in progress in our laboratory to measure the HPLC log k' values of the present series of compounds for further investigation of the relationships among different lipophilic descriptors.

ACKNOWLEDGEMENTS

P.A.B. and M.C.P. were financially supported by the Italian CNR (Roma), Progetto Finalizzato Chimica Fine II.

REFERENCES

1 A. Goodman Gilman, L. S. Goodman, T. W. Rall and F. Murad (Editors), *Goodman and Gilman's The Pharmacological Basis of Therapeutics*, MacMillan, New York, 1985.
2 J. W. Daly, in J. W. Daly, Y. Vuroda, J. W. Phillis, M. Shimizu and M. Ui (Editors), *Physiology and Pharmacology of Adenosine Derivatives,* Raven Press, New York, 1983, pp. 59–69.
3 J. W. Daly, R. F. Bruns and S. H. Snyder, *Life Sci.*, 28 (1981) 2093.
4 C. Silipo and C. Hansch, *Farmaco, Ed. Sci.*, 30 (1974) 35.
5 C. Grieco, C. Silipo and A. Vittoria, *Farmaco, Ed. Sci.*, 33 (1977) 382.
6 C. Silipo and C. Hansch, *J. Med. Chem.*, 19 (1976) 62.
7 K. Bowden and K. R. H. Wooldridge, *Biochem. Pharmacol.*, 22 (1973) 1015.
8 E. J. Lien, K. Mayer, P. H. Wang and G. L. Tong, *Acta Pharm. Jugosl.*, 29 (1979) 181.
9 N. Olaru and Z. Simon, *Rev. Roum. Biochim.*, 18 (1981) 51.
10 N. Olaru and Z. Simon, *Rev. Roum. Biochim.*, 18 (1981) 131.
11 A. W. Hamilton, D. F. Ortwine, D. F. Worth, E. W. Badger, J. A. Bristol, R. F. Bruns, S. J. Haleen and R. P. Steffen, *J. Med. Chem.*, 28 (1985) 1071.
12 Z. Neiman and F. R. Quinn, *J. Pharm. Sci.*, 70 (1981) 425.
13 Z. Neiman and F. R. Quinn, *J. Pharm. Sci.*, 71 (1982) 618.
14 F. Gaspari and M. Bonati, *J. Pharm. Pharmacol.*, 39 (1987) 252.
15 B. Walther, P. A. Carrupt, H. Van de Waterbeemd, N. El Tayar and B. Testa, in J. L. Fauchere (Editor), *QSAR: Quantitative Structure–Activity Relationship in Drug Design*, Alan R. Liss, New York, 1989, pp. 67–70.
16 B. Walther, P. A. Carrupt, N. El Tayar and B. Testa, *Helv. Chim. Acta,* 72 (1989) 507.
17 G. L. Biagi, A. M. Barbaro, M. F. Gamba and M. C. Guerra, *J. Chromatogr.*, 41 (1969) 371.
18 M. C. Pietrogrande P. A. Borea and G. L. Biagi, *J. Chromatogr.*, 447 (1988) 404.
19 Pomona College Medicinal Chemistry Project, *CLOGP Program, Version 3.42*, Pomona College, Claremont, CA, 1986.
20 *Pomona College Medicinal Chemistry Project Data Base,* Pomona College, Claremont, CA.
21 A. Leo, C. Hansch and D. Elkins, *Chem. Rev.*, 71 (1971) 525.
22 A. R. Katritzky (Editor), *Comprehensive Heterocyclic Chemistry*, Vol. 5, Pergamon Press, Oxford, 1984, p. 523.
23 D. D. Perrin, *Dissociation Constants of Organic Bases in Aqueous Solution*, Butterworths, London, 1965.
24 A. M. Barbaro, M. C. Pietrogrande M. C. Guerra, G. Cantelli Forti, P. A. Borea and G. L. Biagi, *J. Chromatogr.*, 287 (1984) 259.
25 A. M. Barbaro, M. C. Guerra, G. L. Biagi, M. C. Pietrogrande and P. A. Borea, *J. Chromatogr.*, 347 (1985) 209.

Journal of Chromatography, 498 (1990) 191–204
Elsevier Science Publishers B.V., Amsterdam — Printed in The Netherlands

CHROM. 21 992

ON-LINE COUPLING OF CAPILLARY ISOTACHOPHORESIS WITH CAPILLARY ZONE ELECTROPHORESIS

D. KANIANSKY*
Institute of Chemistry, Faculty of Science, Komenský University, Mlynská Dolina CH-2, 842 15 Bratislava (Czechoslovakia)
and
J. MARÁK
Institute of Radioecology and Applied Nuclear Techniques, Chrapčiakova 1, 052 01 Spišská Nová Ves (Czechoslovakia)
(Received August 22nd, 1989)

SUMMARY

The on-line combination of capillary isotachophoresis (CITP) with capillary zone electrophoresis (CZE) in the column-coupling configuration of the separation unit was studied. The inherent concentrating power of the ITP stage was effective in achieving a high volume reduction of the injected sample so that the ZE separations with 2–3 μm plate heights could be achieved in 300 μm I.D. capillary tubes for nitrophenols and 2,4-dinitrophenyl-labelled amino acids taken as model analytes. Very reproducible migration times (0.3–1.2% relative standard deviations for 138–350-s migration times) and a high precision of sample injection (0.9–5.1% relative standard deviations for 8-pmol amounts of the analytes) could be typically achieved. Removal of the separated macroconstituents from the separation compartment after the ITP stage prevented column overloading in the ZE stage so that low detection limits could easily be achieved for the analytes (*ca.* 10^{-7} mol/l for a 5-μl injection volume by using a photometric detector) even in a 10^5-fold excess of a sample macroconstituent.

INTRODUCTION

Zone electrophoretic separation is associated with an inherent concentration adaptation of the separated constituents[1–4]. It has been shown that this adaptation process can be advantageously utilized in capillary zone electrophoresis (CZE) to reduce the initial volume of the injected sample[2–4] and, thus, positively influence the efficiency of separation.

The use of a discontinuous buffer system is another alternative for concentrating the sample constituents before their CZE separation[5]. This alternative, analogous to that proposed by Ornstein[6] and Davis[7] for ZE separations in polyacrylamide gels, is in fact a sequential use of isotachophoretic (ITP) concentration with ZE separation.

0021-9673/90/$03.50

It is apparent that such an approach can be beneficial in CZE in general. From a practical point of view, however, tandem coupling of the capillary columns as used in capillary isotachophoresis (CITP) with a concentration cascade of the leading electrolytes[8] and/or its functional equivalent consisting of a capillary column, a sample valve [applicable for the stacking (ITP) phase] and a microsyringe injection block (ref. 9, p. 210) are probably more convenient instrumental solutions than a single capillary column successively filled with a desired sequence of the electrolyte solutions[5].

The column-coupling configuration of the separation unit for ITP (CC-ITP) as first described by Everaerts *et al.*[10] was also shown to be suitable for work with discontinuous buffer systems (see ref. 3, p. 142). In addition, it enables interfering sample constituents to be removed from the separation compartment after the separation in the first (preseparation) column so that mainly the constituents of primary analytical interest are subjected to a final separation in the second column. As such a configuration seems desirable in an on-line combination of CITP with CZE, we preferred the use of the column-coupling configuration of the separation unit in this feasibility study. Our interest in this combination of basic electrophoretic techniques was stimulated by the following facts:

(i) ITP is a separation technique with a well defined concentrating power while the separands migrate stacked in sharp zones, *i.e.*, it can be considered as an ideal sample injection technique for ZE.

(ii) In some instances the detection and quantitation of trace constituents separated by ITP in a large excess of matrix constituents may require the use of appropriate spacing constituents. Such a solution can be very beneficial when a limited number of the analytes need to be determined in one analysis (see, e.g., ref. 11). It becomes less practical (a search for suitable spacing constituents) when the number of trace constituents to be determined in one analysis is high.

(iii) In CZE, high-efficiency separations make possible a multi-component analysis of trace constituents with close physico-chemical properties. However, the separations can be ruined, *e.g.*, when the sample contains matrix constituents at higher concentrations than those of the trace analytes.

(iv) An on-line combination of CITP with CZE appears to be promising for alleviating some of the above practical problems.

This paper presents the results of introductory work obtained with instrumentation intended mainly for CITP. Nitrophenols and 2,4-dinitrophenyl derivatives of amino acids served as model analytes.

EXPERIMENTAL

Instrumentation

A CS Isotachophoretic Analyzer (VVZ PJT, Spišská Nová Ves, Czechoslovakia) that enabled work in the column-coupling mode to be performed was used. The separation unit was assembled from components from the manufacturer and also from those developed in this laboratory.

Laboratory-made columns provided with 0.30 mm I.D. capillary tubes (O.D. $\approx$ 0.65 mm) made of fluorinated ethylene–propylene (FEP) copolymer were employed in both separation stages. The capillary tubes were placed in compartments that allowed efficient dissipation of heat produced on passage of current.

The first column was 10 cm long and was provided with a conductivity sensor[12] to monitor the ITP phase and to provide information necessary for proper switching of the columns by the analyser controller. The second column (ZE stage) was 28 cm long and was provided with a laboratory-made on-column UV–VIS photometric detector with a design similar to that described elsewhere[13]. Detection was performed at 405 nm and a rectangular slit of the detector (0.25 mm in height) was placed 20 cm downstream of the bifurcation point (see Fig. 1).

The samples were injected with the aid of a sampling valve[14] either by a 15-μl internal loop or with the aid of a 10-μl 701 N microsyringe (Hamilton, Bonaduz, Switzerland). When required, both injection alternatives were combined.

An HP 3390 A reporting integrator (Hewlett-Packard, Avondale, PA, U.S.A.) served for peak-area and migration-time measurements in the ZE stage. The data provided by the integrator (peak-height and peak-area ratio) served for the calculation of the column efficiency for the studied separands as described[15].

Chemicals

Chemicals used for the preparation of the electrolyte solutions were obtained from Serva (Heidelberg, F.R.G.), Sigma (St. Louis, MO, U.S.A.) and Lachema (Brno, Czechoslovakia) and were purified by conventional methods. Hydroxyethylcellulose 4000 (HEC) and methylhydroxyethylcellulose 30000 (m-HEC) served as anticonvective additives in the electrolyte solutions. A stock aqueous solution containing 0.5% (w/v) of each of the derivatives was purified on a mixed-bed ion exchanger (Amberlite MB-1; BDH, Poole, U.K.).

Water from a Rodem-1 two-stage demineralization unit (OPP, Tišnov, Czechoslovakia) was further purified by circulation through laboratory-made polytetrafluoroethylene (PTFE) cartridges packed with Amberlite MB-1 mixed-bed ion exchanger. The electrolyte solutions were prepared from freshly recirculated water.

Nitrophenols and 2,4-dinitrophenyl derivatives of amino acids (see Table I) were obtained from Serva and Sigma. The sample solutions were prepared from stock solutions of these preparatives [1 mg dissolved in 1 ml of water–methanol (1:1)]. Sulphate and naphthalene-1,3,6-trisulphonate (NTS) were added at $2 \cdot 10^{-4}$ mol/l concentrations to the sample solutions to prevent adsorption losses of the analytes during sample handling and to suppress their adsorption in the separation compartment during the analysis[11].

RESULTS AND DISCUSSION

Isotachophoresis as a sample injection technique for zone electrophoresis

The on-line combination of CITP with CZE as studied in this work can be divided into several well defined separation phases (Fig. 1). In experiments to investigate the capabilities of ITP as a sample injection technique for ZE, the overall separation scheme consisted of a sequence of three of these phases (successively a, b and e in Fig. 1). In this way, we could separate and concentrate the sample constituents in the ITP stage, remove sulphate and the main part of NTS (see Experimental) after this stage from the separation compartment and separate the transferred sample fraction (the remainder of NTS and the analytes) by ZE in the second column. Part of the injected NTS was transferred into the ZE stage to minimize adsorption of the analytes on the wall of the capillary tube[11,16].

TABLE I

NITROPHENOLS AND 2,4-DINITROPHENYL-LABELLED AMINO ACIDS USED AS MODEL ANALYTES

No.	*Name*[a]	*Abbreviation*
1	DNP-L-cysteic acid	DNP-CYS-SO_3H
2	DNP-L-aspartic acid	DNP-ASP
3	DNP-DL-glutamic acid	DNP-GLU
4	2,6-Dinitrophenol	2,6-DNP
5	2,4,6-Trinitrophenol	2,4,6-TNP
6	2,4-Dinitrophenol	2,4-DNP
7	DNP-glycine	DNP-GLY
8	DNP-L-alanine	DNP-ALA
9	DNP-L-serine	DNP-SER
10	DNP-DL-α-aminobutyric acid	DNP-AABA
11	DNP-L-asparagine	DNP-ASP-NH_2
12	DNP-L-valine	DNP-VAL
13	DNP-DL-methionine	DNP-MET
14	DNP-L-leucine	DNP-LEU
15	DNP-DL-ethionine	DNP-ET
16	DNP-DL-α-aminocaprylic acid	DNP-AACA
17	DNP-γ-aminobutyric acid	DNP-GABA
18	DNP-ε-aminocaproic acid	DNP-EACA

[a] DNP = Dinitrophenyl.

The driving current in the ITP stage (150 μA) was chosen as an experimental optimum considering a rapid ITP separation, sharp zone boundaries and the disturbing role of thermal effects[17]. An optimum value of the driving current for the ZE

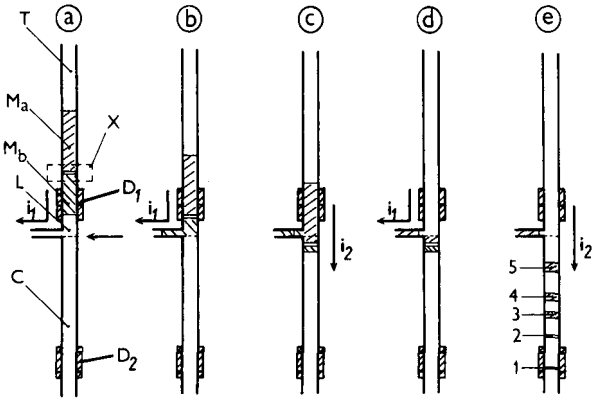

Fig. 1. Schematic illustration of the separation phases in combining ITP with ZE in the column-coupling configuration of the separation unit. (a) ITP separation in the first column (ITP stage); (b) removal of matrix constituent(s), M_b, from the separation compartment; (c) transfer of the sample fraction containing the analyte(s), X, into the second column (ZE stage); (d) removal of matrix constituent(s), M_a, from the separation compartment; (e) ZE separation in the second column (ZE stage). L, T = leading and terminating zones, respectively; C = carrier electrolyte; D_1, D_2 = detectors for ITP and ZE stages, respectively; i_1,i_2 = directions of the driving currents; 1–5 = symbols for the separated constituents in the ZE stage. The arrow on the right in (a) indicates the bifurcation point.

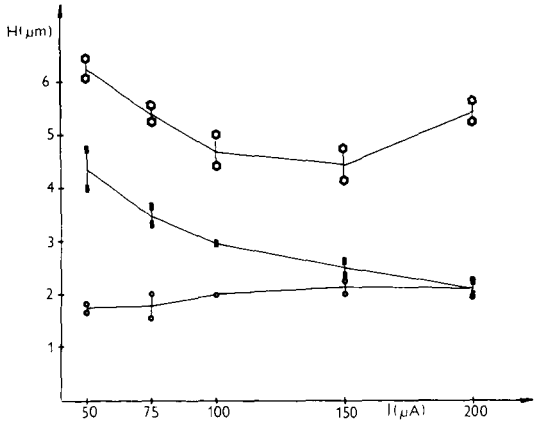

Fig. 2. Dependences of plate height (H) on the driving current (I). The plotted data were obtained for 10-pmol amounts of (○) DNP-ASP, (■) DNP-GLY and (○) DNP-EACA in the operational system listed in Table II. The H values were calculated from the data provided by a computing integrator (see Experimental).

stage was found from experimentally obtained dependences of the heights equivalent to a theoretical plate (H) on the driving current as shown in Fig. 2. A 150-μA driving current was estimated as an optimum for the ZE stage. The values of the driving currents for both stages were higher in comparison with (via current densities) to the values used in CITP and CZE in capillary tubes of similar I.D.[1–4,9,14]. Preliminary experiments revealed that this was possibly due to improved heat dissipation from the capillary tubes in comparison with the column design currently used in our laboratory[14].

An electropherogram (Fig. 3) obtained from the separation of a model mixture

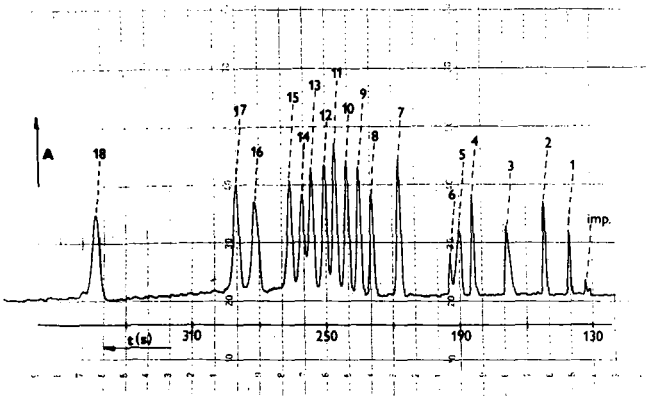

Fig. 3. Electropherogram from the separation of a mixture of nitrophenols and DNP-labelled amino acids. A 5-μl volume of the sample containing the constituents at $2 \cdot 10^{-6}$ mol/l concentrations was injected with a microsyringe. The separation was carried out in the operational system described in Table II (except the pH value of the carrier electrolyte was 5.3). The driving currents were 150 μA in both stages. The total analysis time was slightly less than 10 min. A = increasing light absorption; t = analysis time in the ZE stage; imp = unidentified impurity from the sample. For peak assignments, see Table I.

of anionically migrating constituents (Table I) under the working conditions employed clearly shows the high separation efficiences achieved. In this instance, the detected constituents were present in a sample solution at $2 \cdot 10^{-6}$ mol/l concentrations and were injected in a 5-μl volume with a microsyringe. As expected, none of these constituents was detectable by the conductivity detector under the conditions employed in the ITP stage (see also Fig. 4). As the conductivity detector allowed the detection of isotachophoretically migrating zones as short as 0.2 mm, we can assume that this value corresponded to a maximum length of the sample fraction of interest transferred to the ZE stage. In other words, it represented less than a *ca.* 14-nl injection volume into the 14-μl capillary tube employed for the ZE separation. The ratio of these volumes indicates a very positive role of ITP in achieving the injection volume required for a highly efficient ZE separation[1,2,18]. Experiments carried out with anionically migrating dyes revealed that no visible loss of the sharpness of the sample zone in the bifurcation point (see Fig. 1) occurred. However, this could be due to the fact that a small part (0.5 mm in length) of the leading zone was transferred with the focused dyes into the ZE stage. Hence ITP sharpening effect[9] could be responsible for the suppression of the partial zone dispersion in the bifurcation point (see also below).

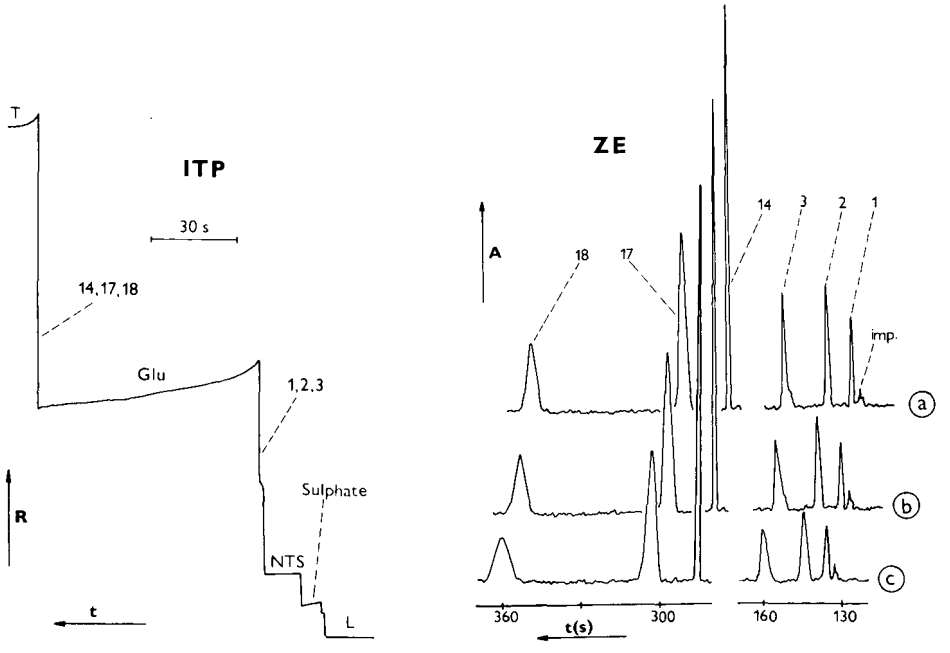

Fig. 4. Influence of interruption of the driving current on the separation efficiency in the ZE stage. The driving current was switched into the ITP stage to remove a sample macroconstituent (glutamate). 95% of the injected glutamate [see the isotachopherogram (ITP) from the conductivity detector in the ITP stage] was removed from the separation compartment after the ITP stage. Electropherograms (ZE) were obtained under the following conditions: (a) 70-s removal step; (b) as in (a) but after constituents 14, 17 and 18 had been transferred into the ZE stage the driving current was disconnected for 490 s; (c) as in (b) but the driving current was disconnected for 1400 s. L, T = leading and terminating zones, respectively. *A*, *t* and R = increasing light absorption, time and resistance, respectively. For the peak assignments see Table I and for working conditions see Table II.

Reproducibilities of migration times, quantification and separation efficiences

A series of experiments were carried out to measure the reproducibilities of the migration times of the studied constituents under the working conditions employed in the ZE stage (Table II). As the ITP separations are very reproducible when the factors influencing the migration velocities are controlled, a very reproducible transfer of the sample fraction of interest into the ZE stage was expected. In addition, for the ZE separations we employed a carrier electrolyte with a sufficient pH buffering capacity (some of the separands were moderately weak acids with pK_a values in the range 4–5). As all precautions concerning uncontrolled movement of the solution in the separation compartment[19] were also taken, high reproducibilities of the migration times (Table III) were achieved. The relative standard deviations of the migration times are in very good agreement with those obtained by CZE in a 0.2 mm I.D. capillary tube[2,3] in which the sample was injected with the aid of a sampling valve.

Mean H values and their reproducibilities obtained in the above series of experiments are summarized in Table III. In general, these values indicate the high separation efficiences achieved. When the electropherograms in Figs. 3 and 6 are compared, it can be seen that the higher H value for 2,4,6-TNP was due to 2,4-DNP (originating from the labelled amino acids) migrating almost unresolved from 2,4,6-TNP. It can also be seen that an unidentified impurity migrating in the front side of the DNP-GLU zone was responsible for a higher H value of this constituent. Although a search for optimum separating conditions in the ZE stage was not the aim of this work, a small pH difference of the carrier electrolytes as used in the run in Fig. 3 and in the remainder of experiments (Figs. 4–6) indicated that at a lower pH we could expect a better resolution of 2,4-DNP and 2,4,6-TNP.

The results published recently by Foret *et al.*[20] show that under our experimental conditions (hydrodynamically closed system) dispersion due to electroosmosis

TABLE II

OPERATIONAL SYSTEM

Discrete spacing constituents: sulphuric, chloric, tartronic, tartaric, malonic, citric, succinic, glutaric, phosphonomethyliminodiacetic, adipic, acetic, dichloroacetic, trichloroacetic, β-bromopropionic, malonic monoethyl ester, iminodiacetic, aspartic, butyric, N-acetylserine, hydroxyethyliminodiacetic, glutamic, succinic monoisopropyl ester, N-acetylleucine, α-aminoadipic and α-aminopimelic acids.

Parameter	*Electrolyte*[a]		
	ITP		*ZE: carrier*
	Leading	*Terminating*	
Solvent	H_2O	H_2O	H_2O
Anion	Cl^-	MES	MES
Concentration (m*M*)	20	10	50
Counter ion	HIS	HIS	HIS
pH	5.5	~5.5	5.5
Additive	HEC; m-HEC	–	HEC; m-HEC
Concentration (%, w/v)	0.1;0.1	–	0.1;0.1

[a] HEC = hydroxyethylcellulose; HIS = histidine; m-HEC = methylhydroxyethylcellulose; MES = morpholinoethanesulphonic acid.

TABLE III

MIGRATION TIMES AND SEPARATION EFFICIENCIES IN THE ZE STAGE (n = 9)

H = height equivalent to a theoretical plate (HETP); $\bar{t}_r$ = average migration time; s_r = relative standard deviation; n = number of data points.

Constituent		*Migration time*		*HETP*	
No.	*Abbreviation*	$\bar{t}_r$ *(s)*	s_r *(%)*	H *(μm)*	s_r *(%)*
1	DNP-CYS-SO_3H	138.4	0.99	2.00	19
2	DNP-ASP	150.3	0.75	2.42	12
3	DNP-GLU	167.1	0.99	5.29	22
4	2,6-DNP	183.4	1.24	2.16	30
5	2,4,6-TNP	190.0	0.59	5.64	23
7	DNP-GLY	215.5	0.41	2.88	5
8	DNP-ALA	227.96	0.46	2.19	18
9	DNP-SER	233.7	0.37	2.73	12
10	DNP-AABA	239.2	0.42	3.27	4
11	DNP-ASP-NH_2	244.5	0.37	3.02	4
12	DNP-VAL	249.2	0.40	3.24	6
13	DNP-MET	255.4	0.39	3.23	6
14	DNP-LEU	259.51	0.35	3.59	7
15	DNP-ET	265.1	0.40	3.18	7
16	DNP-AACA	281.13	0.40	5.00	5
17	DNP-GABA	289.1	0.34	3.91	4
18	DNP-EACA	352.0	0.30	4.22	7

can be dominant. Although the addition of HEC and m-HEC to the electrolyte solutions was a very efficient way of suppressing electroosmosis[21], its experimental comparison with other alternatives[21,22] seemed desirable. In our experiments, ad-

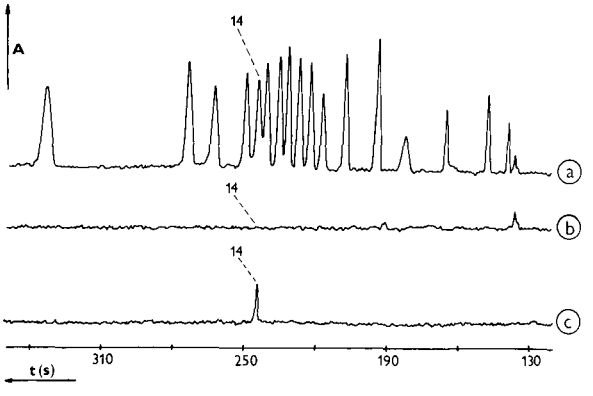

Fig. 5. Role of "ITP" sharpening effect on the detectability of the constituents in the ZE stage. (a) ZE separation of a model mixture containing the separated constituents at $2 \cdot 10^{-6}$ mol/l concentrations (5-μl injection volume); (b) same sample as in (a) except the concentrations of the separands were $8 \cdot 10^{-8}$ mol/l; (c) same as in (b) except the sample contained, in addition, glutamate at $8 \cdot 10^{-3}$ mol/l; 95% of the glutamate was removed after the ITP stage and the remaining part was transferred into the ZE stage to improve the detectability of DNP-LEU (the peak corresponds to 400 fmol of the analyte). The working conditions are described in Table II. The analysis times were *ca.* 10 min.

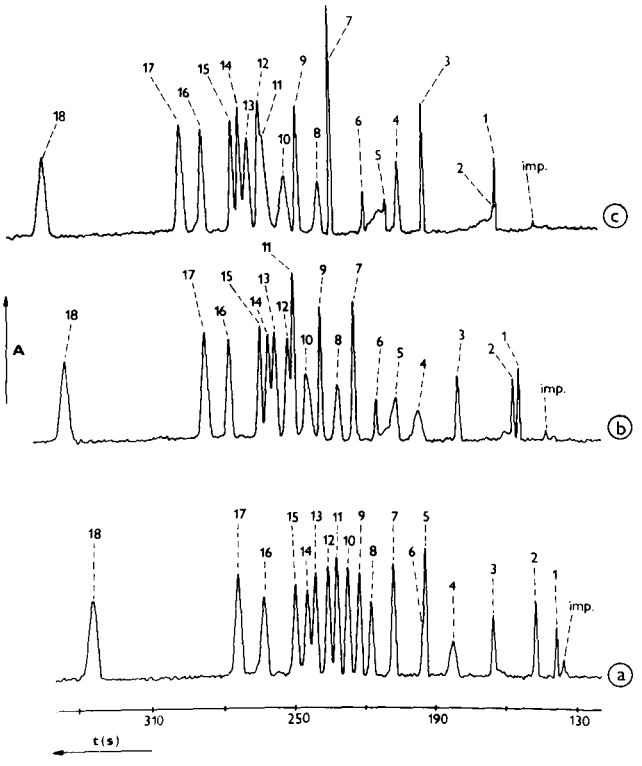

Fig. 6. Influence of a mixture of constituents undetectable in the ZE stage on the separation of nitrophenols and labelled amino acids. (a) 5-μl sample volume containing nitrophenols and 2,4-dinitrophenyl-labelled amino acids at $2 \cdot 10^{-6}$ mol/l concentration; (b) as in (a) except the sample contained, in addition, a 25-component mixture of discrete spacers (each at $4 \cdot 10^{-5}$ mol/l); (c) as in (b) except the concentrations of the spacing constituents were $8 \cdot 10^{-5}$ mol/l. A, t = increasing light absorption and time, respectively; imp = unidentified impurity from the sample. For the peak assignments see Table I and for working conditions see Table II. The composition of the mixture of discrete spacers is given in Table II. The analysis times were *ca.* 10 min.

sorption of the separated constituents was minimized by a dynamic coating of the surface with triply negatively charged NTS. In this respect other alternatives[18,22,23] should also be examined to find the optimum solution for minimizing these undesired dispersive phenomena.

The calibration lines (Table IV) were evaluated for 0.5–5-μl volumes of the sample solution containing the analytes at $2 \cdot 10^{-}6$ mol/l concentrations (1–10 pmol injected). The lowest injected amounts were *ca.* double the estimated detection limits (*ca.* 600–800 fmol). As the response of the detector (transmittance scale) deviated from linearity by more than 5% for 12-pmol amounts of the analytes, we were restricted in our experiments only for the lowest quantifiable concentrations. However, it is necessary to note that 50–80-pmol amounts of the analytes gave zones with migration times identical with those obtained for lower concentrations and with no observable electromigration dispersion[1–3], indicating that a wider concentration

TABLE IV

PARAMETERS OF THE REGRESSION EQUATIONS ($y = a + bx$) AND CORRELATION COEFFICIENTS FOR THE ANALYTES PRESENT IN THE SAMPLES IN 1–10-pmol AMOUNTS

n = Number of data points; r = correlation coefficient; x = sample volume (μl) with $2 \cdot 10^{-6}$ mol/l concentrations of the analytes; y = peak area (thousands of counts of the integrator).

Constituent		a^a	b^a	r	n
No.	*Abbreviation*				
1	DNP-CYS-SO_3H	28	94	0.9869	21
2	DNP-ASP	25	164	0.9947	20
3	DNP-GLU	5	185	0.9896	18
4	2,6-DNP	37	167	0.9877	20
5	2,4,6-TNP	92	198	0.9725	18
7	DNP-GLY	59	308	0.9977	18
8	DNP-ALA	22	231	0.9836	18
9	DNP-SER	25	343	0.9958	17
10	DNP-AABA	50	375	0.9980	17
11	DNP-ASP-NH_2	43	429	0.9985	17
12	DNP-VAL	39	401	0.9971	17
13	DNP-MET	41	410	0.9956	17
14	DNP-LEU	27	356	0.9946	17
15	DNP-ET	48	383	0.9933	17
16	DNP-AACA	76	427	0.9832	17
17	DNP-GABA	31	409	0.9882	17
18	DNP-EACA	74	464	0.9860	17

[a] Thousands of counts of the integrator.

TABLE V

REPRODUCIBILITY OF THE DETERMINATION OF 8-pmol AMOUNTS OF THE ANALYTES ($n = 4$)

$\bar{y}$ = average peak area (thousands of counts of the integrator); s = standard deviation (thousands of counts of the integrator); s_r = relative standard deviation; n = number of data points.

Constituent		$\bar{y}$	s	s_r
No.	*Abbreviation*			*(%)*
1	DNP-CYS-SO_3H	388.0	19.7	5.1
2	DNP-ASP	713.5	21.4	3.0
3	DNP-GLU	765.3	13.0	1.7
4	2,6-DNP	733.8	7.5	1.0
5	2,4,6-TNP	908.3	25.7	2.8
7	DNP-GLY	1324.3	37.7	2.8
8	DNP-ALA	965.7	29.2	3.0
9	DNP-SER	1429.3	25.1	1.8
10	DNP-AABA	1596.3	41.4	2.6
11	DNP-ASP-NH_2	1797.5	32.3	1.8
12	DNP-VAL	1683.0	15.1	0.9
13	DNP-MET	1746.8	18.9	1.1
14	DNP-LEU	1512.5	34.5	2.3
15	DNP-ET	1671.0	29.0	1.7
16	DNP-AACA	1931.0	53.1	2.8
17	DNP-GABA	1734.3	51.7	3.0
18	DNP-EACA	2014.5	41.4	2.1

range is applicable for quantitative analysis by using measurements on the absorbance scale.

Reproducibilities of the determinations of 8-pmol amounts of the analytes (4-μl injection volume) are listed in Table V. The relative standard deviations of the peak areas clearly show that by using microsyringe injection in conjunction with ITP focusing of the separands, the precision in the sample introduction was at least comparable to those achieved by advanced injection systems for CZE in 50–200-μm columns[24,25] with comparable separation efficiencies. These results also suggest that by using ITP as a sample introduction technique for ZE, problems associated with the injection of samples from extremely small sample volumes[24,26] could be alleviated, *e.g.*, by using a microsyringe for low nanolitre volumes[27] for sample handling and injection of the sample into the ITP stage.

Removal of the matrix constituents after the ITP stage

The sample solutions used in the above experiments contained sulphate and NTS as macroconstituents which were removed from the separation compartment after the ITP stage. The sample fractions of analytical interest were transferred into the ZE stage after a short interruption (*ca.* 3 s) in the delivery of the driving current between the phases b and e (see Fig. 1) to switch the columns by the controller of the analyser via a relay. This interruption in the delivery of the driving current had no detectable effect on the efficiency of the ZE separation, as the time was considerably shorter than the migration times. However, as discussed above, in these instances ITP zone sharpening compensated for any dispersion of the zones. From the schematic illustration in Fig. 1 it can be seen that by using a complete sequence of the separation phases the sample fraction transferred into the ZE stage in phase c does not migrate while a less mobile matrix constituent is led out of the separation compartment. Obviously, it is desirable to remove this constituent within the shortest possible time in order to minimize the dispersions of the transferred zones by diffusion. On the other hand, there are inherent restrictions concerning the maximum applied driving current in the ITP stage[9]. The electropherograms in Fig. 4 were obtained in experiments aimed at studying the consequences of such an interruption in the driving current on the ZE separation. Here, the transferred sample fractions were present in the second column for various times before the driving current for the final ZE separation (phase e in Fig. 1) was applied. The interruption of the driving current necessary to remove 95% of the injected glutamate (a in Fig. 4) had no observable influence on the separation efficiencies of constituents 1, 2 and 3 or on their migration times. On the other hand, considerably longer interruptions of the driving current [corresponding to the removal of 8-fold (run b) and 21-fold (run c) larger amounts of glutamate] led to easily detectable decreases in the efficiencies of separation.

As very high reproducibilities in the ITP stage were typical, we could remove more than 99% of the injected glutamate and the migration times of the transferred sample constituents agreed within random error with those obtained for the sample without glutamate (see Table III). Also, no visible differences in the peak shapes were detected in these experiments. When 5% amounts of the injected glutamate were transferred with the labelled amino acids into the ZE stage, a sharp DNP-LEU peak was typical (see Fig. 4) and the migration times of the constituents migrating behind the glutamate zone in the ITP stage (14, 17 and 18) were higher in comparison with

the values obtained without glutamate. Such a behaviour is an obvious consequence of the electromigration dispersion of the glutamate zone in the ZE stage[1–3] accompanied by a strong ITP sharpening effect of the adjacent DNP-LEU zone. As the ZE separations were also reproducible under these conditions, differences in the migration times of constituents 14, 17 and 18 were constant from run to run. These facts led us to investigate the role of the sharpening effect in improving the detectability of the separands in the ZE stage. The electropherograms in Fig. 5 obtained from these experiments clearly illustrate this possibility. For example, in this particular instance the detection limit for DNP-LEU was improved *ca.* 5-fold in comparison with the separations without transferred glutamate. It should be also mentioned that in this way the analyte could be detected with confidence in a sample containing a 10^5-fold excess of glutamate (c in Fig. 5).

In practical situations, the constituents of analytical interest can be present in the samples containing a large number of matrix constituents at concentrations comparable to or slightly higher than those of the analytes. Here, the matrix constituents form very short zones (0.5–1 mm) detectable in the ITP stage by the conductivity detector. Although detectable in the ITP stage, their removal after this stage as described above can be almost impossible, especially when the number of both the analytes and matrix constituents is high. In an ideal case, *i.e.*, with the analytes migrating spaced by the matrix constituents (undetectable in the ZE stage), we could expect sharp peaks of the analytes in the ZE separation with the migration times being influenced by their different injection times and by the electromigration dispersions of the zones of the matrix constituents. However, a time- and labour-consuming search for a suitable operational system seems unavoidable in order to achieve such a goal.

The electropherograms in Fig. 6 illustrate some problems that can be encountered in such instances. In these experiments a model mixture of the analytes was separated with various amounts of a 25-component sample of discrete spacing constituents for the ITP separations of anions at pH 5.5 (Table II). It can be seen that the presence of the spacing constituents in the sample led to sharpening of some zones (Nos. 1, 3, 4 and 7), their "dilution" (Nos. 2, 5 and 10), loss (Nos. 11 and 12) or improvement of the resolution (No. 6). It is apparent that whereas some of the analytes were injected as sharp pulses, another forming mixed zones (spread along the spacing constituents) in the ITP phase gave wide injection pulses. In spite of the fact that a detailed investigation of all factors influencing the ZE separation in such an instance was not made, it appears that the injection of smaller sample amounts or the use of more concentrated electrolyte solutions are, in practice, the simplest alternatives for solving problems of this kind. Here, the choice is not straightforward as the former alternative introduces higher demands on the detection system and the latter can lead to problems associated with thermal effects.

CONCLUSIONS

The results clearly show promising analytical capabilities of on-line coupling of CITP with CZE. As could be expected, a well defined concentration adaptation of the sample constituents in the ITP stage was effective in reducing the volume in which they were transferred into the ZE stage. For example, a 10^2–10^3 volume reduction

was typical under our experimental conditions on injecting 0.5–15-μl sample volumes with the aid of a microsyringe or a sample valve. Thus, by using a microsyringe sample injection, very small sample volumes can be sufficient for the analysis and as no sample splitting is necessary[28] it can be completely transferred for the ZE analysis. It is also important that in this way very reproducible migration times in the ZE stage could be achieved while the precision of the sample injection remained high.

A sample clean-up in the ITP stage can be effective, at least, in removing sample macroconstituents so that the sample volume need not be reduced to avoid column overloading in the ZE stage. It is apparent that in this way it is possible to improve the concentration detection limits for the constituents of analytical interest in CZE. In addition, as the ITP stage also provides analytically important information, an overall evalution of the analysis can be based on the data obtained in both stages in one run.

Our experiments suggest that a defined electromigration dispersion can be effective in improving the detection limits in the ZE stage. However, further research in this respect is necessary to investigate the possibilities of this approach and problems that can occur in its practical use.

Some restrictions concerning the choice of the electrolyte systems (the terminating constituent migrating in the ZE stage) and a need to use a more advanced construction of the instrument are apparent disadvantages of the studied combination of basic electrophoretic techniques. However, only comparative experiments with "pure" techniques can provide more relevant information in this respect.

The use of such a combination in electrophoretic separations with electroosmotic transport of the electrolyte solution in the separation compartment[29] or in electrokinetic chromatography with micellar solutions[30] seems possible. A development of appropriate instrumentation, preferably with well defined control of the electroosmotic flow is necessary, however.

REFERENCES

1 F. E. P. Mikkers, F. M. Everaerts and Th. P. E. M. Verheggen, *J. Chromatogr.*, 169 (1979) 1.
2 F. E. P. Mikkers, F. M. Everaerts and Th. P. E. M. Verheggen, *J. Chromatogr.*, 169 (1979) 11.
3 F. E. P. Mikkers, *Thesis*, University of Technology, Eindhoven, 1980.
4 J. L. Beckers, Th. P. E. M. Verheggen and F. M. Everaerts, *J. Chromatogr.*, 452 (1988) 591.
5 S. Hjertén, K. Elenbring, F. Kilár, J. Liao, A. J. C. Chen, C. J. Siebert and M. Zhu, *J. Chromatogr.*, 403 (1987) 47.
6 L. Ornstein, *Ann. N. Y. Acad. Sci.*, 121 (1964) 321.
7 B. J. Davis, *Ann. N. Y. Acad. Sci.*, 121 (1964) 404.
8 P. Boček, M. Deml and J. Janák, *J. Chromatogr.*, 156 (1978) 323.
9 F. M. Everaerts, J. L. Beckers and Th. P. E. M. Verheggen, *Isotachophoresis: Theory, Instrumentation and Applications*, Elsevier, Amsterdam, Oxford, New York, 1976.
10 F. M. Everaerts, Th. P. E. M. Verheggen and F. E. P. Mikkers, *J. Chromatogr.*, 169 (1979) 21.
11 D. Kaniansky, V. Madajová, J. Marák, E. Šimuničová, I. Zelenský and V. Zelenská, *J. Chromatogr.*, 390 (1987) 51.
12 D. Kaniansky, M. Kovaľ and S. Stankoviansky, *J. Chromatogr.*, 267 (1983) 67.
13 P. Havaši and D. Kaniansky, *J. Chromatogr.*, 325 (1985) 137.
14 D. Kaniansky, *Thesis*, Komenský University, Bratislava, 1981.
15 B. A. Bidlingmeyer and F. W. Warren, Jr., *Anal. Chem.*, 56 (1984) 1583A.
16 I. Zelenský, V. Zelenská and D. Kaniansky, *J. Chromatogr.*, 390 (1987) 111.
17 J. C. Reijenga, Th. P. E. M. Verheggen and F. M. Everaerts, *J. Chromatogr.*, 328 (1985) 353.
18 H. H. Lauer and D. McManigill, *Trends Anal. Chem.*, 5 (1986) 11.

19 I. Zelenský, E. Šimuničová, V. Zelenská, D. Kaniansky, P. Havaši and P. Chaláni, *J. Chromatogr.*, 325 (1985) 161.
20 F. Foret, M. Deml and P. Boček, *J. Chromatogr.*, 452 (1988) 601.
21 J. C. Reijenga, G. V. A. Aben, Th. P. E. M. Verheggen and F. M. Everaerts, *J. Chromatogr.*, 260 (1983) 241.
22 S. Hjertén, *J. Chromatogr.*, 347 (1985) 191.
23 H. H. Lauer and D. McManigill, *Anal. Chem.*, 58 (1986) 166.
24 D. J. Rose, Jr., and J. W. Jorgenson, *Anal. Chem.*, 60 (1988) 642.
25 S. Honda, S. Iwase and S. Fujiwara, *J. Chromatogr.*, 404 (1987) 313.
26 R. A. Wallingford and A. G. Ewing, *Anal. Chem.*, 59 (1987) 678.
27 R. T. Kennedy and J. W. Jorgenson, Anal. Chem., 60 (1988) 1521.
28 M. Deml, F. Foret and P. Boček, *J. Chromatogr.*, 320 (1985) 159.
29 J. W. Jorgenson and K. D. Lukacs, *Anal. Chem.*, 53 (1981) 1298.
30 S. Terabe, K. Otsuka, K. Ichikawa, A. Tsuchiya and T. Ando, *Anal. Chem.*, 56 (1984) 111.

Journal of Chromatography, 498 (1990) 205–211
Elsevier Science Publishers B.V., Amsterdam — Printed in The Netherlands

CHROM. 21 985

ISOTACHOPHORETIC SEPARATION AND BEHAVIOUR OF CATECHOL DERIVATIVES

SHUNITZ TANAKA, TAKASHI KANETA and HITOSHI YOSHIDA*
Department of Chemistry, Faculty of Science, Hokkaido University, Sapporo 060 (Japan)
(First received July 11th, 1989; revised manuscript received September 12th, 1989)

SUMMARY

The separation and migration behaviour of ten catechol derivatives containing electrically neutral species were investigated by capillary tube isotachophoresis. In the usual migration system at pH 7.5 consisting of Tris buffer as the leading electrolyte and histidine as the terminating electrolyte, six of the catechols were separated but the other four with small acid dissociation constants could not be detected. However, by using boric acid as the terminating electrolyte and converting the catechols into anionic catechol–borate complexes in the migrating capillary, all ten catechols could be detected and nine of them could be separated even at pH 7.5.

INTRODUCTION

Catechol and its derivatives form primary structure of dopamine, epinephrine, etc., which act as neurotransmitters and are physiologically important substances[1]. These substances participate in an oxidation–reduction system with *o*-quinone and play important roles in the electron transport system *in vivo*. Analytical separations of these substances have been performed using various types of chromatography[2,3] and flow-injection analysis[4]. Capillary tube isotachophoresis (CITP) is also an excellent separation method but there have been few reports of its application. For the separation of catechols by CITP it is necessary to convert them into ionic species. The hydroxyl group of catechols can dissociate in the alkaline operating system of CITP. However, catechols are oxidized by air in alkaline media to form *o*-quinone and consequently the zones of catechols suffer interferences in the alkaline operating system of CITP. At pH below *ca.* 7, catechols that have small acid dissociation constants cannot migrate because they exist as electrically neutral species.

An efficient method for changing the mobilities of species under isotachophoretic investigation is utilization of complex-forming equilibria. The behaviour of complexes under such conditions was dealt with in detail both theoretically and experimentally by Gebauer *et al.*[5]. We have also reported a new operating system involving reaction with the terminating ion[6]. In this method, sample molecules were converted into negatively charged species with the terminating ion and migrated as a result of complex-forming equilibria. Compared with the conventional method using the com-

0021-9673/90/$03.50

plex-forming equilibria between the sample ions and the counter ion in the leading electrolyte[8,9], this method has the important advantage that the effective mobilities of the sample species become larger according to the strength of the interaction with the terminating ion. Therefore, this method can be applied to the migration of species with low mobilities and electrically neutral species. In a previous paper[10] we demonstrated the probability that electrically neutral catechols can be made to migrate as borate complexes by using borate as the terminating ion.

In this paper, the isotachophoretic behaviour and separation of ten catechol derivatives containing electrically neutral species are described. The order of migration of the catechols was correlated with the acid dissociation constants obtained by potentiometric measurement using acid–base titration. In addition, using boric acid as the terminating electrolyte, the migration system for catechols as borate complexes was investigated. Nine catechols, including some with small acid dissociation constants, could be separated at neutral pH (7.5) in this system.

EXPERIMENTAL

Apparatus

A Model IP-1B capillary tube isotachophoretic analyser equipped with a potential gradient detector (Shimadzu, Kyoto, Japan) was used. The PTFE tube for separation consisted of a main column (150 mm × 0.5 mm I.D.) and a precolumn (40 mm × 1.0 mm I.D.). The capillary tube was filled with electrolyte by pressure of nitrogen gas. In this study the R_E value was used as the index of identification, where R_E is the ratio of the potential gradient of the sample zone to that of the leading zone, *i.e.*, corresponding to the ratio of the mobility of the leading ion to that of the sample ion.

A Model M-8L pH meter (Horiba, Tokyo, Japan) was used to detect neutralization in potentiometric titration.

A Model 174A polarographic analyser (Princeton Applied Research, Princeton, NJ, U.S.A.) was used for measuring cyclic voltammograms. The working electrode was a Metrohm Model E 410 hanging mercury drop electrode (HMDE) and the counter electrode was a glassy-carbon rod. A saturated calomel electrode with a diaphragm tube containing 1 *M* potassium nitrate solution was used as the reference electrode.

Reagent

All reagents were of analytical-reagent grade and solutions were prepared by dissolution in doubly distilled, deionized water. The solutions of catechols were stored in a refrigerator.

2,3-Dihydroxybenzoic acid (2,3-DBA), 3,4-dihydroxybenzoic acid (3,4-DBA), 2,3-dihydroxybenzaldehyde (2,3-DBAL), 3,4-dihydroxybenzaldehyde (3,4-DBAL), 2,3-dihydroxynaphthalene (DN), 4-chlorocatechol (CC) and 4-methylcatechol (MC) were obtained from Tokyo Kasei (Tokyo, Japan), pyrocatechol (PC) from Kanto (Tokyo, Japan) and pyrogallol (PG), hydroxyhydroquinone (HHQ), hydroquinone (HQ) and others chemicals from Wako (Osaka, Japan).

The leading electrolyte was prepared by adding tris(hydroxymethyl)aminomethane to 10 m*M* hydrochloric acid containing $1.25 \cdot 10^{-3}$% poly(vinyl alcohol) to

TABLE I

OPERATING SYSTEM

Parameter	*Leading electrolyte*	*Terminating electrolyte*
Anion	Cl^-	System 1: histidine System 2: germanate System 3: borate
Counter ion	$TrisH^+$	Ba^{2+}
Concentration of anion	10 m*M*	10 m*M*
Additive	$1.25 \cdot 10^{-3}$% poly(vinyl alcohol)	5 m*M* $Ba(OH)_2$
pH	System 1: 7.5 System 2: 8.0 System 3: 7.5	10

adjust the pH. Terminating electrolytes were prepared by adding barium hydroxide to histidine or germanic acid or boric acid solution (pH 10).

The operating systems are summarized in Table I. System 1 consisted of a leading electrolyte of pH 7.5 and a terminating electrolyte of 10 m*M* histidine, system 2 consisted of a leading electrolyte of pH 8.0 and a terminating electrolyte of 10 m*M* germanic acid and system 3 consisted of a leading electrolyte of pH 7.5 and a terminating electrolyte of 10 m*M* boric acid. All terminating electrolytes contained 5 m*M* barium hydroxide.

Acid–base titration

Potentiometric acid–base titration was performed in order to determine the acid dissociation constants of catechols. The dissociation constants were determined

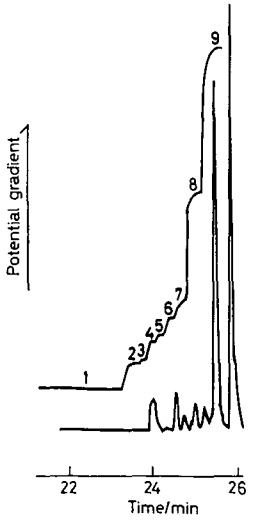

Fig. 1. Isotachopherogram of catechols in system 1. 1 = Chloride; 2 = hydrogencarbonate; 3 = HHQ; 4 = 2,3-DBA; 5 = 3,4-DBA; 6 = 3,4-DBAL; 7 = 2,3-DBAL; 8 = CC; 9 = histidine. Leading electrolyte, 10 m*M* HCl + Tris, $1.25 \cdot 10^{-3}$% PVA, pH 7.5. Sample, 10 μl of a mixed solution of 1 m*M*. Driving current, 100 μA.

by measuring the pH of the mid-point of the titration curve. A 5 or 10 m*M* solution of the sample in 50 m*M* potassium nitrate solution was used as the titrand and 50 m*M* sodium hydroxide solution as the titrant.

RESULTS AND DISCUSSION

Migration of catechol derivatives

The isotachopherogram of the ten catechols obtained by using system 1 in Table I is shown in Fig. 1. Six of the catechols could be detected and separated but the other four were not detected. The effective mobilities of the catechols in this migration system were determined from the acid dissociation constants and the pH of the leading electrolyte. The acid dissociation constants were determined by potentiometric acid–base titration and are given in Table II.

In order of the dissociation constants, 2,3-DBA, 3,4-DBA, 3,4-DBAL, 2,3-DBAL, and CC migrated, 2,3-DBA and 3,4-DBA owing to the dissociation of the carboxyl group and 3,4-DBAL, 2,3-DBAL and CC owing to the dissociation of the hydroxyl group. HHQ had large mobility but its dissociation constant could not be determined. The migration behaviour of HHQ will be described in detail later. The other four catechols, DN, PC, PG and MC, did not migrate because they have small acid dissociation constants and are present as electrically neutral species in this operating system. The mobilities of the catechols increased in alkaline systems such as HCl–NH_3 and HCl–arginine buffer, but the differences in their mobilities decreased and the separation became difficult. Also, some catechols gave unstable zones because they are oxidized by dissolved oxygen in alkaline media.

Migration of catechols as complexes

It is known that polyols, such as catechols and carbohydrates, are complexed with oxy acids such as germanic and boric acid[11,12] and the resulting complexes act as stronger acids than the original germanic and boric acid. These reactions have been used in the titration of boric acid[11], zone electrophoresis of carbohydrates[13,14] and chromatography of carbohydrates[15,16]. In order to utilize this reaction in isotachophoretic separations, we designed a new migrating system using an oxy acid as the terminating electrolyte. In this system, injected catechols might be converted into catechol–oxy acid complexes by reaction with terminating ion and then migrate. In this method it is necessary to satisfy the following requirements for an oxy acid as the terminating electrolyte: (1) the oxy acid should form a stable terminating zone where

TABLE II

ACID DISSOCIATION CONSTANTS (pK_a) OF CATECHOL DERIVATIVES

Compound	pK_a	*Compound*	pK_a
2,3-DBA	3.2	DN	8.4
3,4-DBA	4.5	MC	8.9
3,4-DBAL	7.1	PC	9.1
2,3-DBAL	7.6	PG	8.7
CC	8.4	HHQ	–

the effective mobility is sufficiently different from that of the leading ion, and (2) the catechol–oxy acid complexes formed should have higher effective mobilities than that of the oxy acid.

Germanate and borate were selected as terminating ions and the migration behaviour of catechols in the migration systems shown in Table I was investigated.

Migration as germanate complexes. Fig. 2. shows the isotachopherogram of ten catechols obtained by using germanic acid as the terminating electrolyte (system 2 in Table I). They had high mobilities but except for 2,3-DBA and HHQ they had the mobilities were very similar and the compounds could not be separated. It seems that the germanate–catechol complexes are too stable to be separated using complex-forming equilibria with the terminating ion.

Migration as borate complexes. Fig. 3. shows the isotachopherogram of catechols obtained by using borate as the terminating ion (System 3 in Table I). Some of the catechols that did not migrate in the system 1, could be detected and nine of the catechols could be separated. It seems that the injected catechols form complexes with the boric acid and the complexes act as stronger acids than boric acid in this operating system, as shown by following equations:

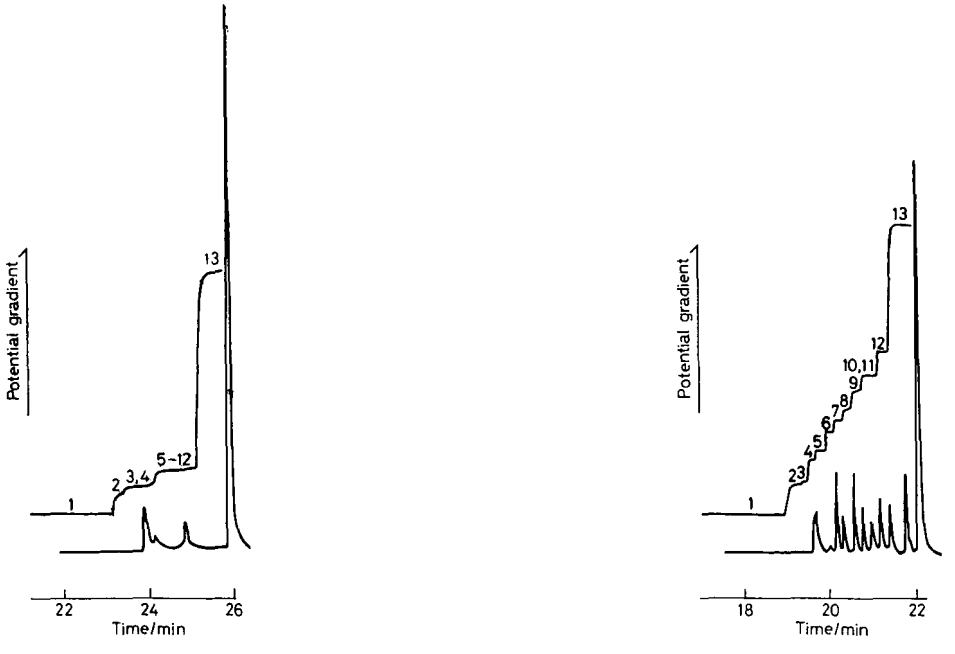

Fig. 2. Isotachopherogram of catechols in system 2. 1 = Chloride; 2 = ~~2,3-DBA; 3 =~~ hydrogencarbonate; 4 = ~~HHQ; 5 =~~ 2,3-DBA; 6 = 3,4-DBAL; 7 = 2,3-DBAL; 8 = DN; 9 = CC; 10 = PC; 11 = PG; 12 = MC; 13 = germanate. Leading electrolyte, 10 m*M* HCl + Tris, 1.25 · 10^{-3}% PVA, pH 8.0. Other conditions as in Fig. 1.

Fig. 3. Isotachopherogram of catechols in system 3. 1 = Chloride; 2 = 2,3-DBA; 3 = hydrogencarbonate; 4 = HHQ; 5 = 3,4-DBA; 6 = 3,4-DBAL; 7 = 2,3-DBAL; 8 = DN; 9 = CC; 10 = PC; 11 = PG; 12 = MC; 13 = borate. Leading electrolyte, 10 m*M* HCl + Tris, 1.25 · 10^{-3}% PVA, pH 7.5. Other conditions as in Fig. 1.

$$C + B \rightleftharpoons CB$$
$$CB + H_2O \rightleftharpoons CBOH^- + H^+$$

where C represents catechols and B represents boric acid. Consequently, the effective mobilities of the catechols become higher than that of the terminating ion. Hydroquinone and resorcinol, which are isomers of pyrocatechol, did not migrate even in this system. It was considered that their borate complexes would have very small stability constants owing to their structures. In operating system 3, only compounds having the catechol structure migrated selectively. Fig. 4 shows the effect of the pH of the leading electrolyte on the R_E values of catechols when boric acid was used as the terminating electrolyte. With increasing pH the effective mobilities became larger but the differences between the effective mobilities became smaller. The operating system adjusted to pH 7.5 was suitable for separating the catechols. The separation of PC and PG, however, could not be achieved in the pH range 7.5–9.0

Behaviour of hydroxyhydroquinone (HHQ)

HHQ has a larger effective mobility than that expected from its structure. The acid dissociation constant of HHQ could not be determined by acid–base titration because the titration curve did not have a well defined end-point. We considered that HHQ was oxidized and the oxide had a high mobility. To confirm this, cyclic voltammetry with HMDE as the working electrode was performed on HQ and HHQ in KH_2PO_4–K_2HPO_4 buffer. Both HQ and HHQ showed the reversible cyclic voltammograms. Fig. 5 shows the relationships between pH and peak potential of the oxidation waves of HQ and HHQ. The slopes for HQ and HHQ were 57 and 86 mV/pH,

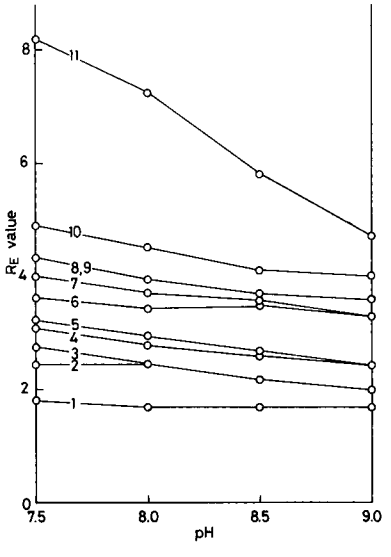

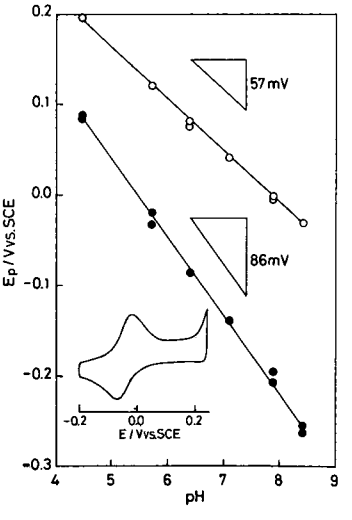

Fig. 4. Effect of pH of the leading electroltyte on R_E values of catechol–borate complexes. 1 = HHQ; 2 = 2,3-DBA; 3 = 3,4-DBA; 4 = 3,4-DBAL; 5 = 2,3-DBAL; 6 = DN; 7 = CC; 8 = PC; 9 = PG; 10 = HC; 11 = borate. Leading electrolyte, 10 m*M* HCl + Tris, $1.25 \cdot 10^{-3}$% PVA. Driving current, 100 μA.

Fig. 5. Relationship between pH and peak potential. ○ = HQ; ● = HHQ. Buffer, 0.1 *M* phosphate.

respectively. It is known that two electrons and two protons participate in the oxidation reaction of HQ. The slope expected theoretically is 59 mV/pH, *i.e.*, in agreement with the experimental value. The slope for HHQ 86 mV/pH, suggested that two electrons and three protons participate in the oxidation reaction of HHQ. That is, the third proton of HHQ is easily dissociated when HHQ is oxidized to form p-quinone as follows:

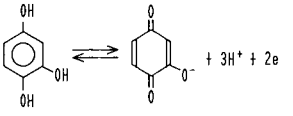

Consequently, the oxidation product of HHQ has a high mobility.

Using boric acid as the terminating electrolyte, nine of the catechols with either large or small mobilities could be separated simultaneously. The utility of complex-forming equilibria between the sample ion and terminating ion was thus confirmed.

REFERENCES

1 W. C. McMurray, *Essentials of Human Metabolism—The Relationship of Biochemistry to Human Physiology and Disease*, Harper & Row, New York, 1983; translated by M. Saito and Y Yojima, *Jintai-no-taisho*, Tokyo Kagaku Dohjin, Tokyo, 1987.
2 T. Ishimitsu and S. Hirose, *Talanta*, 32 (1985) 865.
3 H. Nohta, A. Mitsui, Y. Umegae and Y. Ohkura, *Anal. Sci.*, 2 (1986) 303.
4 H. Satake, Y. Kohri and S. Ikeda, *Nippon Kagaku Kaishi*, (1986) 42.
5 P. Gebauer, P. Boček, M. Deml and J. Janak, *J. Chromatogr.*, 199 (1980) 81.
6 Y. Hirama and H. Yoshida, *J. Chromatogr.*, 322 (1985) 139.
7 S. Tanaka, T. Kaneta and H. Yoshida, *J. Chromatogr.*, 477 (1988) 383.
8 P. Boček, I. Miedziak, M. Deml and J. Janák, *J. Chromatogr.*, 137 (1977) 83.
9 I. Nukatsuka, M. Taga and H. Yoshida, *J. Chromatogr.*, 205 (1981) 95.
10 S. Tanaka, T. Kaneta and H. Yoshida, *Anal. Sci.*, 5 (1989) 217.
11 R.S. Braman, in I.M. Kolthoff and P.J. Elving (Editors), *Treatise on Analytical Chemistry*, Vol. 10, Part II, Wiley, New York, 1975, pp. 37–58.
12 J. Boeseken, *Adv. Carbohydr. Chem.*, 4 (1949) 189.
13 K. W. Fuller and D. H. Northcote, *Biochem. J.*, 64 (1956) 657.
14 R. Piras and E. Cabib, *J. Chromatogr.*, 8 (1962) 63.
15 R. S. Ersser and J. D. Mitchell, *J. Chromatogr.*, 307 (1984) 393.
16 T. Okada and T. Kuwamoto, *Anal. Chem.*, 58 (1986) 1375.

Journal of Chromatography, 498 (1990) 213–221
Elsevier Science Publishers B.V., Amsterdam — Printed in The Netherlands

CHROM. 22 006

ELECTROPHORETIC SEPARATION OF SUGARS AND HYDROLYSATES OF POLYSACCHARIDES ON SILYLATED GLASS-FIBRE PAPER

BEAT BETTLER, RENATO AMADÒ* and HANS NEUKOM
Swiss Federal Institute of Technology, Department of Food Science, ETH-Zentrum, CH-8092 Zurich (Switzerland)
(First received June 5th, 1989; revised manuscript received September 15th, 1989)

SUMMARY

The suitability of silylated glass-fibre paper as a supporting material for the electrophoresis of sugars and hydrolysates of polysaccharides has been studied. Because of the absence of molecular sieving effects by the supporting material, the separation is based only on differences in the molecular charge of the samples. The method described allows the separation of low- and high-molecular-weight substances in the same run.

A mixture of seven sugars was separated into single components within 45 min. To demonstrate the versatility of the method, various polysaccharide hydrolysates were separated electrophoretically. As electrophoresis is based on a different separation principle than chromatographic techniques, this method is considered to be an efficient alternative and/or complement to the chromatography of carbohydrates.

INTRODUCTION

Electrophoresis of carbohydrates has hitherto mainly been performed using paper (cellulose) or unsilylated glass-fibre paper as supporting materials[1–9]. Unfortunately some substantial disadvantages, *e.g.*, a high electroendoosmotic flow, leading to diffuse spots, and adsorption of sample material on the surface of the supporting material, have been demonstrated. Further, paper reacts with many carbohydrate detection reagents, leading to laborious staining procedures.

The aim of this investigation was to develop a simple electrophoretic method that could be used for the rapid identification of sugars and for the characterization of hydrolysates of polysaccharides. Particular attention was given to the choice of the supporting material. Jarvis *et al.*[10] developed an electrophoretic method for the separation of polysaccharides on silylated glass-fibre paper. This technique was successfully used to characterize gelling and thickening agents in foodstuffs[11,12]. Silylated glass-fibre paper does not show any molecular sieving effect, and exhibits a reduced sample adsorption on its surface and a small electroosmotic flow due to the treatment with dimethyldichlorosilane[10,13]. One further advantage compared to other supporting materials (*e.g.*, paper) is that even aggressive chemicals can be used for the detection of carbohydrates after separation.

0021-9673/90/$03.50

The electrophoretic behaviour of different sugars and polysaccharide hydrolysates on silylated glass-fibre paper is described in this paper. The separation is carried out in the presence of sodium tetraborate to form negatively charged carbohydrate–borate complexes. It is known that such complexes are preferentially formed with adjacent *cis*-hydroxyl groups[3,14]. The results obtained demonstrate the suitability of silylated glass-fibre paper as a supporting material for the electrophoresis of neutral sugar mixtures and of polysaccharide hydrolysates. The use of this supporting material makes it possible to separate low- and high-molecular-weight substances in the same run. The versatility of the method is demonstrated by analysing different hydrolysates of polysaccharides. The method turns out to be an alternative and an additional possibility to chromatographic techniques used for the characterization of carbohydrates.

EXPERIMENTAL

Equipment

Electrophoresis on a cooling plate was performed using an LKB (Bromma, Sweden), 2117 Multiphor apparatus.

Suspended-strip electrophoresis was carried out in a Shandon universal chamber (without cooling) for horizontal electrophoresis using a Vokam power supply (Shandon, London, U.K.).

Chemicals

Glass-fibre paper GF/C and filter-paper were obtained from Whatman (Maidstone, U.K.), 10-μl micropipettes from Brand (Wertheim, F.R.G.), Saran film from Dow Chemical (Horgen, Switzerland) and Triton X-100 and Tween 20 from Fluka (Buchs, Switzerland).

All sugars were of analytical-reagent grade and purchased from Fluka, except for the stationary marker 2,3,4,6-tetra-O-methyl-D-glucose (Koch-Light Labs., Colnbrook, U.K.). The polysaccharides were kindly provided by Obipektin (Bischofszell, Switzerland) (sodium pectate), Dow Chemical [methylcellulose Methocel A4C prem. (MC) and hydroxypropylmethylcellulose Methocel F4M prem. (HPMC)] and Kelco (San Diego, CA, U.S.A.) (gellan).

Chloroform, dimethyldichlorosilane, sodium tetraborate decahydrate, ethanol, trifluoroacetic acid (TFA), sulphuric acid (all from Fluka) and 1,3-naphthalenediol (Riedel de Haën, Seelze, F.R.G.) were of analytical-reagent grade.

Preparation of silylated glass-fibre paper

Silylated glass-fibre paper was prepared by modification of the method described by Jarvis *et al.*[10]. For electrophoresis on the cooling plate the glass-fibre paper was cut into strips 25.6 cm in length and for suspended-strip electrophoresis 16 cm in length. Organic material in the glass-fibre paper was removed by heating at 400°C for 2 h. Silylation was performed by immersion of the glass-fibre paper in 5% (w/w) dimethyldichlorosilane solution in chloroform for 24 h at room temperature. Before use the strips were rinsed in toluene and dried.

Hydrolysis of polysaccharides

Polysaccharide samples (10 mg) were hydrolysed with 2 *M* TFA (1 ml) in a nitrogen atmosphere at 120°C for 1 h in an oil-bath, using Pyrex screw-capped hydrolysis tubes (Auer-Bittmann-Soulié, Dietikon, Switzerland). After hydrolysis, TFA was removed by a stream of compressed air at room temperature. Residual TFA was removed from the hydrolysate by washing three times with 1 ml of deionized water and repeating the above procedure. Finally, the hydrolysate was dissolved in 0.5–2 ml of deionized water. Hydrolysates containing uronic acid lactones were treated with dilute sodium hydroxide solution (pH $\leqslant 8$) to yield the free uronic acids[15,16].

Sugar and marker solutions

Aqueous sugar solutions (0.2%, w/v) and an aqueous sugar mixture containing 0.2% (w/v) of each component (sucrose, maltose, rhamnose, mannose, glucose and galacturonic acid) were prepared. Aqueous marker solutions of MC and sodium pectate were prepared at a concentration of 0.25% (w/v).

Electrophoresis

Cooled plate method. Silylated glass-fibre paper was soaked for 1 day in a buffer solution (0.05 *M* sodium tetraborate solution, pH 9.2) containing 0.2% (v/v) Triton X-100. Excess of electrolyte was removed by slightly blotting the wet silylated glass-fibre paper before use. Wicks of filter-paper (Whatman No. 3) were wrapped in Saran film, taking care that no air bubbles remained trapped between the cooling plate and the glass-fibre paper. The system was pre-equilibrated for 15 min under the running conditions, then samples (5–15 μl) were applied to the supporting material as a fine uniform line (1–2 cm long) by the aid of a micropipette. Electrophoresis was performed at a constant current of 40 mA, resulting in a potential gradient of about 30 V/cm when a strip width of 8.5 cm was used. Cooling was achieved by running tap water of 8–10°C. Separation was achieved within 45 min. Glucose (M_{Glc}) was used as a mobility marker, whereas low-viscosity MC or 2,3,4,6-tetra-O-methyl-D-glucose served as a stationary marker.

Suspended-strip method. For the suspended strip technique the procedure described by Bettler *et al.*[12] was adopted.

Staining

A 0.2-g amount of 1,3-naphthalenediol was dissolved in 100 ml of ethanol; 4 ml of concentrated sulphuric acid were added before use. The separated carbohydrates were located by thoroughly spraying both sides of the hot air-dried electrophoresis strips (hair dryer) with the staining reagent. Heating at 110°C allowed the colour to develop in about 10 min.

Determination of the electrophoretic mobility, M_e

The electrophoretic mobility, M_e, was determined by calculating the ratio of the distance between the substance and stationary marker to the distance between the mobility marker [glucose (M_{Glc}) or sodium pectate ($M_{Pect.}$)] and the stationary marker.

RESULTS AND DISCUSSION

Electroendoosmosis, stationary and mobility marker

Stationary markers were used in order to take into account additional factors affecting the separation, such as electroendoosmosis of the dimethyldichlorosilane-treated support material or heating effects. Experiments with the stationary marker 2,3,4,6-tetra-O-methyl-D-glucose, which exhibits no complexation with borate, resulted in a migration on the cooling plate of approximately 3–5 cm/h towards the cathode. With the suspended-strip method, the endoosmotic flow was almost suppressed (0–1 cm/h) owing to the superimposed heating effect during the run. In comparative experiments tetramethylated glucose and low-viscosity MC exhibited the same migration properties. As MC showed a smaller diffusion, this polysaccharide was chosen as the preferred stationary marker.

For calculation of the electrophoretic mobilities of the separated sugars, glucose and sodium pectate were used as mobility markers. Glucose has commonly been used as a mobility marker to calculate the electrophoretic mobilities of mono- and oligosaccharides[17]. In this work, glucose was used as a mobility marker for the electrophoresis on the cooling plate, the mobility being 12.5 cm with respect to the stationary marker. On the other hand, sodium pectate has already been used for this purpose for the electrophoresis of polysaccharides on silylated glass-fibre paper[12]. Because of its minimal diffusion properties, this substance is especially suitable for suspended-strip electrophoresis. Comparison with other published data was possible by converting the $M_{\text{Pect.}}$ data from suspended-strip electrophoresis into M_{Glc} data by division by 0.91.

Electrophoresis of sugar mixtures

Glass-fibre paper shows a small electrophoretic resistance, thus allowing the use of higher potential gradients, leading to shorter analysis times compared with electrophoresis on other supporting materials. The small electrophoretic resistance allows the use even of simple suspended-strip electrophoresis (Fig. 1). Electrophoresis on a cooled plate allows much higher potential gradients to be used than in uncooled suspended-strip electrophoresis, thus leading to a better separation in a shorter time. The resolution is improved and diffusion is reduced (Fig. 2).

The mobilities obtained by electrophoresis on silylated glass-fibre paper (Table I) are comparable to those described for electrophoresis on cellulose paper and on unsilylated glass-fibre paper (reproducibility 4–7%[17]). The same mobility values are obtained by using electrophoresis on a cooled plate or the uncooled suspended-strip technique.

Electrophoresis of polysaccharide hydrolysates

One of the general methods for the partial characterization of polysaccharides is hydrolysis to their monomeric constituents and subsequent analysis by gas chromatography (GC) or thin-layer chromatography (TLC)[18–20]. As pointed out by Friese[20], it is very difficult to perform acid hydrolysis of polysaccharides quantitatively because of incomplete hydrolysis (different stability of the glycosidic linkages towards acids[21] and losses due to subsequent reactions. Further, many decomposition products undergo reversion reactions.

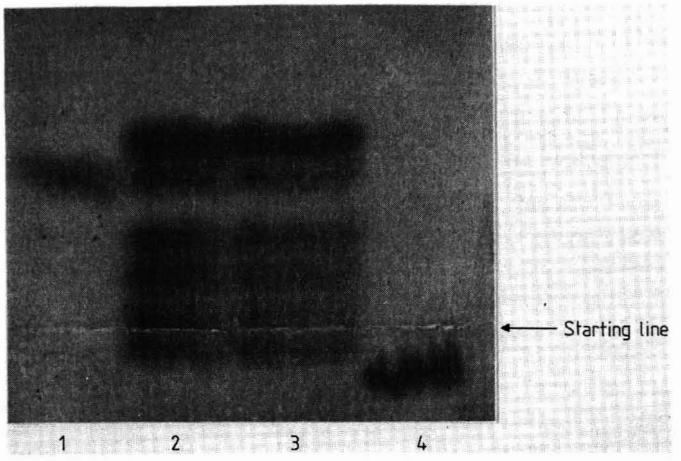

Fig. 1. Suspended-strip electrophoresis of sugars. 0.05 *M* borax (pH 9.2), 6 V/cm, 90 min, detection with 1,3-naphthalenediol reagent. 1 = Glucose (mobility marker), 10 μl; 2 and 3 = mixture of sucrose, rhamnose, maltose, mannose, glucose, 5 μl, and galacturonic acid, 10 μl; 4 = MC (stationary marker) 10 μl.

In contrast to most chromatographic techniques (*e.g.*, GC), electrophoresis on silylated glass-fibre paper detects most of the degradation products. This method permits the analysis of both low-(monosaccharides, oligosaccharides) and high-molecular-weight carbohydrates (polysaccharides[1,2]) in the same run. As electrophoretic separations are based on a different principle than chromatographic methods,

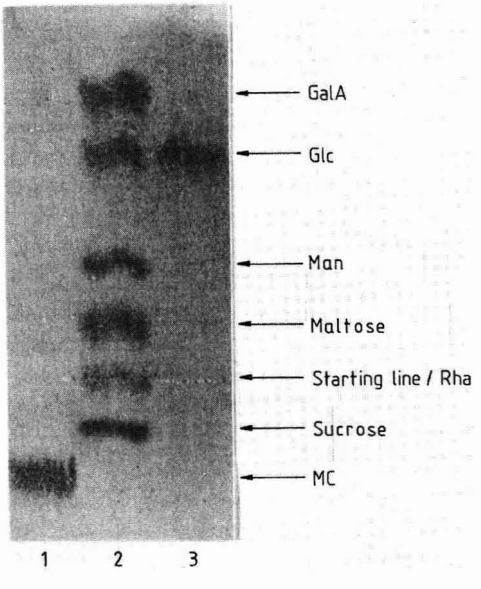

Fig. 2. Electrophoresis on a cooling plate of sugars. 0.05 *M* borax (pH 9.2), 40 mA, 45 min, detection with 1,3-naphthalenediol reagent. 1 = MC (stationary marker), 10 μl; 2 = mixture of sucrose, rhamnose, maltose, mannose, glucose, 5 μl and galacturonic acid, 10 μl; 3 = glucose (mobility marker), 10 μl.

TABLE I

ELECTROPHORETIC MOBILITIES OF CARBOHYDRATES ON SILYLATED GLASS-FIBRE PAPER EXPRESSED AS $M_{Pect.}$ AND M_{Glc}

Electrophoresis on a cooling plate, 0.05 *M* borax (pH 9.2) 40 mA, 45 min.

Mobility reference	$M_{Pect.}$	M_{Glc}
Mannose	0.63	0.69
Galactose	0.82	0.90
Lactose	0.38	0.42
Maltose	0.31	0.34
Sucrose	0.15	0.16
Glucose	0.91	1.00
Arabinose	0.83	0.91
Fructose	0.80	0.88
Xylose	0.91	1.00
Rhamnose	0.46	0.50
Galacturonic acid	1.09	1.20

the use of electrophoresis is suitable for a first characterization of polysaccharide hydrolysates especially for partially hydrolysed polysaccharides.

Electrophoretic patterns of MC and HPMC on the cooling plate are shown in Fig. 3. Commercially available MCs have degrees of substitution between 1.64 and 1.92[22]. In Table II the substitution pattern of MC is given together with the corresponding electrophoretic mobilities on cellulose paper as determined by Foster[1].

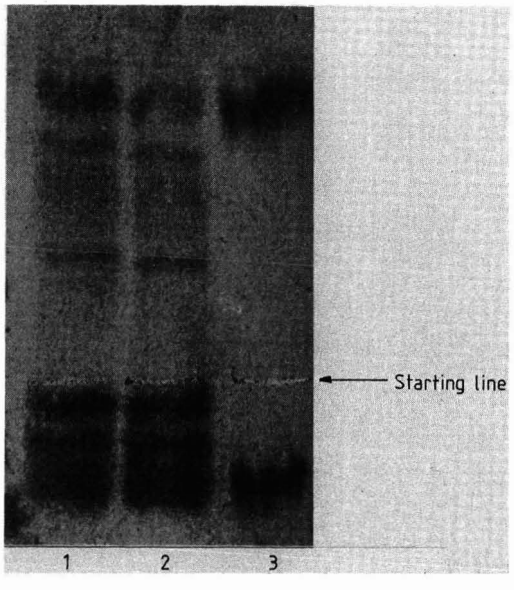

Fig. 3. Electrophoresis on a cooling plate of hydrolysates of cellulose derivatives. 0.05 *M* borax (pH 9.2), 40 mA, 45 min, detection with 1,3-naphthalenediol reagent. 1 = Hydrolysate HPMC, 10 μl; 2 = hydrolysate MC, 10 μl; 3 = mixture of MC (stationary marker) and glucose (mobility marker), 10 μl.

TABLE II

GLUCOSE ETHER SUBSTITUTION PATTERN OF MC WITH REFERENCE MOBILITIES (M_{Glc}) AND MIGRATION ZONES OF MC HYDROLYSATE

Conditions as in Table I. The formation of traces of additional glucose ethers (terminal constituents) is possible.

Glucose ether	M_{Glc} [a]	M_{Glc} *migration zones, hydrolysate of MC* [b]
Unsubstituted glucose	1.00	1.00
2-O-Methylglucose	0.23	0.21
3-O-Methylglucose	0.80	0.86
6-O-Methylglucose	0.80	0.86
2,3-Di-O-methylglucose	0.12	0.14
2,6-Di-O-methylglucose	–	–
3,6-Di-O-methylglucose	–	–
2,3,6-Tri-O-methylglucose and incompletely hydrolysed MC	0.00	0.00
No reference mobility	–	0.58
No reference mobility	–	1.07

[a] Ref. 1.

[b] According to the electrophoretic mobilities, M_{Glc}, assigned to the glucose ethers.

According to these reference mobilities, the zones of the electrophorograms obtained on the cooling plate were assigned to the different glucose ethers (Table II); 2,6- and 3,6-di-O-methyl-D-glucose could not be assigned because of lack of corresponding reference mobilities. Throughout the whole migration area, further diffuse zones are visible. These may be explained by additional degradation products caused by incomplete acid hydrolysis of the analysed MC.

HPMC is an MC that has been additionally reacted with small amounts of

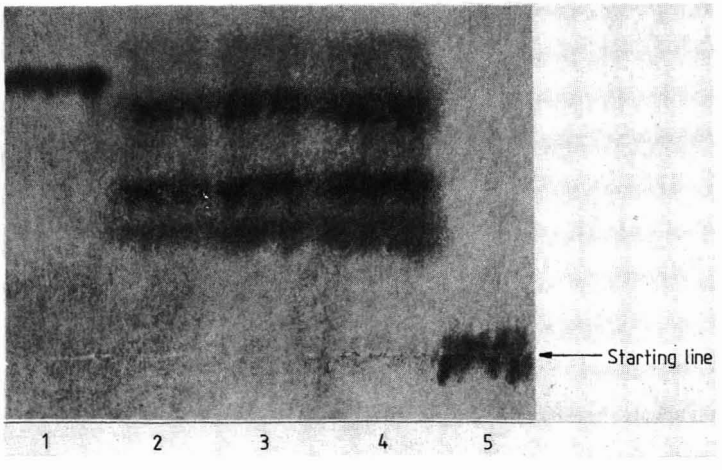

Fig. 4. Suspended-strip electrophoresis of a hydrolysate of gellan. 0.05 *M* borax (pH 9.2), 6 V/cm, 90 min, detection with 1,3-naphthalenediol reagent. 1 = Sodium pectate (mobility marker), 10 μl; 2, 3 and 4 = hydrolysate gellan, 5, 10 and 15 μl, respectively; 5 = MC (stationary marker), 10 μl.

propylene oxide. The HPMC used in this work contained 27–30% methoxy and 4–7.5% hydroxypropyl groups[22]. After electrophoresis, the HPMC hydrolysate shows the same electrophoretic pattern as MC. This can be explained by the same content of methoxy groups in MC and HPMC. The low degree of hydroxypropyl substitution has no influence on the electrophoretic pattern.

As an example of the electrophoresis of polysaccharide hydrolysates, the suspended-strip electrophoresis of a gellan hydrolysate is shown in Fig. 4. Gellan is a polysaccharide containing rhamnose, glucose and glucuronic acid in a molar ratio of 1:2:1[23]. On the basis of results obtained by electrophoresis of free sugars (Table I), three of the four migration zones were assigned to rhamnose, glucose and glucuronic acid. The unidentified migration zone ($M_{Pect.}$ 0.62) shows the mobility of mannose. This sugar can be excluded because it is not a constituent of gellan. This was confirmed by GC analysis, where no mannose could be detected[24]. Miles *et al.*[23] described the high stability of the glucuronic acid–(1,4)-glucose linkage. It is assumed that the unidentified zone represent an aldobiuronic acid (glucuronosylglucose) obtained by incomplete hydrolysis of gellan. This would also explain the low glucose:rhamnose ratio of 1.43:1 as determined by GC[24]. Similarly, other polysaccharides containing uronic acids could also, on incomplete hydrolysis, form acid resistant fragments such as aldobiuronic acids.

This investigation has clearly shown that electrophoresis on silylated glass-fibre paper could be used as a method of choice for a rapid characterization of polysaccharides. The advantages of electrophoresis over other separation and identification techniques are that electrophoresis needs only modest instrumentation, the silylation of glass-fibre paper is simple and several strips can be prepared at the same time. The electrophoretic method needs no derivatization procedure and allows the detection of most of the degradation products. Especially interesting is the fact that high- and low-molecular-weight carbohydrates can be separated in the same run. Electrophoresis may also be helpful for the confirmation of gas chromatograms, for example, by revealing sugar constituents or higher molecular weight fragments not detectable by GC. Finally, electrophoresis is an efficient alternative and complement to TLC methods[21,25] for the screening of polysaccharide hydrolysates. Sugar constituents difficult to separate by TLC often are easily separated by electrophoresis in a short time.

REFERENCES

1 A. B. Foster, *Adv. Carbohydr. Chem.*, 12 (1957) 81.
2 J. L. Frahn and J. A. Mills, *Aust. J. Chem.*, 12 (1959) 65.
3 H. Weigel, *Adv. Carbohydr. Chem.*, 18 (1963) 61.
4 A. Haug and B. Larsen, *Acta Chem. Scand.*, 15 (1961) 1395.
5 J. A. Rendlemann, *Adv. Carbohydr. Chem.*, 21 (1966) 209.
6 M. J. St. Cyr, *J. Chromatogr.*, 47 (1970) 284.
7 S. J. Angyal and J. A. Mills, *Aust. J. Chem.*, 32 (1979) 1993.
8 S. Stoll and Y. Prat, *Ann. Falsif. Expert. Chim.*, 54 (1962) 159.
9 E. J. Bourne,A. B. Foster and P. M. Grant, *J. Chem. Soc.*, (1956) 4311.
10 M. C. Jarvis, D. R. Threlfall and J. Friend, *Phytochemistry*, 16 (1977) 849.
11 H. Schäfer and H. Scherz, *Z. Lebensm.-Unters.-Forsch.*, 77 (1983) 193.
12 B. Bettler, R. Amadò and H. Neukom, *Mitt. Geb. Lebensmittelunters. Hyg.*, 76 (1985) 69.
13 G. Bonn, M. Grünwald, H. Scherz and O. Bobleter, *J. Chromatogr.*, 370 (1986) 485.
14 E. A. Malcolm, J. W. Green and H. A. Swenson, *J. Chem. Soc.*, (1964) 4669.

15 O. Raunhardt, H. W. H. Schmidt and H. Neukom, *Helv. Chim. Acta*, 50 (1967) 1267.
16 J. D. Blake and G. N. Richards, *Carbohydr. Res.*, 8 (1968) 275.
17 S. C. Churms (Editor), in G. Zweig and J. Sherma (Editors in Chief), *Handbook of Chromatography, Carbohydrates*, Vol. 1, CRC Press, Boca Raton, FL, 1982, p. 155.
18 E. Mergenthaler and H. Scherz, *Z. Lebensm.-Unters.-Forsch.*, 162 (1976) 25.
19 A. Preuss and H. P. Thier, *Z. Lebensm.-Unters.-Forsch.*, 179 (1984) 17.
20 P. Friese, *Fresenius Z. Anal. Chem.*, 301 (1980) 389.
21 R. R. Selvendran and M. S. DuPont, in R. D. King (Editor), *Developments in Food Analysis Techniques 3*, Elsevier Applied Science, Barking, New York, 1984, p. 1.
22 M. Glicksmann, *Food Hydrocolloids*, Vol. III, CRC Press, Boca Raton, FL, 1986, p. 121.
23 M. J. Miles, V. J. Morris and M. A. O'Neill, in G. O. Philipps, D. J. Wedlock and P. A. Williams (Editors), *Gums and Stabilisers for the Food Industry 2*, Pergamon Press, Oxford, New York, Toronto, Sidney, Paris, Frankfurt, 1984 p. 485.
24 B. Bettler, *PhD Thesis*, No. 8501, ETH, Zürich, 1988.
25 B. Mann, *J. Chromatogr.*, 407 (1987) 369.

Journal of Chromatography, 498 (1990) 223–230
Elsevier Science Publishers B.V., Amsterdam — Printed in The Netherlands

CHROM. 22 007

ELECTROPHORESIS OF URONIC ACIDS, NEUTRAL SUGARS AND HYDROLYSATES OF ACIDIC POLYSACCHARIDES ON SILYLATED GLASS-FIBRE PAPER IN ELECTROLYTES OF BIVALENT CATIONS

BEAT BETTLER, RENATO AMADÒ* and HANS NEUKOM
Swiss Federal Institute of Technology, Department of Food Science, ETH-Zentrum, CH-8092 Zurich (Switzerland)
(First received June 5th, 1989; revised manuscript received September 15th, 1989)

SUMMARY

The separation of different uronic acids, oligogalacturonic acids and neutral sugars by electrophoresis on silylated glass-fibre paper is described. As electrolytes 0.1 *M* solutions of barium, zinc and calcium acetate were used. In these solutions the separation of acid constituents was possible without interference from neutral sugars. Depending on the electrolytes, a mixture of galacturonic, mannuronic, glucuronic and guluronic acid was separatad within 90–165 min. The partial characterization of acid polysaccharides such as pectin, alginate and mixtures thereof is described.

INTRODUCTION

Different workers have described the electrophoretic separation of uronic acids or glycosaminoglycans, having uronic acids as monomeric constituents, in electrolytes containing bivalent metal ions, using cellulose or derivatives thereof as supporting materials[1–7]. A review of previous work was published by Deyl[8].

In our previous work[9], electrophoresis on silylated glass-fibre paper was used to separate neutral sugars and polysaccharide hydrolysates. Compared with supporting materials such as cellulose acetate and cellulose paper, the chemically inert glass-fibre paper exhibits different advantages, such as small electroendoosmotic flow and little adsorption of the sample at the surface, and permits the staining of the separated substances even with aggressive chemical reagents. Further, electrophoresis on glass-fibre paper allows the simultaneous separation of low- and high-molecular-weight substances. The 0.05-*M* borate buffer (pH 9.2) used gives good separations of neutral sugars. However, this buffer system is not suitable for the separation of uronic acids.

The aim of this investigation was to develop an electrophoretic method that could be used for the identification of uronic acids and other hydrolysis products of acidic polysaccharides without interference from occasionally present neutral sugars.

In the experiments described here, electrophoresis on silylated glass-fibre paper was used for this purpose. Various electrolyte systems were tested (as described by

0021-9673/90/$03.50

Deyl[8]), in order to achieve optimal separations. Further, the possibility of characterizing acidic polysaccharides after hydrolysis without previous fractionation and/or derivatization processes is demonstrated.

EXPERIMENTAL

Equipment

For electrophoresis an LKB (Bromma, Sweden) 2117 Multiphor instrument equipped with a cooling plate was used.

Chemicals

Zinc acetate dihydrate, calcium acetate and barium acetate, all of analytical-reagent grade, were purchased from Fluka (Buchs, Switzerland). The following reference substances were used: oligogalacturonic acids (prepared by enzymatic degradation of sodium pectate and separated according to Hasegawa and Nagel[10]), galacturonic acid (GalA), glucuronic acid (GlcA), mannuronic acid (ManA) lactone and myo-inositol (Sigma, St. Louis, MO, U.S.A.), guluronic acid (GulA) [not available commercially; a hydrolysate of sodium alginate or propylene glycol alginate with 2 *M* trifluoroacetic acid (TFA) containing sufficient GulA was used[9]]. Apple pectins, degree of esterification (*DE*) 37% and 73% and amidated pectin, degree of amidation (*DA*) 28.6% and 18.4% were obtained from Obipektin (Bischofszell, Switzerland), sodium alginate and propylene glycol alginate from Kelco (San Diego, CA, U.S.A.), Protan (Drammen, Norway) and Fluka (Buchs, Switzerland).

Hydrolysis of polysaccharides

The preparation of polysaccharide hydrolysates was performed as described in the accompanying paper[9].

Electrolytes

Solutions (0.1 *M*) of zinc, barium and calcium acetate in deionized, deaerated water were used as electrolytes for the electrophoretic experiments.

Electrophoresis

Electrophoresis was carried out at a constant current of 50 mA. Depending on the electrolyte used, a potential gradient of 16–26 V/cm was built up. The system was cooled with tap water at 8–10°C and equilibrated for 15 min prior to sample application. The time needed for optimum separation of the samples was dependent on the electrolyte–buffer used. Electrophoresis in zinc and calcium acetate solution was carried out for 90–120 min and in barium acetate solution for up to 165 min. The current was increased to 70 mA in this buffer system. After each electrophoretic run, the platinum electrodes were cleaned in 1 *M* hydrochloric acid. With calcium acetate buffer, the electrodes had to be cleaned from deposits during the electrophoretic run to prevent a sudden increase in the potential gradient. With glucose (Glc) taken as zero, the mobilities were measured and expressed relative to the mobility of glucuronic acid (GlcA) and reported as M_{GlcA}.

The migration zones were stained with 1,3-naphthalenediol reagent[9]. For the detection of cyclitols, the glass-fibre paper was sprayed with a 0.5% (w/v) solution of potassium permanganate in 1 *M* sodium hydroxide.

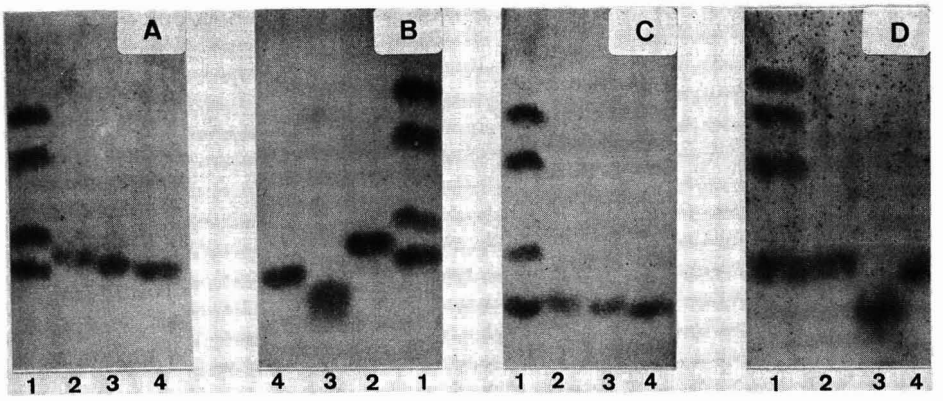

Fig. 1. Electrophoresis of uronic acids and neutral sugars. 0.1 *M* electrolytes of bivalent cations; detection with 1,3-naphthalenediol reagent. (A) 0.1 *M* barium acetate (70 mA, 125 min): 1 = uronic acid mixture (GalA, ManA and GlcA)–Glc; 2 = 2,3,4,6-tetra-O-methyl-D-Glc; 3 = Rha; 4 = Ara. (B) 0.1 *M* barium acetate (70 mA, 140 min): 1 = uronic acid mixture–Glc; 2 = 2,3,4,6-tetra-O-methyl-D-Glc; 3 = Rib; 4 = Frc. (C) 0.1 *M* zinc acetate (50 mA, 120 min): 1 = uronic acid mixture–Glc; 2 = 2,3,4,6-tetra-O-methyl-D-Glc; 3 = Man; 4 = Gal. (D) 0.1 *M* calcium acetate (50 mA, 120 min): 1 = uronic acid mixture–Glc; 2 = 2,3,4,6-tetra-O-methyl-D-Glc; 3 = Rib; 4 = Frc.

RESULTS AND DISCUSSION

Migration properties of uronic acids

In the electrophoresis, a reference mixture composed of Glc (mobility taken as zero), ManA, GalA and GlcA (mobility marker) was applied. The separation of the examined acids was complete in all three electrolytes used (Fig. 1). The mobility values determined in the zinc and calcium acetate solutions corresponded to those obtained by St. Cyr[2] (Table I). However, the mobility values in the barium acetate solution are

TABLE I

ELECTROPHORETIC MOBILITIES (M_{GlcA}) OF URONIC ACIDS ON SILYLATED GLASS-FIBRE PAPER

0.1 *M* electrolytes of bivalent cations, 50 mA for zinc and calcium acetate and 70 mA for barium acetate, 90–165 min.

Uronic acid	*Barium acetate*		*Zinc acetate*		*Calcium acetate*	
	M_{GlcA}[a]	*Cyr*[b]	M_{GlcA}[a]	*Cyr*[b]	M_{GlcA}[a]	*Cyr*[b]
Glucuronic acid	1.00	1.00	1.00	1.00	1.00	1.00
Mannuronic acid	0.74	0.79	0.76	0.75	0.81	0.77
Galacturonic acid	0.24	0.42	0.30	0.30	0.55	0.50
Guluronic acid[c]	—[d]	0.26	0.41	0.44	0.41	0.40

[a] Mobility of Glc taken as zero.

[b] Electrophoretic mobilities (M_{GlcA}) determined by St. Cyr[2]. Mobility of myo-inositol taken as zero.

[c] No reference substance available. Mobility determined by electrophoresis of an alginate hydrolysate.

[d] Mobility in the range of neutral sugars.

different. As will be discussed below, this cannot be explained by the fact that St. Cyr used a different marker as zero (myo-inositol). Miyamoto and Nagase[3] reported a poor resolution of uronic acids using barium acetate buffer. This finding conflicts with our results obtained with electrophoresis on silylated glass-fibre paper (Fig. 1A and B), which gave a clear separation of uronic acids.

It is important that all lactones of the uronic acids be transformed into the acidic form prior to electrophoresis. Treatment with sodium hydroxide to split lactones must be done according to the method described previously[11]. Excess of sodium hydroxide should be avoided, and the pH should not be higher than 8.

Migration properties of neutral sugars

The high-voltage electrophoresis experiments of Angyal and Mills[7] with sugars, sugar derivatives and cyclitols showed that an axial–equatorial–axial sequence of three hydroxyl groups on a six-membered ring or three consecutive *cis*-hydroxyl groups on a five-membered ring form a favourable arrangement for complex formation with metal cations. Carbohydrates lacking this sequence exhibit only poor mobility. The common sugars in polysaccharides do not form strong complexes. Ribose, a frequent sugar in nature, has the required sequence for complex formation. However, this sugar is not a constituent of polysaccharides. In electrophoresis, complexed neutral sugars move towards the cathode and therefore do not interfere with uronic acids, which move towards the anode.

For the calculation of mobility values, the mobility of Glc was taken as zero. To compare the mobility values with literature data, the cathodic migration of Glc relative to the stationary marker 2,3,4,6-tetra-O-methyl-D-Glc was determined in all three electrolytes used. In addition, the migration properties of some common constituents of polysaccharides, galactose (Gal), rhamnose (Rha), mannose (Man) and arabinose

TABLE II

ELECTROPHORETIC MOBILITIES (M_{GlcA}) OF NEUTRAL SUGARS ON SILYLATED GLASS-FIBRE PAPER IN 0.1 *M* BARIUM ACETATE (70 mA, 120–165 min) WITH RESPECT TO 2,3,4,6-O-TETRAMETHYL-D-GLUCOSE AND GLUCOSE

Mobility taken as zero	M_{GlcA}	
	2,3,4,6-Tetra-O-methyl-D-glucose	*Glucose*
Glucose	−0.08	0.00
Arabinose	−0.12	−0.03
Mannose	−0.12	−0.04
Galactose	−0.09	−0.01
Rhamnose	−0.07	0.00
Fructose	−0.20	−0.11
Ribose	−0.35	−0.26
Myo-inositol	−[a]	−0.10
2,3,4,6-Tetra-O-methyl-D-glucose	0.00	−0.08

[a] No experimentally determined mobility value. Simultaneous staining of 2,3,4,6-tetra-O-methyl-D-Glc and myo-inositol is not possible with the detection reagent. Referring to eqn. 3 a mobility of M_{GlcA} −0.19 is calculated.

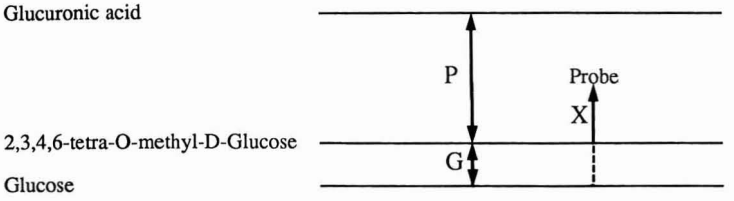

Fig. 2. Conversion of M_e values.

(Ara), were investigated. Ribose (Rib), a sugar forming strong complexes, and fructose (Frc) were also examined.

In 0.1 *M* barium acetate, Glc shows M_{GlcA} −0.08 relative to the stationary marker 2,3,4,6-tetra-O-methyl-D-Glc (Table II, Fig. 1A and B). For comparative purposes, all mobilities in the Tables I–III can be converted to values relative to 2,3,4,6-tetra-O-methyl-D-Glc, as follows (Fig. 2):

$$M_{e1} = (X + G)/(P + G) \tag{1}$$

$$M_{e2} = X/P \tag{2}$$

where $M_{e1} = M_e$ value with Glc taken as zero mobility and $M_{e2} = M_e$ value with 2,3,4,6-tetra-O-methyl-D-Glc as stationary marker. Extension of eqn. 1 with P/P gives

$$M_{e1} = (X/P + G/P)/(P/P + G/P) = (M_{e2} + G/P)/(1 + G/P)$$

leading to

$$M_{e2} = M_{e1}(1 + G/P) - G/P \tag{3}$$

The ratio G/P was determined experimentally and has a value of 0.08 in 0.1 *M* barium acetate.

In the experiments of St. Cyr[2], the mobility of myo-inositol was taken as zero. In 0.1 *M* barium acetate, different mobility data were obtained for the uronic acids. To check whether this is a consequence of the different markers taken as zero, the mobility of myo-inositol was also determined. Myo-inositol shows a mobility of M_{GlcA} −0.10 relative to glucose. Even taking into consideration the higher cathodic movement of myo-inositol, the mobility values of St. Cyr are not comparable to those obtained in our experiments. Ribose, as expected, has the highest mobility in 0.1 *M* barium acetate (Fig. 1B). In contrast to other sugars, ribose migrates as a diffuse zone. The distance for the determination of the electrophoretic mobility of ribose was measured in the zone centre. For the mobilities of the other neutral sugars, see Table II.

In 0.1 *M* zinc acetate, the tested neutral sugars had no measurable cathodic movement (Fig. 1C).

In 0.1 *M* calcium acetate, only a slight migratory difference was observed between the stationary marker 2,3,4,6-tetra-O-methyl-D-Glc and unsubstituted Glc. All sugars examined showed a small cathodic movement. Ribose exhibits the highest mobility as on electrophoresis in a barium acetate electrolyte (Fig. 1D).

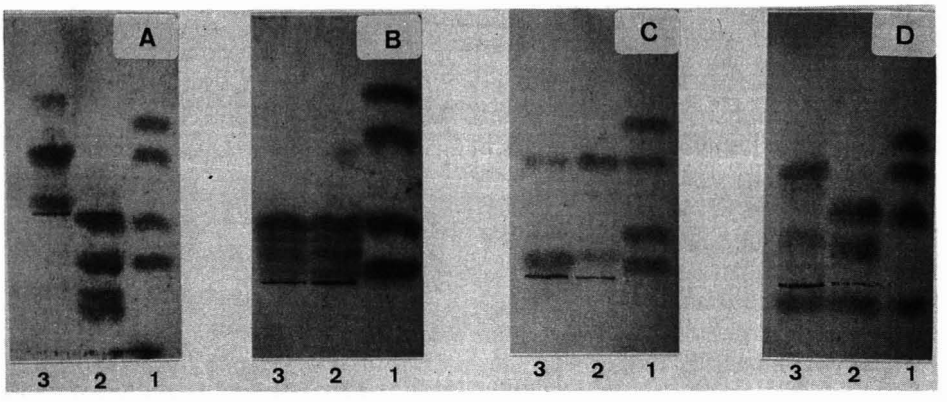

Fig. 3. Electrophoresis of polysaccharide hydrolysates. 0.1 *M* electrolytes of bivalent cations, detection with 1,3-naphthalenediol reagent. (A) 0.1 *M* zinc acetate (50 mA, 90 min): 1 = uronic acid mixture (GalA–ManA and GlcA)–Glc; 2 = hydrolysate of pectin (*DE* 37%); 3 = hydrolysate of propylene glycol alginate. (B) 0.1 *M* barium acetate (70 mA, 165 min): 1 = uronic acid mixture–Glc; 2 = hydrolysate of amidated pectin; 3 = hydrolysate of pectin (*DE* 37%). (C) 0.1 *M* barium acetate (70 mA, 120 min): 1 = uronic acid mixture–Glc; 2 = hydrolysate of propylene glycol alginate; 3 = hydrolysate of sodium alginate. (D) 0.1 *M* calcium acetate (50 mA, 120 min): 1 = uronic acid mixture–Glc; 2 = hydrolysate of pectin (*DE* 73%); 3 = hydrolysate of sodium alginate.

Migration properties of polysaccharide hydrolysates

The electrophoresis method described in this paper is especially suitable for the characterization of hydrolysates of acidic polysaccharides, as uronic acids are efficiently separated. The separation is not disturbed by neutral sugars, hence a selective analysis of the acidic constituents in polysaccharides without interference from neutral sugars is possible. Further, the method is also suitable for the characterization of partially hydrolysed acidic polysaccharides, the separation of low- and high-molecular-weight degradation products in the same run being possible.

As typical examples, the zone patterns obtained by electrophoresis of hydrolysates of pectins, alginates and propylene glycol alginates are discussed. These polysaccharides are easy to distinguish by their different uronic acid constituents (Fig. 3A–D). Hydrolysates of pectins show identical zone patterns independently of *DE* and *DA*. Propylated derivatives of alginates also have a zone pattern independent of *DE*.

TABLE III

ELECTROPHORETIC MOBILITIES (M_{GalA}) OF GALACTURONIC ACID OLIGOMERS ON SILYLATED GLASS-FIBRE PAPER

0.1 *M* electrolytes of bivalent cations, 50 mA for zinc and calcium acetate and 70 mA for barium acetate 90–165 min.

Electrolyte (0.1 M)	*Mono-GalA*	*Di-GalA*	*Tri-GalA*	*Penta-GalA*
Zinc acetate	0.30	0.00	−0.27	−0.40
Barium acetate	0.24	0.18	0.11	0.06
Calcium acetate	0.55	0.40	0.32	0.27

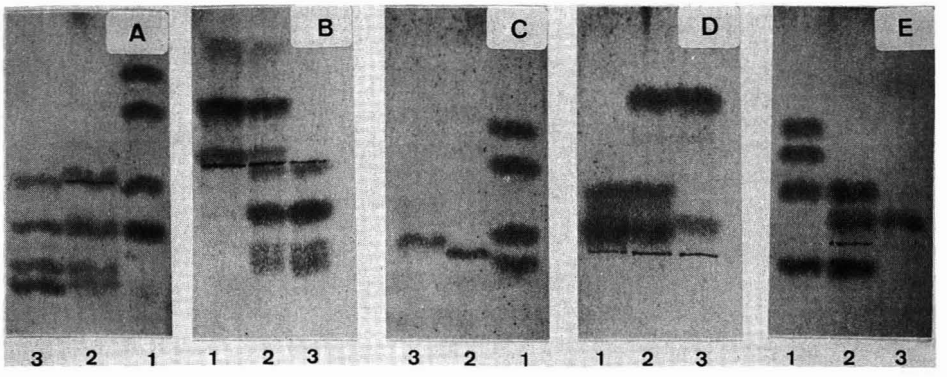

Fig. 4. Electrophoresis of hydrolysates of polysaccharide mixtures and oligo-GalA. 0.1 *M* electrolytes of bivalent cations, detection with 1,3-naphthalenediol reagent. (A) 0.1 *M* zinc acetate (50 mA, 115 min): 1 = uronic acid mixture (GalA, ManA and GlcA)–Glc; 2 = hydrolysate of amidated pectin; 3 = GalA oligomer mixture (mono-, di-, tri-, penta-GalA). (B) 0.1 *M* zinc acetate (50 mA, 120 min): 1 = hydrolysate of propylene glycol alginate; 2 = hydrolysate of mixture of propylene glycol alginate–pectin (*DE* 73%); 3 = pectin (*DE* 73%). (C) 0.1 *M* barium acetate (70 mA, 120 min): 1 = uronic acid mixture–Glc; 2 = penta-GalA; 3 = di-GalA. (D) 0.1 *M* barium acetate (70 mA, 120 min): 1 = hydrolysate of pectin (*DE* 73%); 2 = hydrolysate of mixture of pectin (*DE* 73%)–propylene glycol alginate; 3 = hydrolysate of propylene glycol alginate. (E) 0.1 *M* calcium acetate (50 mA, 95 min): 1 = uronic acid mixture–Glc; 2 = hydrolysate of pectin (*DE* 73%); 3 = GalA oligomer mixture (di-, tri-, penta-GalA).

In addition to the zones of galacturonic acid and neutral sugars, pectins form additional cathodic moving spots (Fig. 3A, Table III) in 0.1 *M* zinc acetate. The components of a mixture of oligo-GalA (mono-, di-, tri- and penta-GalA) are separated using zinc acetate as electrolyte (Fig. 4A). Di-GalA has almost zero mobility. Obviously, the zinc complexation shifts di-GalA to a nearly neutral form. The fractions with M_{GlcA} −0.27 and −0.34 to −0.45 have the mobilities of tri- and penta-GalA, respectively. Penta-GalA forms a distinct zone. The corresponding zone in pectin hydrolysates is broader. This is explained by the fact that tetra-GalA is not completely separated from penta-GalA. A reference sample of tetra-GalA was not available. Even in mixtures with pectins, alginates are easily detected by their uronic acid constituents (Fig. 4B). Alginates form an additional weak zone of M_{GlcA} 1.13 in addition to the two uronic acid fractions. This zone possibly originates from incomplete acid hydrolysis or subsequent reactions. Neutral sugar fractions are detectable in sugar-standardized samples. In addition to the formation of distinct zones, a diffuse smear is visible, probably also as consequence of subsequent reactions during incomplete hydrolysis. Only electrophoresis in zinc acetate produces fractions moving towards the cathode. In 0.1 *M* barium acetate solutions oligo-GalA shows a low mobility on electrophoresis (Fig. 4C, Table III). In pectin hydrolysates, oligo-GalA separates only after a prolonged analysis time. In the hydrolysates of alginates, distinction of GulA from the neutral sugar fraction is difficult. However, alginates are easily identified in mixtures with pectins by the constituent ManA (Fig. 4D). In 0.1 *M* calcium acetate solutions, GulA has a slightly higher mobility than oligo-GalA in pectin hydrolysates (Figs. 3D and 4E, Table III). An identification of the components of a pectin–alginate mixture is possibly by identification of GalA and ManA.

An analysis of acidic constituents by electrophoresis in electrolytes of bivalent cations improves the electrophoresis in borate solutions. Acidic polysaccharides are easily characterized by differences in their uronic acid constituents. In addition to the characterization of acidic polysaccharides, a possible application of this method is the analysis of gelling and thickening agents, especially those which cannot be differentiated by electrophoresis as intact polysaccharides[12].

ACKNOWLEDGEMENT

The authors thank Miss M. Fischer for her help in preparing the manuscript.

REFERENCES

1 A. Haug and B. Larsen, *Acta Chem. Scand.*, 15 (1961) 1395.
2 M. J. St. Cyr, *J. Chromatogr.*, 47 (1970) 284.
3 I. Miyamoto and S. Nagase, *Anal. Biochem.*, 115 (1981) 308.
4 E. Wessler, *Anal. Biochem.*, 26 (1968) 439.
5 P. Oreste and G. Torri, *J. Chromatogr.*, 195 (1980) 398.
6 M. Breen, H. G. Weinstein, L. J. Blacik, M. S. Borcherdin and R. A. Sittig, *Methods Carbohydr. Chem.*, 7 (1976) 101.
7 S. J. Angyal and J. A. Mills, *Aust. J. Chem.*, 32 (1979) 1993.
8 Z. Deyl, in Z. Deyl (Editor), *Electrophoresis, a Survey of Techniques and Applications, Part B: Applications* (*Journal of Chromatography Library*, Vol. 18B), Elsevier, Amsterdam, Oxford, New York, 1983, p. 13.
9 B. Bettler, R. Amadò and H. Neukom, *J. Chromatogr.*, 498 (1990) 213.
10 S. Hasegawa and C. W. Nagel, *J. Food Sci.*, 31 (1966) 838.
11 O. Raunhardt, H. W. H. Schmidt and H. Neukom, *Helv. Chim. Acta*, 50 (1967) 1267.
12 B. Bettler, R. Amadò and H. Neukom, *Mitt. Geb. Lebensmittelunters. Hyg.*, 76 (1985) 69.

Journal of Chromatography, 498 (1990) 231–236
Elsevier Science Publishers B.V., Amsterdam — Printed in The Netherlands

CHROM. 22 003

Note

Rapid analysis of light hydrocarbons in stabilized crude oils by gas chromatography

W. K. AL-THAMIR
North Oil Company, Central Laboratories Department, P.O. Box 5271, Baghdad (Iraq)
(First received April 12th, 1989; revised manuscript received September 12th, 1989)

The direct analysis of crude oil in order to determine the constituents up to C_7^+ is a significant test for reservoir and production studies, and may reflect some of the characteristics of crude oil from the evaluation point of view. Gas chromatography provides excellent separations of very complex hydrocarbon mixtures in terms of accuracy, rapidity and simplicity.

Martin and Winters[1] were the first to attempt to determine the composition of crude oil up to C_7 by direct analysis in two stages. The volatile components were first separated from the crude oil by a precolumn and then passed into three chromatographic columns. All the columns were operated at room temperature and employed two internal standards, *cis*-2-pentene and ethyl acetate, and the time of analysis was *ca.* 3 h. Although this work was useful, the use of multiple columns to analyse complex samples boiling over a wide range is complicated and time consuming.

The Institute of Petroleum published a standard method[2] for the analysis of crude oils for C_2–C_6 hydrocarbons by using Porapak Q precolumn and analytical columns and 2,2-dimethylbutane as an internal standard. However, this method was originally developed[3] for North Sea crude oil, in which 2,2-dimethylbutane is not normally present. When the method is applied to other crudes, which may well contain 2,2-dimethylbutane, the latter is unsuitable as an internal standard.

British Petroleum[4] developed another method, using a long capillary column attached to a precolumn and a backflushing technique, which is capable of determining individual hydrocarbons up to *n*-heptane, benzene and toluene and the carbon number distribution to C_9. An indirect method for analysing crude oils has also been attempted[5] in which distillation and gas chromatography using a capillary column and 1-pentene as an internal standard with temperature programming from 10 to 300°C are used to determine C_2–C_{20} hydrocarbons. This type of procedure may result in inaccurate data, as losses of light hydrocarbons during the distillation are inevitable; in addition, the method is lengthy and requires considerable amounts of sample.

However, the analysis of crude oils for compounds above C_7 is not essential from the petroleum engineering point of view, where reporting of C_6 and C_7 as groups is the final goal and moving to a higher range will lead to erroneous results owing to the presence of sulphur, nitrogen and oxygen compounds in addition to the difficulty of providing high resolution for all hydrocarbons[6]. This paper described a rapid and

0021-9673/90/$03.50

simple method for the analysis of crude oil employing a single conventional column with a precolumn containing a powerful adsorbent to eliminate sulphur-, nitrogen- and oxygen-containing compounds[7] in addition to asphaltenic materials in order to obtain "genuine" hydrocarbons. For quantitative analysis, a non-hydrocarbon internal standard was added to the crude oil that would elute without interfering with the hydrocarbons of interest and that would meet the usual conditions for an internal standard.

EXPERIMENTAL

A Varian 3700 gas chromatograph equipped with a flame ionization detector (thermal conductivity detector is an alternative) and a Spectra-Physics 4270 computing integrator was used. Helium (purity 99.995%) was employed as the carrier gas and maintained at flow-rate of 25 ml/min in all experiments. A stainless-steel analytical column (4.5 m × 2.3 mm I.D.) packed with 10% (w/w) of Apiezon L on Chromosorb P AW (80–100 mesh) was used in conjunction with a stainless-steel precolumn (50 mm × 2.3 mm I.D.) packed with a 50:50 (w/w) mechanical mixture of molecular sieve type 5A and Fuller's earth (both 80–100 mesh). The operating conditions were as follows: column temperature, programmed from 60 to 180°C at 7°C/min; injection temperature, 150°C; detector temperature, 200°C; chart speed, 0.5 cm/min; sample size, 2 μl; and attenuation, 32.

High-purity chloroform was found to be a suitable internal standard, with good linearity over wide-range. Optimization was carried out, which indicated that addition of 4–5% (w/w) of chloroform to a known amount of stabilized crude oil was adequate. A sample of this mixture was shaken vigorously and introduced immediately by syringe into the gas chromatograph. To measure relative response factors, chloroform was mixed with known concentrations of high-purity hydrocarbons.

The crude oil sample was stored in a refrigerator before analysis. The addition of the internal standard may be done at ambient temperature and care was taken to minimize losses of light ends, and hence to improve the accuracy. Replacement of the precolumn packing after 25 injections is recommended in order to prevent contamination of the analytical column.

RESULTS AND DISCUSSION

Chromatographic analysis of hydrocarbons is normally effected with a non-polar liquid stationary, and in this work thermally stable Apiezon L on Chromosorb P was selected. The precolumn packing of a molecular sieve and Fuller's earth mixture was chosen on account of these adsorbents' ability to retain strongly sulphur-, nitrogen- and oxygen- containing compounds and asphaltenic materials; in addition, this packing provided the possibility to elute chloroform cleanly in the middle of chromatogram without interfering with hydrocarbons.

To confirm the accuracy of the results, standard mixtures of high-purity hydrocarbons and chloroform were prepared at different concentrations as indicated in Table I; the relative standard deviation did not exceed 0.55% in any instance.

Typical chromatogram of crude oil analysis is shown in Fig. 1, which illustrates a rapid separation in less than 10 min, including hexane components (the residue is

TABLE I

HYDROCARBON CONCENTRATIONS (%, w/w) IN STANDARD MIXTURES DETERMINED BY GAS CHROMATOGRAPHY (GC) WITH A FIXED AMOUNT OF CHLOROFORM

Component	*Sample 1*		*Sample 2*		*Sample 3*	
	Actual concentration	*GC measured*[a]	*Actual concentration*	*GC measured*[a]	*Actual concentration*	*GC measured*[a]
n-Pentane	33.37	33.20	20.66	20.43	12.52	12.48
2,2-Dimethylbutane	2.93	2.96	1.50	1.49	0.74	0.73
n-Hexane	17.13	17.16	30.49	30.50	22.94	22.88
Benzene	5.73	5.55	7.57	7.62	9.36	9.28
n-Heptane	14.44	14.56	23.72	23.88	18.06	18.11
n-Octane	14.28	14.29	8.93	8.99	13.90	13.92
n-Nonane	8.61	8.57	2.58	2.64	16.69	16.65
n-Decane	3.51	3.71	4.55	4.45	5.79	5.95

[a] Average of five runs.

considered to be C_7^+). Fig. 2 shows an analysis in the presence of the internal standard, chloroform.

To obtain reliable results, relative response factors of hydrocarbons were

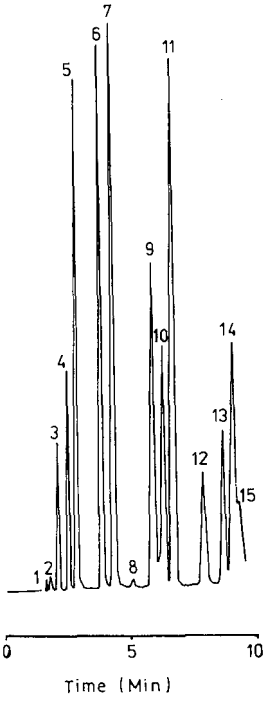

Fig. 1. Chromatogram of C_1–C_6 hydrocarbons in stabilized crude oil eluted from Apiezon L column by direct injection under conditions specified under Experimental. Peaks: 1 = C_1; 2 = C_2; 3 = C_3; 4 = iso-C_4; 5 = *n*-C_4; 6 = iso-C_5; 7 = *n*-C_5; 8–15 = C_6 components.

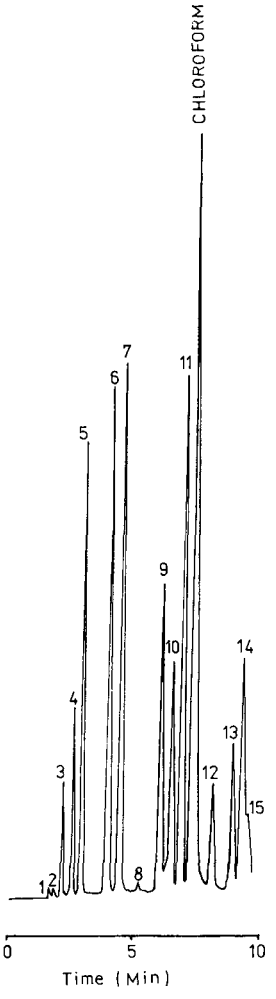

Fig. 2. Chromatogram of stabilized crude oil with chloroform as internal standard. Conditions and peaks as in Fig. 1.

calculated, and subsequently the concentrations of the hydrocarbons of interest were calculated by the equation

$$\text{Component (wt.\%)} = \left(\frac{TS}{GN}\right) \cdot 100 \cdot RRF$$

where T = peak area of component, G = peak area of chloroform, S = weight of chloroform, N = weight of crude oil and RRF = Relative response factor.

Table II gives results for the determination of light hydrocarbons in different types of stabilized crude oils yielded by a field separator (final stage of the production line). The determination of individual hydrocarbons up to C_5 in crude oils (produced

TABLE II

GAS CHROMATOGRAPHIC ANALYSIS OF DIFFERENT TYPE OF STABILIZED CRUDE OILS OBTAINED FROM A FIELD SEPARATOR

Results are expressed in % (w/w).

Component	*Crude oil A (API = 40)*	*Crude oil B (API = 36)*	*Crude oil C (API = 27)*
C_1	0	0.03	0
C_2	0.01	0.05	0.01
C_3	0.12	0.25	0.27
iso-C_4	0.15	0.42	0.20
n-C_4	0.57	1.09	0.80
iso-C_5	1.60	1.47	0.69
n-C_5	3.55	1.59	0.99
C_6 (group)	6.99	4.74	2.59
C_7^+	87.01	90.36	94.45
Total	100.00	100.00	100.00

under different conditions) is vital for selecting optimum conditions for field production, and Table III shows the analysis of a crude oil (API gravity 38) derived from a degassing operation by a laboratory separator at temperatures of 26, 50, 70 and 99°C, where the dramatic effect of temperature on the isolation of light hydrocarbons is observed.

A drawback of this method is the difficulty of injecting heavy crude oil (API gravity less than 20), which may be overcome by dilution with a suitable amount of an hydrocarbon heavier than C_7 (*e.g.*, xylenes).

TABLE III

GAS CHROMATOGRAPHIC ANALYSIS OF CRUDE OIL (API GRAVITY 38) OBTAINED FROM A LABORATORY SEPARATOR AT DIFFERENT TEMPERATURES

Results are expressed in % (w/w).

Component	*26°C*	*50°C*	*70°C*	*99°C*
C_1	Trace	0	0	0
C_2	0.04	0.03	0.01	0
C_3	0.31	0.25	0.19	0.05
iso-C_4	0.33	0.22	0.12	0.05
n-C_4	1.28	1.15	0.59	0.28
iso-C_5	1.41	1.29	1.23	0.43
n-C_5	2.06	1.95	1.25	0.79
C_6 (group)	8.08	7.91	5.72	4.45
C_7^+	86.49	87.20	90.89	93.95
Total	100.00	100.00	100.00	100.00

CONCLUSION

The gas chromatographic determination of the light hydrocarbons composition up to C_7^+ in stabilized crude oils was accomplished in less than 10 min by a direct method using chloroform as a non-hydrocarbon internal standard. Genuine hydrocarbon peaks were obtained when a short precolumn packed with a molecular sieve and Fuller's earth mixture was incorporated to remove sulphur-, nitrogen- and oxygen-containing compounds.

REFERENCES

1 R. L. Martin and J. C. Winters, *Anal. Chem.*, 31 (1959) 1954.
2 Institute of Petroleum, *Methods for Analysis and Testing*, IP 344, Part 1, Vol. 2, 1980, Heyden, London.
3 British Gas, Research and Technology Division, London, personal communication, 1988.
4 British Petroleum Research International, Sunbury Research Centre, Sunbury-on-Thames, personal communication, 1988.
5 E. H. Osjord, H. P. Ronningsen and L. Tau, *J. High Resolut. Chromatogr. Chromatogr. Commun.*, 8 (1985) 683.
6 K. H. Altgelt and T. H. Gouw (Editors), *Chromatography in Petroleum Analysis*, Marcel Dekker, New York, 1979, p. 71.
7 W. K. Al-Thamir, *J. Chromatogr. Sci.*, 26 (1988) 345.

Journal of Chromatography, 498 (1990) 237–240
Elsevier Science Publishers B.V., Amsterdam — Printed in The Netherlands

CHROM. 22 025

Note

Comparison of phenyl- and octyl-Sepharose CL-4B in the hydrophobic interaction chromatography of simple aliphatic and aromatic compounds

W. J. GELSEMA* and C. L. DE LIGNY
Laboratory for Analytical Chemistry, University of Utrecht, Croesestraat 77A, 3522 AD Utrecht (The Netherlands)
(Received August 28th, 1989)

Previously we have published a series of papers[1–7] dealing with the hydrophobic interaction chromatography of simple aliphatic compounds on octyl-Sepharose CL-4B. We now report some results of analogous experiments with phenyl-Sepharose CL-4B, again using simple compounds, for this purpose aliphatic and aromatic in nature. For comparison, the same compounds were also chromatographed on octyl-Sepharose CL-4B.

Comparisons of these two hydrophobic adsorbents have been published before[8–12]. However, they were based on experiments with test compounds of more complicated structure, *i.e.*, proteins and polynucleotides, which obviously hampers the interpretation of the results. Nevertheless, certain peculiar effects, *e.g.*, reversal of the elution order of a particular protein or polynucleotide pair on the two materials, lead to speculations about a specific "aromatic" or "stacking" interaction mechanism[11,12] on phenyl-Sepharose. Such a detail should in principle be more readily discernible using aliphatic and aromatic compounds of much simpler structure.

EXPERIMENTAL

The experimental procedure has been fully described[1]. Test compounds (Aldrich, Brussels, Belgium; purity $\geqslant 98\%$, used without further purification) were dissolved in the eluent at a concentration of 0.1–0.5 mg ml^{-1}. In some instances saturated solutions in the eluent were used. Aliquots of 1 ml of the sample solutions were applied to thermostatically controlled (25°C) columns of phenyl- and octyl-Sepharose CL-4B (Pharmacia, Uppsala, Sweden) having bed volumes of about 120 ml and eluted at a flow-rate of 15–20 ml h^{-1}. The eluent was a 25 m*M* sodium phosphate buffer of pH 7.10 (analytical-reagent grade; Baker, Deventer, The Netherlands); detection was performed by measuring the UV absorbance at 206 or 254 nm (Uvicord S; LKB, Bromma, Sweden).

From the elution volume, the (partial molal) standard free energy change, $\Delta G°$, for the partition of the test compound between the gel phase and the eluent was calculated using eqns. 3–6 in ref. 1. In these calculations the following values for the specific bed weight, β (milligrams of matrix material per millilitre of gel bed) and the

0021-9673/90/$03.50

density, ρ, of the dry gel were used: $\beta_{os} = 36.3$ mg ml^{-1}, $\beta_{ps} = 38.0$ mg ml^{-1} and $\rho_{os} = \rho_{ps} = 1.6$ g ml^{-1}.

The degree of substitution of both gels is sufficiently high to permit the above treatment of the retention data in terms of a partition process[1,2].

RESULTS

In Fig. 1, ΔG° values for the partition on both gels are shown for three series of test compounds, *viz.*, carboxylic acids, $CH_3(CH_2)_{n-1}COOH$ ($n=6$–10), *p*-alkylbenzoic acids, $CH_3(CH_2)_{n-1}C_6H_4COOHN$ ($n=0$–4), and ω-phenylcarboxylic acids, $C_6H_5(CH_2)_nCOOH$ ($n=0$–4). Except for *p*-isopropylbenzoic acid ($n=3$), the test compounds contained *n*-alkyl chains. Note that at the pH of the eluent the acids are more than 99% dissociated (their pK values range from 4.2 for benzoic acid to 5.0 for undecanoic acid).

The slopes, $-\Delta\Delta G^\circ(CH_2)$, obtained by least-squares treatment of the data in Fig. 1 (only that for benzoic acid was omitted) are given in Table I.

DISCUSSION

We confine the discussion to the values of $-\Delta\Delta G^\circ(CH_2)$ in Table I, which represent the contribution of a CH_2 group in the alkyl chains of the test compounds to the free energy change on hydrophobic interaction with octyl- and phenyl-Sepharose.

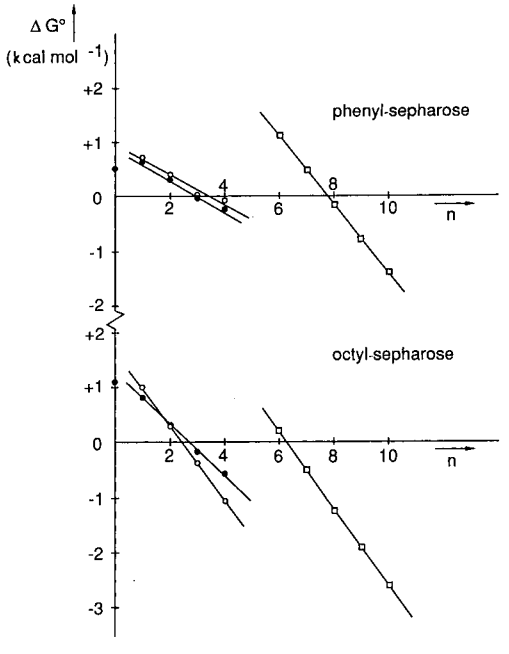

Fig. 1. Standard free energy change at 25°C *versus* alkyl chain length for (□) carboxylic acids, (○) *p*-alkylbenzoic acids and (●) ω-phenylcarboxylic acids on phenyl- and octyl-Sepharose CL-4B at pH 7.10.

TABLE I

VALUES OF $-\Delta\Delta G^{\circ}(CH_2)$ FOR THE RETENTION OF THE THREE SERIES OF TEST COMPOUNDS AT 25°C ON PHENYL- AND OCTYL-SEPHAROSE CL-4B AT pH 7.10

Compounds	$-\Delta\Delta G^{\circ}(CH_2)$ *(kcal mol^{-1})*	
	Octyl-Sepharose	*Phenyl-Sepharose*
Carboxylic acids	0.70 ± 0.01	0.61 ± 0.02
p-Alkylbenzoic acids	0.69 ± 0.02	0.27 ± 0.04
ω-Phenylcarboxylic acids	0.47 ± 0.02	0.29 ± 0.03

Focusing first on the results with octyl-Sepharose, the value of 0.70 kcal mol^{-1} for the carboxylate ions is slightly smaller than that (0.74 kcal mol^{-1}) reported previously[1] for the corresponding uncharged acids at pH 3.52. Small effects of the charge were found previously[7] for the partition of carboxylic acids and alkylamines on octyl-Sepharose. Further, it was shown[7] that for both carboxylate and alkylammonium ions the $-\Delta\Delta G^{\circ}(CH_2)$ values tend to decrease with decreasing n. The cause of this effect is probably[1,7] an increasing influence of the charged head group on the solvation of CH_2 groups with decreasing n. This conclusion is corroborated by the results presented in this paper: for *p*-alkylbenzoate ions and carboxylate ions the $-\Delta\Delta G^{\circ}(CH_2)$ values are identical within experimental error (in both series the CH_2 group is far from the polar head), whereas for ω-phenylcarboxylate ions, where the CH_2 group is much closer to the charged head, $-\Delta\Delta G^{\circ}(CH_2)$ is much smaller (0.47 kcal mol^{-1}).

Turning now to the results with phenyl-Sepharose, it appears that $-\Delta\Delta G^{\circ}(CH_2)$ for aliphatic carboxylate ions is smaller than that on octyl-Sepharose (0.61 *versus* 0.70 kcal mol^{-1}). This reflects the lower hydrophobicity of phenyl compared with octyl groups. As only the hydrophobic interaction of a CH_2 group with the gels is expressed in these figures, we conclude that the ratio of hydrophobicities of the gels is phenyl/octyl = 61/70 = 0.87. We think that this is a more meaningful estimate of this ratio than those reported previously, which were based on interactions of proteins with the gels, often in the presence of high salt concentrations. The latter estimates, mostly expressed as a normal alkyl chain equivalence of a phenyl group (φ), are generally smaller than our estimate [compare, for instance, $\varphi \approx C_3$–C_4 (ref. 11) and $\varphi < C_5$ (ref. 9)]. The most peculiar results in Table I are the (within experimental error) identical and relatively small $-\Delta\Delta G^{\circ}(CH_2)$ values for the two series of aromatic carboxylate ions. A $-\Delta\Delta G^{\circ}(CH_2)$ value of 0.61 kcal mol^{-1} for *p*-alkylbenzoate ions is expected: as for aliphatic carboxylate ions, it represents the interaction of a CH_2 group, far from the charged head, with phenyl groups. The actual value is, however, less than half this. This might be explained by assuming that the interaction mechanism in this instance (and in that of the ω-phenylcarboxylate ions) is not a simple partition, but a bimolecular association of the test compounds with phenyl groups on the gel. The present results can then tentatively be interpreted as follows: the aromatic test compounds are held on the gel primarily by phenyl–phenyl bimolecular interaction. This phenyl–phenyl interaction fixes the orientation of the aromatic test compounds with respect to other phenyl groups, and to the glycidyl spacer arms connecting the

phenyl groups to the Sepharose chains. This orientation is probably not optimal for interaction of their alkyl chains with the phenyl-Sepharose, and thus a lower value of $-\Delta\Delta G°(CH_2)$ results than is found for the aliphatic test compounds. Evidence for strong phenyl–phenyl interaction is afforded by the $\Delta G°$ value of benzoic acid on phenyl-Sepharose, which is lower than that on octyl-Sepharose (see Fig. 1), whereas the reverse holds for most other compounds.

In conclusion, we think that these results provide evidence for a special "aromatic" mechanism for the retention of aromatic compounds on phenyl-Sepharose. This mechanism differs from that of aliphatic compounds on phenyl-Sepharose and from that of aliphatic and aromatic compounds on octyl-Sepharose.

REFERENCES

1 W. J. Gelsema, P. M. Brandts, C. L. de Ligny, A. G. M. Theeuwes and A. M. P. Roozen, *J. Chromatogr.*, 295 (1984) 13.
2 P. M. Brandts, C. M. Middelkoop, W. J. Gelsema and C. L. de Ligny, *J. Chromatogr.*, 356 (1986) 247.
3 P. M. Brandts, W. J. Gelsema and C. L. de Ligny, *J. Chromatogr.*, 322 (1985) 399.
4 P. M. Brandts, W. J. Gelsema and C. L. de Ligny, *J. Chromatogr.*, 333 (1985) 41.
5 P. M. Brandts, W. J. Gelsema and C. L. de Ligny, *J. Chromatogr.*, 354 (1986) 19.
6 P. M. Brandts, W. J. Gelsema and C. L. de Ligny, *J. Chromatogr.*, 437 (1988) 337.
7 P. M. Brandts, W. J. Gelsema and C. L. de Ligny, *J. Chromatogr.*, 438 (1988) 181.
8 J. C. Janson and T. Låås, in R. Epton (Editor), *Chromatography of Synthetic and Biological Polymers. Vol. 2. Hydrophobic, Ion Exchange and Affinity Methods.* Ellis Horwood, Chichester, 1978, Ch. 4, p. 60.
9 J. Rosengren, S. Påhlman, M. Glad and S. Hjérten, *Biochim. Biophys. Acta*, 412 (1975) 51.
10 W. Kissing and R. Reiner, *J. Solid-Phase Biochem.*, 4 (1979) 221.
11 B. H. J. Hofstee and N. F. Otillio, *J. Chromatogr.*, 161 (1978) 153.
12 J. L. Ochoa, J. Kempf and J. M. Egly, in J. M. Egly (Editor), *Chromatographie d'affinité et Interactions Moléculaires— Affinity Chromatography and Molecular Interactions, Symposium Proceedings, Strasbourg*, INSERM, Paris, 1979, p. 293.

Journal of Chromatography, 498 (1990) 241–247
Elsevier Science Publishers B.V., Amsterdam — Printed in The Netherlands

CHROM. 21 984

Note

Separation of hordenine and N-methyl derivatives from germinating barley by liquid chromatography with dual-electrode coulometric detection

I. M. JOHANSSON and B. SCHUBERT*
University of Uppsala, Equine Drug Research Laboratory, Ulleråker, S-750 17 Uppsala (Sweden)
(First received November 2nd, 1987; revised manuscript received September 12th, 1989)

Hordenine [4-(2-dimethylaminoethyl)phenol] is chemically closely related to tyramine and several other compounds normally present in mammalian tissues and body fluids. Hordenine itself, however, has not been reported to be a normal constituent in mammals. Hordenine has earlier been used in both human and veterinary medicine in the treatment of diarrhoea and other intestinal disturbances[1,2].

Hordenine has been detected in the urine of race horses[3]. To date, the Medication Control Programme of Swedish horseracing has found four urine samples to contain hordenine, mainly in the form of an acid-labile conjugate, in the concentration range 1–43 μg/ml. The analysis was performed by thin-layer chromatography (TLC) and the presence of hordenine was confirmed by gas chromatography–mass spectrometry (GC–MS).

This work is part of a larger study in which various horse feeds on the Swedish market and plant materials were analysed for the presence of hordenine. Further, the pharmacokinetics of hordenine in the horse and the effects on cardiorespiratory and blood lactate responses to exercise in the horse were studied[4]. Feeding one horse 733 g of germinating barley, a natural source of hordenine containing 63 μg/g of hordenine, resulted in hordenine concentrations in the urine comparable to those mentioned above[4]. The hordenine content in the germinating barley was analysed both by GC–MS[4] and by the present liquid chromatographic (LC) method. Dried barley seedlings (from the malthouse industry) and parts of reed canary grass, also a natural source of hordenine, were analysed by LC with ultraviolet detection[4].

The present chromatographic study of hordenine also included the corresponding N-desmethyl derivatives, tyramine and N-methyltyramine. These are precursors in the formation of hordenine in barley seedlings and certain other plants, and have been reported to occur in dried barley seedlings from the malthouse industry, as also does N-trimethyltyramine (candicin)[5]. Pholedrine [4-(2-methylaminopropyl)phenol] was tested for comparison.

EXPERIMENTAL

Apparatus

The LC system consisted of a Constametric III pump (LDC, Riviera Beach,

0021-9673/90/$03.50

FL, U.S.A.), a Wisp 710B automatic injector (Waters Assoc., Milford, MA, U.S.A.) and either a UV detector (Spectro Monitor III; LDC) operated at 273 nm or an electrochemical detector (Model 5100 A; ESA, Bedford, MA, U.S.A.). The electrochemical detection system consists of a coulometric guard cell (Model 5020) and a solid-state analytical cell containing dual coulometric working electrodes made from porous graphite (Model 5010). The guard cell, operated at +0.8 V, was connected between the pump and injector to reduce the background current at the analytical cell resulting from oxidation of contaminants in the eluent. For the detection of hordenine and related compounds, the first working electrode (D_1) was set at +0.5 V, a potential at which hordenine just begins to oxidize according the hydrodynamic voltammogram of hordenine obtained for the LC system with phosphate buffer (pH 3.0) –methanol (80:20, v/v) as the eluent. The electro-oxidation of the compounds was then effected at the working electrode (D_2) at +0.75 V. The signal from D_2 was recorded and integrated using a Chromatopac C-RIB integrator (Shimadzu, Kyoto, Japan).

The pH of the chromatographic eluent was recorded with a Metrohm (Herisau, Switzerland) Model 620 pH meter.

Chemicals and reagents

Hordenine hemisulphate was obtained from Sigma (St. Louis, MO, U.S.A.) and tyramine hydrochloride from Merck (Darmstadt, F.R.G.). N-Methyltyramine and N-trimethyltyramine iodide (candicin) were synthesized according to Gruenke *et al.*[6] and Buck *et al.*[7], respectively. The structures of the compounds are given in Fig. 1.

N,N-Dimethyl-N-octylamine (DMOA) was obtained from ICN Pharmaceuticals (Planview, NY, U.S.A.) and sodium octylsulphate from Merck. Tetrabutylammonium (TBA) hydroxide was prepared from tetrabutylammonium iodide (Merck)[8] and the titre was determined by the picric acid method[9].

The phosphate buffers were prepared from sodium dihydrogenphosphate and orthophosphoric acid. Methanol of analytical-reagent grade (Merck) was used.

Barley

First-class barley was soaked in water for 24 h and was then spread out on wet paper for 5 days.

To 1 g of germinating barley in a centrifuge tube were added 15 ml of 1 *M* hydrochloric acid and the tube was placed in a water-bath at 95°C for 30 min. The mixture was then homogenized (Ultra-Turrax; Janke and Kunkel, Staufen, F.R.G.) for 3 min and centrifuged. The supernatant was diluted 10 fold with the chromatographic eluent and 20 μl were injected onto the column.

Liquid chromatography

Initially the separation was made on a LiChroCART column system with a

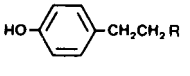

Fig. 1. Structures of the compounds. R = NH_2, tyramine; $NHCH_3$, N-methyltyramine; $N(CH_3)_2$, hordenine; $N^+(CH_3)_3$, N-trimethyltyramine.

LiChrosorb RP Select B cartridge (7-μm particle size; type 16365; Merck). The dimensions were 125 mm × 4.0 mm I.D. The eluent was a mixture of 0.1 *M* NaH_2PO_4 or 0.01 *M* NaH_2PO_4 (pH = 4.6) with methanol (90:10, v/v). In some experiments, DMOA (0.8 m*M*) and/or sodium octylsulphate (1–3 m*M*) were added. The flow-rate was 0.8 ml/min. The influence of DMOA in the eluent on the capacity factor and the peak shape on the LiChrosorb RP Select B column was compared with the results obtained with a 100 mm × 3.0 mm I.D. column packed with 10-μm Spherisorb ODS (Phase Separations, Queensferry, U.K.). To determine peak symmetry, the perpendicular from the peak maximum was drawn and the peak width at 13,5% of the height was used[10].

Later, a strong cation-exchange column, Nucleosil SA, 5-μm particle size (Macherey, Nagel & Co., Düren, F.R.G.) was used. The dimensions of the column were 200 mm × 4.6 mm I.D. The eluent was phosphate buffer (pH 3.0, ionic strength = 0.1)–methanol (80:20, v/v) at a flow-rate of 1.0 ml/min.

RESULTS AND DISCUSSION

Addition of dimethyloctylamine (DMOA) to the eluent

The LiChrosorb RP Select B column is designed to give a good chromatographic performance with basic substances[11]. Nevertheless, the peaks obtained for hordenine and its N-methyl derivatives tailed significantly, giving A_s = 2.3–3.3 with 0.1 *M* NaH_2PO_4 as the eluent. An improvement in peak symmetry and the influence on retention on reversed-phase columns by DMOA in the eluent have been demon-

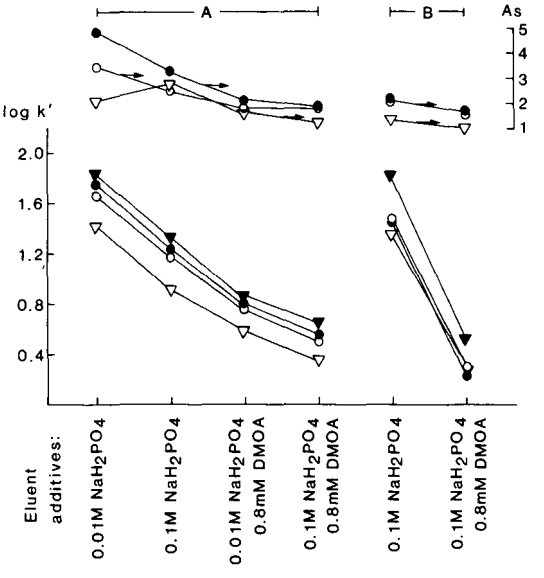

Fig. 2. Comparison of the capacity factors and peak symmetry. Column (A) LiChroCART with LiChrosorb RP Select B; (B) Spherisorb ODS. Eluents: mixture of 0.1 *M* NaH_2PO_4 or 0.01 *M* NaH_2PO_4 (pH = 4.6) with methanol (90:10 v/v), containing 2 m*M* octylsulphate and with 0.8 m*M* DMOA added to three of the systems as indicated. Sample: ▽ = tyramine; ▼ = pholedrine; ○ = hordenine; ● = N-trimethyltyramine.

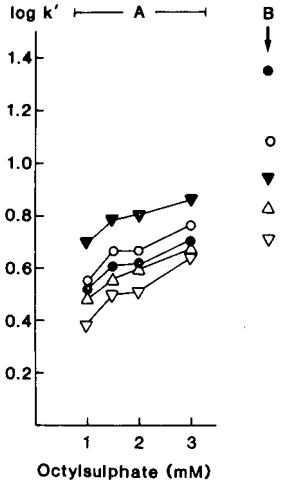

Fig. 3. Comparison of capacity factors. (A) Column: LiChroCART with LiChrosorb RP Select B. Eluent: 10% methanol in 0.01 *M* NaH_2PO_4 (pH = 4.6) containing DMOA (0.8 m*M*) and octylsulphate. (B) Column: Nucleosil SA. Eluent: 20% methanol in phosphate buffer (pH 3.0, ionic strength = 0.1). Sample: ▽ = tyramine; △ = N-methyltyramine; ▼ = pholedrine; ○ = hordenine; ● = N-trimethyltyramine.

strated for more hydrophobic amines[12–16]. Addition of 0.8 m*M* DMOA to the eluent in this study improved the peak symmetry (*As* = 1.3–2.3). However, the retention of all substances decreased and the capacity factor for hordenine decreased from 14.6 to 3.3. The decrease in retention was even greater on the Spherisorb ODS column. Small changes in selectivity were obtained with both columns on addition of DMOA. The results are summarized in Fig. 2. The improvement in peak symmetry was most pronounced for candicin. A similar marked effect of additives in chromatographic solvents on other quaternary ammonium compounds has been reported[17].

However, the resulting retention times were too short to resolve the compounds of interest fully. Addition of octylsulphate to the eluent at concentrations up to 3 m*M* increased the retention (Fig. 3) but the separation was still not adequate. A change of the eluent pH to 3, a reduction in the ionic strength to 0.01 or exchange of methanol for acetonitrile did not improve the separation on the LiChrosorb RP Select B column.

Data from separations on the Spherisorb ODS column showed that the addition of a methyl group to the α-carbon of N-methyltyramine (giving pholedrine) gives an increase in log *k'* of 0.4 units. Methyl substitution at the nitrogen (giving hordenine) increases log *k'* by only 0.05 units. This ODS column seems to give a poor selectivity for different substituents at the nitrogen atom.

Different selectivities can often be observed with various columns of the same type, as for non-steroidal anti-inflammatory drugs on C_{18} columns (Spherisorb ODS *vs.* LiChrosorb RP-18)[18]. This is obviously due to different degrees of end-capping and other dissimilarities in manufacture. Some other brand of C_{18} material, not investigated by us, might possibly separate the compounds studied here. However, our present data suggest that a sufficient separation on this type of column cannot be

obtained, even if the number of theoretical plates could be reasonably increased, *e.g.*, by the use of longer columns and/or smaller particle size. Reversed-phase columns have been used previously to determine tyramine[19–21].

A considerable improvement in the separation was obtained with the Nucleosil SA column (Fig. 3), and this column was exclusively used subsequently in the study. The peak symmetries on the Nucleosil SA correspond to those on the Spherisorb ODS column (A_s = 1.5–2.2) without the addition of DMOA to the eluent. Catecholamines have also been separated on this type of column, which were shown to give cleaner chromatograms in the analysis of plasma and urine samples compared with LiChrosorb RP-18 columns[22,23].

Electrochemical detection

Hordenine showed an electrochemical response with the ESA coulometric detector and required a relatively high oxidation potential of +0.75 V. The same potential has been used for the coulometric detection of octopamine and tyramine[24]. Use of the ESA coulometric detector required a buffer system that generated low currents at both working electrodes. Hydrodynamic voltammograms recorded between 0.0 and +1.3 V showed that the background current was increased considerably by the addition of DMOA (Fig. 4). In this experiment, 24% acetonitrile in phosphate buffer (pH 3.25; ionic strength = 0.01) was used. In contrast, TBA did not increase the noise and could be used as an additive to the eluent for electrochemical detection at the high potential necessary to detect hordenine and related compounds. The separation of a standard mixture of the compounds on the Nucleosil SA column at a potential of +0.75 V is shown in Fig. 5. The calibration graph for hordenine was linear in the range 0.56–28 μM (0.092–4.6 μg/ml). The regression equation for the curve was $y = 38.5\,x - 24.2$ (r = 0.993; n = 8) and the detection limit was 0.33 μM (0.054 μg/ml) measured at three times the background noise.

In our earlier investigations[4], hordenine was determined by high-performance liquid chromatography with ultraviolet detection. It has a fairly strong absorbance at 275 nm (molar absorptivity ε = 1606 at pH 3.15), but the present method gave a 25-fold improvement in the detection limit (1.35 *vs.* 0.054 μg/ml).

Analysis of germinating barley and horse urine

A chromatogram of an extract of germinating barley is shown in Fig. 6. Peaks with the same retention times as tyramine, N-methyltyramine and hordenine were

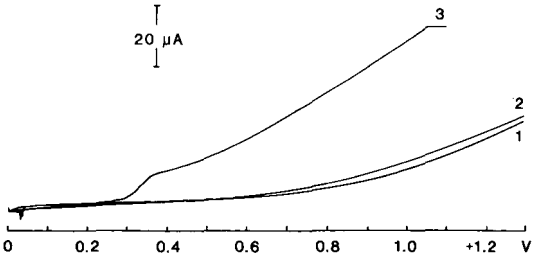

Fig. 4. Hydrodynamic voltammograms with different additives in the eluent. Eluent: 24% acetonitrile in phosphate buffer (pH 3.25, ionic strength = 0.01). 1 = eluent; 2 = elutent + TBA (0.8 mM); 3 = eluent + DMOA (0.8 mM).

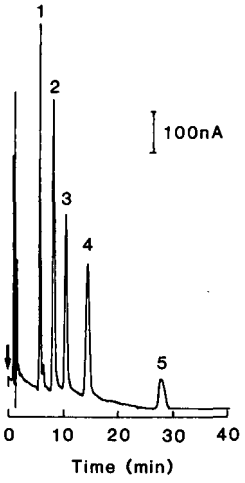

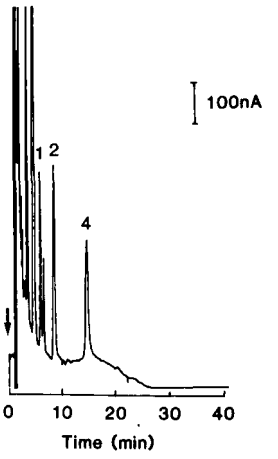

Fig. 5. Chromatogram of 10–19 ng of standards with D_1 1 at +0.5 V and D_2 at +0.75 V. Flow-rate: 1.0 ml/min. Column: Nucleosil SA. Eluent: 20% methanol in phosphate buffer (pH 3.0, ionic strength = 0.1). Peaks: 1 = tyramine (119 pmol); 2 = N-methyltyramine (129 pmol); 3 = pholedrine (93 pmol); 4 = hordenine (114 pmol); 5 = N-trimethyltyramine (67 pmol).

Fig. 6. Chromatogram of extract from germinating barley. Chromatographic conditions and peaks as in Fig. 5.

obtained. Determination of the concentrations from peak areas compared with standards analysed under the same conditions indicated that 1 g of barley contained 26 μg of tyramine, 48 μg of N-methyltyramine and 63 μg of hordenine. The presence of hordenine was confirmed by GC–MS[4].

The relative standard deviation for hordenine added to 1 *M* hydrochloric acid and treated as described under Experimental for barley extraction was 8.8% at the 26 μ*M* (4.3 μg/ml) level (n = 8). The yield through the sample work-up was 105%.

Samples of horse urine were diluted 10-fold with chromatographic eluent (without treatment with hydrochloric acid) and 20-μl aliquots were injected. However, this procedure proved unsuccesful for the determination of hordenine in the urine of horses that had received this compound. Unfortunately, horse urine contains large amounts of phenols and other electroactive compounds that seriously interfere with the determination of hordenine using electrochemical detection, and contamination of the electrode surfaces necessitates extensive cell cleaning every 4–6 injections.

REFERENCES

1 H. Thoms, *Handbuch der Praktischen und Wissenschaftlichen Pharmazie*, Vol. 6, Urban and Schwartzenberg, Berlin, 1928, p. 1025.
2 P. Gengoux, *Pharmacodynamie Générale de Thérapeutique Vétérinaire*, 2nd ed., Duculot, Gembloux, 1971, p. 459.
3 M. S. Moss, personal communication, 1986.
4 B. Schubert, P. Kallings, M. Johansson, Å. Ryttman and U. Bondesson, presented at the *7th International Conference of Racing Analysts and Veterinarians, Louisville, KY, April 10–14, 1988.*
5 G. Rabitzsch, *Planta Med.*, 7 (1959) 268.

6 L. D. Gruenke, L. C. Craig, F. D. Klein, T.-L. Nguyen, B. A. Hitzemann, J. W. Holaday, H. H. Loh, L. Braff, A. Fischer, I. D. Glick, F. Hartmann and D. M. Bissel, *Biomed. Mass Spectrom.*, 12 (1985) 707.
7 J. S. Buck, R. Baltzly and W. S. Ide, *J. Am. Chem. Soc.*, 60 (1938) 1789.
8 K. Gustavii and G. Schill, *Acta Pharm. Suec.*, 3 (1966) 259.
9 K. Gustavii and G. Schill, *Acta Pharm. Suec.*, 3 (1966) 241.
10 P. A. Bristow, *LC in Practice*, HETP, Handforth, Wilmslow, 1976, p. 17.
11 *R.P. Select B, Information Booklet*, E. Merck, Darmstadt, 1987.
12 S.-O. Jansson, I. Andersson and B. A. Persson, *J. Chromatogr.*, 203 (1981) 93.
13 S.-O. Jansson, *J. Chromatogr.*, 5 (1982) 677.
14 S.-O. Jansson and S. Johansson, *J. Chromatogr.*, 242 (1982) 41.
15 S.-O. Jansson, I. Andersson and M.-L. Johansson, *J. Chromatogr.*, 245 (1982) 45.
16 B.-A. Persson, S.-O. Jansson, M.-L. Johansson and P.-O. Lagerström, *J. Chromatogr.*, 316 (1984) 291.
17 A. Sokolowski and K.-G. Wahlund, *J. Chromatogr.*, 189 (1980) 299.
18 I. M. Johannson and M.-L. Eklund, *J. Liq. Chromatogr.*, 7 (1984) 1609.
19 J. Scaro, J. L. Morrisey and Z. K. Shihabi, *J. Liq. Chromatogr.*, 3 (1980) 537.
20 P. C. Waldmeier, K.-H. Antonin, J.-J. Feldtrauer, C. Grunenwald, E. Paul, J. Lauber and P. Bieck, *Eur. J. Clin. Pharmacol.*, 25 (1983) 361.
21 R. C. Causon and M. J. Brown, *J. Chromatogr.*, 317 (1984) 319.
22 B.-M. Eriksson and B.-A. Persson, *J. Chromatogr.*, 228 (1982) 143.
23 B.-M. Eriksson, S. Gustavsson and B.-A. Persson, *J. Chromatogr.*, 278 (1983) 255.
24 R. J. Martin, B. A. Bailey and R. G. H. Downer, *J. Chromatogr.*, 278 (1983) 265.

Journal of Chromatography, 498 (1989) 248–253
Elsevier Science Publishers B.V., Amsterdam — Printed in The Netherlands

CHROM. 22 021

Note

High-performance liquid chromatography of alkylnaphthalenes and phenylnaphthalenes on alumina

JANA PUNČOCHÁŘOVÁ, JINDŘICH VAŘEKA, LUDĚK VODIČKA and JOSEF KŘÍŽ*
Laboratory of Synthetic Fuels, Institute of Chemical Technology, Suchbátarova 5, CS-16628 Prague 6 (Czechoslovakia)

(First received June 21st, 1989; revised manuscript received September 20th, 1989)

The relationship between the molecular structure of mono- and diaromatic hydrocarbons and their adsorptivity on silica and alumina has been studied by Snyder[1,2], Klemm *et al.*[3] and, more precisely, by Popl and co-workers[4–6]. The influence of molecular structure on the intermolecular interactions with the adsorbent (hydroxylated and silanized silica gels) and eluent has been studied by Ageev *et al.*[7,8], using polymethyl- and monoalkylbenzenes and also five alkylnaphthalenes among other polynuclear aromatic hydrocarbons as test compounds.

Adsorption systems with long-term equilibration of the water content between the mobile and the stationary phases have been used for the high-performance liquid chromatographic (HPLC) study of the retention behaviour of some alkylbenzenes[9], alkylnaphthalenes[10] and alkylbiphenyls[11] on silica and alkylbenzenes on alumina[12].

The aim of this study was to obtain HPLC data for alkylnaphthalenes in order to study the relationship between their molecular structure and retention behaviour on alumina.

EXPERIMENTAL

Apparatus

A Model 8500 liquid chromatograph (Varian, Palo Alto, CA, U.S.A.) with a syringe pump was used. Sample injection was performed by the stop-flow technique with a 5-μl syringe (Hamilton, Bonaduz, Switzerland). A UVM-4 multi-wavelength UV detector (Vývojové dílny ČSAV, Prague, Czechoslovakia) was operated at 254 nm. Chromatograms were recorded and retention times were measured with a Model 3390A reporting integrator (Hewlett-Packard, Avondale, PA, U.S.A.).

A stainless-steel column (150 mm × 4 mm I.D.) was packed using the slurry-packing technique with 7.5-μm alumina (Alusorb 160 Neutral; Lachema, Brno, Czechoslovakia). The water content in the recycling mobile phase was maintained by a moisture control system (MCS) incorporated in a closed circuit. The MCS was filled with 150 g of silica containing 0.5, 1 and 2% of water. The MCS apparatus was described in detail previously[10]. Both the column and the MCS were maintained at 25 ± 0.1°C. Retention data were calculated on a Hewlett-Packard HP-85 computer equipped with a 82905B impact printer, 82901M dual-disk drive and 7475A plotter. Visicalc software was used to prepare, compute and print the data.

0021-9673/90/$03.50

Chemicals

A series of alkylnaphthalene isomers were used. Some of them were commercial products from various manufacturers and the others were kindly donated by Dr. Fryčka of Urxovy závody (Valašské Meziříčí, Czechoslovakia).

Mobile phase

Pure *n*-pentane (VEB Jenapharm, Laboratorchemie Apolda, G.D.R.) was used as the mobile phase. Before use, it was distilled on a glass perforated-plate column with exclusion of moisture and stored over Nalsit A4 molecular sieves (Chemické Závody Juraja Dimitrova, Bratislava, Czechoslovakia). The flow-rate of the mobile phase was 60 ml/h.

Procedure

Three or four measurements were used for each sample. The samples were 10% solutions in isooctane. The column was stabilized before the measurement by washing with fresh mobile phase. The time for equilibration of the column depends on the amount of water contained in the MCS. The column activity was checked before the beginning of the measurement, several times during the analysis and after completion of the measurement, by injecting a test mixture of benzene, naphthalene and biphenyl in isooctane. The dead time of the column was determined as the time interval from the moment of injection to the time when the trace for the solvent disturbance crossed the baseline. The solvent disturbance peak was generated by *n*-hexane.

RESULTS AND DISCUSSION

The retention times, t_R, and capacity factors, k', for 0.5, 1 and 2% water in the MCS are given in Table I. Each value represents an average of three or four measurements for individual alkylnaphthalenes; the reproducibility is within the range 1–2%.

Three main factors that affect the adsorption of alkylbenzenes on silica and alumina[9,12] and alkylnaphthalenes on silica[10] have been discussed previously: (i) the number and shape of the alkyl groups, (ii) the length of the alkyl groups and (iii) the arrangement of the alkyl groups (*ortho* effect).

Number of alkyl groups

Fig. 1 shows the dependence of $\log k'$ on the number of carbon atoms for some of the measured compounds. With increasing number of carbon atoms, the range of the retention data broadens.

In relation to the adsorption of alkylnaphthalenes on alumina, the retention is significantly influenced by the number of alkyl groups. The retention increases with increasing number of methyl groups in every position. Similar behaviour has been observed for alkylbenzenes adsorbed on alumina[12].

Length of alkyl groups

Not enough compounds were available for the effect of increasing the chain length of the alkyl groups on retention to be studied in more detail. However, both ethylnaphthalenes studied have shorter retentions than the corresponding methyl

TABLE I

RETENTION DATA FOR ALKYLNAPHTHALENES ON ALUMINA

t_R = Retention time (min); k' = capacity factor = $(t_R - t_0)/t_0$, where t_0 = retention time of unretained compound (hexane) = 1.95 min; MCS = moisture control system.

Compound	*Abbreviation*	*Concentration of water in MCS (%)*					
		0.5		*1*		*2*	
		t_R	k'	t_R	k'	t_R	k'
Naphthalene	N	6.76	2.47	6.23	2.19	4.20	1.15
1-Methylnaphthalene	1-MN	8.68	3.45	7.97	3.09	4.92	1.52
2-Methylnaphthalene	2-MN	8.70	3.46	8.05	3.13	4.94	1.53
1-Ethylnaphthalene	1-EN	7.94	3.07	7.31	2.75	4.59	1.35
2-Ethylnaphthalene	2-EN	7.82	3.01	7.09	2.64	4.50	1.31
1,2-Dimethylnaphthalene	1,2-DMN	12.02	5.16	10.79	4.53	6.00	2.08
1,3-Dimethylnaphthalene	1,3-DMN	11.70	5.00	10.48	4.37	5.91	2.03
1,4-Dimethylnaphthalene	1,4-DMN	12.26	5.29	11.03	4.66	6.10	2.13
1,6-Dimethylnaphthalene	1,6-DMN	12.10	5.21	10.83	4.55	6.03	2.09
1,7-Dimethylnaphthalene	1,7-DMN	12.20	5.26	10.85	4.56	6.01	2.08
1.8-Dimethylnaphthalene	1,8-DMN	14.56	6.47	12.72	5.52	6.82	2.50
2,3-Dimethylnaphthalene	2,3-DMN	14.78	6.58	12.89	5.61	6.87	2.52
2,6-Dimethylnaphthalene	2,6-DMN	12.04	5.17	10.73	4.50	6.01	2.08
2,7-Dimethylnaphthalene	2,7-DMN	12.36	5.34	11.00	4.64	5.98	2.07
1-Allylnaphthalene	1-AN	11.23	4.76	9.67	3.96	5.56	1.85
1,3,7-Trimethylnaphthalene	1,3,7-TMN	18.41	8.44	16.52	7.47	7.78	2.99
2,3,5-Trimethylnaphthalene	2,3,5-TMN	23.91	11.26	20.69	9.61	9.47	3.86
2,3,6-Trimethylnaphthalene	2,3,6-TMN	22.94	10.76	20.17	9.34	9.15	3.69
1-Phenylnaphthalene	1-PhN	15.92	7.16	13.45	5.90	7.52	2.86
2-Phenylnaphthalene	2-PhN	51.00	25.15	38.00	18.49	17.75	8.10
Acenaphthene	Acen	14.30	6.33	12.59	5.46	6.61	2.39

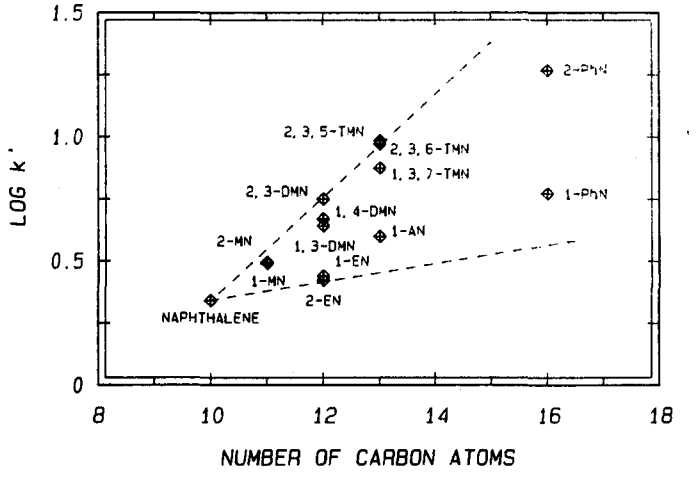

Fig. 1. Dependence of log k' on the number of carbon atoms in alkylnaphthalenes. The range of the retention of all the alkylnaphthalenes is limited by dashed lines. Column, 150 × 4 mm I.D. packed with 7.5-μm alumina. Eluent, *n*-pentane, 1% water in the MCS. Abbreviations are given in Table I.

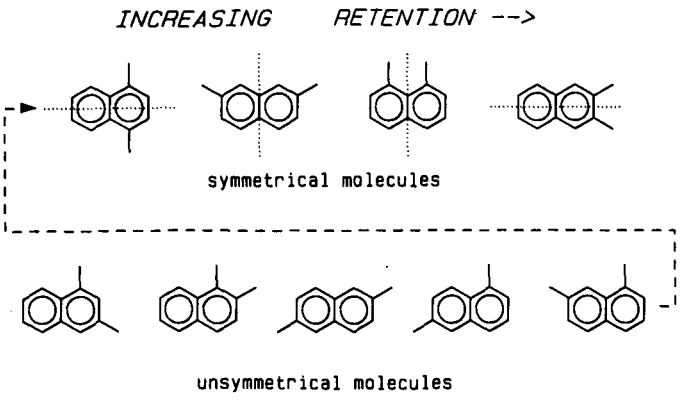

Fig. 2. Scheme illustrating the retention order of symmetrical and non-symmetrical dimethylnaphthalenes.

derivatives (see Fig. 1). On comparing the behaviour of alkylbenzenes on alumina with our results it can be expected that a further increase in chain length will not influence the retention to a great extent.

Arrangement of the alkyl groups

Dimethylnaphthalene homologues can serve as an example for studying the influence of the arrangement of methyl groups on retention. While the distance between the two methyl groups is the main factor that affects the retention of dimethylnaphthalenes on silica[10], there is a new influencing factor on alumina, namely the symmetry of the molecule. The longest retention times are shown by derivatives with axes of symmetry. For the symmetrical compounds, the retention increases with decrease in the distance between the two methyl groups owing to the change of the electron density distribution in the molecule and therefore stronger non-specific interaction with the stationary phase[7,8]. The retention order of all measured

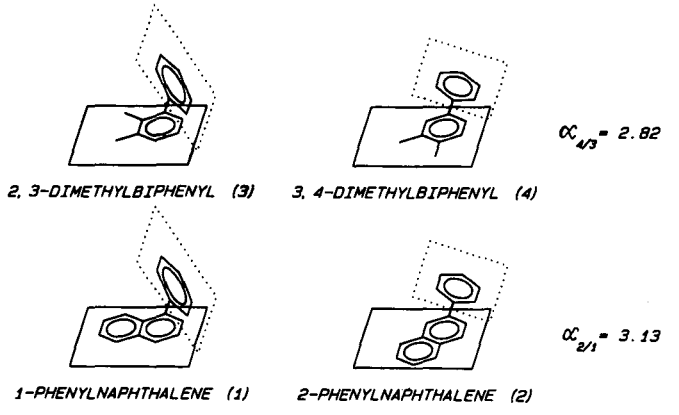

Fig. 3. Influence of the geometrical arrangement of molecules on retention. The selectivities are compared for the pairs 2,3- and 3,4-dimethylbiphenyl and 1- and 2-phenylnaphthalene.

symmetrical and non-symmetrical dimethylnaphthalenes is based on the scheme shown in Fig. 2. The retention of acenaphthene is close to that of 1,8-dimethylnaphthalene, a compound with a similar structure.

The influence of α- and β-substitution on retention has been mentioned by several workers. Snyder[2] and Kucharczyk *et al.*[13] found that 2-methylnaphthalene eluted before 1-methylnaphthalene, whereas Klemm *et al.*[3] found the same retention for both compounds. Popl *et al.* [5,6] reported that 2-methyl- and 2-ethylnaphthalene have lower retentions than the 1-substituted derivatives and that the retention of 2-phenylnaphthalene is substantially higher than that of 1-phenylnaphthalene.

In the present experimental arrangement, for all concentrations of water in MCS the differences between the retentions of the compounds substituted by small alkyl groups are not significant; 2-methyl- has a higher retention than 1-methylnaphthalene whereas 2-ethyl has a shorter retention than 1-ethylnaphthalene.

In agreement with Popl *et al.*'s work[5], a significant difference was found for the pair of phenylnaphthalenes; the substantionally higher retention of 2-phenylnaphthalene can be explained by the rotation of the benzene ring around the naphthalene–phenyl bond. Owing to a higher interaction of a phenyl group located in the α-position with the naphthalene skeleton (steric hindrance), the interplanar angle of 1-phenylnaphthalene is larger than that of 2-phenylnaphthalene and therefore the ability of the former to be adsorbed on the surface of alumina is smaller. Such behaviour is similar to the adsorption of biphenyl molecules on alumina[14], where the retention of the molecules is strongly influenced by the rotation of both phenyl rings owing to substitution in the sterically sensitive 2- and 6-positions (see Fig. 3).

Influence of water content in the mobile phase

The elution times of alkylnaphthalenes decrease with increasing water content in the mobile phase. Fig. 4 shows the dependence of log k' on the water content as determined by MCS. The retention decreases monotonously and the selectivity is not influenced to a great extent.

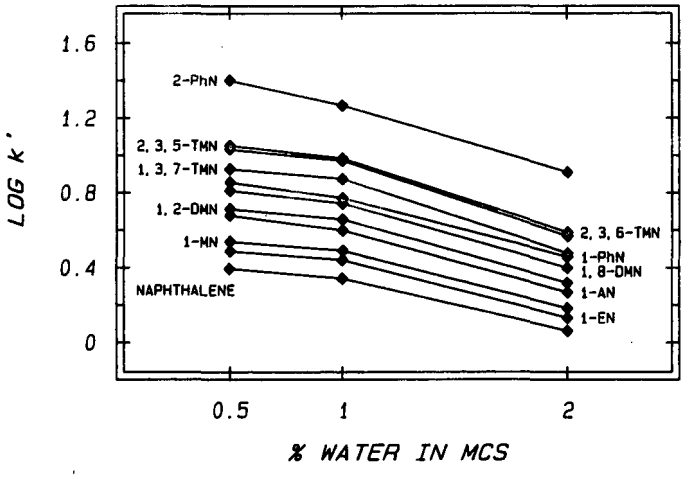

Fig. 4. Variation of log k' for several alkylnaphthalenes with concentration of water in the moisture control system (MCS).

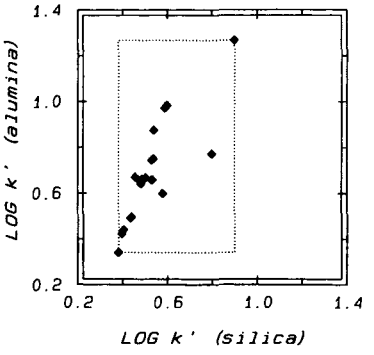

Fig. 5. Comparison of log k' values for all measured alkylnaphthalenes on alumina and silica. Silica[10] column (250 × 8 mm I.D.) packed with 7.5-μm silica gel (Silasorb; Lachema).

Comparison of alumina and silica

The retention behaviour of all the measured compounds using both alumina and silica[10] adsorbents is show in Fig. 5. It is evident that for the alkylnaphthalenes investigated alumina provides a better separation than silica.

REFERENCES

1 L. R. Snyder, *The Principles of Adsorption Chromatography*, Marcel Dekker, New York, 1968.
2 L. R. Snyder, *J. Chromatogr.*, 6 (1961) 22.
3 L. H. Klemm, D. S. W. Chia, C. E. Klopfenstein and K. B. Desay, *J. Chromatogr.*, 30 (1967) 476.
4 M. Popl, V. Dolanský and J. Mostecký, *J. Chromatogr.*, 117 (1976) 117.
5 M. Popl, V. Dolanský and J. Mostecký, *J. Chromatogr.*, 91 (1974) 649.
6 M. Popl, V. Dolanský and J. Mostecký, *Collect. Czech. Chem. Commun.*, 39 (1974) 1836.
7 A. N. Ageev, A. V. Kiselev and Ya. I. Yashin, *Chromatographia*, 13 (1980) 669.
8 A. N. Ageev, A. V. Kiselev and Ya. I. Yashin, *Chromatographia*, 14 (1981) 638.
9 J. Kříž, L. Vodička, J. Punčochářová and M. Kuraš, *J. Chromatogr.*, 219 (1981) 53.
10 J. Punčochářová, L. Vodička and J. Kříž, *J. Chromatogr.*, 267 (1983) 222.
11 J. Kříž, J. Punčochářová and L. Vodička, *J. Chromatogr.*, 354 (1986) 145.
12 J. Kříž, J. Punčochářová, L. Vodička and J. Vařeka, *J. Chromatogr.*, 437 (1988) 177.
13 N. Kucharczyk, J. Fohl and J. Vymětal, *J. Chromatogr.*, 11 (1963) 55.
14 J. Kříž, L. Vodička and E. A. Johnson, in preparation.

Journal of Chromatography, 498 (1990) 254
Elsevier Science Publishers B.V., Amsterdam — Printed in The Netherlands

CHROM. 22 078

Book Review

Modern supercritical fluid chromatography, edited by C. M. White, Hüthig, Heidelberg, 1988, XII + 239 pp., price DM 98.00, ISBN 3-7785-1569-1.

In a new field advances are rapid and are being made on many fronts so that it is inevitably almost impossible for a single work to provide a coverage that is both coherent and cohesive, while still being up-to-date and relevant. As a consequence, all the books on supercritical fluid chromatography (SFC) that have appeared so far have been edited multiauthor works and, as in this case, derived from a meeting or symposium. This usually ensures that a range of topics of active interest are covered and this is also true of the present compilation edited by Curt White. It is also a reflection of the breadth of interest in SFC that, unlike some other new areas, there is little overlap between the contributors to this and other SFC books.

The book opens with a chapter by Klesper, the founder of modern SFC, on the use of composition gradients. The separation methods available to the chromatographer are described in a number of chapters. A general review of packed-column SFC is provided by Pacholec and colleagues. The evolution of the early work in SFC of hydrocarbons is exemplified by a chapter on the application of SFC in the petroleum industry by Schwartz, Levy and Guzowski. Of more interest to the pharmaceutical industry is a survey of the application of SFC for the separation of basic nitrogen compounds by Ashraf-Khorassani and Taylor. They describe a wide range of stationary phases and illustrate the effects of a modifier. In a more specific and little explored area, Khosah considers the application of alumina as a stationary phase and a final brief chapter by Widmer considers the industrial significance of SFC.

Vorhees *et al.* report the successful role of SFC coupled with mass spectrometry, an area which has done much to advance the chromatographic technique. Pariente and Griffiths briefly look at capillary SFC and SFC–Fourier transform infrared spectroscopy. The potential of the ion mobility spectrometer for SFC is suggested by Hill and Morrissey.

The collection is completed by two specialised chapters. Restrictor performance in capillary columns is compared by Wright and Smith and then Maguire and Denyszyn discuss the solubility of organic modifiers in liquid carbon dioxide.

Overall the book ranges from the specialist practical to the theoretical. It shows the range of the ways in which SFC has been used in industry and areas of research interest but the reviews are often brief and tend to give an insight into only a small area. Consequently, it would probably be difficult for a newcomer to the field to gain an overall impression of the state of SFC from this book and with few exceptions little guidance is given in the selection and operation of an SFC system. Although from an American conference, capillary SFC does not dominate and many of the chapters discuss the role and advantages of packed columns. This book will be of primary interest to those in the field and for observers of developments in SFC. However, those contemplating venturing into SFC still await a comprehensive general introduction, which is needed to overcome some of the mystic which still surrounds SFC.

Loughborough (U.K.) ROGER M. SMITH

Journal of Chromatography, 498 (1990) 255–256
Elsevier Science Publishers B.V., Amsterdam — Printed in The Netherlands

CHROM. 22 013

Book Review

Fat soluble vitamin assays in food analysis—A comprehensive review, by G. F. M. Ball, Elsevier Applied Science, London, New York, 1988, 326 pp., price £45.00, ISBN 1-85166-239-1.

As its subtitle rightly suggests, this book presents a comprehensive review of modern methods for the determination of fat-soluble vitamins in foods and feeds. It contains a wealth of useful data on assay principles, practice and results, which will be appreciated particularly by newcomers to the field and those who are only occasionally confronted with the analysis of foods. For these workers, the availability of an authoritative review saves the pain of going through time-consuming literature searches before the analyses can be started. The book has been clearly and concisely written. The authors are thoroughly familiar with modern analytical concepts and have reviewed the specific literature in great detail (although in certain sections, *e.g.*, that on high-performance liquid chromatography of carotenoids, several important references are lacking).

The book can be divided into two main parts, a general one, describing the principles and the background of fat-soluble vitamin asays (Chapters 1–5), and one concerned with the various techniques available for each individual vitamin, *i.e.*, non-chromatographic procedures (Ch. 6), gas chromatography (Ch. 7) and high-performance liquid chromatography (Ch. 8). In the last three chapters, an introduction to the technique itself, which is sometimes too lengthy, precedes the actual description of the vitamin assays.

The book's content is generally scientifically sound and subject to few criticisms. However, some gaps should be filled and some corrections made in a possible second edition. Gas chromatography–mass spectrometry is ignored as an analytical technique and modern thin-layer chromatography (especially high-performance thin-layer chromatography and densitometry also is not discussed. No mention is made of the important short excitation wavelength in the fluorescence spectrum of vitamin E (p. 44). Non-aqueous reversed-phase chromatography is not necessarily compatible with the injection of extracts in hexane; this is only so when the eluent (based on hexane itself) is totally miscible with it. β-Cryptoxanthin is not the predominant (non-provitamin A) carotenoid in maize, but lutein.

As far as the overall structure of the book is concerned, the authors have opted for an arrangement according to techniques rather than individual vitamins. The disadvantage of this approach is that the general principles and background information for each vitamin (including structural and physico-chemical properties) have to be grouped in a separate chapter (Ch. 2) (to avoid repetition), which in our opinion is too far from the chapters supposedly describing the application of these principles. This may partly account for some stylistic inconsistencies. For example, in Ch. 8 the section on carotenoids again starts with a brief discussion on analytical considerations, whereas other sections (*e.g.*, on vitamin D) do not.

The overall consistency could indeed have been improved in general. For example, the chapter on high-performance liquid chromatography contains many tables, but the chapter on gas chromatography has none. Many details now given in the text could easily be moved to tables, *e.g.*, data concerning gas chromatographic columns, derivatization, internal standards and even results (recovery, precision). Sometimes, as in Ch. 8, information in the text merely duplicates that in the tables. Also, some subdivision (with or without headings) in each section, *e.g.*, according to the type of biological matrix analysed or the nature of the clean-up procedures, would have added to the clarity. This would have been preferable to a detailed chronological discussion of the papers, which leads to repetitions on assay principles and methodology.

The book is extensively illustrated, although some figures (*e.g.*, those showing the separation of standards) are less relevant. Some abbreviations used in the references are not standard (*e.g., J. Chromat.* instead of *J. Chromatogr.*).

In conclusion, the format of this book is capable of improvement and some errors should be corrected, but this does not detract from its value as a very useful compendium for analytical chemists who are active in the area of fat-soluble vitamins.

Ghent (Belgium) H. J. NELIS and A. P. DE LEENHEER

Vol. 498, No. 1

journal of chromatography news section

2nd INTERNATIONAL SYMPOSIUM ON APPLIED MASS SPECTROMETRY IN THE HEALTH SCIENCES, BARCELONA, SPAIN APRIL 17–20, 1990

The new deadline for submission of abstracts and for registration is January 20, 1990. Acceptance of abstracts for inclusion in the book of abstrcts will be communicated to authors by mid February 1990. Registered participants may submitt stop press last minute contributions up to March 30, 1990.

The opening of the symposium will take place on the evening of April 17 with a welcome reception. Scientific sessions will start April 18. Manuscripts for the proceedings volume to be published by Elsevier as a special issue of the *Journal of Chromatography, Biomedical Applications* must be delivered April 17.

Posters will be the main form of data presentation and discussion so that even invited lectures will be complemented by the corresponding poster presentation. Each poster will be in place till the end of the Symposium and there will be no parallel sessions.

Topics will cover the whole field of applied mass spectrometry in the health sciences. These will include all of the following:

— New developments in MS instrumentation and techniques
— Recent trends and perspectives in combined chromatographic and MS techniques: GC–MS, LC–MS, SFC–MS, CZE–Ms
— FAB and tandem MS
— Desorption and ionization techniques
— Isotope dilution MS and Isotope probes
— Applications in clinical studies and diagnosis; Metabolic and biochemical studies; preptide mapping and protein sequencing; high molecular weight biopolymers; respiratory gas analysis; environmental chemistry; food chemistry; toxicology and doping control; drug assay methods; pharmacology; microbiology, stereochemical isomers; quantitative determinations and
— Fundamental studies and fragmentation mechanisms of biomolecules

A technical exhibition of mass spectrometric instrumentation and related suplies will be located on the same floor as the coffee area and lecture and poster Halls.

For further details, contact: Professor Emilio Gelpi, Symposium Secretariat. 2nd International Symposium on Applied Mass Spectrometry in the health Sciences. Palau de Congressos. Dept. Convencions, Av. Reina Ma Cristina s/n, 08004 Barcelona, Spain. Tel.: (343) 423 31 01. ext. 8208; Telex: 53117; Fax: 426 28 45.

PUBLICATION SCHEDULE FOR 1990

Journal of Chromatography and Journal of Chromatography, Biomedical Applications

MONTH	J	F	
Journal of Chromatography	498/1 498/2 499	500 502/1 502/2	The publication schedule for further issues will be published later
Cumulative Indexes, Vols. 451–500		501	
Bibliography Section		524/1	
Biomedical Applications	525/1	525/2	

INFORMATION FOR AUTHORS

(Detailed *Instructions to Authors* were published in Vol. 478, pp. 453–456. A free reprint can be obtained by application to the publisher, Elsevier Science Publishers B.V., P.O. Box 330, 1000 AH Amsterdam, The Netherlands.)

Types of Contributions. The following types of papers are published in the *Journal of Chromatography* and the section on *Biomedical Applications:* Regular research papers (Full-length papers), Notes, Review articles and Letters to the Editor. Notes are usually descriptions of short investigations and reflect the same quality of research as Full-length papers, but should preferably not exceed six printed pages. Letters to the Editor can comment on (parts of) previously published articles, or they can report minor technical improvements of previously published procedures; they should preferably not exceed two printed pages. For review articles, see inside front cover under Submission of Papers.

Submission. Every paper must be accompanied by a letter from the senior author, stating that he is submitting the paper for publication in the *Journal of Chromatography*. Please do not send a letter signed by the director of the institute or the professor unless he is one of the authors.

Manuscripts. Manuscripts should be typed in double spacing on consecutively numbered pages of uniform size. The manuscript should be preceded by a sheet of manuscript paper carrying the title of the paper and the name and full postal address of the person to whom the proofs are to be sent. Authors of papers in French or German are requested to supply an English translation of the title of the paper. As a rule, papers should be divided into sections, headed by a caption (*e.g.*, Summary, Introduction, Experimental, Results, Discussion, etc.). All illustrations, photographs, tables, etc., should be on separate sheets.

Introduction. Every paper must have a concise introduction mentioning what has been done before on the topic described, and stating clearly what is new in the paper now submitted.

Summary. Full-length papers and Review articles should have a summary of 50–100 words which clearly and briefly indicates what is new, different and significant. In the case of French or German articles an additional summary in English, headed by an English translation of the title, should also be provided. (Notes and Letters to the Editor are published without a summary.)

Illustrations. The figures should be submitted in a form suitable for reproduction, drawn in Indian ink on drawing or tracing paper. Each illustration should have a legend, all the *legends* being typed (with double spacing) together on a *separate sheet*. If structures are given in the text, the original drawings should be supplied. Coloured illustrations are reproduced at the author's expense, the cost being determined by the number of pages and by the number of colours needed. The written permission of the author and publisher must be obtained for the use of any figure already published. Its source must be indicated in the legend.

References. References should be numbered in the order in which they are cited in the text, and listed in numerical sequence on a separate sheet at the end of the article. Please check a recent issue for the layout of the reference list. Abbreviations for the titles of journals should follow the system used by *Chemical Abstracts*. Articles not yet published should be given as "in press" (journal should be specified), "submitted for publication" (journal should be specified), "in preparation" or "personal communication".

Dispatch. Before sending the manuscript to the Editor please check that the envelope contains three copies of the paper complete with references, legends and figures. One of the sets of figures must be the originals suitable for direct reproduction. Please also ensure that permission to publish has been obtained from your institute.

Proofs. One set of proofs will be sent to the author to be carefully checked for printer's errors. Corrections must be restricted to instances in which the proof is at variance with the manuscript. "Extra corrections" will be inserted at the author's expense.

Reprints. Fifty reprints of Full-length papers, Notes and Letters to the Editor will be supplied free of charge. Additional reprints can be ordered by the authors. An order form containing price quotations will be sent to the authors together with the proofs of their article.

Advertisements. Advertisement rates are available from the publisher on request. The Editors of the journal accept no responsibility for the contents of the advertisements.

For Superior Chiral Separation

CHIRALCEL, CHIRALPAK and CROWNPAK are now available from DAICEL and include 15types of HPLC columns which provide superior resolution of racemic compounds.

Drugs directly resolved on our DAICEL columns are given as follows;

SUBSTANCE	α	column	SUBSTANCE	α	column	SUBSTANCE	α	column
Alprenolol	3.87	OD	Gauifenesin	2.40	OD	Oxapadol	complete resolution	CA-1
Amphetamine	1.2	CR	Hexobarbital	1.7	CA-1			
Atenoloi	1.58	OD	Homatropine	3.13	OD	Oxazepan	4.36	OC
Atropine	1.62	OD	Hydroxyzine	1.17	OD	Oxazolam	1.67	OF
Baclofen	1.39	CR	Indapamide	1.58	OJ	Oxprenolol	6.03	OD
Carbinoxamine	1.39	OD	Ketamine	complete resolution	CA-1	Perisoxal	1.33	OF
Carteolol	1.86	OD					1.27	OD
Chlophedianol	2.82	OJ	Ketoprofen	1.46	OJ	Pindolol	5.07	OD
Chlormezanone	1.47	OJ	Mephobarbital	5.9	OJ	Piprozolin	1.7	CA-1
Cyclopentolate	2.47	OJ		2.3	CA-1	Praziquantal	complete resolution	CA-1
Diltiazem	1.46	OD	Methaqualone	2.8	CA-1			
	2.36	OF		7.3	OJ	Propranolol	2.29	OD
	1.75	OG	Methsuximide	2.68	OJ	Rolipram	complete resolution	CA-1
Disopyramide	2.46	OF	Metoprolol	complete resolution	OD			
Ethiazide	1.54	OF				Sulconazole	1.68	OJ
Ethotoin	1.40	OJ	Mianserin	1.75	OJ	Suprofen	1.6	OJ
Fenoprofen	1.35	OJ	Nilvadipine	complete resolution	OT	Trimebutine	1.81	OJ
Glutethimide	2.48	OJ				Warfarin	1.96	OC

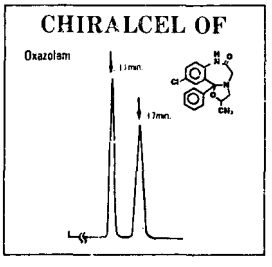

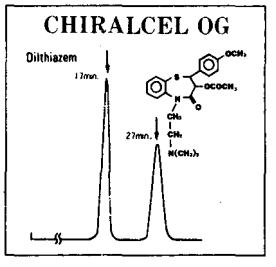

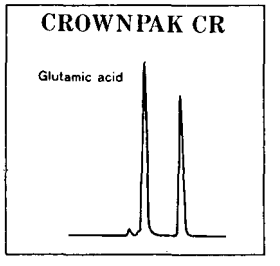

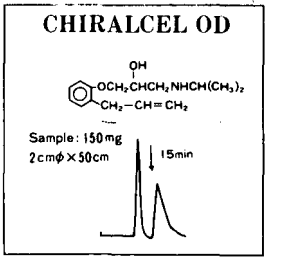

In addition to the drugs listed above, our chiral columns permit resolution also of the following: FMOC amino acids and Carboxylic acids, and Pesticides, for example Isofenfos, EPN and Acephate, and Synthetic intermediate 4-hydroxy cyclophentenone etc, Many other compounds besides these can be readily resolved.

▶ *Separation Service*

- A pure enantiomer separation in the amount of 100g~10kg is now available.
- Please contact us for additional information regarding the manner of use and application of our chiral columns and how to procure our separation service.

For more information about our Chiral Separation Service and Columns, please contact us!

DAICEL CHEMICAL INDUSTRIES, LTD.

8-1, Kasumigaseki 3-chome, Chiyoda-ku, Tokyo 100, Japan Phone: 03(507)3151 FAX: 03(507)3193

DAICEL (U.S.A.), INC.
Fort Lee Executive Park
Two Executive Drive, Fort Lee,
New Jersey 07024
Phone: (201)461-4466
FAX: (201)461-2776

DAICEL (U.S.A.), INC.
23456 Hawthorne Blvd.
Bldg. 5, Suite 130
Torrance, California. 90505.
Phone: 213-791-2030
FAX: 213-791-2031

DAICEL (EUROPA) GmbH
Königsallee 92a.
4000 Düsseldorf 1, F.R. Germany
Phone: (0211)134158
Telex: (41)8588042 DCEL D
FAX: (0211)879-8329

DAICEL CHEMICAL (ASIA) PTE.LTD.
65 Chulia Street #40-07
OCBC Centre, Singapore 0104.
Phone: 5332511
FAX: 5326454